Spring 2014

Chemical investigation of fungicolous and endophytic fungi

Nisarga Laxman Phatak
University of Iowa

CHEMICAL INVESTIGATION OF FUNGICOLOUS AND ENDOPHYTIC FUNGI

by

Nisarga Laxman Phatak

A thesis submitted in partial fulfillment
of the requirements for the Doctor of
Philosophy degree in Chemistry
in the Graduate College of
The University of Iowa

May 2014

Thesis Supervisor: Professor James B. Gloer

Graduate College
The University of Iowa
Iowa City, Iowa

CERTIFICATE OF APPROVAL

_____

PH.D. THESIS

_____

This is to certify that the Ph.D. thesis of

Nisarga Laxman Phatak

has been approved by the Examining Committee
for the thesis requirement for the Doctor of Philosophy
degree in Chemistry at the May 2014 graduation.

Thesis Committee: _____
James B. Gloer, Thesis Supervisor

_____
Leonard R. MacGillivray

_____
Ned B. Bowden

_____
Amanda J. Haes

_____
Horacio F. Olivo

To
Aai and Baba

Do not brood over your past mistakes and failures as they will only fill your mind with grief, regret, and depression. Do not repeat them in future.

Swami Sivananda
Unknown

ACKNOWLEDGMENTS

First and foremost, Dr. Gloer. There are no words that can describe my gratitude for him. For all the patience, support, and encouragement that you have shown to me during my stay here. For guiding and supporting me through some tough times. For teaching me some of the most wonderful lessons of life. You are someone I can only dream of emulating.

Dr. Don Wicklow for all the samples that made my PhD possible. Your enthusiasm is contagious. I would also like to thank Dr. Patrick F. Dowd at the USDA for conducting the antiinsectan bioassays. I am grateful to my committee members, Drs. Ned Bowden, Len MacGillivray, Amanda Haes, and Horacio Oilivo for their guidance, thoughtful comments, and support during my graduate career.

Dr. Santhana Velupillai of the University of Iowa NMR Central Research Facility for providing some insights into theoretical NMR and always willing to help. Dr. Lynn Teesch and Mr. Vic Parcell of the University of Iowa High Resolution Mass Spectrometry Facility are very much appreciated. I would like to thank Dr. Dale C. Swenson of the University Of Iowa Department Of Chemistry X-Ray Crystallography Facility for conducting X-ray diffraction analyses.

I would like to thank all former and current Gloer group members. I would like to especially thank Lori for inducting me into this research group. Amni for all the help, pep talks and all the good times. Dinith for cheering me up always.

All my friends in Iowa City who have made my stay here memorable. Gupto, Suman, Nirmal, Oishik, Mayuresh, Ipshita, Aashay, Bhakti, Pradeep for supporting me during some tough times and being the family away from my own family and for never making me feel lonely. Special thanks to Oishik, Sudipta Sen for all the paneer and biryani. Oishik, Nirmal, Gupto, Suman and Ipshita for being my closest friends.

My family and friends back in India, for their constant support and encouragement. My maternal uncle and aunt, Shailendra mama and Hema mavshi and paternal uncle and aunt –aatya and kakaji- for all that you have done for me, will never be forgotten. I do not feel indebted to you because you are my closest family I would not be here without your support all through my life. Prasad, Arshad, Rohit for giving me the peace of mind and someone to rely on in time of need.

And finally my parents-aai and papadi. You have been the pillars of my life. The very foundation that I stand on. For being so strong and supportive of all my decisions. For giving me the freedom to choose my path. For enduring so many hardships to give me all the possible opportunities. For never doubting me or my will. I live for you both and I hope that someday I will be able to give you everything that you sacrificed.

TABLE OF CONTENTS

LIST OF TABLES

Table

LIST OF FIGURES

Figure

LIST OF SCHEMES

Scheme

CHAPTER 1

INTRODUCTION

Fungi are estimated to be second only to insects in species diversity. It is estimated that there are at least 1.5 million species of fungi, which is more than five times the estimated number of plant species and 50 times the estimated number of bacterial species.[1] Of the 1.5 million species, only about 5 – 10% have so far been described by taxonomists, leaving a very large number of unexplored fungal species in the environment. Moreover, these estimates are now considered conservative, and new data suggest that there are an estimated 3.5 – 5.1 million fungal species.[2,3] Fungi in general are known to produce a variety of secondary metabolites with a wide range of biological activities. The roles of such metabolites in nature are rarely clear. However, it is possible that fungi, which often thrive in competitive environments, would experience evolutionary pressure to produce such metabolites in some instances for defensive or offensive functions.[4]

Fungi are often associated with producing toxins such as aflatoxins (**1.1** – aflatoxin B_1), ochratoxins, fumonisins (**1.2** – fumonisin B_1), trichothecenes, and others that sometimes contaminate food crops. One common example, *Aspergillus flavus*, is a pathogenic fungus known to cause ear rot in corn and yellow mold in peanuts. It is an opportunistic human and animal pathogen and causes aspergillosis in immunocompromised individuals. It is also known to produce aflatoxins, which are among the most carcinogenic substances known and are associated with liver cancer.[5] Aflatoxins produce acute necrosis, cirrhosis, and carcinoma of the liver in a number of animal species. LD_{50} value ranges from 0.5 to 10 mg/kg body weight.[6] The U.S. FDA allows only 20 – 300 ppb of aflatoxins in animal feeds.[7]

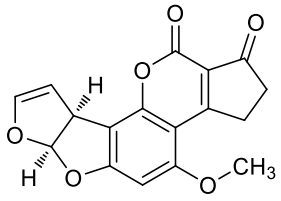

1.1

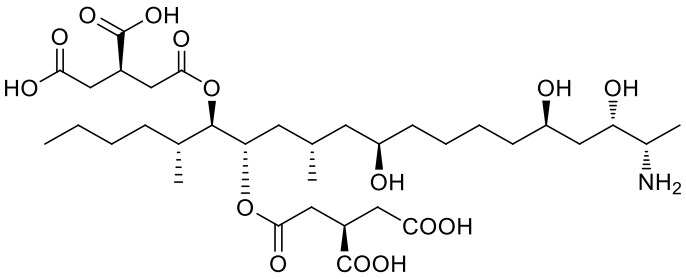

1.2

Many of the secondary metabolites produced by fungi have potent biological activities which in some cases include toxicity. Fungi are resistant towards their own toxic secondary metabolites through metabolite-specific resistance pathway.[8,9] This self-resistance to has been attributed to various factors such as the presence of an enzyme-modifying compound,[10,11] export mechanisms,[12,13] compartmentalization,[14] or specific mutations in the target enzyme.[15] Gliotoxin (**1.3**) is a cytotoxic secondary metabolite produced by *Aspergillus fumigatus*. Deletion of a single gene, *gliT* in the gliotoxin gene cluster (Δ*gliT*), renders the organism highly sensitive to exogenous gliotoxina and completely disrupts gliotoxin secretion. However addition of glutathione to Δ*gliT* strains relieved glitoxin inhibition.[10] Another example is cercosporin (**1.4**) produced by the tobacco pathogenic fungus *Cercospora nicotianae*. The production of and resistance to cercosporin is regulated by *CRGI* (cercosporin resistance gene 1), a gene encoding a zinc cluster transcription factor. Disruption of this factor causes the fungus to become highly sensitive to cercosporin.[12]

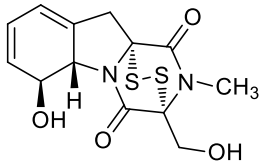

1.3

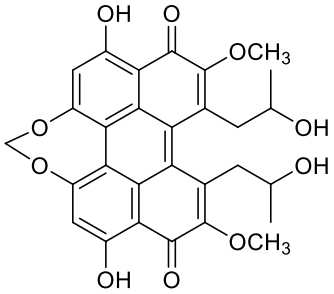

1.4

Despite the negative reputation often ascribed to fungi, some are also known to produce secondary metabolites with important pharmacological activities. Many drugs with antibiotic, antifungal, immunosuppressant and cholesterol-lowering properties have been discovered through chemical studies of fungi.[16-19] Lovastatin (**1.5**) also known as (Mevacor®), originally isolated from *Aspergillus terreus*, was the lead compound in the development of the statin class of drugs widely used to lower blood cholesterol. Other well-known examples are penicillins (e.g., penicillin G - **1.6**) that were first isolated from *Penicillium notatum*, which are vitally important antibiotics.

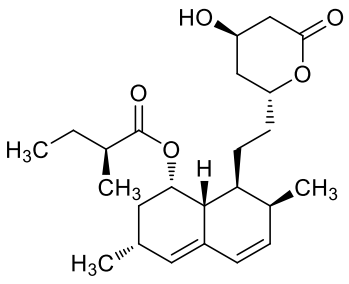

1.5

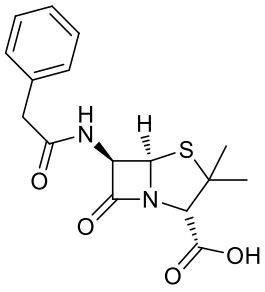

1.6

Fungal secondary metabolites are biosynthesized via four major pathways including polyketide, shikimate, terpenoid, and amino acid/peptide biogenesis, with some being of mixed biogenetic origin. Members of this class of metabolites often show biological activity, and sometimes display unusual features not common to other peptides. Several representatives of this class were encountered in the course of the research described in this thesis. This chapter mainly consists of a review of non-ribosomally synthesized fungal peptides, with emphasis on their biosynthesis and representative members of this class discovered since reviewed by Lee in 1997, along with some not covered in that report.[20] Isolation and structure elucidation of a variety of new and known compounds encountered in this research, including several fungal non-ribosomal peptides, will be discussed in subsequent chapters of this thesis.

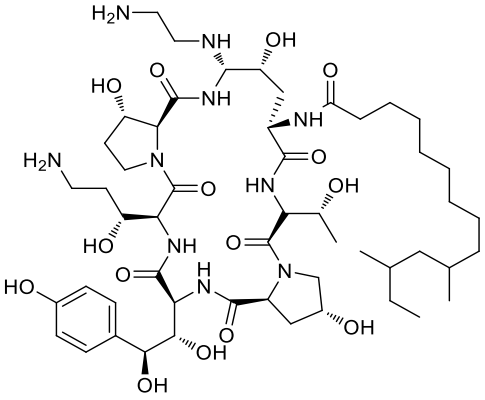

1.7

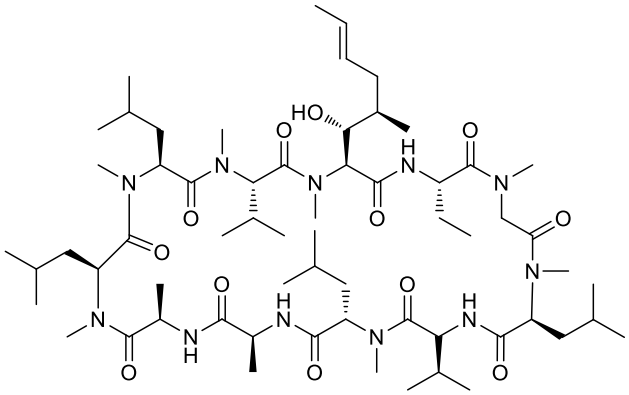

1.8

Non-ribosomally synthesized peptides (NRPs) produced by a variety of fungi and bacteria show extraordinary structural diversity and exhibit a wide range of biological activities including antibiotic, immunosuppressant, and cytostatic effects.[16] Prime examples from fungal sources include caspofungin (**1.7**),[17] a clinically useful antifungal agent belonging to the echinocandin family, and cyclosporin A (**1.8**),[18] an immunosuppressant with applications in organ transplantation. The latter was originally

isolated from the fungus *Tolypocladium inflatum*, but can be found as a metabolite of many other fungi as well. Its activity arises because it interferes with lymphokine biosynthesis. It has also been shown to inhibit HIV-I replication.[21]

Bacteria also make important NRPs. For example, bleomycin A_2 (**1.9**),[22] a glycopeptide produced by *Streptomyces verticillus* exhibits cytostatic activity and finds application in cancer treatment.

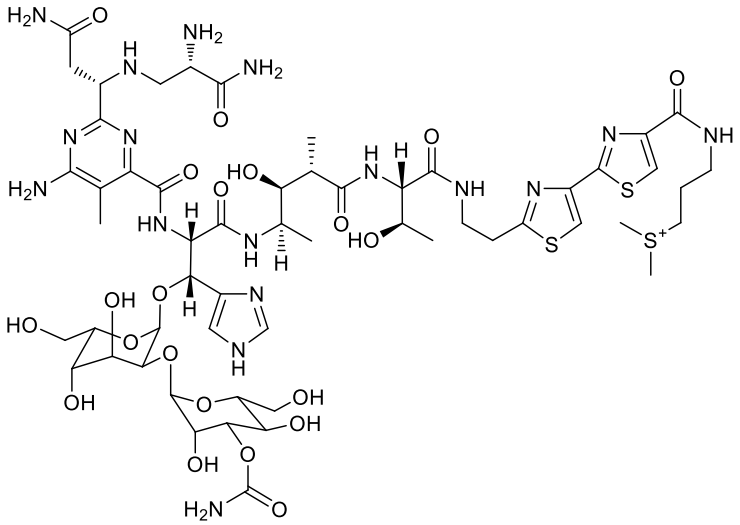

1.9

NRPs display a wide variety of structural features that are different from those of normal peptides and proteins which are synthesized in cell ribosomes. Ribosomal peptides usually contain only the 20 common amino acids as building blocks, whereas many other amino acids and hydroxy acids are found in NRPs.[23] NRPs are assembled independent of ribosomes in a nucleic acid-independent pathway by a group of multi-modular enzymes called non-ribosomal peptide synthetases (NRPSs). This pathway can use not only the 20 standard amino acids found in ribosomal peptides, but can employ D-configured amino acids, methylated, glycosylated, phosphorylated units, and fatty acid or polyketide units. NRPs can also contain non-proteinogenic amino acids like ornithine or

(4*R*)-4-[(*E*)-2-butenyl]-4-methyl-L-threonine, as in **1.8**, and some amino acids can be modified to form oxazoline or thiazoline moieties. These capabilities lead to tremendous structural diversity, with distinctive features that are often essential for biological activity.[16]

Biosynthesis of NRPs

NRPSs are modularly organized multi-enzyme complexes. A module is a section of the NRPS polypeptide chain that is responsible for the incorporation of one amino acid (or other units) into the peptide. Each module is further subdivided into domains that enzymatically catalyze individual steps of NRP synthesis. The functions of these domains include substrate recognition and activation (the adenylation-(A)-domain), transport to respective catalytic centers (the peptidyl carrier protein (PCP) domain), and peptide or ester bond formation (the condensation-(C)-domain) (Figure 1.2).[24]

The first step involves selection of a specific substrate (typically an amino acid or hydroxy acid) and is catalyzed by an adenylation domain (A) followed by the generation of an aminoacyl AMP-mixed anhydride through ATP hydrolysis. The next step involves transport of these activated amino acids and elongation intermediates between the catalytic centers through the peptidyl carrier protein (PCP) unit. However, the PCP is first activated by post-translationally transferring the 4'-phosphopantetheine (PPan) cofactor from coenzyme A to a conserved serine residue of PCP, converting the inactive *apo*-PCP to the active *holo*-PCP (Figure 1.1). Activated amino acids and peptides are then covalently bound as thioesters to the free thiol of the PPan cofactor and transported between catalytic sites. In the next stage, peptide bond formation is catalyzed by the condensation (C) domain. The resulting intermediate is then translocated for any further construction or modification steps. Final product release is catalyzed by a thioesterase (TE) domain.[16] In addition to these four domains, other domains often involved in NRP synthesis include epimerization (E), *N*-methyltransferase (Mt), cyclization (Cy),

oxidation (Ox), reduction (R), and formyltransferase (F) domains that may or may not be involved and act in conjunction to carry out various modifications.

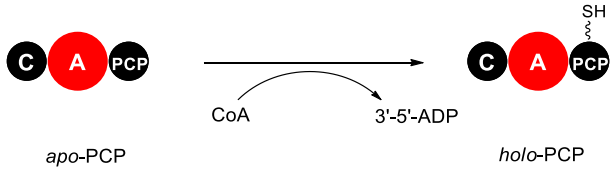

Figure 1.1. Activation of peptidyl carrier protein (PCP)

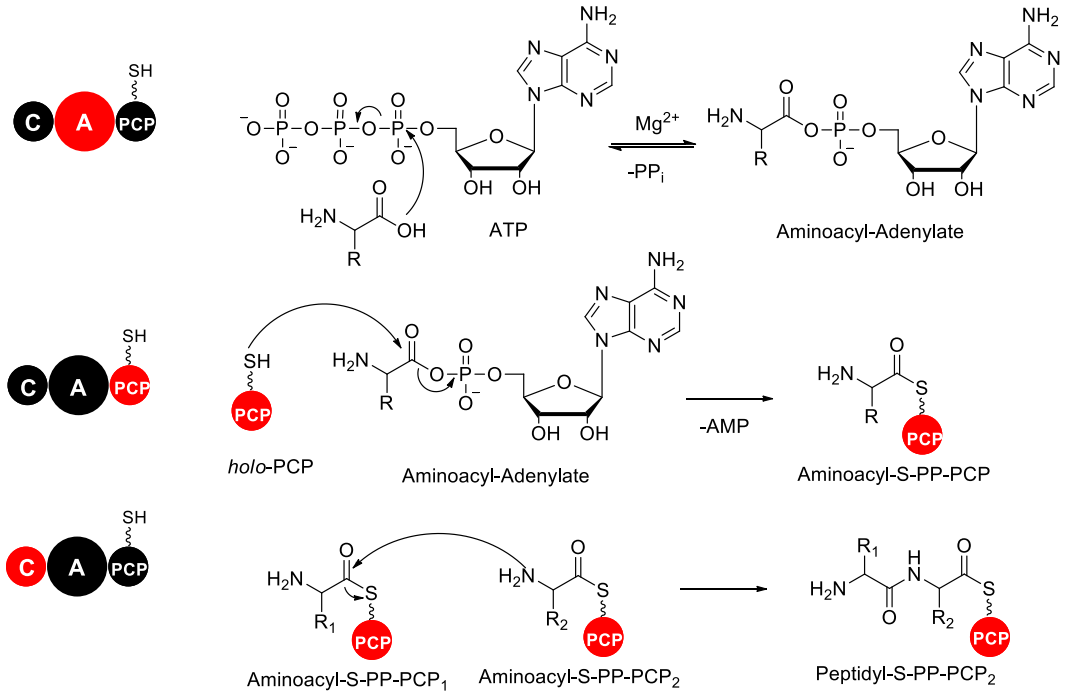

Figure 1.2. Reactions catalyzed by three NRPS domains: A, PCP, and C. The cofactor 4'-phosphopantetheine (PPan) is attached to the carrier domain PCP.[16]

Non-Ribosomal Peptides from Fungi

The NRP synthesis pathway and the many kinds of modifications that can occur, lead to a vast array of diversity in the structures of NRPs. As noted earlier, many of the distinctive modifications carried out in these processes are responsible for observed biological activities of the final products. The following section contains a review of the structures and bioactivities of fungal NRPs. These peptides are classified as lipopeptides, glycopeptides, peptaibols, and depsipeptides.

Lipopeptides

As the name implies, lipopeptides consist of lipids connected to peptides. This group is exemplified by the echinocandin family of compounds that have been a source of clinically important antifungal drugs. Echinocandins are amphiphilic cyclic hexapeptides with an *N*-linked acyl lipid side chain. The amino acids used in their construction include dihydroxyornithine, 4-hydroxyproline, 3-hydroxyproline, 3-hydroxy-4-methylproline, dihydroxyhomotyrosine, and threonine, most of which are uncommon amino acids. Echinocandins exhibit potent antifungal properties by inhibiting the synthesis of 1,3-β-glucan, a key component of the fungal cell wall which is absent in mammalian cells. It is presumed that the long side chains intercalate with the phospholipid bilayer of the cell membrane.[17] However, one problem with this class of compounds was that some echinocandins hemolyze human and mouse erythrocytes in vitro at therapeutically useful concentrations.[25] Solubility issues were also somewhat problematic. A semi-synthetic analogue cilofungin (**1.10**) was prepared from echinocandin B_0 (**1.11**) with a modified side chain. Although **1.10** proved non-lytic to red blood cells (RBCs), it showed little improvement in solubility, and because of solvent toxicity in formulations, development of this drug was halted. Subsequent research led to discovery of the semi-synthetic analogue anidulafungin (**1.12**) which has been marketed as Eraxis® by Pfizer. Related to the echinocandins, pneumocandin B_0 (**1.13**) was

discovered by researchers at Merck & Co. The key structural differences between the pneumocandins and the echinocandins were the presence of a 3*R*-hydroxyglutamine in place of the threonine unit and a 10*R*, 12*S*-dimethylmyristoyl side chain rather than a linoleoyl group, respectively. These differences made echinocandins non-lytic to RBCs.[26] Subsequent efforts to improve water-solubility, stability, and antifungal properties led to the development of a semisynthetic analogue called caspofungin (**1.7**), now marketed as Cancidas® by Merck & Co. The precursor to caspofungin (**1.7**), pneumocandin B_0 (**1.13**), was discovered from *Glarea lozoyensis*, which had previously been classified as *Zalerion arboricola* along with several other compounds belonging to the pneumocandin family.[27-29] Compound **1.13** showed potent in vitro activity in the glucan synthase assay with IC_{50} values of 70 nM. However, its limited water-solubility (<0.1 mg/mL) was a major problem. To overcome this, a semi-synthetic, relatively water-soluble (~0.4 mg/mL) derivative (**1.7**) was synthesized. Compound **1.7** was found to be more potent in antifungal assays than **1.13**, and had improved pharmacokinetic properties (Table 1.1).[26,30]

Table 1.1. Antifungal activity for pneumocandin B_0 (**1.13**) and caspofungin (**1.7**)

	C. albicans GS (IC_{50}, nM)	*C. albicans* MFC (μg/mL)	*A. Fumigatus* MEC (μg/mL)
1.13	70	0.25	1
1.7	0.60	0.125	0.008

GS: 1,3-β-D-glucan synthase assay using *C. albicans* protoplast membranes; IC_{50} the concentration at which the compound inhibits formation of 50% of trichloroacetic acid-precipitable polysaccharides generated by membrane preparation from *C. albicans* protoplasts; MFC: minimum fungicidal concentration, lowest concentration of drug showing no growth or fewer than four colonies per spot.; MEC The minimum effective concentration, or lowest drug concentration that results in the formation of blunt attenuated hyphal structures as viewed microscopically.[25,31]

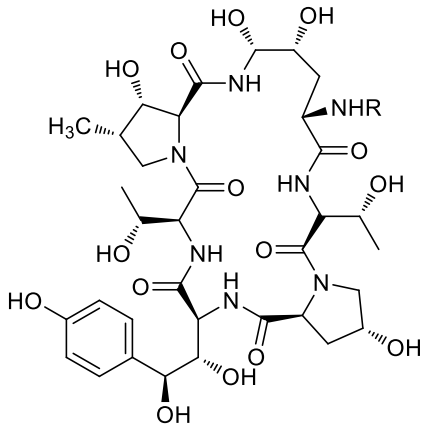

1.10

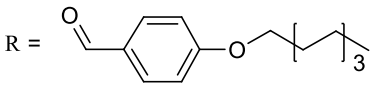

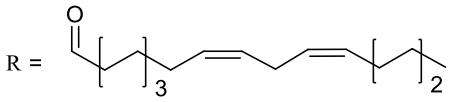

1.11

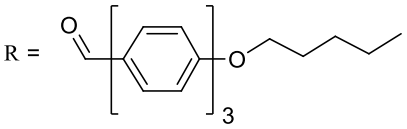

1.12

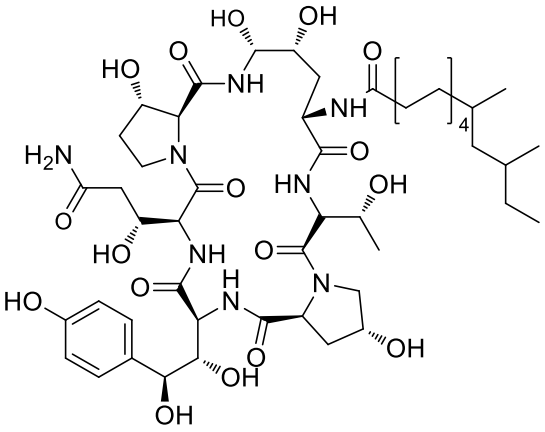

1.13

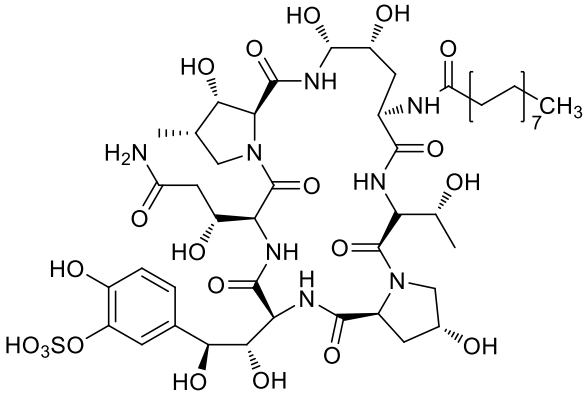

1.14

Another antifungal pneumocandin analogue, FR901379 (**1.14**) was developed into micafungin (**1.15**),[32] marketed as Mycamine® by Astellas. FR901379 (**1.14**) was isolated from *Coleophoma empetri* and was similar in structure to other pneumocandins, but contained a sulfonate group on the homotyrosine unit and a palmitoyl side chain.[33] It inhibited 1,3-β-glucan synthase prepared from *C. albicans* with an IC_{50} value of 0.7

μg/mL and also displayed potent antifungal activity against *C. albicans*. It was highly water-soluble (>50 mg/mL), which was attributed largely to the sulfonate group.[32] This compound overcame the problems associated with solubility of **1.13**. However, **1.14** displayed hemolytic activity. To reduce the hemolytic activity and to improve the antifungal activity, **1.15**, a semi-synthetic compound was prepared, having a modified side chain containing an isoxazole ring. It displayed improved activity against *C. albicans* and *A. fumigatus* and showed reduced hemolytic effects.

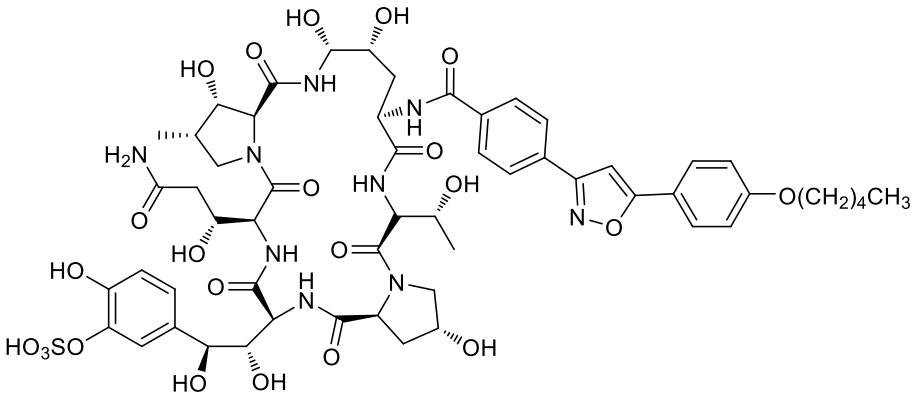

1.15

Additional members of the pneumocandin class have recently been isolated from *Coleophoma empetri* (**1.16 - 1.20**), *Tolypocladium parasiticum* (**1.21**), and *Chalara* sp. (**1.22**).[34-37] They have the same basic core structure, with differences in oxygenation and side chains.

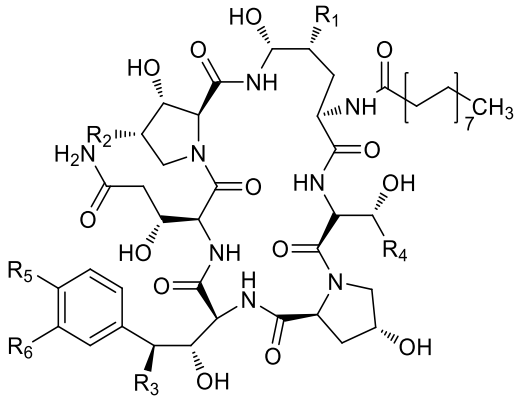

1.16 R_1 = OH, R_2 = CH_3, R_3 = H, R_4 = H, R_5 = H, R_6 = OSO_3H

1.17 R_1 = OH, R_2 = H, R_3 = H, R_4 = H, R_5 = H, R_6 = OSO_3H

1.18 R_1 = H, R_2 = CH_3, R_3 = H, R_4 = H, R_5 = H, R_6 = OSO_3H

1.19 R_1 = OH, R_2 = CH_3, R_3 = H, R_4 = CH_3, R_5 = OSO_3H, R_6 = H

1.20 R_1 = OH, R_2 = H, R_3 = H, R_4 = CH_3, R_5 = OSO_3H, R_6 = H

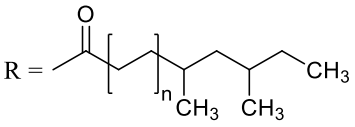

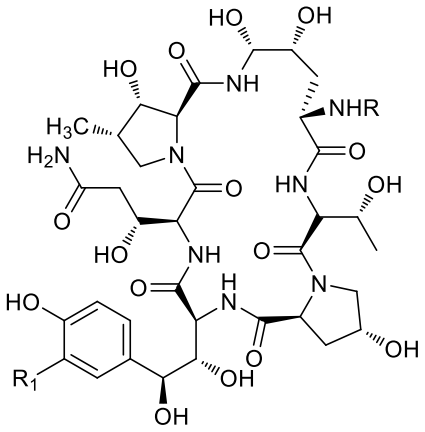

1.21 n = 4 R_1 = OSO_3H

1.22 n = 5 R_1 = OSO_3H

1.23 n = 4 R_1 = H

Compounds **1.16** - **1.23** were tested for inhibition of 1,3-β-glucan synthase in comparison with **1.14** and the results are summarized in Table 1.2.[34-37]

Table 1.2. Inhibitory activities of **1.14** and **1.16** - **1.23** against 1,3-β-glucan synthase prepared from *Candida albicans*. [34-37]

Compound	IC_{50} (μg/mL)
1.16	0.49
1.17	0.64
1.18	0.72
1.19	36.2
1.20	19.7
1.21	0.87
1.22	2.0
1.23	0.20[25]
1.14	0.77

Compounds **1.16** - **1.18** showed higher potency than **1.14** in the glucan synthase assay. The major structural differences were the amino acid units in these compounds. Compounds **1.16** - **1.20** contain a homophenylalanine residue and a linear 16-carbon side chain instead of the homotyrosine found in **1.14**. Compounds **1.16** - **1.18** contain a serine residue in place of a threonine unit. Compounds **1.19** and **1.20** were about 50-fold and 25 fold weaker than **1.14** in the glucan assay, respectively. The only major difference between **1.19**, **1.20**, and **1.14** was the presence of a homotyrosine unit in **1.14** and the locations of the sulfonate group on the aryl ring.

FR190293 (**1.21**) is similar to pneumocandin A_0 (**1.23**), but has an additional sulfonate group. However, it is four times less potent than **1.23** in the glucan synthase assay.[25] Although the sulfonate group increases water solubility, it decreases the inhibition of 1,3-β-glucan synthase. FR 227673 (**1.22**), having a longer side chain, was more potent than **1.21** in the antifungal assays against *C. albicans* and *A. fumigatus*. However, it was less active than **1.21** in the glucan synthase assay.[37]

Fusaristatins A (**1.24**) and B (**1.25**) are two lipophilic cyclic depsipeptides reported from a *Fusarium* sp. No stereochemical information was presented for either depsipeptide. Compound **1.25** showed moderate antibacterial properties by inhibiting topoisomerases I (IC_{50} 73 µm) and II (IC_{50} 98 µm). The compounds also showed cytotoxicity towards LU 65 (lung cancer) cells with IC_{50} values of 23 and 7 µm for **1.24** and **1.25**, respectively.[38]

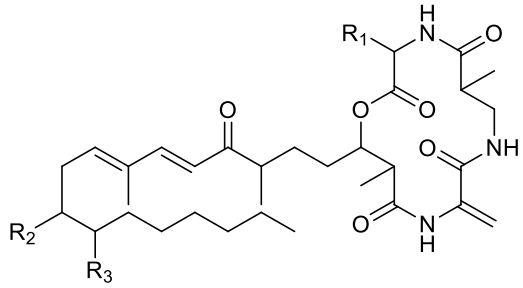

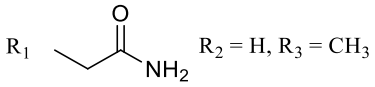

1.24

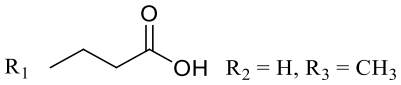

1.25

Fellutamides are linear tetrapeptides that have been isolated from three different fungi. Fellutamides A (**1.26**) and B (**1.27**) were isolated from *Penicillium fellutanum* and fellutamides C (**1.28**) and D (**1.29**) were reported from an unidentified fungal isolate. However, other analogues isolated from *Aspergillus versicolor* were also named fellutamides. One of them was given the same name as **1.28** (fellutamide C - **1.30**) while another was called fellutamide F (**1.31**).[39-42] For the purpose of this review, **1.30** will be designated as fellutamide C'.

Compounds **1.26** and **1.27** showed potent cytotoxic activity against murine leukemia P388 (IC_{50} 0.2 and 0.1 µg/mL, respectively), L1210 (IC_{50} 0.8 and 0.7 µg/mL, respectively), and human epidermoid carcinoma KB cells (IC_{50} 0.5 and 0.7 µg/mL, respectively).[39] Compound **1.28** was active against *C. albicans*, *C. tropicalis*, *C.*

glabrata, *C. krusei*, and *C. parapsilosis* with MIC values between 2 and 4 μg/mL. Compound **1.29** was also active against these fungi with MIC values ranging from 8 – 16 μg/mL. These metabolites also showed equal potency against fungal proteasome, with IC_{50} values of 0.2 μg/mL and MIC values of 1.25 μg/mL.

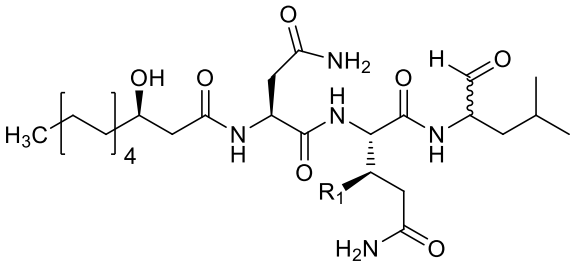

1.26 n = 4 R = OH

1.27 n = 4 R = H

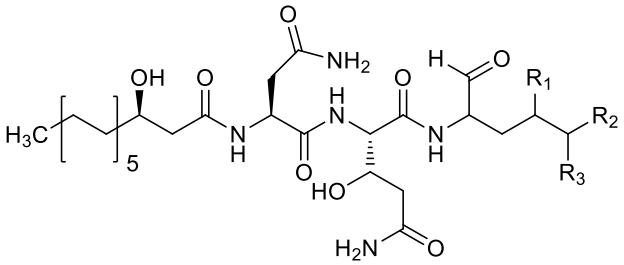

1.28 $R_1 = CH_3$ R_2, $R_3 = H$

1.29 $R_1 = H$ R_2, $R_3 = CH_3$

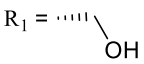

$R_2 = CH_3$ R_3, $R_4 = H$

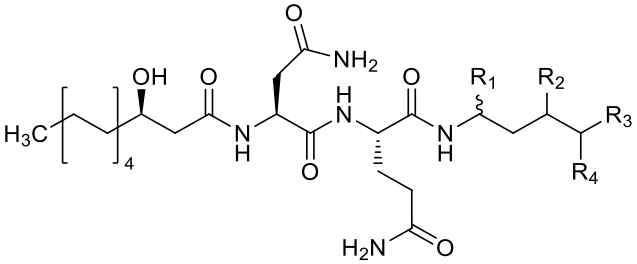

1.30

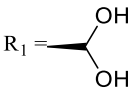

$R_2 = H$ R_3, $R_4 = CH_3$

1.31

Compounds **1.28** and **1.29** also showed proteasome activity against human tumor cell lines, potently inhibiting the growth of PC-3 prostate carcinoma cells with IC_{50} values of 440 ± 60 and 160 ± 20 nM, respectively.[42] Compounds **1.30** and **1.31** also showed significant potency against human CNS cancer cells and colon cancer cells (Table 1.3).[41]

Table 1.3. Cytotoxicity data for **1.30** and **1.31**[41]

Compound	A549	SK-OV-3	SK-MEL-2	XF 498	HCT15
1.30	18.42	13.28	2.83	2.16	1.74
1.31	1.81	1.20	0.67	0.14	0.13
Doxorubicin (control)	0.01	0.06	0.04	0.12	0.18

Note: Data expressed in ED_{50} values (μg/mL). The 50% inhibitory concentration (ED_{50}) was defined as the concentration that reduced the absorbance (520 nm) by 50% compared to the control level in the untreated wells. A549, human lung cancer cells;SK-OV-3, human ovarian cancer cells; SK-MEL-2, human skin cancer cells; XF498, human CNS cancer cells; HCT15, human colon cancer cells.

Depsipeptides

Depsipeptides contain one or more ester bonds in the backbone in addition to standard amide bonds, with the ester linkage typically formed by esterification between hydroxyl groups and amino acids. Fusaristatins A (**1.24**) and B (**1.25**) discussed in the previous section are depsipeptides that have lipophilic units connected to their core structures. IB01212 (**1.32**), a cytotoxic cyclodepsipeptide, was isolated from *Clonostachys* sp.[43] It is a cyclic dimer formed by two chains of L-*N*,*N*-Me_2Leu-L-Ser-L-*N*-MeLeu-L-*N*-MePhe bound by two ester moieties.

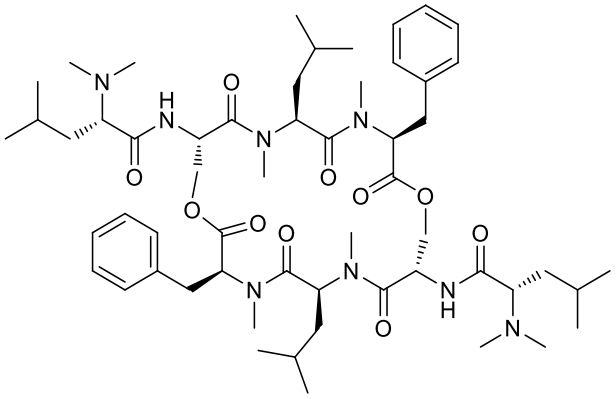

1.32

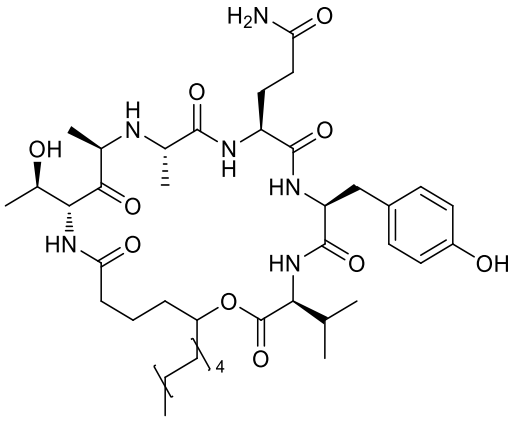

1.33

Compound **1.32** showed potent activity against prostate cancer, breast cancer, colon cancer, and cervix cancer cells with a GI_{50} (50% growth inhibition) values on the order of 10 nM.

Cordycommunin (**1.33**), was isolated from the insect pathogenic fungus *Ophiocordyceps communis*. It contains a 5-hydroxy tetradecanoic acid unit along with an unusual D-*allo*-Thr unit. It exhibited weak activity against *Mycobacterium tuberculosis* with an MIC of 15 µM and weak cytotoxicity against human oral cavity carcinoma (IC_{50} 45 µM).[44] Trichodepsipeptides A (**1.34**) and B (**1.35**) were isolated from *Trichothecium* sp. These two depsispeptides are close analogues, with trichodepsipeptide B containing an extra methylene unit. Neither compounds showed significant activity against human tumor cell lines.[45] Guangomides A (**1.36**) and B (**1.37**) and homodestcardin (**1.38**) were isolated from an unidentified sponge-derived fungus.[46] Both **1.36** and **1.37** contain D-Ala and D-*N*-MePhe, in addition to L-Ala, L-*N*-MeAla, and L-*N*-MePhe units. Compound **1.36** also contains *S*-hydroxyisocaproic acid (Hic) and *S*-dihydroxyisovaleric acid (Dhiv) units, while **1.37** contains *S*-Hic and *S*-hydroxyvaleric acid (S-Hiv). Compounds **1.36** and **1.37** showed weak antibacterial activity against *Staphylococcus epidermis* and

Enterococcus durans (MIC = 100 μg/mL). Homodestcardin (**1.38**) was the first destruxin analogue to be reported from a marine fungal isolate.[46] Biological activity was not reported for **1.38**. Destruxins comprise a well-known class of cyclic depsipeptides first reported in 1961 from *Metarrhizium anisopliae*. Dextruxins are composed of an α-hydroxy acid and five amino acid residues. Members of this group exhibit a wide spectrum of phytotoxic and insecticidal activities.[47,48]

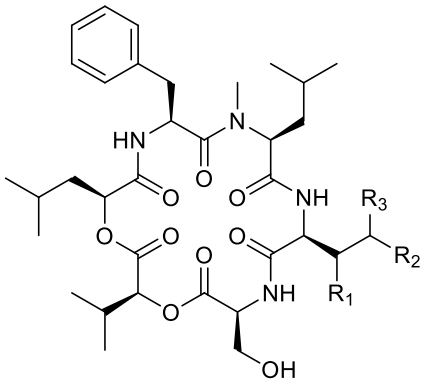

1.34 R_1 = H R_2, R_3 = CH_3

1.35 R_1 = CH_3 R_2, R_3 = H

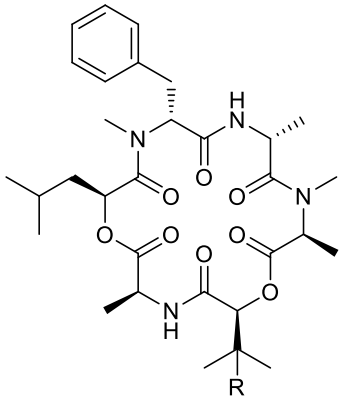

1.36 R = OH

1.37 R = H

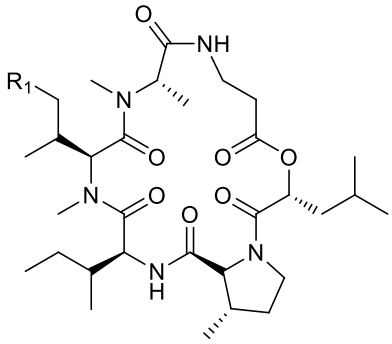

1.38 R_1 = CH_3

1.39 R_1 = H

Roseocardin (**1.39**), another destruxin analogue, was reported from *Trichothecium roseum*.[49] Roseocardin was evaluated for cardiotonic activity and was found to increase the contractile force of the right atrium (20 μM) and also prolonged the inter-contraction interval.

Peptaibols

Peptaibols comprise a class of linear peptides that are characterized by a high proportion of α,α-dialkylated amino acids such as α-aminoisobutyric acid (Aib) or isovaline (Iva), and typically contain an acyl substituted *N*-terminus and a *C*-terrminal amino alcohol unit. Peptaibols are known as membrane modifying, pore-forming peptides. They are organized in amphipathic helices which interact with phospholipid bilayers and increase their permeability. They are known to promote voltage-dependent ion channel formation in lipid bilayer membranes. They are mostly active against gram positive bacteria. Longer-sequence members of the class (18-20 residues) tend to be the most potent.[50] Detailed structural studies on alamethicin (**1.40**) have shown that the Aib residues help in forming the helical structures of peptaibols.[51] The amphipathic nature of **1.40** causes aggregation and formation of helical bundles with hydrophobic exteriors that contact the lipid layer. The hydrophilic interior of the channels contain multiple Gln and Glu residues that are important for conductance.[52] Such compounds often exhibit potent activity against gram positive bacteria, and sometimes show cytotoxic activity against eubacteria and cancer cell lines.[53,54] At present >450 peptaibols have been identified from soil fungi, of which ~50% have been isolated from *Trichoderma* spp.[51] This review will cover representative examples that have been reported since 2001.

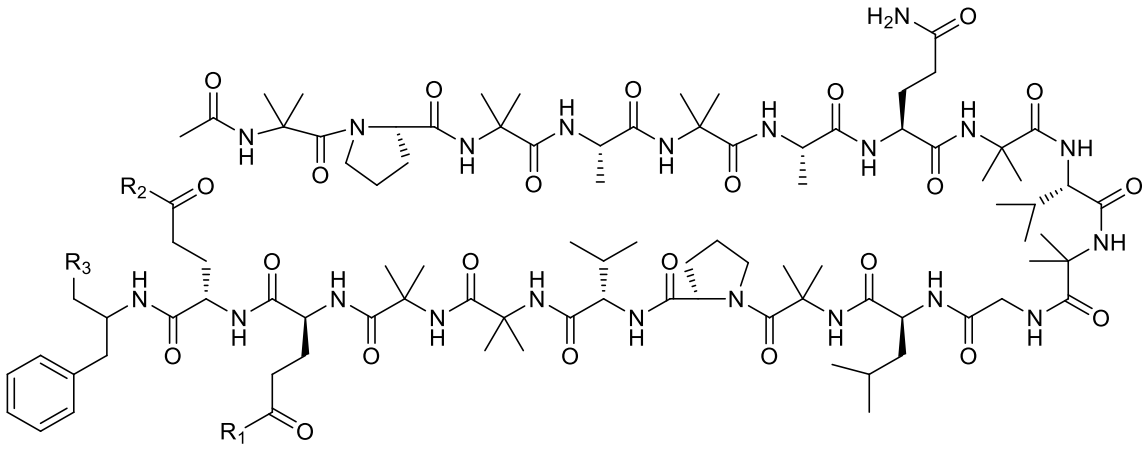

1.40 R_1 = OH R_2 = NH_2 R_3 = OH

1.41 R_1 = OH R_2 = NH_2 R_3 = $^{+}NH_2CH_2CH_2OH$ **1.42** R_1 = NH_2 R_2 = OH R_3 = $^{+}NH_2CH_2CH_2OH$

Septocylindrins A (**1.41**) and B (**1.42**) were isolated from *Septocylindrium* sp. They are similar to alamethicin, but have an extended C-terminus. Septocylindrin A (**1.41**) showed antibacterial and antifungal activity with MIC values between 16 – 32 µg/mL against *S. aureus*, *Enterococcus faecium, E.coli*, and *C. albicans*, **1.42** exhibited MIC values of 8 µg/mL against *S. aureus, E. faecium,* and *E.coli*.[53]

Atroviridins A - C (**1.43 - 1.45**), and neoatroviridins A - D (**1.46- 1.49**) were reported as metabolites of *Trichoderma atroviride*. Atroviridins have 20 amino acid residues and neoatriviridins have 18 amino acid residues. All of the amino acid configurations including the amino alcohol and phenylalaninol units were found to have the L- configuration, except for the Iva unit which was found to have D-configuration.

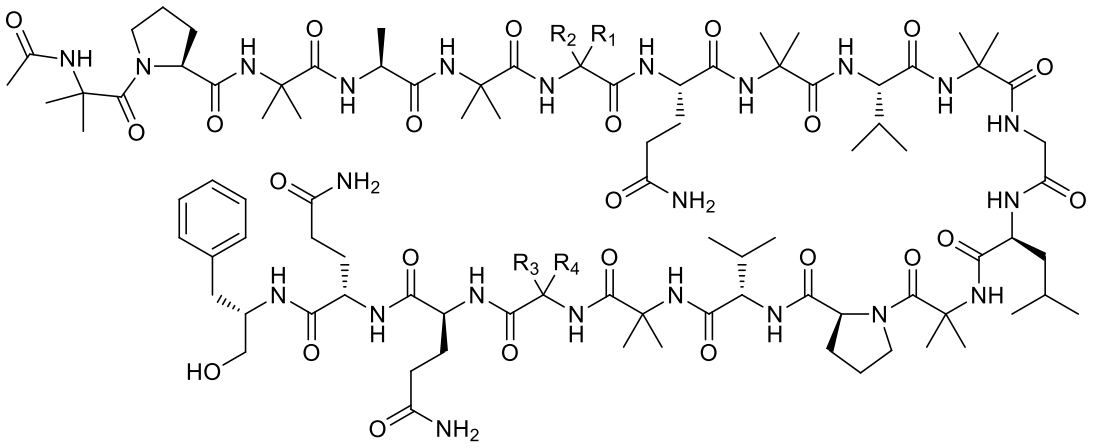

1.43 $R_1 = H$ $R_2 = R_3 = R_4 = CH_3$

1.44 $R_1 = H$ $R_2 = R_3 = CH_3$ $R_4 = CH_2CH_3$ **1.45** $R_1 = R_2 = R_3 = CH_3$ $R_4 = CH_2CH_3$

Atroviridins and neoatroviridins exhibited strong antifungal effects against *Curavularia inaqualis*, *Colletotrichum dematium*, and *Fusarium oxysporum* and antibacterial activity against *B. subtilis* and *S. aureus* in disc diffusion assays.[50] They also showed significant cytotoxic activity against prostate, melanoma, and leukemia cell lines with IC_{50} values in the range of 2 – 4 µg/mL.[50,55]

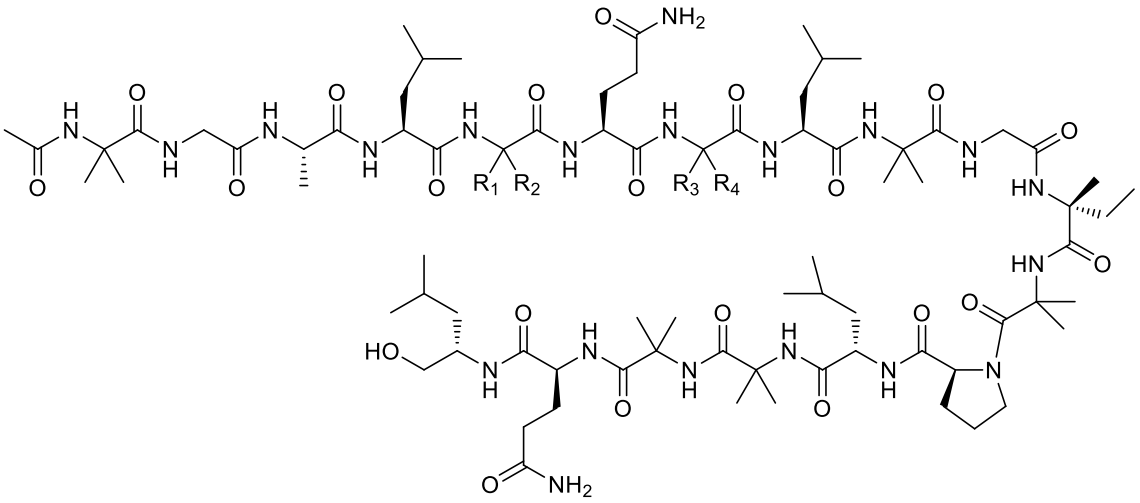

1.46 $R_1 = R_2 = R_3 = R_4 = CH_3$

1.47 $R_1 = CH_2CH_3\ R_2 = R_3 = R_4 = CH_3$

1.48 $R_1 = R_2 = R_3 = CH_3\ R_4 = CH_2CH_3$

1.49 $R_1 = R_3 = CH_2CH_3\ R_2 = R_4 = CH_3$

Cephaibols (**1.50** – **1.55**), were isolated from *Acremonium tubakii*.[56] All of the amino acid residues in **1.50** – **1.55** were found to have the L-configuration except for the Iva and Phe-ol units, which could not be determined. Compounds **1.50** and **1.52** showed antibacterial properties, with MIC values between 2.5 – 10 µg/mL against *S. aureus* and *S. pyogenes*. Compound **1.50** also caused 100% lethality against larvae of the parasite *Ascaria galli* at 25 µg/mL, and 60% lethality at 12.5 µg/mL. It was also 100% lethal at 250 µg/mL against the parasite *Cimex lectularius* and caused 80% mortality at 62.5 µg/mL.

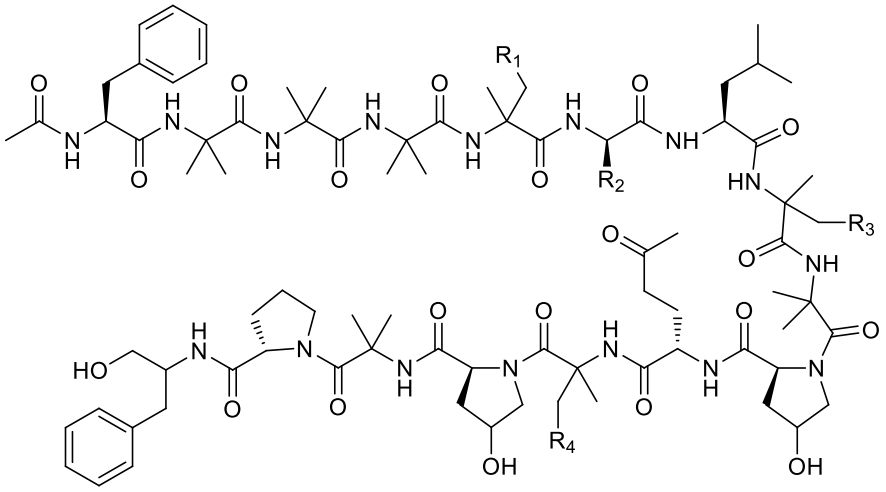

1.50 $R_1 = R_2 = H\ R_3 = R_4 = CH_3$

1.51 $R_1 = H\ R_2 = R_3 = R_4 = CH_3$

1.52 $R_2 = H\ R_1 = R_3 = R_4 = CH_3$

1.53 $R_1 = R_2 = R_4 = H\ R_3 = CH_3$

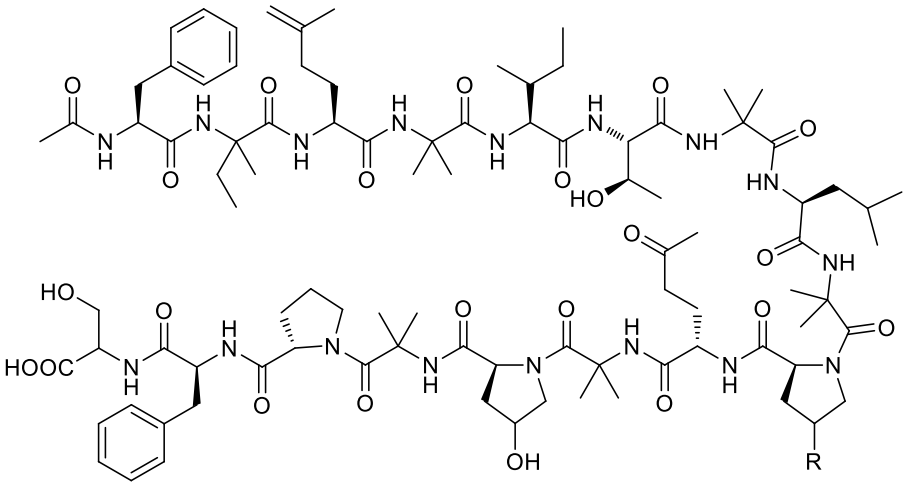

1.54 R = OH

1.55 R = H

Cicadapeptins I (**1.56)** and II (**1.57**) were isolated from *Cordyceps heteropoda*.[57] All the amino acids were found to have the L-configuration. The α-carbon of the unusual C-terminal diamine was postulated to have the L-configuration based on its presumed L-Leu-derived biosynthesis. Compounds **1.56** and **1.57** produced clear inhibition zones in disk assays against *Bacillus cereus* (13 and 12 mm respectively), *B. subtilis* (13 and 11 mm respectively), and *E. coli* (16 mm each) at 100 µg/disk.

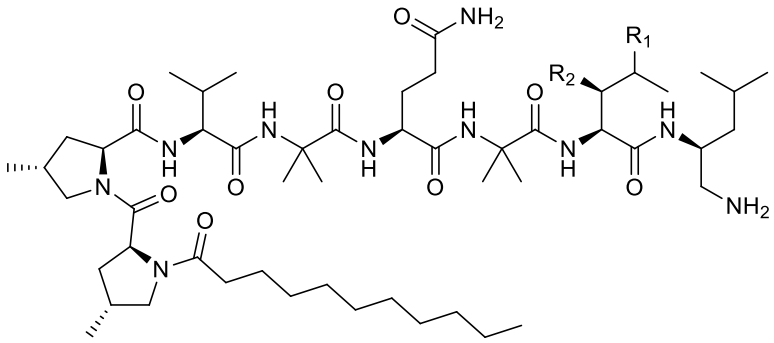

1.56 $R_1 = CH_3$ $R_2 = H$

1.57 $R_1 = H$ $R_2 = CH_3$

Glycopeptides

Glycopeptides are peptides with carbohydrate moieties covalently attached to the side chain of amino acid residues. Glycopeptides are commonly isolated from bacteria, but are relatively rare as secondary fungal metabolites. There has been one report of isolation of glycopeptide from fungi since 2000.

Dictyonamide B (**1.58**) was obtained from an unidentified marine fungal isolate.[58] All the amino acid residues were found to have the L-configuration and the fructose unit

was found to have the D-configuration. It was reportedly tested only against cyclin-dependent kinase 4, and showed no acitivity.

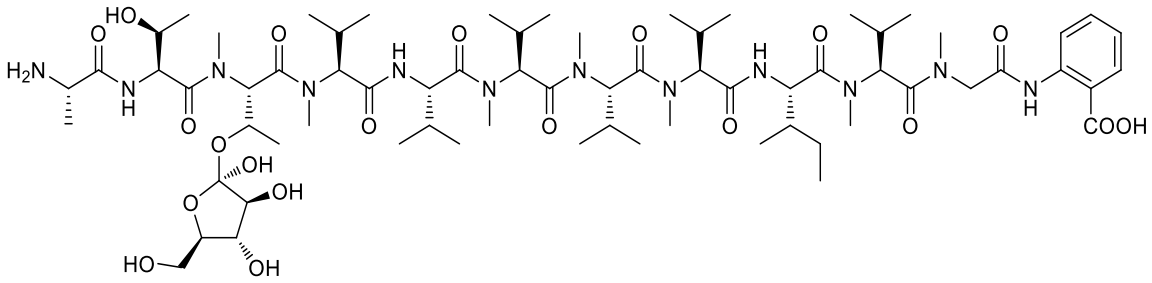

1.58

Fungi have proven to be a source of many natural products with antibiotic, anticancer, and immunosuppressive properties.[59] The metabolites reviewed in this chapter are representative of the structural diversity and biological activities associated with fungal non-ribosomally synthesized peptides. Various echinocandins and alamethicin-type compounds exhibit particularly strong antifungal and antibacterial properties and, as noted earlier, some echinocandins have already proven to be clinically important.

The following five chapters will cover in detail the chemical investigation of fungicolous and endophytic fungal cultures that led to several known and some new secondary metabolites. In particular, chapters three and four will describe the isolation and characterization several of new non-ribosomally synthesized decapeptides and glycodepsipeptides.

CHAPTER 2

SCREENING OF FUNGAL ISOLATES

Fungi have long been an excellent source of biologically active secondary metabolites. The fungal kingdom contains approximately 3.5 million species, of which only a small number (<5%) have been studied.[2,3] Fungi found in different competitive environments could produce secondary metabolites for either offensive and/or defensive roles. For example, one species may produce secondary metabolites to inhibit the growth of a competitor. Chemical studies of such fungal interactions could lead to the discovery of novel secondary metabolites with antifungal properties, and could therefore have practical implications. However, such interactions have not been widely studied, especially from a chemical standpoint.[4]

Our research has focused on studies of selected groups of fungi. For example, mycoparasitic fungi colonize and parasitize other fungi and sometimes cause damage to the host. Such damage could be due at least in part to production of antifungal or secondary metabolites by the mycoparasite. However, such interactions have rarely been studied in detail. The term "fungicolous" is often employed to describe species that colonize other fungi without necessarily causing any harm to the host, or for which no such harm (or ecological relationship) has been clearly demonstrated. Studies of such fungi in our research group have led to isolation of numerous new biologically active secondary metabolites.[60-63]

Another group of fungi that have been targeted in our research are the endophytic fungi. Endophytic fungi colonize the inner tissues of plants in a symbiotic or a non-symbiotic manner. They may or may not be necessary for growth, defense, and/or survival of the plant host. They may protect plants from attack by other pathogens by producing secondary metabolites that inhibit the growth of other pathogenic organisms.[59] Many secondary metabolites isolated from endophytic fungi reportedly show biological

activity, including anticancer, anti-diabetic, insecticidal, antimicrobial, and immunosuppressive properties.[59]

The process of discovering of new biologically active secondary natural products from such sources involves several steps, beginning with selection of source material, plating of portions of the material to produce fungal colonies, and isolation of individual colonies. After preliminary sorting and selection to minimize duplication and focus on distinctive or unusual isolates, the target fungi are subjected to solid substrate fermentation. Extraction of the fermented substrate and biological testing of the extracts, affords a set of bioactive extracts for chemical investigation. Separation of extracts to isolate secondary metabolites, structure elucidation of these metabolites, and testing of the purified compounds in different biological assays then follows. All fungal selection and collection for the work described in this thesis was done by Dr. Donald T. Wicklow and his colleagues at the United Stated Department of Agriculture (USDA) National Center for Agricultural and Utilization Research (NCAUR) in Peoria, IL. Fungicolous fungi are typically collected from surfaces of fruiting bodies of polypores and other long-lived fungal bodies that are commonly encountered in nature. Such bodies and which tend to be rich in nutrients and are therefore particularly susceptible to attack and colonization by other fungi. Fermentation extracts of many fungicolous fungal isolates show antifungal and antiinsectan activity and a subset of eight of those screened were chosen for work described here (Table 2.1). Endophytic fungi are typically obtained from plant material following surface sterilization and dissection to access the infected tissues. Ten endophytic fungal extracts that exhibited antifungal and antiinsectan activity were chosen for further analysis as described here.

Substrate samples were plated onto potato dextrose agar (PDA) petri plates and incubated for 14 days at 25 ºC. Fungal colonies were then isolated and cultured. After preliminary taxonomic evaluation and selection fungal spore suspensions were used to carry out solid-substrate fermentation on rice. Fermentation cultures were extracted with

EtOAc and these extracts were then tested for antifungal activity against *Aspergillus flavus* and *Fusarium verticillioides*. *A. flavus* and *F. verticillioides* cause ear rot in corn, are opportunistic human pathogens, and produce problematic mycotoxins such as aflatoxins and fumonisins. Both of these types of mycotoxins cause significant economic losses to producers of corn-based foods, poultry, and other livestock. *A. flavus* also causes aspergillosis, which can affect the respiratory system of immune-compromised individuals. Thus, activity against these fungi could have value in agriculture or medicine.

The extracts were also tested for activity against *Spodoptera frugiperda* (fall armyworm), an economically important crop pest that causes damage to corn leaves and ears. Several fungicolous and endophytic fungal extracts that showed antifungal and antiinsectan activity (Table 2.1) were selected for chemical investigations described in this thesis. The EtOAc extracts were subjected to partitioning between CH_3CN and hexanes to separate background lipids from the more polar components of the extract, which are nearly always those responsible for observed activity. However, the hexanes extract are retained for possible analysis in cases where activity is not recovered. The CH_3CN fractions were then analyzed by NMR and fractions that displayed NMR resonances suggestive in some way of the possible presence of potential new or unusual compound classes were further investigated.

CH_3CN fractions were then subjected to various chromatographic techniques including column chromatography using silica gel or Sephadex LH-20, C_{18} high pressure liquid chromatography (HPLC), and/or preparative thin layer chromatography (TLC). Compounds isolated from or detected in the resulting fractions were then characterized by NMR and MS. Comparison of NMR and MS data with literature data and databases generally enabled identification of known compounds.

Table 2.1. Antifungal and antiinsectan bioassay results for the EtOAc extracts of selected fungicolous/Mycoparasitic (MYC) and endophytic (ENDO) fungal cultures.

Culture #	Organism	*Aspergillus flavus*[a]		*Fusarium verticillioides*[b]		*Spodoptera frugiperda*
		2-day	4-da	2-da	4-da	%RGR
MYC-2023	Unidentified	mz=5	mz/rg=5	mz=6	mz=2+rg2	(-)
MYC-2164	*Penicillium* sp.	cz=19	cz=17	cz=18	cz12+mz6	50%
MYC-2141	Unidentified	cz=10	cz=5	mz=7	mz=2+rg=4	(-)
MYC-1876	*Fusarium* sp.	mz/rg=4	(-)	mz=4	mz/rg=3	(-)
MYC-2146	*Penicillium* sp.	cz=12	cz=10	cz=7	cz=6	>75
MYC-2113	Unidentified	mz=12	mz=12	mz=7	mz/rg=3	50
MYC-1881	*Sesquicillium microspora*	(-)	(-)	rg/mz=3	rg=20	(-)
MYC-2025	*Phaeoacremonium* sp	(-)	(-)	mz/rg=5	mz=2+rg=10	(-)
ENDO-3094	*Alternaria alternata*	mz=5	mz=4	mz=7	mz=3	M=>75
ENDO-3149	Unidentified	cz10+mz5	mz=15	mz=5	(-)	75
ENDO-3087	*Penicillium oxalicum*	(-)	(-)	(-)	(-)	M=>90
ENDO-3525	*Setophoma terrestris*	cz=11	cz=10	cz5+mz7	cz=3	(-)
ENDO-3541	Unidentified	cz=6	cz=3	cz5+mz10	cz=3	(-)
ENDO-3531	Unidentified	cz/mz=3	rg=3	mz=8	(-)	(-)
ENDO-3288	Unidentified	mz=2	(-)	mz=3	rg=3	(-)
ENDO-3289	Unidentified	mz=5	(-)	cz/mz=7	mz=7	(-)
ENDO-3323	Unidentified	cz/mz=3	rg=3	mz=4	(-)	(-)
ENDO-3417	*Phoma* sp.	(-)	(-)	mz=3	(-)	(-)

Note. [a]These assays were performed at a concentration of 500 μg of extract per disk (disk diameter = 12.5 mm), and the diameters of the resulting inhibition zones are given in mm. cz = clear zone (no growth throughout zone, agar surface to dish bottom); mz = mottled zone (mosaic of clear zone areas and appearance of patch colony growth, a result of retarded development of individual tiny colonies spread rapidly to fully cover the agar surface); rg = reduced growth (fungus fully covers the agar surface, but colony development suppressed when contrasted with colony development outside the zone of inhibition); (-) = not active; NT = not tested. [b]These assays were performed at a 2000 ppm dietary level; % RGR = % reduction in growth rate relative to controls (M = % mortality).

Several new compounds were encountered in this research, and details of their structures and characterization are presented in the following chapters. Details of work leading to previously known compounds, along with four new compounds that were found to be

very close analogues of previously known metabolites, are summarized in this chapter, but are presented in much less detail because identification of these compounds was far more straightforward.

The EtOAc extract of the unidentified fungicolous isolate MYC-2023 exhibited antifungal activity against *A. flavus* and *F. verticillioides*. Chemical investigation of this extract led to isolation of the two known compounds stemphol **(2.1)**[64,65] and lamellicolic anhydride (**2.2**),[66] along with two new analogues of **2.1** (**2.3** and **2.4).** Compound **2.1** had previously been reported from *Stemphylium majusculum* and *Pleospora herbarum* and was found to show antifungal activity against *Pleospora herbarum*.[9,10] It has also been reported to inhibit sea urchin embryogenesis. Compound **2.2** has been reported from *Verticillium lamellicola*.[66]

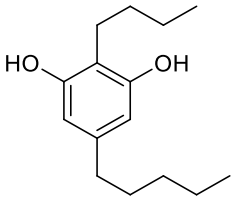

2.1

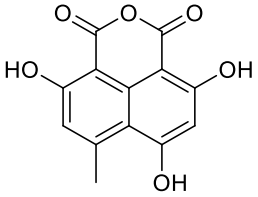

2.2

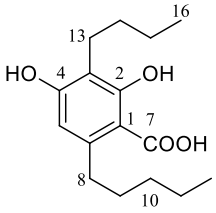

2.3

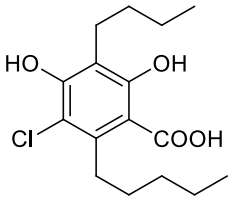

2.4

The molecular formula of **2.3** was determined to be $C_{16}H_{24}O_4$ based on HRESITOFMS data ($[M-H]^-$ at *m/z* 279.1598, Δ 0.2). It was identified as an alkylated

resorcinol similar to **2.1** based on NMR (Table 2.2) and MS data. The lengths of the alkyl groups were determined as shown based on facile loss of C_3H_7 and C_4H_8 (via benzylic cleavage) to give major ions at *m/z* 193 and 180 in the EI mass spectrum. The positions of these groups were determined based on HMBC correlations (Table 2.2).

Table 2.2. NMR data for Compound **2.3** ($CDCl_3$) and **2.4** (CD_3OD)

Pos	δ_H[a] (mult; *J* in Hz)	δ_C[c]	HMBC (H→C#)	δ_H[b] (mult; *J* in Hz)
#	**2.3**			**2.4**
1		146.9		
2		164.1		
3		113.7		
4		158.8		
5	6.22 (s)	110.5	1, 3, 4, 6, 8	
6		103.3		
7		175.4		
8	2.86 (t, 8.0)	36.3	1, 5, 6, 9, 10	3.20* (t, 7.2)
9	1.2-1.6 (ov)	31.4	8, 10, 11, 12	1.2-1.6 (ov)
10	1.2-1.6 (ov)	32.0		1.2-1.6 (ov)
11	1.2-1.6 (ov)	22.6		1.2-1.6 (ov)
12	0.88 (t, 6,9)	13.8		0.94 (t, 6.9)
13	2.60 (t, 7.6)	22.5	2, 3, 4, 14, 15	2.65* (t, 7.4)
14	1.2-1.6 (ov)	30.9		1.2-1.6 (ov)
15	1.2-1.6 (ov)	22.8		1.2-1.6 (ov)
16	0.88 (t, 6.9)	13.8		0.93* (t, 7.2)

Note. [a] ^1H NMR measured at 600 MHz, [b] ^{13}C NMR measured at 100 MHz, [c] ^{13}C measured at 100 MHz, ov = overlapping signals * These assignments are interchangeable

The molecular formula of **2.4** was determined to be $C_{16}H_{23}O_4Cl$ based on HRESITOFMS data ($[M-H]^-$ at *m/z* 313.1204, Δ 0.3), along with an ion at *m/z* 315.1180 corresponding to the ^{37}Cl- containing species (33% relative intensity). The ^1H NMR data for this minor metabolite were similar to those of **2.3**, but with the absence of the aromatic proton singlet resonance. Structure **2.4** was proposed for this metabolite, having a chlorine atom in place of the aromatic hydrogen found in **2.3**, but this could not be fully confirmed by 2D NMR because of severe sample limitations. Compounds **2.2**, **2.3**, and **2.4** displayed significant activity against *Bacillus subtilis*, affording inhibition zone diameters in standard disk assays of 10 (100 µg/disk), 20 (200 µg/disk) and 20 mm (100 µg/disk), respectively. Compounds **2.3** and **2.4** also displayed antifungal activity against *F. verticillioides* (mz = 20 mm at 100 µg/disk for **2.3** and 200 µg/disk for **2.4**, respectively in disk assays). Thus, the presence of compounds **2.3** and **2.4** account for at least some of the activity of the initial extract against *F. verticillioides*. Compounds **2.1** and **2.2** did not exhibit any activity in antifungal assays.

Chemical investigation of the crude extract of another unidentified Hawaiian fungicolous isolate (MYC-2141) showed antifungal activity against *A. flavus* and *F. verticillioides* and afforded three known compounds (palmacordacins A - C **2.5** - **2.7**) and one new isocoumarin analogue (**2.8**).

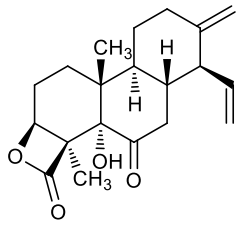

2.5

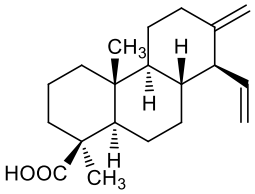

2.6

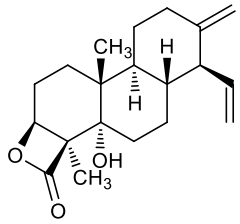

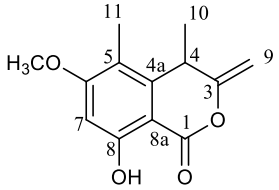

2.7 **2.8**

Diterpenoids **2.5** - **2.7** were originally isolated from fungicolous isolate of *Coniothyrium palmarum* (MYC-1551) by another member of our research group.[61] Comparison of NMR and MS data for these samples with those obtained in the earlier work enabled their identification. In the prior studies, palmacordacins A – C exhibited antibacterial activity against *S. aureus* and **2.7** displayed antifungal activity agains *C. albicans*, *A. flavus*, and *F. verticillioides*.[61]

Table 2.3. ^{1}H NMR data for **2.8**

Position	δ_H (mult; *J* in Hz)	Position	δ_H (mult; *J* in Hz)
4	3.79 (q, 7.2)	10	1.36 (d, 7.2)
7	6.36 (s)	11	2.06 (s)
9a	4.54 (d, 1.8)	6-OCH_3	3.84 (s)
9b	4.76 (dd, 0.6, 1.8)	8-OH	11.0 (s)

Note. $CDCl_3$, 400 MHz

Unrelated compound **2.8** was identified by analysis of ^{1}H NMR data (Table 2.3) as a close analogue of known compound **2.9**, lacking only one of the methoxy signals. Compound **2.9** had been previously isolated from a fungicolous *Verticillium* sp. by

another member of our research group, and displayed antifungal activity against *A. flavus* and *F. verticillioides*.[61]

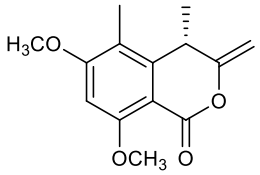

2.9

The structure of **2.8** was assigned based on comparison of ^{1}H NMR data with those of **2.9**. The aromatic proton was recognized and located based on its upfield shift (δ 6.36 in **2.8** *vs* δ 6.40 in **2.9**), making it *ortho* to both the hydroxy and the methoxy groups. The relative position of the methoxy group was determined based on the downfield shift of the resonance for phenolic proton (δ 11.0), which is charecterisitc of an intramolecularly hydrogen-bonded phenolic OH. Efforts were not undertaken to elucidate further structural or spectroscopic details of **2.8** because of its close similarity to the previously known compound.

The EtOAc extract from cultures of a fungicolous isolate of *Fusarium* sp. (MYC-1876) showed antifungal activity against *A. flavus* and *F. verticillioides*. Chemical investigation of this extract led to the isolation of apicidin B (**2.10**), a cyclic tetrapeptide that had been previously reported from an endophytic isolate of *Fusarium pallidoroseum*.[67,68] Apicidins comprise are a novel class of cyclic tetrapeptides that exhibit potent antiprotozoal activity against the apicomplexan family of protozoa, including *Plasmodium* spp. (malarial parasites), *Toxoplasma gondii, Crytosporidium* spp., and *Eimeria* sp. They reversibly inhibit histone deacetylase (HDAC) activity. HDAC, in conjunction with histone acetylase (HAT), plays a key role in gene transcription. Blockade of deacetylation causes hyperacetylation, which leads to cell death. Compound **2.10** reportedly displayed MIC values of 12.8, 411, and 189 nM

against *Besnoitia jellisoni*, *E. tenella*, and *P. falciparum*, respectively. Compound **2.10** also displayed significant antifungal activity in our assays against .*F. verticillioides* (mz = 33 mm diameter at 200 µg/disk concentration), and is therefore likely responsible for the activity observed for the original extract.

The EtOAc extract of cultures of a third unidentified fungicolous fungal isolate (MYC-2113) was found to be active against *A. flavus* and *F. verticillioides*. It also showed 50% RGR against *S. frugiperda*. Chemical investigation of this extract led to the isolation of hypothemycin (**2.11**). This compound was originally reported from *Hypomyces trichothecoides* and displayed moderate antibiotic activity against the protozoan *Tetrahymena furgasoni* and the plant pathogenic fungi *Ustilago maydis* and *Botrytis allii*. It also displayed cytotoxicity against several tumor cell lines, with IC_{50} values ranging from 0.25 to 1.5 µg/mL.[69] In our antifungal disk assays, it displayed significant activity against *A. flavus* (mz = 30 mm) and *F. verticillioides* (mz = 22 mm) at 200 µg/disk concentration

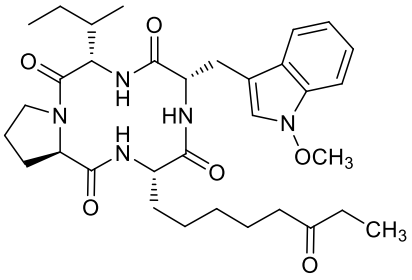

2.10

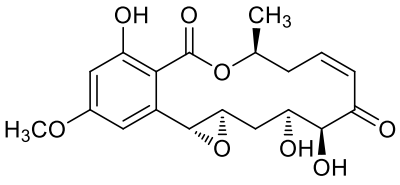

2.11

The EtOAc extract of a fermentation culture of an unidentified endophytic fungus (ENDO-3323) isolated from the seed of a praire dropseed, displayed antifungal activity against *A. flavus* and *F. verticillioides*. Chemical investigation of this extract led to the isolation of the two known perylenequinones stemphylotoxins II (= altertoxin II) (**2.12**)

and III (**2.13**), and along with alternariol monomethyl ether (**2.14**). These compounds were identified based on comparison of NMR and MS data with literature values.[65,70,71]

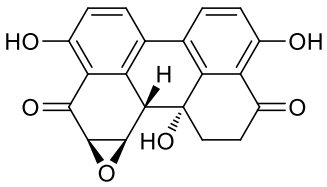

2.12

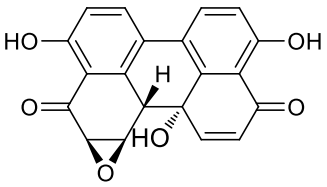

2.13

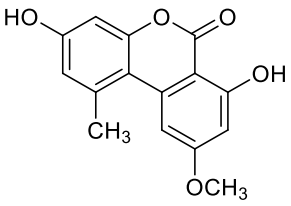

2.14

Compounds **2.12** and **2.13** were originally reported from *Stemphylium botryosum var. lactucum* and *Alternaria alternata*, which are similar morphologically. Species of *Alternaria* are plant pathogens and common decay organisms, while *S. botryosum* causes leaf spot in lettuce. The phytotoxicity of these fungi has been associated with the production of these metabolites. The compounds also exhibited potent mutagenic activities in the Ames *Salmonella typhimurium* assay, and show antibacterial activity in vitro against *B. subtilis*, *B. cereus*, and *E. coli*. These activities have been shown to be associated with the presence of the epoxy groups.[71-73] Alternaria toxin **2.14** was isolated from *Alternaria alternata*, and exhibited activity against *S. typhimurium* and *E. coli*. It also showed toxicity against lymphoma 5178Y and Hela cells in tissue culture.[70]

The EtOAc extract of an endophytic fungal isolate of *Alternaria alternata* (ENDO-3094), isolated from a seed of sorghum, showed antifungal activity against *A. flavus* and *F. verticillioides*, as well as anti-insectan activity vs. *S. frugiperda*, causing greater than 75% mortality at the standard extract concentration used. Chemical investigation of this extract led to the isolation of three known polyketide-derived metabolites; heptacyclosordariolone (**2.15**), 3-deooxyisoochracinic acid (**2.16**), and **2.17**. These were identified based on comparison of NMR and MS data with literature data. Compound **2.15** was previously described as a metabolite of *Sordaria macrospora*.[74] Its

stereochemical configuration was not reported. Compounds **2.16** and **2.17** had been previously isolated by another member of our research group from another *Alternaria* sp.[75] Compound **2.16** displayed antibacterial activity against *B. subtilis*. Compound **2.17** had also been reported from *Sordaria macrospora* as an epimeric mixture,[75,76] but no stereochemical information for the individual constituents was provided. Since it did not exhibit any antifungal and antibacterial activity in our assays, efforts to determine the stereochemical configuration were not undertaken.

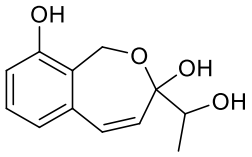

2.15

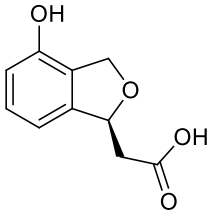

2.16

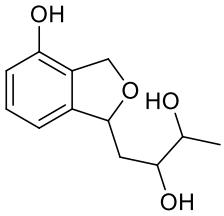

2.17

The EtOAc extract from fermentation cultures of another unidentified endophytic fungus (ENDO-3288) collected from the seed of a switch grass, showed moderate antifungal activity. Chemical investigation of this extract led to the isolation of sorokinianin (**2.18**), a phytotoxin that had previously been isolated from the phytopathogenic fungus *Bipolaris sorokiniana*.[77] Its relative configuration was originally proposed based on ^{1}H NMR and NOE data, in conjunction with an energy-minimized model. The absolute configuration was not assigned. It reportedly inhibited the growth of barley seedlings, and displayed mild antibacterial activity against *B. subtilis*. It also displayed antifungal activity in our assays against *A. flavus* (mz = 26 mm) at 200 µg/disk concentration.

The EtOAc fermentation culture of an unidentified fungal isolate (ENDO-3289), obtained from a seed of blue grama grass, displayed antifungal activity. Chemical

investigation of the EtOAc extract led to the isolation and identification of equisetin (**2.19**) based on literature NMR and MS data. Equisetin (**2.19)** was originally reported from *Fusarium equiseti* and *F. pallidoroseum*, but has been encountered with some frequency from other fungal isolates in our own research.[78] It displays strong antibiotic and cytotoxic activity, and inhibits mitochondrial ATPases and HIV-1 integrase.[79] Compound **2.19** displayed antibacterial activity in our assays, at 200 µg/disk against *B. subtilis* and *S. aureus* showing inhibitory zone sizes of 18 and 10 mm, respectively. It also showed significant antifungal activity at 200 µg/disk against *A. flavus* (mz = 19 mm) and *F. verticillioides* (mz = 17 mm).

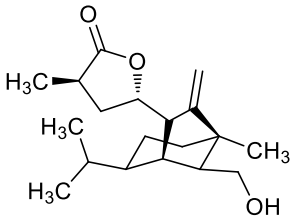

2.18

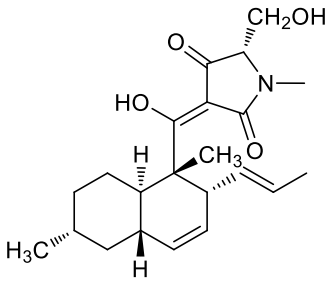

2.19

The EtOAc extract of another unidentified endophytic culture (ENDO-3531), collected from a corn stem, showed modest antifungal activity. Chemical investigation of this extract led to an encounter with the known benzofuran derivative **2.20** and a new analogue (**2.21)**. Compound **2.20** was obtained as a 1:0.13 mixture with **2.21**. ESIMS data, including ions at *m/z* 211 $[M+H]^+$, 233 $[M+Na]^+$ and 197 $[M+H]^+$ for the mixture initially suggested that the molecular formula of **2.20** was $C_{10}H_{10}O_5$. However, detailed analysis of NMR and MS data and comparison with literature values[80] identified **2.20** as a known compound with the molecular formula $C_{10}H_{12}O_4$. It had previously been reported

from *Epicoccum purpurascens*.[80] On the other hand, the molecular formula of **2.21** was determined to in fact be $C_{10}H_{10}O_5$ based on ESIMS data (*m/z* 211 $[M+H]^+$, 233 $[M+Na]^+$). In retrospect, it appears that the greater ionizability of the minor component (**2.21**) led to initial misidentification of the molecular ion of **2.20** in the mixture of **2.20** and **2.21**. ^1H NMR data for **2.21** indicated its similarity to another known compound (**2.22**),[80] with the presence of an additional methoxy group. The structure was assigned based on analysis of ^1H NMR and ESIMS data, and comparison with literature values.[80] Because of its close similarity to the known compounds, efforts to assign the regiochemistry were not undertaken. Compound **2.21** did exhibit any antifungal activity.

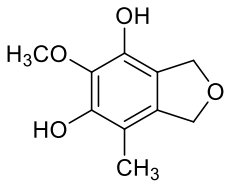

2.20

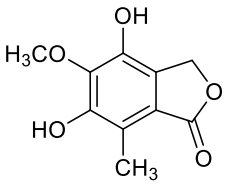

2.21

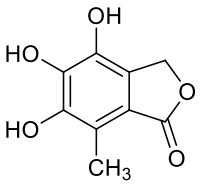

2.22

Chemical investigation of an EtOAc extract of a fermentation of an endophytic isolate of the plant pathogen *Macrophomina phaseolina* NRRL 13663 led to the isolation of the known compounds involutin (**2.23**) and striatisporolide A (**2.24**) based on comparison of NMR data with literature values.[81] Compound **2.23** was originally reported from an isolate of *Paxillus involutus*, while **2.24** was originally isolated from *Penicillium striatisporum*. Neither absolute configuration nor biological activity was reported for either compound.[81,82] They did not exhibit any antifungal activity in our disk assays.

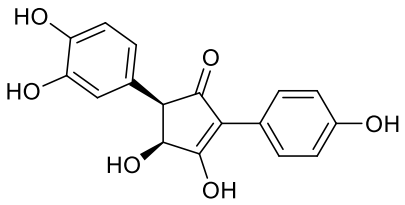

2.23

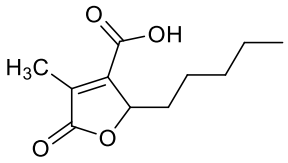

2.24

The secondary metabolites described in this chapter belong to a variety of different structural and biosynthetic classes, and include terpenes, polyketides, and peptides. They displayed a wide range of activities including antifungal and antibacterial effects. However because they were previously known or very closely related to previously known compounds, further studies of them beyond those summarized here were not pursued. The next four chapters will discuss in detail the chemical investigation of additional fungicolous and endophytic fungal isolates that led to the isolation and characterization of new secondary metabolites. Additional known compounds that were isolated together with new compounds from a given isolate will also be described in these chapters.

CHAPTER 3

CHEMICAL INVESTIGATION OF A FUNGICOLOUS ISOLATE OF *SESQUICILLIUM MICROSPORA*

Our studies of mycoparasitic and fungicolous fungi have resulted in discovery of many bioactive natural products that display antifungal, antibacterial, and/or antiinsectan activity.[60,62,83] A fungal culture (MYC-1881) was isolated from a basidioma of *Phellinus gilvus* found growing on a dead branch in a lowland wet forest, Lava Tree State Park, Puna District, Hawaii. The culture was identified as *Sesquicillium microspora* based on a nucleotide-to-nucleotide blast search of the GenBank database, and was deposited in the USDA NCAUR collection. *Sesquicillium* spp. have been reported to produce several different types of secondary metabolites including candelalides A (**3.1**) and B (**3.2**),[84] sescandelins,[85] and leptopsin C (**3.3**).[86] Candelalides have shown to be potential immunosuppresants and leptosins have exhibited antitumor properties.

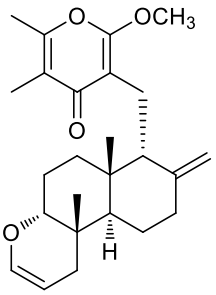

3.1

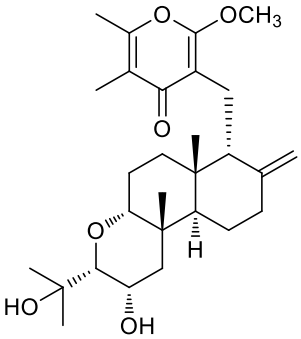

3.2

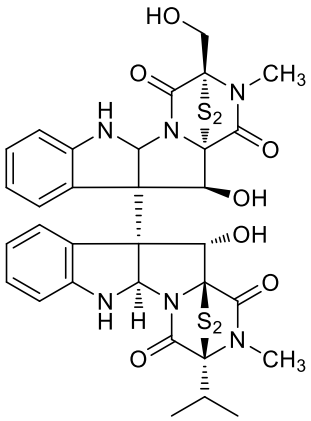

3.3

The ethyl acetate extract of a solid-substrate fermentation culture of this isolate of *S. microspora* showed antifungal activity against *Fusarium verticillioides*. Chemical investigation of this extract led to the isolation of three new cyclic decapeptides that we named sesquilarins A – C (**3.4 - 3.6**). The separation process resulting in the isolation of these metabolites is summarized in Scheme 3.1

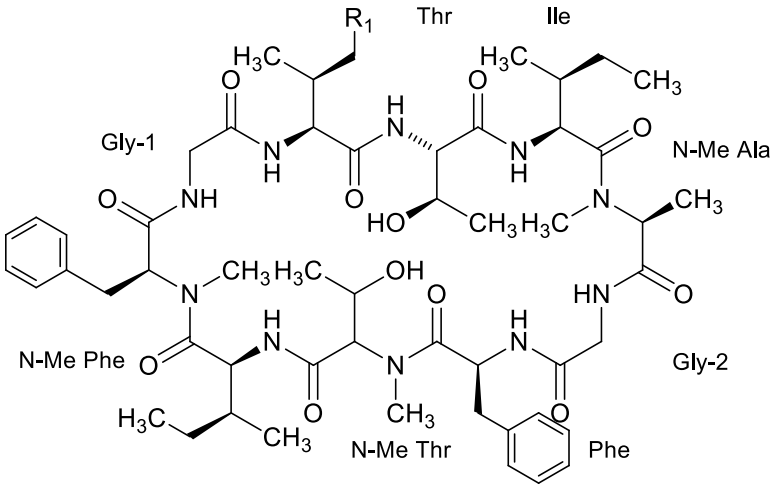

3.4 $R_1 = R_2 = H$

3.5 $R_1 = CH_3$ $R_2 = H$

3.6 $R_1 = R_2 = CH_3$

Scheme 3.1. Isolation of metabolites from *Sesquicillium microspora*

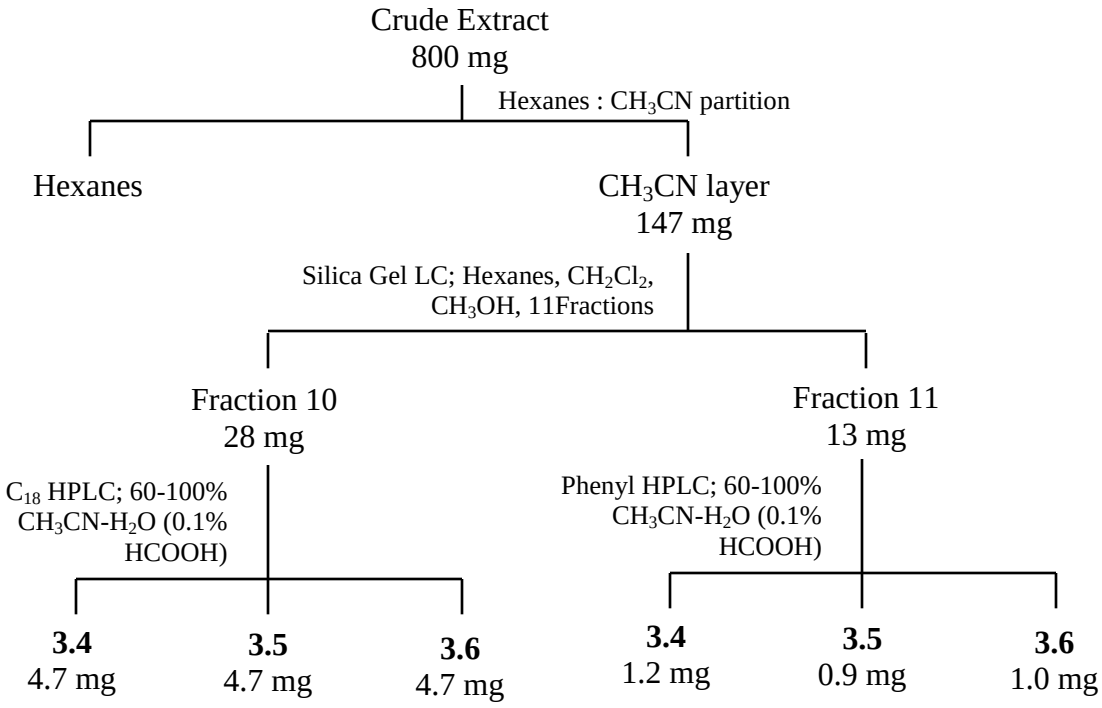

Structure elucidation of sesquilarins A – C (**3.4** - **3.6**)

The molecular formula of sesquilarin A (**3.4**) was determined to be $C_{52}H_{78}N_{10}O_{12}$ by analysis of HRESITOFMS (*m/z* 1035.5887 $[M+H]^+$; $C_{52}H_{79}N_{10}O_{12}$, Δ = - 0.8 mDa) and NMR data (Table 3.1). The ^{1}H NMR data (Table 3.1) were characteristic of a peptide, and the presence of seven amide NH and three N-CH_3 resonances suggested a decapeptide. The identities of the individual amino acid units present and assignments for their ^{1}H NMR resonances were established on the basis of TOCSY data. These assignments were later confirmed by GCMS analysis of the *N*-trifluoroacetyl-*sec*-butyl ester derivatives of the amino acids obtained upon hydrolysis. These experiments indicated that **3.4** is a cyclic decapeptide consisting of two Gly units, two Val units, and one of each of the following: Ile, Thr, Phe, N-MeThr, N-MeAla, and N-MePhe. The

complete sequence was determined by extensive analysis of HMBC, ROESY, and HRESITOFMSMS data (Figure 3.1 - Figure 3.3).

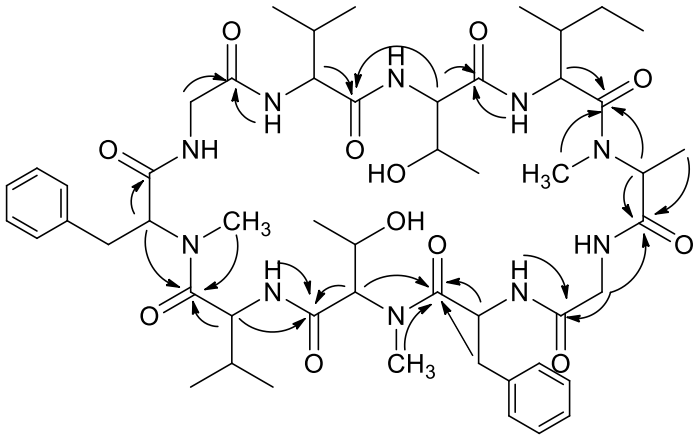

a

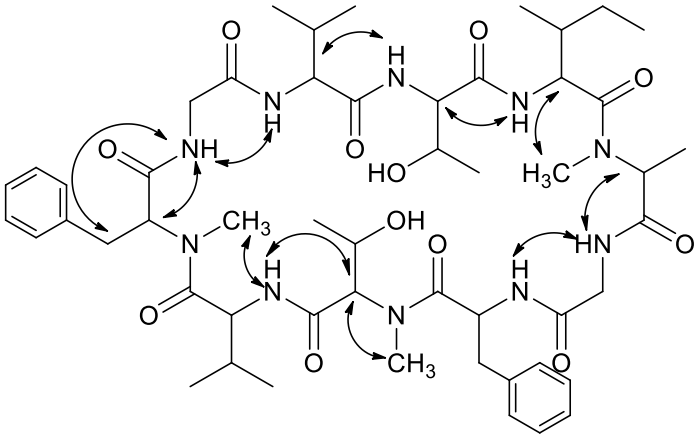

b

Figure 3.1 Sequence-relevant **a**. HMBC (→) and **b**. ROESY (↔) correlations for sesquilarin A (**3.4**)

An HMBC correlation from the α-proton of Thr to the carbonyl carbon of the Val-1 unit and a ROESY correlation between the α-proton of Val-1 and the amide NH of Thr

indicated that Val-1 acylated Thr in the sequence. A cross-peak consistent with an HMBC correlation from the amide NH of the Ile unit to the carbonyl carbon of Thr was present, but was inconclusive because of signal overlap. However, a ROESY correlation between the α-proton of Thr and the amide NH of Ile extended the sequence by indicating acylation of the Ile unit by the Thr unit. The N-MeAla unit was acylated by Ile based on an HMBC correlation from the N-CH_3 signal to the carbonyl of Ile. HMBC correlations from the α-protons of Gly-2 to the carbonyl of N-MeAla further extended the partial sequence. This was supported by observation of an *m/z* 456.2806 ion in the HRESITOFMS data corresponding to a $C_{21}H_{38}N_5O_6$ fragment. HMBC correlations from the methylene protons of the Phe unit and the N-CH_3 of the N-MeThr unit to the carbonyl of the Phe unit indicated that Phe acylates the N-MeThr unit. A ROESY correlation between the amide NH of Val-2 and the α-proton of N-MeThr, and an HMBC correlation from the amide NH of Val-2 to the carbonyl of N-MeThr extended the sequence by acylating Val-2 with N-MeThr. An HMBC correlation from the N-CH_3 of the N-MePhe unit to the carbonyl carbon of Val-2 completed another partial sequence (Phe → N-MeThr → Val-2 →N-MePhe). An HMBC correlation from the amide NH of the Phe unit to the carbonyl carbon of Gly-2 indicated acylation of Phe by Gly-2. By default, the only remaining amino acyl unit (Gly-1) must be located between the N-MePhe and Val-1 units. This was supported by ROESY correlations between the NH of Gly-1 and both the amide NH of Val-1 and the α-proton of N-MePhe.

These connections were supported by HRESITOFMS and HRESITOFMSMS data (Figure 3.2 and Figure 3.3). Observation of an ion at *m/z* 320.1592 (Gly-2 – Phe – N-MeThr; $C_{16}H_{22}N_3O_4$, Δ = 1.8 mDa) supported the acylation of Phe by Gly-2. Assignment of this unit was also supported by observation of an ion at *m/z* 716.4347 (peptide minus Gly-2 – Phe – N-MeThr; $C_{36}H_{58}N_7O_8$, Δ = - 0.01 mDa). An additional minor ion *m/z* 580.3084 corresponding to $C_{31}H_{42}N_5O_6$ supported the partial sequence from Phe through Gly-1

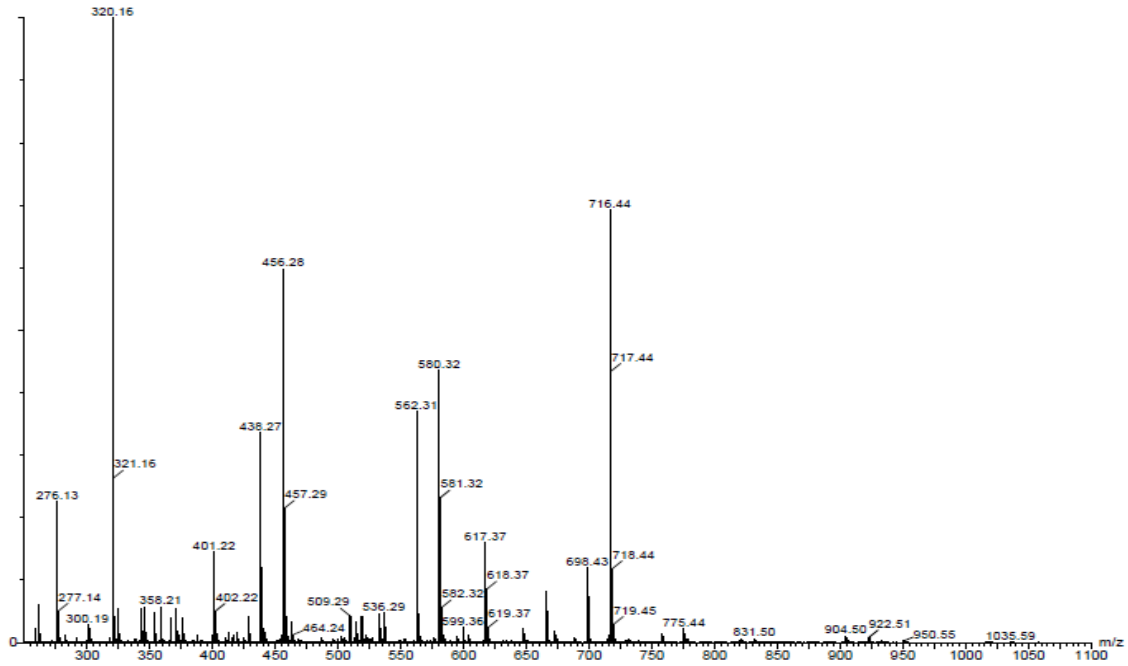

Figure 3.2. TOFMSMS data for sesquilarin A (**3.4**) for *m/z* 1035.5887 $[M+H]^+$

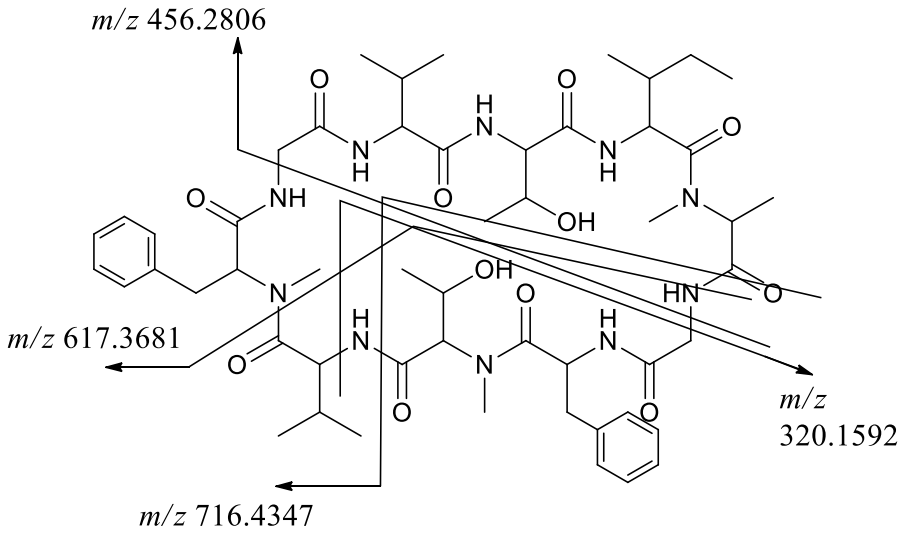

Figure 3.3. Key HRESITOFMSMS fragments for sesquilarin A (**3.4**) for *m/z* 1035.5887 $[M+H]^+$

Table 3.1. ^{1}H and ^{13}C NMR data for sesquilarin A (**3.4**)

Position	δ_H (mult; *J* in Hz)	δ_C	Position	δ_H (mult; *J* in Hz)	δ_C	Position	δ_H (mult; *J* in Hz)	δ_C
N-MeThr			**Gly 1**			**Val 2**		
α	5.35 (d, 9.5)	62.7	α_1	4.04 (dd, 18, 6.1)	42.8	α	4.52 (dd, 11, 9.9)	53.6
β	3.98 (m)	64.5	α_2	3.87 (dd, 18, 6.1)		β	2.08 (m)	30.3
γ-CH_3	1.00 (d, 6.2)	17.2	N-H	6.05 (br s)		γ-CH_3	0.93 (d, 6.4)	17.8
N-CH_3	2.96 (s)	30.2	C=O		168.87	γ-CH_3	0.91 (d, 6.4)	19.6
C=O		168.2	**Gly 2**			NH	8.48 (d, 9.9)	
N-MePhe			α_1	4.55 (dd, 17, 9.2)	42.4	C=O		171.9
α	3.72 (dd, 11.0, 4.0)	68.4	α_2	3.26 (ov)		**Ile**		
β_1	3.41 (dd, 14, 4.0)	34	N-H	6.31 (br s)		α	4.82 (dd, 10, 9.9)	52.7
β_2	3.28 (ov)		C=O		171.88	β	2.17 (m)	30.5/36.0[a]
Phenyl	7.13-7.32 (ov)	125-135	**N-MeAla**			γ-CH_3	0.87 (d, 6.6)	15.9
N-CH_3	2.78 (s)	39.9	α	3.55 (q, 7.0)	61.2	γ-$CH_{2\alpha}$	1.54 (m)	24.5
C=O		169.0	β-CH_3	1.54 (d, 7.0)	12.7	γ-$CH_{2\beta}$	1.22 (m)	
Val 1			N-CH_3	3.37 (s)	38.3	δ-CH_3	0.92 (t, 7.9)	10.9
α	4.26 (dd, 10, 8.6)	58.9	C=O		169.4	N-H	8.89 (d, 9.9)	
β	2.17 (m)	30.5/36.0[a]	**Phe**			C=O		172.7
γ-CH_3	1.03 (d, 6.6)	19	α	4.79 (m)	51.9	**Thr**		
γ-CH_3	0.96 (d, 6.6)	18.8	β_1	3.31(ov)	36.8	α	5.37 (dd, 9.6, 4.3)	56.3
N-H	7.71 (d, 9.2)		β_2	3.10 (dd, 13, 4.8)		β	3.77 (ov)	67.9
C=O		171.1	Phenyl	7.13-7.32 (ov)	125-135	γ-CH_3	1.06 (d, 6.2)	17.9
$CDCl_3$; 600 MHz (^{1}H) and 150 MHz (^{13}C)			N-H	8.06 (d, 6.6)		N-H	6.53 (br d)	
[a]Assignment interchangeable, ov: overlap			C=O		174.7	C=O		168.91

The absolute configurations of the amino acid units present were determined by GCMS analysis of *N*-TFA-(±)-2-butyl ester derivatives of the amino acids obtained upon hydrolysis of **3.4** in comparison with standards. This method enabled verification of the amino acids present, and the assignment of their absolute configuration. The *N*-TFA-(±)-2-butyl ester derivatives of standards of the amino acids in the acid hydrolyzate of **3.4** were prepared using standards of L-Val, L-Ile, L-alloIle, L-Thr, L-alloThr, L-Phe, L-MeAla, and L-MePhe and analyzed using GCMS. The identity of each peak was confirmed by comparison of the TIC (total ion current) chromatograms of the *N*-TFA-(±)-2-butyl derivatives to TIC chromatograms of *N*-TFA-(*S*)-(+)-2-butyl ester derivatives. Most of the amino acids present in **3.4** were found to have the L-configuration, although the N-MeThr configuration could not be assigned with certainty by this method because of the commercial unavailability of the *allo* N-MeThr isomer. Also, the two diasteromeric derivatives of N-MeAla did not resolve by GC and hence its configuration also could not be assigned using this technique. Fortunately, an X-ray crystal structure was later obtained for the closely related analogue sesquilarin C (**3.6**) enabling assignment of the L-configuration for both the N-MeThr and the N-MeAla units of **3.4** by analogy.

The molecular formula of sesquilarin B (**3.5**) was determined to be $C_{53}H_{80}N_{10}O_{12}$ (one methylene unit more than **3.4**) by analysis of HRESITOFMS (*m/z* 1049.6050 $[M+H]^+$; $C_{53}H_{81}N_{10}O_{12}$, Δ = - 1.5 mDa) and NMR data (Table 3.2). The ^{1}H NMR data were very similar to those of **3.4**, indicating that **3.4** and **3.5** are closely related analogues. Analysis of TOCSY data suggested that one of the Val units in **3.4** was replaced by an Ile or Leu unit, but these options could not be clearly differentiated by TOCSY due to signal complexity and overlap in the upfield region. Analysis of COSY data determined this unit to be an Ile moiety. The corresponding (Ile) α-proton showed correlations to two protons in the upfield region that were later assigned to the Ile β-methylene carbon. As expected for an Ile unit, these β-protons showed further correlations to a methyl and

another methylene unit. The sequence of the amino acids in **3.5** was independently determined by analysis of HMBC, ROESY, and HRESITOFMSMS data (Figure 3.4). As a result, it was determined that the Val-1 in **3.4** was replaced by an Ile unit in **3.5**. This was also supported by observation of an ion at *m/z* 470.2974 in the HRESITOFMSMS data for **3.5** (Figure 3.4) that was complimentary to the *m/z* 456.2806 ion in the data for **3.4** (Figure 3.3).

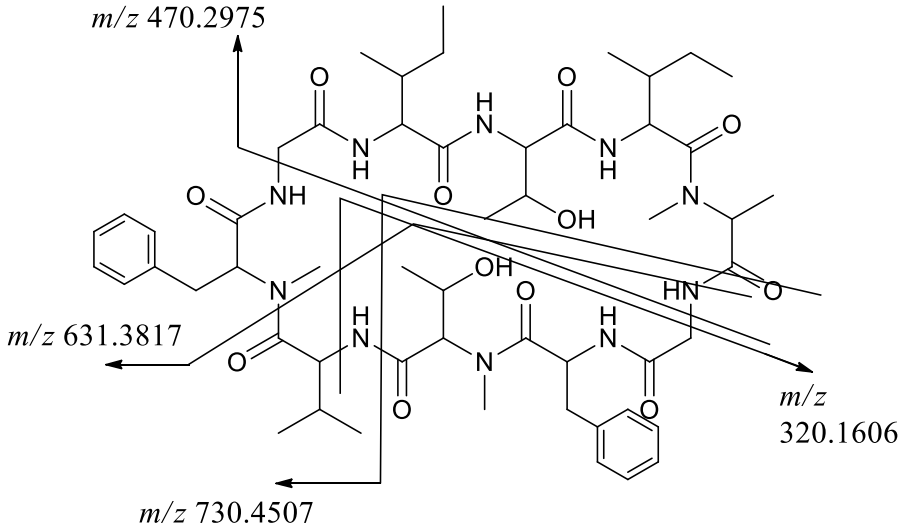

Figure 3.4. Key HRESITOFMSMS fragments for sesquilarin B (**3.5**) *m/z* 1049.6050 $[M+H]^+$

Upon hydrolysis, derivatization, and GCMS analysis in comparison to standards as described for **3.4**, all of the amino acids in **3.5** were again determined to have the L-configuration except for N-MeThr and N-MeAla, which could not be definitively assigned by this method.

The molecular formula of sesquilarin C (**3.6**) was determined to be $C_{54}H_{82}N_{10}O_{12}$ (one methylene unit larger than **3.5**) based on HRESITOFMS (1063.6204 $[M+H]^+$; $C_{54}H_{83}N_{10}O_{12}$, Δ = - 1.2 mDa) and NMR data (Table 3.3). The similarity in the ^1H NMR data for **3.6** clearly indicated its close analogy to **3.4** and **3.5**. Detailed analysis of TOCSY and COSY data revealed that the remaining Val unit present in **3.5** was replaced by an Ile unit in **3.6**. Observation of an ion at *m/z* 594.3290 (Phe through Gly-1) in HRESITOFMSMS data corresponding to an analogous ion at *m/z* 580.3084 observed in **3.4** supported this conclusion. The sequence of **3.6** was again independently confirmed by analysis of HMBC, ROESY, and HRESITOFMSMS data (Figure 3.5).

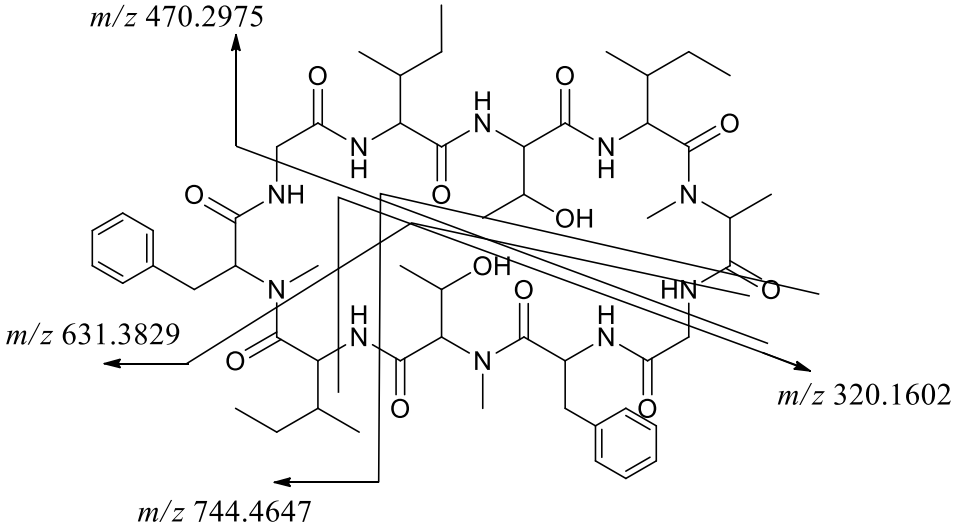

Figure 3.5. Key HRESITOFMSMS fragments for sesquilarin C (**3.6**) for *m/z* 1063.6204 $[M+H]^+$

The absolute configurations of the amino acids that could be assigned in this manner were again verified by GCMS analysis of the *N*-trifluoroacetyl-*sec*-butyl ester

derivatives generated from the acid hydrolyzate of **3.6**. In the case of **3.6**, however, suitable crystals were obtained from CH_2Cl_2 (5% hexanes) and an X-ray crystal structure was obtained. The resulting ORTEP plot is shown in Figure 3.6. This confirmed the proposed sequence of the sesquilarin C (**3.6**), and supported those proposed earlier for sesquilarin A (**3.4**) and B.(**3.5**). In addition this result enabled the absolute configurations of all of the amino acids to be independently assigned. All amino acids present, including N-MeThr and N-MeAla, were determined to have L-configuration. The analogous amino acids present in **3.4** and **3.5** are presumed to have the same configuration.

Sesquilarins A – C (**3.4 - 3.6**) did not exhibit any antifungal activity against *A. flavus* or *F. verticillioides* in disk assays at 50 µg/disk, nor did they exhibit any antibacterial activity against *E. coli*, *S. aureus,* and *B. subtilis* when tested at 20 µg/disk. Although the majority of the silica gel column fractions contained simple lipids, a few fractions contained mainly simple aromatic compounds which could potentially account for the activity initially observed for *S. microsporum* extract. However, these compounds were not purified further due to their lack of structural distinctiveness or interest.

Although cyclic peptides are encountered frequently as natural products, cyclic decapeptides are relatively rare. A literature search for such metabolites yielded only eighteen previously isolated decapeptides, of which only two have been reported from a quite different fungal source (*Cortinarius* sp., a mushroom).[87] None of these eighteen decapeptides have any structural similarity to the sesquilarins. A search of similar sequences yielded veruccamides,[88] cyclic tetradecapeptides isolated from another fungi (*Myrothecium verrucaria*). They contained the same Val-2 → Val-1 four amino acid fragment that is found in sesquilarin A (**3.4**). This chapter describes the isolation and structure elucidation of three new decapeptides from *Sesquicillium microspora*. To the best of our knowledge this is the first report of peptide-type metabolites from a member of this genus.

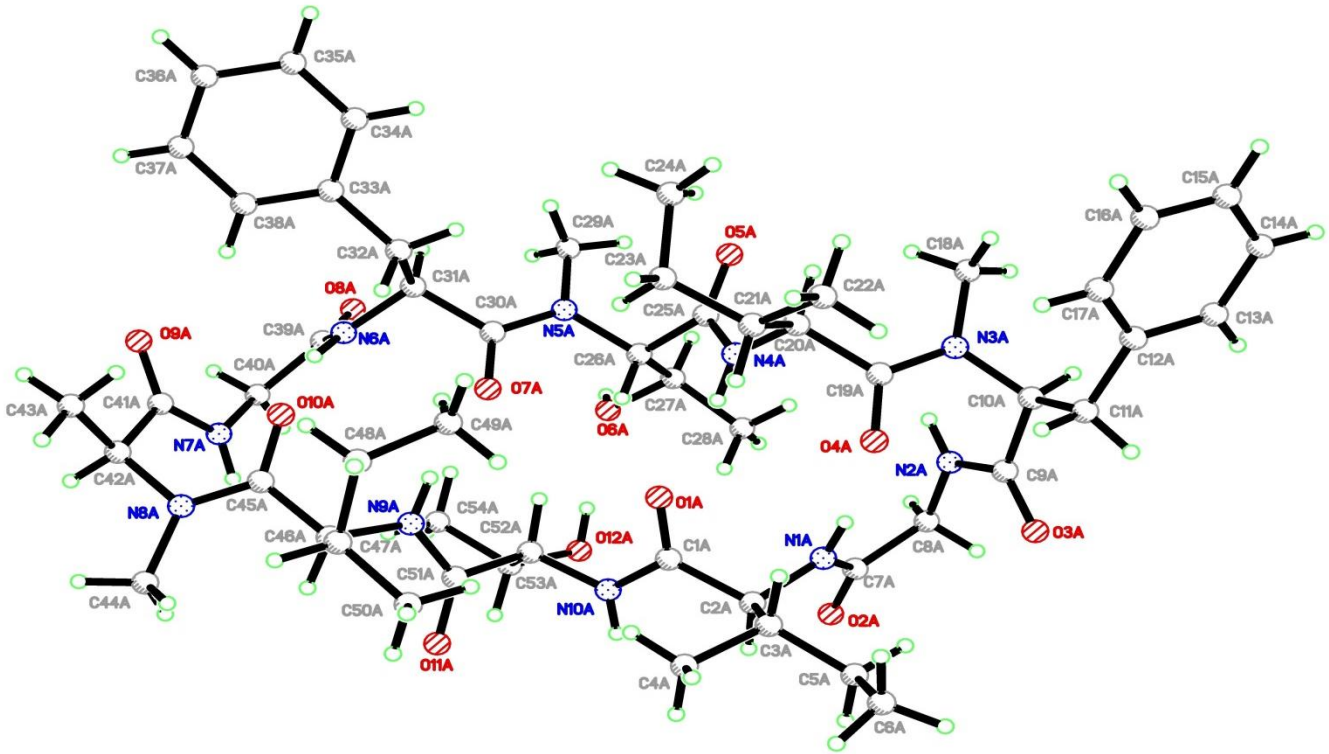

Figure 3.6. ORTEP image for sesquilarin C (**3.6**)

Table 3.2. ^{1}H and ^{13}C NMR data for sesquilarin B (**3.5**)

Position	δ_H (mult; *J* in Hz)	δ_C	Position	δ_H (mult; *J* in Hz)	δ_C	Position	δ_H (mult; *J* in Hz)	δ_C
N-MeThr			**Gly 1**			**Val**		
α	5.36 (d, 9.1)	62.7	α_1	4.0 (dd, 17, 6.3)	43.0	α	4.51 (t, 9.2)	53.5
β	3.97 (dd, 9.1, 6.1)	64.5	α_2	3.90 (dd, 17, 6.5)		β	2.07 (m)	30.8
γ-CH_3	1.01 (d, 6.1)	17.8	N-H	6.06 (br s)		γ-CH_3	0.93 (d, 7.5)[a]	17.6[a]
N-Me	2.96 (s)	30.2	C=O		169	γ-CH_3	0.91 (d, 7.6)[a]	19.8[a]
C=O		168.3	**Gly 2**			NH	8.49 (d, 9.2)	
N-MePhe			α_1	4.56 (dd, 17, 9.3)	42.5	C=O		171.8
α	3.71 (dd, 11, 3.8)	68.4	α_2	3.25 (dd, 17, 5.1)		**Ile 2**		
β_1	3.39 (ov)	34.0	N-H	6.36 (br s)		α	4.83 (t, 10)	53.1
β_2	3.27 (ov)		C=O		172.1	β	2.19 (m)	36.3
Phenyl	7.13-7.32 (ov)	125-137	**N-MeAla**			γ-CH_3	0.87 (d, 6.8)	15.8
N-CH_3	2.77 (s)	39.9	α	3.55 (d, 6.7)	61.3	γ-$CH_{2\alpha}$	1.57 (m)	24.4
C=O		169.3	β-CH_3	1.56 (d, 6.7)	12.7	γ-$CH_{2\beta}$	1.20 (m)	
Ile 1			N-CH_3	3.36 (s)	38.3	δ-CH_3	0.86 (t, 7.2)	ov
α	4.31 (t, 8.6)	57.2	C=O		169.6	N-H	8.9 (d, 10)	
β	1.98 (m)	37.3	**Phe**			C=O		172.8
γ-CH_3	0.93 (d, 7.0)	15.4	α	4.78 (m)	52.1	**Thr**		
γ-$CH_{2\alpha}$	1.60 (ov)	25.1	β_1	3.31 (t, 13)	36.5	α	5.38 (dd, 9.3, 5.6)	56.4
γ-$CH_{2\beta}$	2.0 (ov)		β_2	3.09 (dd, 13, 4.7)		β	3.77 (ov)	67.8
δ-CH_3	0.92 (t, 6.8)	ov	Phenyl	7.13-7.32 (ov)	125-137	γ-CH_3	1.06 (d, 5.9)	17.3
N-H	7.74 (d, 8.6)		N-H	8.05 (d, 6.6)		N-H	6.55 (d, 9.3)	
C=O		171.2	C=O		174.7	C=O		168.9
$CDCl_3$; 500 MHz (^{1}H) and 125 MHz (^{13}C) [a] Assignment interchangeable, ov: overlap								

Table 3.3. ^{1}H and ^{13}C NMR data for sesquilarin C (**3.6**)

Position	δ_H (mult; *J* in Hz)	δ_C	Position	δ_H (mult; *J* in Hz)	δ_C	Position	δ_H (mult; *J* in Hz)	δ_C
N-MeThr			**Gly 1**			**Ile 3**		
α	5.37 (d, 9.5)	62.4	α_1	4.0 (ov)	42.7	α	4.59 (t, 9.5)	52.4
β	3.98 (ov)	64.2	α_2	3.9 (dd, 6.4, 17)		β	1.90 (m)	36.7
γ-CH_3	1.04 (d, 6.2)	17.5	N-H	6.00 (t, 6.2)		γ-CH_3	0.96 (d, 6.7)[a]	-
N-Me	2.98 (s)	30	C=O		169	γ-CH_2	1.52 (ov), 1.05 (ov)	-
C=O		167.9	**Gly 2**			δ-CH_3	0.93	-
N-MePhe			α_1	4.53 (dd, 8.1, 17)	42.3	NH	8.53 (d, 9.5)	
α	3.71 (dd, 4.2, 11)	68.1	α_2	3.23 – 3.31		C=O		171.8
β_1	3.40 (dd, 4.2, 14)	33.7	N-H	6.25 (br d, 8.1)		**Ile 2**		
β_2	3.23-3.31 (ov)		C=O		171.8	α	4.82 (t, 10)	52.8
Phenyl	7.13-7.32 (ov)	125-137	**N-MeAla**			β	2.17 (m)	36
N-CH_3	2.82 (s)	39.6	α	3.53 (q, 7.0)	60.9	γ-CH_3	0.86 (d, 6.7)	NA
C=O		169.3	β-CH_3	1.57 (d, 7.0)	12.2	γ-$CH_{2\alpha}$	1.56 (ov)	24.4
Ile 1			N-CH_3	3.37 (s)	37.8	γ-$CH_{2\beta}$	1.18(ov)	
α	4.28 (t, 8.8)	57.2	C=O		169.5	δ-CH_3	0.93 (ov)	NA
β	2.03 (m)	36.5	**Phe**			N-H	8.88 (d, 10)	
γ-CH_3	0.95 (d, 6.7)	-	α	4.79 (m)	51.9	C=O		172.4
γ-$CH_{2\alpha}$	1.60 (ov)	-	β_1	3.11 (dd, 5.3, 13)	36.3	**Thr**		
γ-$CH_{2\beta}$	1.26 (ov)		β_2	3.23 – 3.31 (ov)		α	5.36 (dd, 4.4, 9.5)	55.9
δ-CH_3	0.93 (ov)	-	Phenyl	7.13-7.32 (ov)	125-137	β	3.79 (dd, 4.4, 6.6)	67.5
N-H	7.74 (d, 9.1)		N-H	8.01 (d, 6.4)		γ-CH_3	1.08 (d, 6.6)	16.8
C=O		171	C=O		174.7	N-H	6.51 (br d, 9.5)	
$CDCl_3$ 600 MHz (^{1}H) and 125 MHz (^{13}C), ov: overlap						C=O		168.6

CHAPTER 4

CHEMICAL INVESTIGATION OF AN ISOLATE OF *PHAEOACREMONIUM* SP.

Our studies of mycoparasitic and fungicolous fungi have afforded a variety of bioactive natural products. During our ongoing studies of these types of fungi, a culture of *Phaeoacremonium* sp. (MYC 2025 = NRRL 54515) was isolated from black stromata of a pyrenomycete found on a dead hardwood branch in a Hawaiian lowland wet forest, Mackenzie State Park, Puna District, Hawaii. *Phaeoacremonium* species have been associated with opportunistic human infections of skin and nails, as well as stunted growth and die-back of various woody hosts, especially grapevines.[89] About 23 species of *Phaeoacremonium* have been described. However, the genus is relatively unexplored from a chemical standpoint, with only a few secondary metabolites having been reported.[90] This is the first report of a peptide-type natural product from a member of this genus.

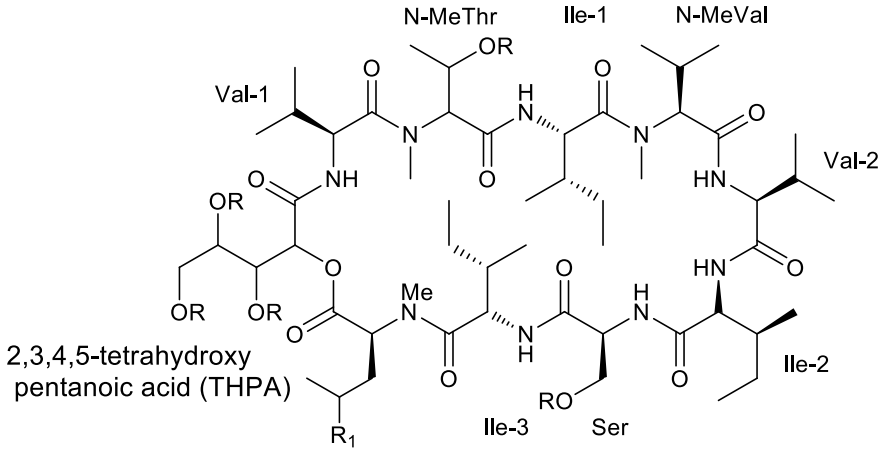

4.1 R = H, $R_1 = CH_3$

4.2 R = H, $R_1 = CH_2CH_3$

4.3 R = Ac, $R_1 = CH_3$

4.4 R = Ac, $R_1 = CH_2CH_3$

The EtOAc extract of solid-state fermentation cultures of MYC-2025 showed antifungal activity against F*usarium verticillioides*. Chemical studies of this extract afforded two new cyclic depsipeptides that we called phaeoacramides A (**4.1**) and B (**4.2**). The isolation process involved in obtaining **4.1**and **4.2** is summarized in Scheme 4.1.

Scheme 4.1. Isolation of metabolites from *Phaeoacremonium* sp.

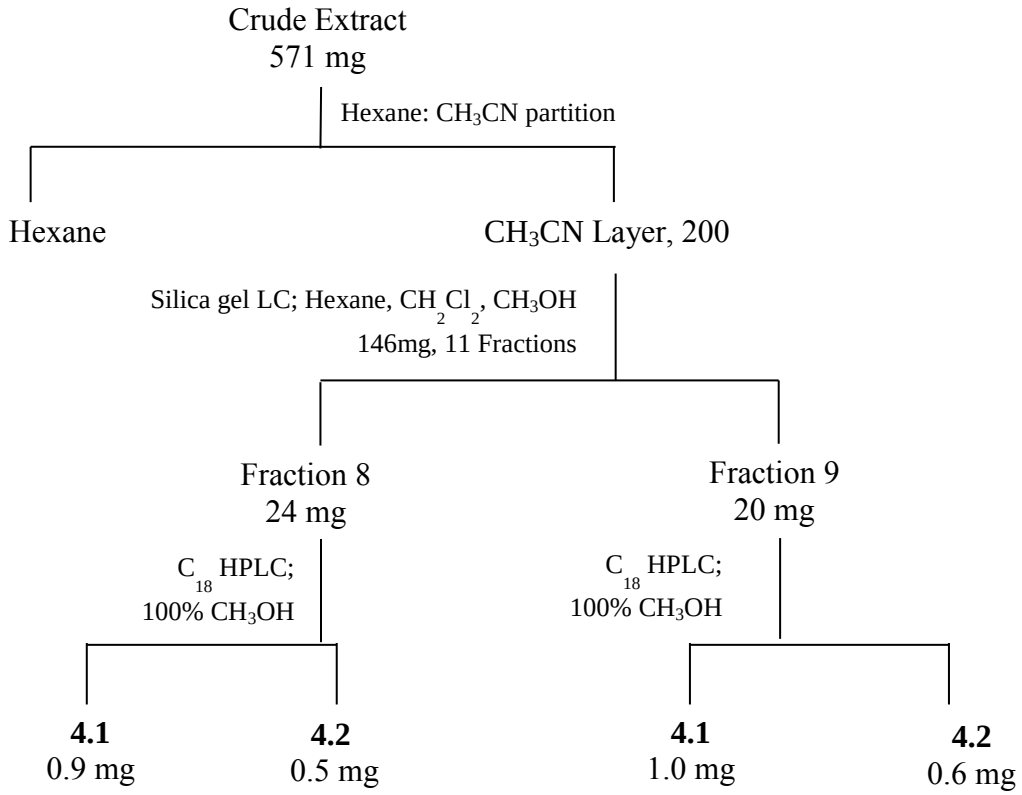

The EtOAc extract was partitioned between CH_3CN and hexanes to partly separate the more polar fractions from routinely encountered lipids. The CH_3CN fraction was further separated by silica gel chromatography. The majority of the silica fractions contained residual lipids and mixtures of simple phenolics. However, some fractions

contained peptides, as judged by NMR analysis, and these were separated by C_{18} HPLC to obtain **4.1** and **4.2**, which we named phaeoacramides A and B, respectively. Compound **4.2** was ultimately found to contain additional interesting structural feature not present in **4.1** and hence will be discussed first in detail.

Structure elucidation of phaeoacramide B (**4.2**)

The molecular formula for phaeoacramide B (**4.2**) was initially assigned to be $C_{54}H_{100}N_{11}O_{15}$ on basis of NMR and HRESITOFMS data (*m/z* 1142.7372 $[M+H]^+$ Δ -2.8 mDa). This HRESITOFMS measurement, determined using a reference lock mass ion at *m/z* 556.2771 $[M+H]^+$, was only later found to be inaccurate. At this stage, however, the initially assigned molecular formula was used in efforts to determine the structure. The ^{1}H NMR data were characteristic of a peptide, with the presence of six amide NH doublets and three N-CH_3 resonances (Table 4.1). All of the individual amino acids present and their spin-systems were assigned based on TOCSY data and were later confirmed by GCMS analysis of *N*-trifluoroacetyl-*sec*-butyl ester derivatives of the amino acids obtained upon hydrolysis of a sample of **4.2**. The amino acids were were identified as three Ile units, two Val units, and one unit each of Ser, N-MeThr, and N-MeVal. TOCSY data also suggested the presence of a homo-isoleucine (HomoIle) spin-system (an isoleucine with an extra methylene unit) which is very unusual in naturally occurring peptides.[91] To our knowledge, there are twelve naturally occurring compounds that contain a HomoIle unit, of which only have been isolated from a fungal source (*Claviceps purpurea*).[92] The presence of this unit was supported by the GC-MS data for the derivatized hydrolyzate, which showed a peak with a characteristic fragmentation pattern consistent with the presence of an additional methylene unit in a spectrum otherwise characteristic of an N-MeIle derivative (Figure 4.1). For example, GC-MS fragments for the N-MeIle derivative includes a of fragment at *m/z* 196, resulting from cleavage between the α-carbon and the carbonyl. Correspondingly, a fragment *m/z* 210

was observed for the N-MeHomoIle derivative indicating the presence of an extra methylene unit in the fragment.

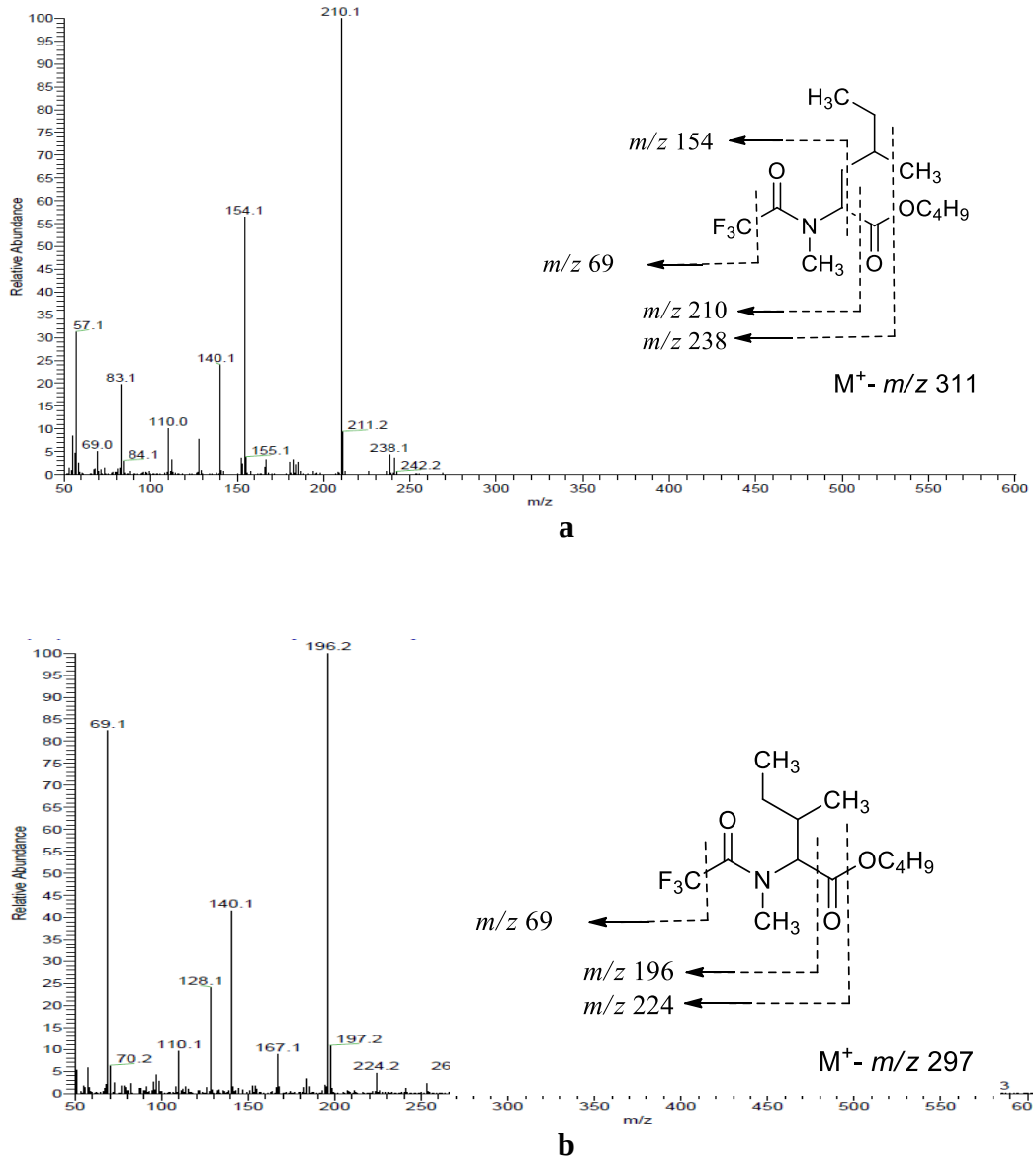

Figure 4.1. GC EIMS data for *N*-TFA-(*S*)-(+)-2-butyl ester of **a**. N-MeHomoIle **b**. N-MeIle

TOCSY data also revealed a highly oxygenated spin-system consistent with the presence of a sugar unit in **4.2**, but a specific substructure could not be assigned at this point because of signal overlap in the ^{1}H NMR spectrum and the inability to add the observed units up to match the molecular formula predicted by the HRESITOFMS data. Even so, these data indicated that **4.2** was a glycopeptide consisting of a sugar unit, three Ile units, two Val units, and one unit of each Ser, N-MeThr, N-MeHomoIle, and N-MeVal. After determining the amino acid composition, HMBC and ROESY data were collected in an effort to determine the amino acid sequence. Three-bond HMBC correlations from the α-proton or N-methyl signals to the carbonyl carbon of the acylating unit were sought in order to determine connections between amino acids. However, only a few such connections were observed. A partial structure could be assigned (Figure 4.2) based on the sparse HMBC data and on ROESY correlations. Reasons for a shortage of useful correlations included extensive overlap in the α-proton and carbonyl regions, and the somewhat broad signals observed in the ^{1}H NMR spectrum.

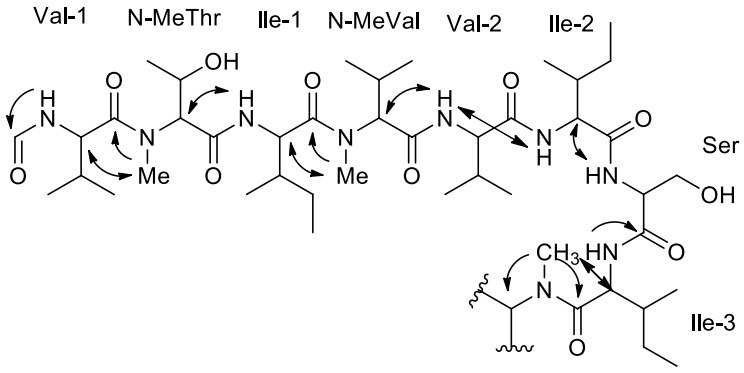

Figure 4.2. HMBC (→) and ROESY (↔) correlations for phaeoacramide B (**4.2**)

Assignment of the partial structure in Figure 4.2 left the elemental composition $C_9H_{19}N_2O_4$ unaccounted for, along with two degrees of unsaturation. The carbon skeleton of the N-MeHomoIle unit attached to Ile-3 accounted for another $C_6H_{11}O$ beyond the partial sequence shown in Figure 4.2, leaving $C_3H_8N_2O_3$ to be accounted for. However, the TOCSY data indicated the presence of a sugar unit in which an oxygenated C*H* at δ 5.2 showed HMBC correlations to two carbonyl carbons. These contradictory data precluded the assignment of a reasonable structure at this stage.

In an effort to overcome this problem, **4.2** was treated with acetic anhydride to obtain pentaacetate **4.4**. The much-improved ^{1}H NMR peak shapes and signal resolution obtained for **4.4** helped significantly in assigning the complete structure using 2D NMR data (Table 4.2 and Figure 4.3). The data obtained for the pentaacetate were in complete agreement with the partial sequence assigned earlier and confirmed the acylation of Val-1 by the sugar unit. Because of the incompatibility between the originally assigned molecular formula for **4.2** and the structural features indicated by the NMR data, HRESITOFMS data were collected again for **4.2** using a lock mass of *m/z* 1111.5464 $[2M+H]^+$ of the Leu-Enkephalin standard instead of its $[M+H]^+$ ion at *m/z* 556.2771, which had been used for the original measurement. The closer proximity of this higher lock mass to the target mass improved the accuracy of the measurement. The new data suggested that the molecular formula of **4.2** was actually $C_{55}H_{99}N_9O_{16}$ (*m/z* 1142.7301 $[M+H]^+$, Δ 1.3 mDa), rather than $C_{54}H_{99}N_{11}O_{15}$, and this conclusion was supported by the HRESITOFMS data for **4.4** ($C_{65}H_{109}N_9O_{21}Na$; *m/z* 1374.7672 $[M+Na]^+$). This was also in much better agreement with the NMR data for **4.2** (and **4.4**). This new molecular formula and the partial structure assignment discussed earlier left an elemental composition $C_4H_8O_4$ unaccounted for (not counting the carbonyl carbon of the sugar unit shown in the partial sequence in Figure 4.2). This was in good agreement for the presence of a five-carbon sugar unit acylating Val-1, as shown in the pentaacetate structure (Figure 4.3).

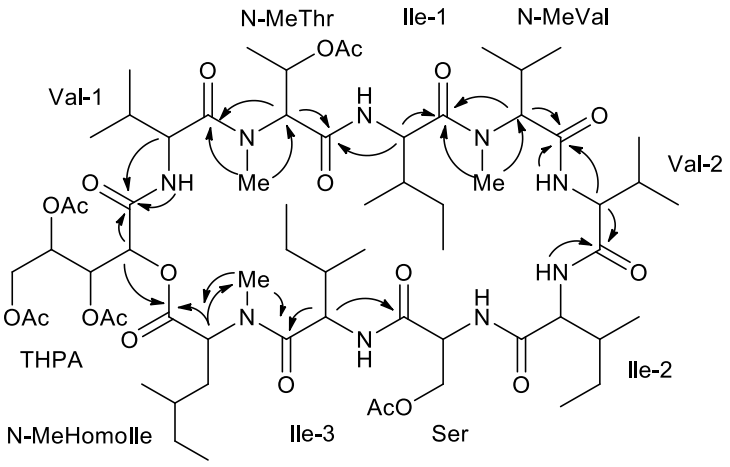

Figure 4.3. Key HMBC (→**)** correlations for phaeoacramide B pentaacetate (**4.4**)

All of the methines and methylenes bearing free OH groups in **4.2** were assigned based on their significant downfield shifts in the ^{1}H NMR spectrum of **4.4**. These signals were assigned to the Ser, N-MeThr, and sugar units based on the TOCSY data for **4.4**. The signals for the sugar unit were significantly better resolved in **4.4**, leading to its identification as a pentose derivative (tetrahydroxy pentanoic acid; THPA) based on HMBC and COSY data.

The entire sequence of **4.4** (and therefore **4.2**) was independently assigned by analysis of 2D NMR data. The α-proton for the pentose-like unit (THPA) showed HMBC correlations to carbonyl resonances at δ 169.6 (N-MeHomoIle) and 166.0 (THPA), thereby indicating acylation of the THPA unit by the N-MeHomoIle unit (Figure 4.3). A ROESY correlation between the amide proton of Val-1 and this THPA α-proton indicated the location of the THPA unit between N-MeHomoIle and Val-1 (Figure 4.4).

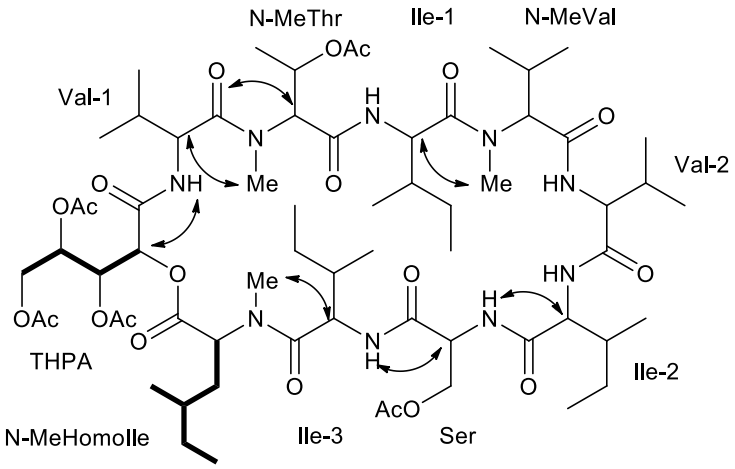

Figure 4.4. Key ROESY (↔) and COSY (**—**) correlations for phaeoacramide B pentaacetate (**4.4**)

The N-MeHomoIle → THPA → Val-1 subunit further acylated N-MeThr based on an HMBC correlation from the N-CH_3 of N-MeThr to the carbonyl carbon of Val-1. This was supported by observation of a major fragment ion at *m/z* 486.2805 in HRESITOFMSMS data for **4.2** corresponding to the loss of a N-MeHomoIle → THPA → Val-1 → N-MeThr fragment (Figure 4.5). Ile-1 was acylated by N-MeThr based on an HMBC correlation from the α-proton of Ile-1 to the carbonyl carbon of N-MeThr. An HMBC correlation from the N-CH_3 of N-MeHomoIle to the carbonyl carbon of Ile-3 indicated that the N-MeHomoIle was acylated by Ile-3. This partial structure was also supported by observation of *m/z* 730.4586 in the HRESITOFMSMS data for **4.2**, corresponding to loss of the Ile-3 to Ile-1 portion of the molecule. This subunit was further connected to N-MeVal based on an HMBC correlation from the N-CH_3 of N-MeVal to the carbonyl carbon of Ile-1. The presence of the N-MeThr → Ile-1 → N-MeVal sequence was supported by observation of an ion at *m/z* 342.2353 in the HRESITOFMSMS for **4.2**. N-MeVal was found to acylate Val-2 by the virtue of HMBC correlations from the amide and α-protons of Val-2 to the carbonyl carbon of N-MeVal.

This partial sequence was further extended to include Ile-2 based on an HMBC correlation from the amide proton of Ile-2 to the carbonyl carbon of Val-2. By default, and to accomodate the degrees of unsaturation required, the Ser residue must be acylated by Ile-2. This connection was supported by a ROESY correlation between the amide proton of Ser and the α-proton of Ile-2, and between the amide proton of Ile-3 and the α-proton of Ile-2, thereby completing the cyclic structure.

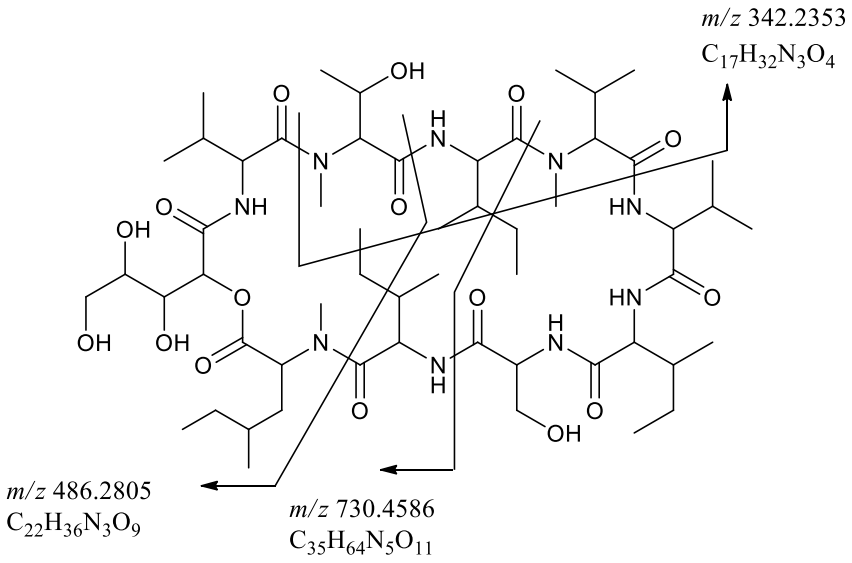

Figure 4.5. Key HRESITOFMSMS fragments for phaeoacramide B (**4.2**)

The absolute configurations of the amino acyl units were determined by GCMS analysis of *N*-trifluoroacetyl (TFA)-(*S*)-(+)-2-butyl ester derivatives of the amino acids obtained upon hydrolysis. This method not only leads to identification of the amino acids present (*via* GCMS), but also enables assignment of their absolute configurations by chromatographic comparison to standards.[93] The *N*-TFA-(±)-2-butyl ester derivatives of standards of the amino acids in the acid hydrolyzate of **4.2** were prepared using all

possible stereoisomers and analyzed by GCMS. However, standards for all isomers of N-MeThr and N-MeHomoIle, were not commercially available, so their configurations were not assigned by this method. The identity of each peak was confirmed by comparison of the TIC (total ion current) chromatograms of the *N*-TFA-(±)-2-butyl derivatives to *N*-TFA-(*S*)-(+)-2-butyl ester derivatives prepared using enantiopure amino acid standards. All of the amino acids present for which standards were available were found to have the L-configuration.

Several approaches were explored in an effort to determine the absolute configuration of the THPA residue. Under acid hydrolysis conditions, THPA would be expected to cyclize into a lactone.[94,95] Three of the four possible isomers of the pentanoic acid derivative were available and diastereomers of these isomers (xylonic acid, ribonic acid, and arabinoic acid) were prepared by bromine oxidation of of D-ribose, D-xylose, and D-arabinose, respectively using a literature procedure[96] (eg., Figure 4.6).

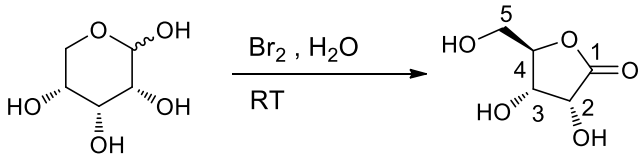

Figure 4.6. Br_2 Oxidation of D-ribose[96]

Under the set of reaction conditions, the five membered 1,4-lactone is preferred over the 1,5-lactone, except with xylose, in which 1,5-xylono lactone is the preferred product. The resulting lactones were characterized by comparison of the ^{1}H NMR spectra with literature values.[96-98] The ^{1}H NMR spectrum of a pentose sugar consists of a

characteristic downfield anomeric resonance that is eliminated in the lactone. In addition, other proton resonances, especially those at C-2 and C-4, are shifted downfield as compared to the pentose sugar. The resulting lactones were then derivatized with trifluoroacetic anhydride and analyzed by GCMS for comparison to the data for the derivatized hydrolyzate of **4.2**. However, because the lactone is susceptible to ring opening under the reaction conditions, these products tend to exist in equilibrium among the major 1,4-lactone (or 1,5-lactone) and minor free acid form.[96] Hence, in each case, multiple peaks were observed in the GCMS chromatogram. Corresponding peaks for the TFA derivatives of the THFA in the sample could not be clearly detected by GCMS, presumably due to the limited sample size of **4.2** available for hydrolysis experiments and the complexity of the mixtures resulting upon hydrolysis and derivatization.

In an alternative approach to detect the hydrolysis product and assign its relative configuration, another sample of **4.2** was hydrolyzed and the hydrolyzate was analyzed directly by ^{1}H NMR in comparison with the available standard samples of the sugar acids prepared as described above.[97-99] However, due to extensive signal overlap, sample complexity, broad lines, and poor signal-to-noise ratio, resonances could not be detected for the expected lactones in the NMR spectrum of the crude hydrolyzate. Trimethylsilyl derivatives of the components of the **4.2** hydrolyzate and 1,4-ribonolactone (Figure 4.6) were prepared for analysis by GCMS.[100] However, sample limitations and the complexity of the hydrolyzate product mixture again resulted in failure to detect any pentanoic acid TMS derivatives in the derivatized hydrolyzate of **4.2** by GCMS. Attempts to separate the pentose sugar from other amino acids by extraction of the hydrolyzate into organic solvent would not be expected to work because both the sugar and the amino acid residues would have greater solubility in water than in organic solvents. Multiple attempts to crystallize **4.2** in separate efforts to overcome these difficult stereochemical problems by employment of X-day crystallography were not successful.

Table 4.1. ^{1}H and ^{13}C NMR data for phaeoacramide B (**4.2)**

Position	δ_H (mult; *J* in Hz)	δ_C	Position	δ_H (mult; *J* in Hz)	δ_C	Position	δ_H (mult; *J* in Hz)	δ_C	Position	δ_H (mult; *J* in Hz)	δ_C
Ile 1			**Ile 2**			THPA			**N-Me Val**		
α	4.59-4.69 (ov)	53.0	α	4.59-4.69 (ov)	56.4	α	5.20(br s)	74.7	α	3.10 (d, 11.3)	76.3
β	1.94 (ov)	35.4	β	1.93-2.03 (ov)	36.0	β	4.18 (br s)	70.7	β	2.75 (m)	26.4
γ_1	1.41(m)		γ_1	1.51 (m)		γ	3.50 (m)	71.4	γ-CH_3	0.97 (d, 6.2)	18.2
γ_2	1.11 (m)	24.0	γ_2	1.26 (m)	25.0	δ_1	3.54 (ov)		γ-CH_3	1.08 (d, 6.7)	20.4
γ-CH_3	0.84 (d, 6.2)	15.6	γ-CH_3	0.89 (d, 6.6)	14.8	δ_2	3.42 (ov)	62.9	N-CH_3	3.35 (s)	41.8
δ-CH_3	0.76 (d, 7.3)	9.8	δ-CH_3	0.83 (t, 7.3)	9.42	C=O		168.81	C=O		168.0
N-H	8.98 (d, 9.7)		N-H	7.80 (br d, 8.3)		**Val 1**			**Val 2**		
C=O		172.6	C=O		NA	α	4.59-4.69 (ov)	54.8	α	4.59-4.69 (ov)	57.4
N-Me HomoIle			**Ile 3**			β	2.3 (m)	30.3	β	2.63 (m)	30.2
α	3.65 (m)	62.1	α	4.78 (t, 9.7)	52.9	γ-CH_3	0.97 (d, 7.0)	18.9	γ-CH_3	0.93 (d, 6.5)	19.3
β_1	2.16 (t, 11.8)		β	1.93 (ov)	35.8	γ-CH_3	0.87 (d, 7.1)	18.0	γ-CH_3	0.78 (d, 6.8)	15.3
β_2	1.76 (t, 11.8)	35.4	γ_1	1.47 (ov)		N-H	7.90 (d, 8.5)		N-H	6.53 (d, 10.2)	
γ	1.19-1.35 (ov)	30.3	γ_2	1.08 (ov)	23.8	C=O		173.8	C=O		70.7
δ-CH_3	0.92 (d, 6.3)	18.5	γ-CH_3	0.80 (d, 6.2)	15.3	**N-Me Thr**			**Ser**		
δ-CH_2	1.19-1.35 (ov)	29.8	δ-CH_3	0.76-0.81 (ov)	10.5	α	5.37 (d, 9.4)	61.9	α	4.99 (br s)	53.9
ε-CH_3	0.83 (t, 8.0)	11.0	N-H	8.74 (d, 9.9)		β	4.1 (br s)	64.0	β_1	3.55 (ov)	61.8
N-Me	3.25	39.6	C=O		172.2	γ-CH_3	0.98 (ov)	18.5	β_2	3.45 (ov)	
C=O		169.8				N-CH_3	3.39 (s)	31.4	N-H	8.15 (br s)	
$CDCl_3$, 600 MHz (^{1}H) and 150 MHz (^{13}C)						C=O		169.3	C=O		169.9

Table 4.2. ^{1}H and ^{13}C NMR data for phaeoacramide B pentaacetate (**4.4**)

Position	δ_H (mult; *J* in Hz)	δ_C	Position	δ_H (mult; *J* in Hz)	δ_C	Position	δ_H (mult; *J* in Hz)	δ_C	Position	δ_H (mult; *J* in Hz)	δ_C
Ile 1			**Ile 2**			THPA			**N-Me Val**		
α	4.61 (br d, 9.3)	53.2	α	4.42 (dd, 9.1, 7.8)	57.1	α	5.47 (d, 6.5)	70.2	α	3.13 (d, 11)	76.0
β	1.89-1.91 (ov)	36.0	β	1.94-1.98 (ov)	37.4	β	5.40 (dd, 6.5, 4.3)	69.3	β	2.7 (m)	26.7
γ_1	1.39 (m)		γ_1	1.51 (m)		γ	5.55 (dt, 6.5, 4.3)	69.6	γ-CH_3	1.10 (d, 6.7)	20.6
γ_2	1.03 (m)	24.12	γ_2	1.28 (m)	25.0	δ_1	4.21 (dd, 12, 4.3)		γ-CH_3	0.98 (d, 6.5)	19.3
γ-CH_3	0.83 (d,7.4)	15.88	γ-CH_3	0.90 (d, 8.6)	15.1	δ_2	4.03 (dd, 12, 4.3)	61.8	N-CH_3	3.32 (s)	41.6
δ-CH_3	0.77 (dd, 8.3, 8.1)	10.81	δ-CH_3	0.86-0.88 (ov)	13.9	C=O		166.0	C=O		168.6
N-H	8.8 (d, 10)		N-H	7.73 (d, 9.2)		**Val 1**			**Val 2**		
C=O		172.2	C=O		171.4	α	4.60 (ov)	55.0	α	4.53 (dd, 10, 2.9)	57.8
N-Me HomoIle			**Ile 3**			β	2.18 (m)	30.8	β	2.65 (m)	29.8
α	3.60 (dd, 3.7, 10)	62.4	α	4.78 (dd, 9.6, 9.4)	53.0	γ-CH_3	0.98 (d, 6.5)	18.7	γ-CH_3	0.94 (d, 7.1)	19.5
β_1	2.09 (ov)		β	1.86-1.88 (ov)	37.7	γ-CH_3	0.89 (d, 6.7)	18.4	γ-CH_3	0.82 (d, 6.7)	16.1
β_2	1.85 (ov)	35.8	γ_1	1.42 (ov)		N-H	7.7 (d, 8.3)		N-H	6.44 (d, 10)	
γ	1.36 (ov)	31.0	γ_2	1.04 (ov)	24.1	C=O		174.3	C=O		170.7
δ-CH_3	0.95 (d, 6.6)	18.5	γ-CH_3	0.82 (d, 7.4)	15.1	**N-Me Thr**			**Ser**		
δ-CH_2	1.64 (m), 1.51 (m)	30.0	δ-CH_3	0.80 – 0.83 (ov)	10.8	α	5.51 (d, 9.6)	59.2	α	5.61 (m)	51.2
ε-CH_3	0.86 (t, 7.9)	11.0	N-H	8.83 (d, 9.5)		β	5.33 (dd, 9.6, 6.3)	66.6	β_1	4.40 (dd, 12, 6.8)	63.8
N-Me	3.23 (s)	39.2	C=O		172.1	γ-CH_3	1.15 (d, 6.3)	17.2	β_2	4.05 (dd, 12, 3.9)	
C=O		169.6				N-CH_3	3.29 (s)	31.5	N-H	6.71 (br s)	
$CDCl_3$, 600 MHz (^{1}H) and 150 MHz (^{13}C)						C=O		168.4	C=O		168.9

Structure Elucidation of Phaeoacramide A (**4.1**)

The molecular formula of **4.1** was determined to be $C_{54}H_{98}N_9O_{16}$ based on observation of a HRESITOFMS ion at *m/z* 1128.7151 $[M+H]^+$ using the lock mass of *m/z* 1111.5464 $[2M+H]^+$ of the Leu-Enkephalin standard in conjunction with NMR data (Table 4.3). These data revealed that **4.1** is a close analogue of **4.2**, having one less methylene unit. However, as was the case with **4.2**, the complete sequence could not be assigned with certainty on the basis of HMBC, ROESY, and HRESITOFMSMS data alone due to broad NMR lines, signal overlap, and absence of correlations to certain key resonances. Hence, **4.1** was similarly treated with acetic anhydride to obtain pentaacetate **4.3** (Table 4.4). Analysis of TOCSY data for **4.3** revealed that the N-MeHomoIle unit in **4.2** was replaced by a more common N-MeLeu unit, and this was supported by HMBC and COSY data. The sequence of the peptide was independently determined by extensive analysis of HMBC and ROESY data for **4.3** and HRESITOFMSMS data for **4.1** (Figure 4.7) and was found to be analogous to that of **4.2**.

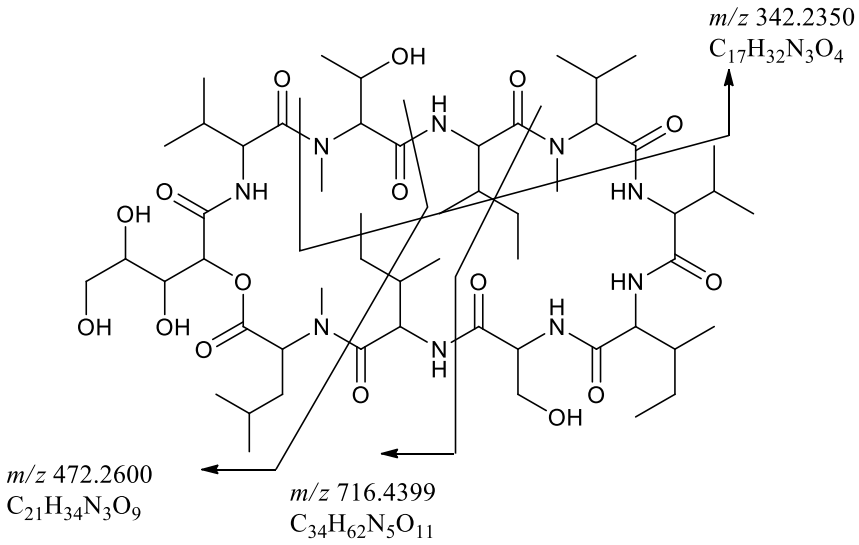

Figure 4.7. Key HRESITOFMSMS fragments of phaeoacramide A (**4.1**)

The common amino acids present were again all determined to have the L-configuration by GCMS analysis of the *N*-trifluoroacetyl-(*S*)-(+)-2-butyl ester derivatives as described earlier for **4.2**. However, as before, because standard samples of the isomers of N-MeThr and N-MeLeu were not available, their configurations were not determined by this method and remain unassigned, as does the configuration of the THPA unit.

Neither phaeoacramide A (**4.1**) nor B (**4.2**) showed any antifungal activity against *A. flavus* or *F. verticillioides* or any antibacterial activity against *E. coli*, *S.aureus,* or *B. subtilis* in standard disk assays at 50 µg/disk. There were other major silica fractions that were not examined further because they contained only lipids and simple aromatic compounds. These fractions may account for the originally observed activity of the extract. There have been only seven reports of naturally occurring compounds from the genus *Phaeoacremonium*, none of which are peptides. The configurations of N-MeHomoIle, M-MeLeu, N-MeThr, and the sugar unit occurring in these compounds remain unassigned. To assign the stereochemistry of these units, additional amounts of the two phaeoacramides would need to be produced and isolated, and the possible isomers of the corresponding amino acids would need to be synthesized. It is conceivable that the sugar acid unit could be separated from the hydrolyzate and analyzed if the work could be done on a significantly larger scale. It is also possible that larger sample of **4.1** and **4.2** might provide a better chance for success in crystallization. However, in view of the lack of detected activity, the extensive work necessary to pursue these questions further was not considered justifiable.

Table 4.3. ^{1}H NMR data for phaeoacramide A (**4.1)**

Position	δ_H (mult; *J* in Hz)	Position	δ_H (mult; *J* in Hz)	Position	δ_H (mult; *J* in Hz)	Position	δ_H (mult; *J* in Hz)
Ile 1		**Ile 2**		**THPA**		**N-Me Val**	
α	4.60-4.73 (ov)	α	4.60-4.73 (ov)	α	5.20(br s)	α	3.14 (d, 10.9)
β	1.93-2.03 (ov)	β	1.93-2.03 (ov)	β	4.19 (br s)	β	2.77 (m)
γ_1	1.44-1.58 (ov)	γ_1	1.44-1.58 (ov)	γ	3.52 (m)	γ-CH_3	1.12 (d, 6.5)
γ_2	1.06-1.19 (ov))	γ_2	1.26-1.33 (m)	δ_1	3.56 (ov)	γ-CH_3	1.0 (d, 6.5)
γ-CH_3	0.87 (d, 6.3)	γ-CH_3	0.86 (t, 7.1)	δ_2	3.45 (ov)	N-CH_3	3.38 (s)
δ-CH_3	0.79 (d, 7.5)	δ-CH_3	0.93 (d, 6.4)	C=O		C=O	
N-H	9.06 (d, 9.5)	N-H	7.84 (br d, 7.1)	**Val 1**		**Val 2**	
C=O		C=O		α	4.60-4.73 (ov)	α	4.60-4.73 (ov)
N-Me Leu		**Ile 3**		β	2.33 (m)	β	2.65 (m)
α	3.65 (m)	α	4.80 (d, 12, 7.3)	γ-CH_3	1.0 (d, 6.9)	γ-CH_3	0.96 (d, 6.3)
β_1	1.87 (ov)	β	1.93-2.03 (ov)	γ-CH_3	0.89 (d, 6.9)	γ-CH_3	0.84 (d, 6.7)
β_2	1.62 (ov)	γ_1	1.44-1.58 (ov)	N-H	7.96 (d, 7.1)	N-H	6.56 (d, 9.8)
γ	2.03 (ov)	γ_2	1.06-1.19 (ov)	C=O		C=O	
δ-CH_3	0.97 (d, 7.0)	γ-CH_3	0.82 (d, 6.2)	**N-Me Thr**		**Ser**	
δ-CH_3	0.93 (d, 7.0)	δ-CH_3	0.82 (ov)	α	5.04 (br s)	α	5.38 (d, 8.8)
N-Me	3.38 (s)	N-H	9.06 (d, 9.5)	β	3.57 (ov)	β_1	4.1 (br s)
C=O		C=O		γ-CH_3	3.49 (ov)	β_2	1.0 (d, 4.4)
				N-CH_3	8.28 (br s)	N-H	3.42 (s)
$CDCl_3$, 600 MHz (^{1}H) and 150 MHz (^{13}C)				C=O		C=O	

Table 4.4. ^{1}H and ^{13}C NMR data for phaeoacramide A pentaacetate (**4.3**)

Position	δ_H (mult; *J* in Hz)	δ_C	Position	δ_H (mult; *J* in Hz)	δ_C	Position	δ_H (mult; *J* in Hz)	δ_C	Position	δ_H (mult; *J* in Hz)	δ_C
Ile 1			**Ile 2**			**THPA**			**N-Me Val**		
α	4.63 (br d, 9.3)	53.5	α	4.45 (dd, 9.1, 8.1)	56.9	α	5.48 (d, 6.8)	70.2	α	3.13 (d, 11)	75.7
β	1.89-1.91 (ov)	35.9	β	1.94-1.98 (ov)	37.3	β	5.42 (dd, 6.8, 4.3)	69.2	β	2.73 (m)	26.5
γ_1	1.41-1.47 (ov)		γ_1	1.52 (m)		γ	5.58 (ddd, 7.0, 4.7, 4.3)	69.5	γ-CH_3	1.13 (d, 7.5)	20.6
γ_2	1.03-1.09 (ov)	24.0	γ_2	1.31 (m)	24.9	δ_1	4.24 (dd, 12, 4.7)		γ-CH_3	1.0 (d, 6.7)	19.3
γ-CH_3	0.86 (d, 7.4)	16.0	γ-CH_3	0.92 (d, 7.6)	10.9	δ_2	4.03 (dd, 12, 7.0)	61.7	N-CH_3	3.34 (s)	41.5
δ-CH_3	0.79 (t, 8.1)	11.0	δ-CH_3	0.90 (ov)	13.9	C=O		165.9	C=O		168.8
N-H	8.87 (d, 9.3)		N-H	7.78 (d, 9.2)		**Val 1**			**Val 2**		
C=O		172.0	C=O		171.23	α	4.62 (br d, 9.6)	54.8	α	4.55 (d, 10, 2.8)	57.7
N-Me Leu			**Ile 3**			β	2.20 (m)	30.7	β	2.68 (m)	29.7
α	3.59 (dd, 7.4, 6.8)	62.3	α	4.78 (dd, 9.6, 9.4)	52.8	γ-CH_3	1.0 (d, 7.7)	18.7	γ-CH_3	0.96 (d, 7.0)	19.5
β_1	1.94-1.98 (ov)		β	1.89-1.91 (ov)	37.8	γ-CH_3	0.91 (d, 7.8)	18.3	γ-CH_3	0.84 (d, 6.7)	16.0
β_2	1.94-1.98 (ov)	37.8	γ_1	1.41-1.47 (ov)		N-H	7.73 (d, 8.3)		N-H	6.46 (d, 10)	
γ	1.63-1.69 (ov)	24.7	γ_2	1.03-1.09 (ov)	24.0	C=O		174.1	C=O		170.5
δ-CH_3	0.99 (d, 7.2)	21.4	γ-CH_3	0.84 (d, 7.2)	15.2	**N-Me Thr**			**Ser**		
δ-CH_3	0.96 (d, 7.2)	23.0	δ-CH_3	0.83-0.86 (m)	11.1	α	5.51 (d, 10)	59.1	α	5.63 (m)	50.9
N-Me	3.26 (s)	39.1	N-H	8.87 (d, 10)		β	5.35 (dd, 10, 6.4)	66.6	β_1	4.4 (dd, 11, 7.1)	63.6
C=O		169.4	C=O		172.1	γ-CH_3	1.15 (d, 6.4)	17.2	β_2	4.07 (dd, 11, 3.7)	
						N-CH_3	3.31 (s)	32.0	N-H	6.91 (br s)	
$CDCl_3$, 600 MHz (^{1}H) and 150 MHz (^{13}C)						C=O		168.3	C=O		168.8

CHAPTER 5
CHEMICAL INVESTIGATION OF FUNGAL BIS-NAPHTHOPYRONES AND THEIR ACTIVITY AGAINST BOTULINUM NEUROTOXIN A

Significance of Botulinum Neurotoxins

Botulinum neurotoxins (BoNTs) are among the most potent known toxins. Seven distinct BoNT serotypes are produced by the anaerobic gram positive bacteria *Clostridium botulinum, C.* baratii, and *C. butyricum.* BoNTs consist of a heavy chain (HC) of 100 kDa covalently attached by a disulfide bond to a light chain (LC) 0f 50 kDa. The HC mediates the binding of BoNTs with receptors at the neuronal surface, which is followed by endocytosis. BoNTs are potent metalloendoproteases and, after cellular uptake, are capable of targeting and cleaving various soluble N-ethylmaleimide-sensitive factor (NSF) attachment protein (SNAP) receptors (SNAREs), inhibiting release of acetylcholine at the neuromuscular junction, thereby causing neuromuscular blockage and descending flaccid paralysis that is known as botulism.[101] They typically have LD_{50} values of 0.5 – 1 ng/kg in mice and approximately 1 ng/kg in humans. Very recently, a new variant has been discovered (BoNT/H) that is believed to be the most potent BoNT. Exposure to approximately 0.08 – 0.5 ng of BoNT/H can be fatal for an adult, as compared to 0.09 – 0.90 µg of BoNT/A.[102-104] Exposure can occur by ingestion of toxin or bacterial spores, by inhalation, or by infection through a wound. Thus, widespread dispersal of the toxin could occur.

Interestingly, despite their toxicity, BoNTs also find applications as therapeutic and cosmetic agents. Local application of BoNT in extremely low doses has been effective in treating various medical conditions, including chronic pain, muscular dysfunction, and inflammation. Genetically mutated versions have been produced to increase substrate specificity and cleavage of non-neuronal SNAREs to extend their

therapeutic applications and to attenuate their overall toxicity. They are also widely used in cosmetics, with product names that include Botox, Dysport, Xeomin, and Myobloc.[105]

Because of their lethality, potency, ease of production, transport, and dispersal, BoNTs have the potential to be used as bioterrorism agents. A risk of intentional or accidental misuse of these toxins has led to increased efforts to find effective treatments to remediate BoNT exposure.[106]

A pentavalent botulinum toxoid (PBT) vaccine has been studied as a potential treatment, but it displays declining immunogenicity, so improved botulinum toxoid and recombinant vaccines are being investigated.[101] However, the multitude of clinical uses of BoNT makes mass vaccinations against these toxins undesirable. Currently, the only FDA-approved therapeutic treatment for BoNT intoxication consists of passive immunization with equine-based antitoxin for BoNT/A and B. Although such antitoxins can neutralize and clear toxins from the circulatory system, early treatment is essential for efficacy, as they cannot intervene in the pathogenesis of the disease after cellular uptake. Hence, in the event of a bioterrorism attack, these inhibitors would not be effective because exposure to the toxin would not be known until after cellular uptake. A more effective inhibitor would act both pre- and post-cellular uptake of the toxins.[101]

Screening Methods and Results

Previous in silico screenings and tiered biochemical assays (enzymatic, in vitro, and ex vivo) successfully identified five quinolinol derivatives as effective inhibitors of BoNT/A.[107] Of these quinolinols, **5.1** was found to be the most potent BoNT/A inhibitor that was active in an ex vivo mouse phrenic nerve hemidiaphragm assay (MPNHDA). Using similar strategy, researchers at the U. S. Army Medical Research Institute of Infectious Diseases (AMRIID) carried out further in silico screening by computationally docking compounds from the NIH molecular library small molecule repository

(MLSMR) collection of ~ 350000 compound structures to the catalytic binding site of BoNT/A protein target (Figure 5.1).

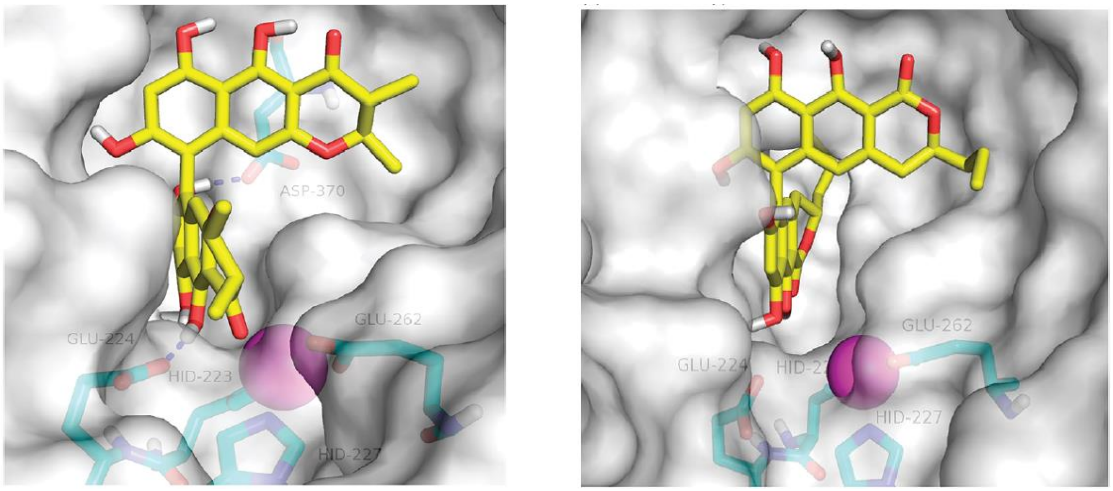

a **b**

Figure 5.1. Proposed binding mode of (**c**) Chaetochromin A (**5.2**) and (**d**) Talaroderxine B (**5.4**) in the active site of BoNT/A.[108]

After several such screenings, 100 compounds were selected and samples were obtained for actual testing for inhibition of the protease activity of BoNT/A LC.[108] Chaetochromin A (**5.2**), a known fungal bis-naphthopyrone, was obtained from our research group as it had been previously isolated from *Chaetomium arcuatum* (NRRL 25243). Chaetochromin A (**5.2**) was found to be active in these assays with up to 74% inhibition in the BoNT/A protease assay (Table 5.1). It was identified as chaetochromin A based on comparison of NMR, MS, and CD data with literature values.[109]

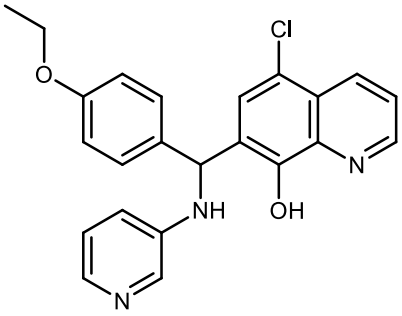

5.1

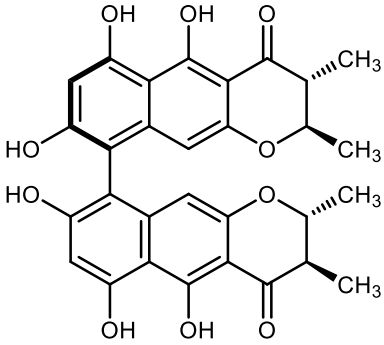

5.2

Based on these results, a search of our compound collection for other structurally similar compounds resulted in selection of five other previously known fungal bis-naphthopyrones for evaluation (**5.3 – 5.6**). These compounds were tested for inhibition of the protease activity of BoNT/A Light Chain (LC) and were all found to be active. While secalonic acid (**5.5**) and cephalochromin (**5.6**) showed activity similar to that of chaetochromin A (**5.2**), talaroderxines A (**5.3**) and B (**5.4**) were found to be more active than **5.2** (Table 5.1). These results validated the initial in silico screening results and prompted more thorough characterization of these compounds.

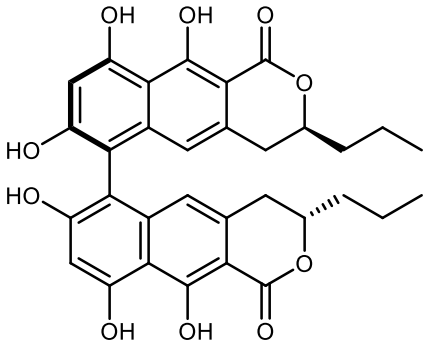

5.3

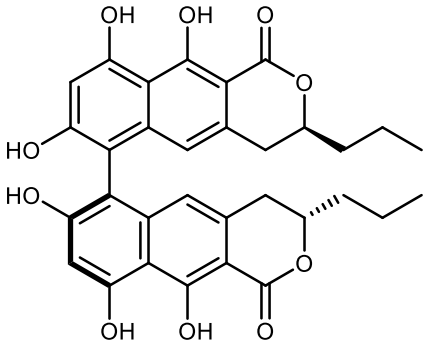

5.4

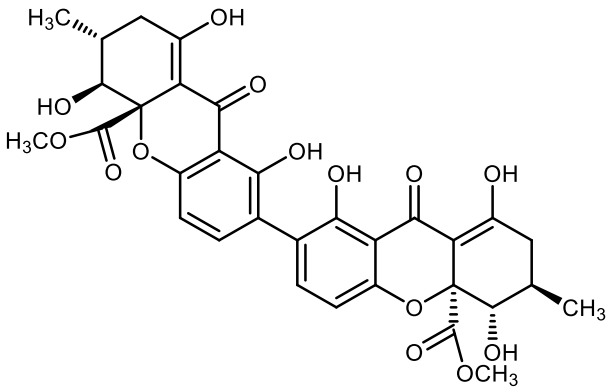

5.5

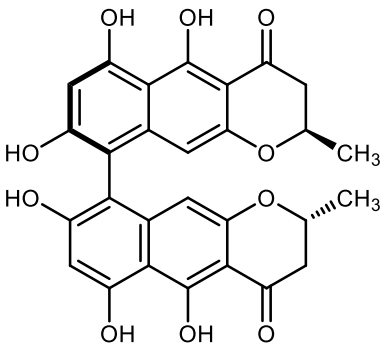

5.6

Table 5.1. BoNT/A protease assay results for fungal bis-naphthopyrones[108]

	BoNT/A protease assay % inhibition (μM)		
Sample	100	20	IC_{50} (μM)
5.1	98.0	96.2	2.1
5.2	74.0	55.0	24.6
5.3	96.0	85.0	3.7
5.4	80.3	67.0	10.1
5.5	64.5	39.1	28.6
5.6	72.0	45.0	29.2
5.7	74.0 (200 μM)	51.0	23.5

Talaroderxines A (**5.3**) and B (**5.4**) had been isolated in our group from a coprophilous *Delitschia* sp. (JS 300), but had reported once before from *Talaromyces derxii*.[110,111] While most of the ^{1}H and ^{13}C NMR signals for these diastereomers were superimposable, some of the ^{1}H NMR signals showed slight differences. In addition, the two compounds gave somewhat gave different $[\alpha]_D$ values. They were originally identified in our lab based on comparison of NMR and MS data with literature values, but had not been studied further at the time because they were previously known.[111] In view

of the bioactivity results, there was a desire to confirm the identities and stereochemical assignments of these compounds. The measured $[\alpha]_D$ values [**5.3**: -40° (*c* 0.4, CH_3OH) and **5.4**: -47 (*c* 0.3, CH_3OH)] were similar to those originally reported (-75.4 and -86.8 for **5.3** and **5.4,** respectively)[111], but the reasons for the differences were unclear. Moreover, this small difference was judged to be insufficient to enable definitive assignment, so a re-assessment was in order. Fortunately, a synthesis of **5.3** and **5.4** had been underataken by Shaw, et al.[112] The synthetic samples of **5.3** and **5.4** showed $[\alpha]_D$ values of +67.1 and -71.8, respectively, which were inconsistent with original literature values.[112] In an effort to clear up this issue, the original culture of *Delitschia* sp. was re-fermented and processed as previously done in our lab to afford a mixture of talaroderxines A and B which was provided to Prof. Shaw's research group for purification using the protocols employed in their synthetic work. The purified talaroderxine A and B samples were found to have $[\alpha]_D$ values of +118 and -215, respectively, suggesting that samples used previously for collecting $[\alpha]_D$ data (both in the original literature and in our work) were not optically pure and that the sign of the rotation of talaroderxine A originally reported was incorrect.[111,112] Because of this confusion, electronic circular dichroism (ECD) data were collected. Due to the barrier to rotation between the individual aryl units, **5.3** and **5.4** have an atropisomeric relationship and give opposite ECD curve shapes. A bisignate ECD spectrum exhibiting negative first (or positive first) and positive second (or negative second) cotton effects because of the coupling between the two bis-naphthopyrone chromophores, corresponds to a counterclockwise (or clockwise) (Figure 5.2) twist along the axial connection (C9 – C-9' bond). This axial chirality is designated as a*R* (or a*S*).[109,113] Based on the ECD curves (Figure 5.3), and their comparison to chaetochromin A (**5.2**), it was realized that the identities of the talaroderxine samples from earlier work in our lab had been switched (i.e., the sample labelled talaroderxine A was actually B, and vice versa. This

mislabeling was done due to lack of detailed interest at the time and was based only on comparison with the literature values, which proved to be incorrect).

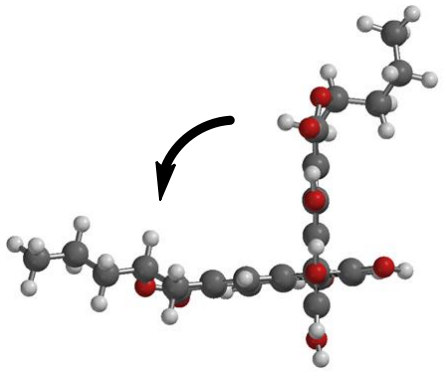

Figure 5.2. Counterclockwise twist along the axial C-9 – C9' bond in talaroderxine B (**5.4**)

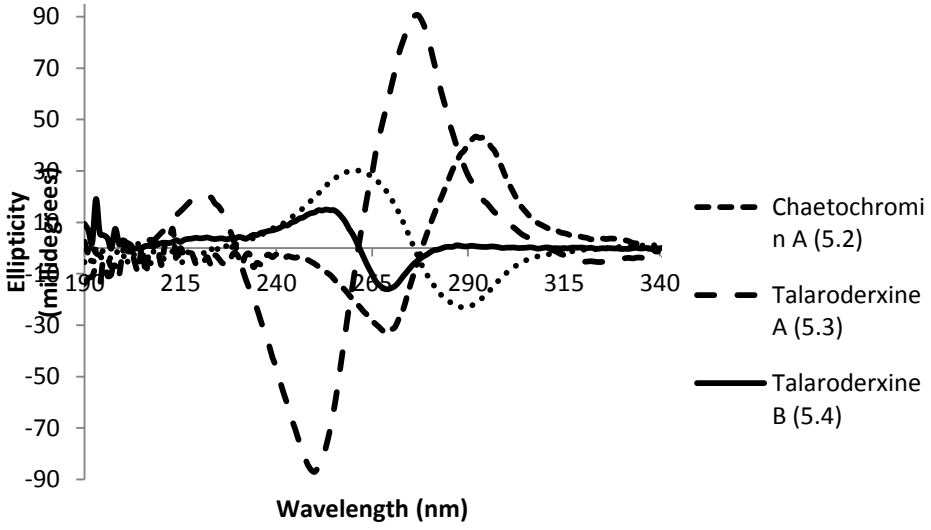

Figure 5.3. ECD curves for **5.3** and **5.4** in CH_3OH, and for **5.2** and **5.7** in dioxane

Another sample of material that was clearly closely related to chaetochromin A (**5.2**) had previously been obtained in our laboratory from a fungicolous isolate of *Acremonium cavaraeanum* (NRRL 29884). It was originally identified as a chaetochromin analogue with a gross structure shown in **5.7** based on comparison of NMR data with literature values,[63,114,115] but was again not investigated further at that time because it did not show activity in our antifungal or insect assays and the gross structure was not new. However, this sample was found to be active in the BoNT/A protease assay (Table 5.1).

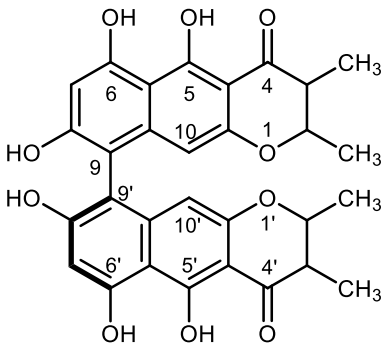

5.7

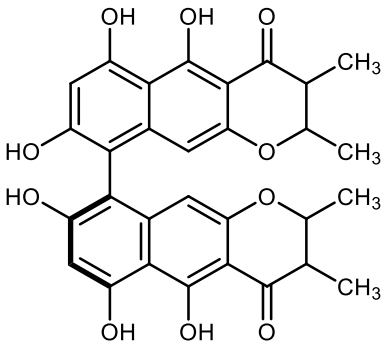

5.8

In view of this bioactivity, efforts were undertaken to completely characterize this sample. The $[\alpha]_D$ value measured for **5.7** [-505º (*c* 0.05, dioxane)] closely matched the literature value reported for isochaetochromin B2 (**5.8**), a literature compound with the same gross structure whose stereochemistry was never assigned.[115] However, observed differences in the ^{1}H NMR data suggested that **5.7** was different in some way, and was therefore a possible new stereoisomer. To explore this, the axial chirality was assessed and established as a*R* by ECD analysis (Figure 5.3). The relative configurations at the C-2, C-3 and C-2', C-3' subunits were established as either *trans* and *cis*, based on 11 Hz and 3.3 Hz couplings observed between H-2 and H-3 or H-2' and H-3', respectively.

However, it was not clear which was which, and the question of absolute configuration at the four sp^3 centers was also a particularly daunting one. Establishment of the absolute configuration at these positions seemed likely to require either X-ray crystallography or synthesis. Given the availability of a relatively large sample in this instance, it was felt that efforts to crystallize the compound would be worthwhile. Because some more impurities were evident by NMR analysis, efforts were undertaken to further purify the sample prior to attempting crystallization.

Several attempts were made to purify **5.7** using different methods including chromatography on C_{18}, silica gel, or Sephadex LH-20, and C_{18} HPLC. Surprisingly, the latter techniques afforded two peaks of similar intensities. The EtOAc extract of the NRRL 29884 culture extract was partitioned between and CH_3CN and hexanes. All the attempts to purify the CH_3CN fraction using Sephadex LH-20 or C_{18} column chromatography resulted in a mixture of two samples. All the fractions containing the two samples were eventually combined together and were separated by C_{18} HPLC to obtain two pure samples (Scheme 5.1). Confusingly, the ^1H NMR data for the two samples (Figure 5.4) did not match each other, neither of them matched the signals observed for the original sample of **5.7**. However, it was apparent that each had the same gross structure, with four characteristic aromatic proton resonances, four methyl doublets, and the corresponding sp^3 methines, which identified these two compounds as unsymmetrical bis-naphthopyrone isomers.

Scheme 5.1. Isolation Scheme for compounds **5.9** and **5.10**

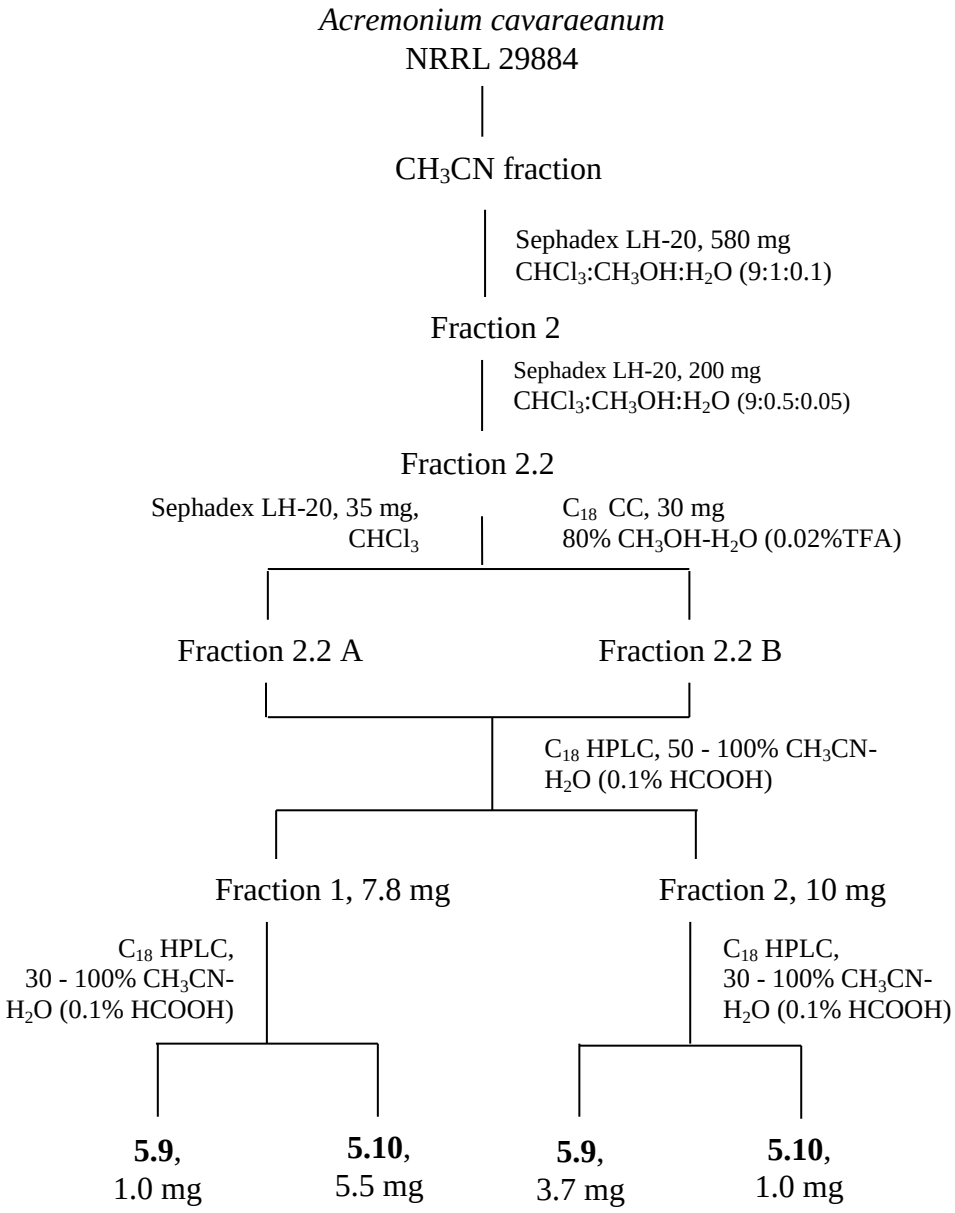

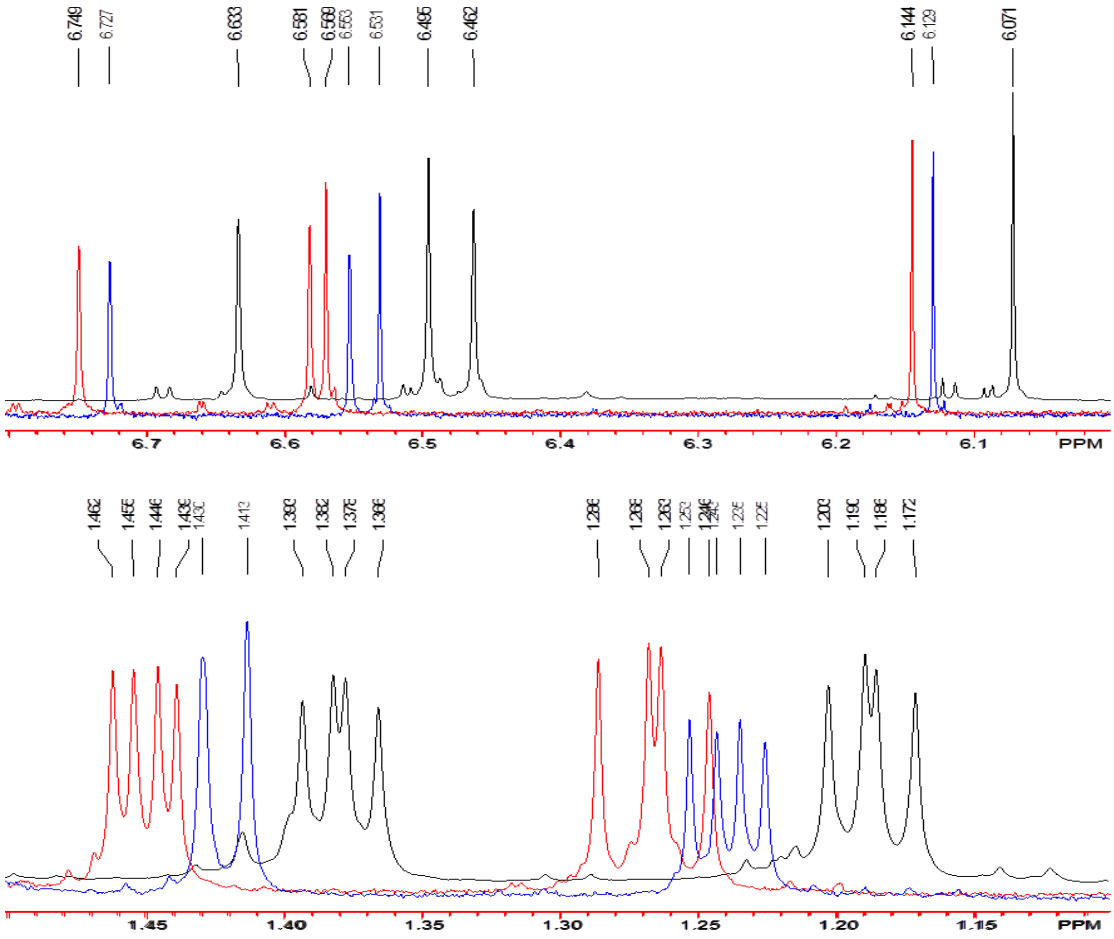

Figure 5.4. ^{1}H NMR data (aromatic and methyl regions) for the two components of **5.7** shown in different colors

Because neither spectrum matched that of the original **5.7** sample, ^{1}H NMR data for a remaining subsample of **5.7** were collected to check for changes or decomposition. Surprisingly, two sets of signals were observed in the ^{1}H NMR spectrum in this instance confirming that **5.7** is actually a mixture. In an effort to judge whether this was the result of decomposition or a concentration-based effect, ^{1}H NMR data on the **5.7** sample were collected at various concentrations (Figure 5.5).

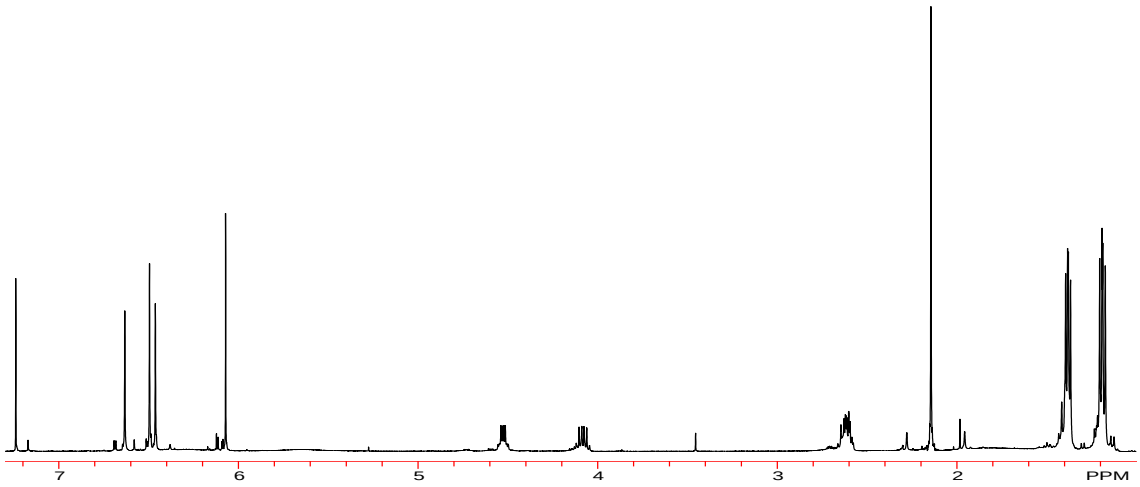

a

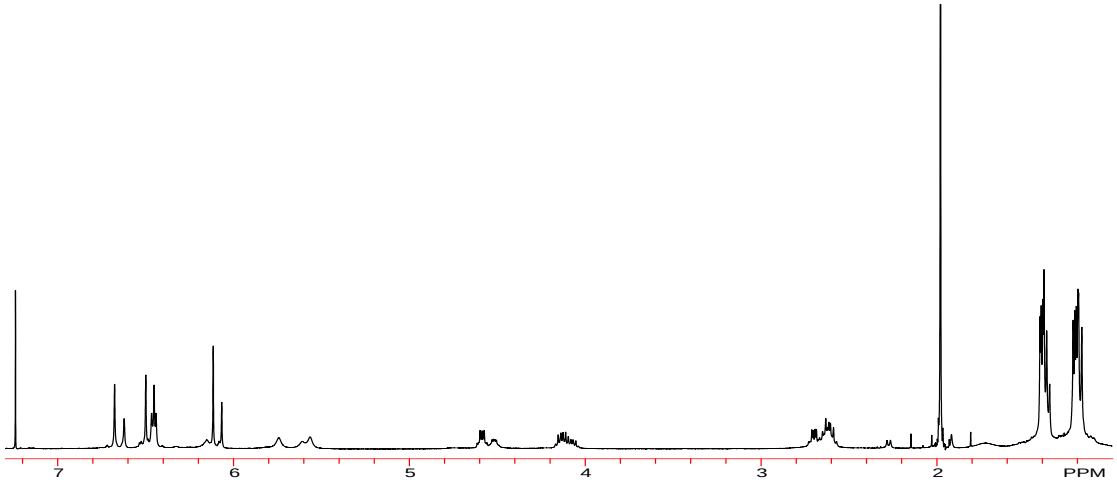

b

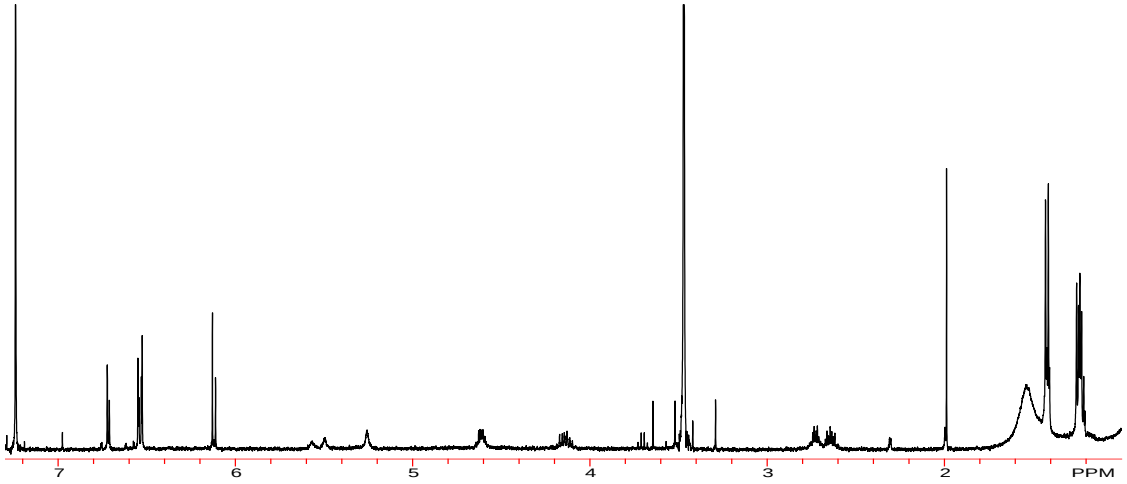

c

Figure 5.5. ^{1}H NMR spectra of the **5.7** sample in $CDCl_3$: (**a**) original spectrum at ca.100 mg/mL (**b**) 44 mg/mL (**c**) 1.2 mg/mL

The results showed resolution (and shifting) of the two sets of ^{1}H NMR signals with decreasing concentration, supporting the observation that the **5.7** sample was indeed a mixture of the two isomers. Samples of the individual components (**5.9** and **5.10**) collected by HPLC were individually tested for biological activity against BoNT/A protease. Interestingly, each was found to be more active than the original **5.7** sample, with **5.10** showing twice the activity of **5.9**, (IC_{50} of 9.3 µg/mL for **5.10** *vs.* 18 µg/mL for **5.9** *vs.* 23.5 µg/mL for **5.7**). Upon collection of ECD data for the separated samples, it became clear that one difference between them was the axial chirality, as the curves were of opposite shape (Figure 5.6). Thus the structures could be differently depicted as shown in **5.9** and **5.10**, but questions still remained regarding the other stereochemical features. The NMR data for **5.9** and **5.10** were consistent (Table 5.2 and Table 5.3) with those of known chaetochromin analogues.[109,114-116]

The axial chirality was established as a*S* and a*R* for **5.9** and **5.10,** respectively by comparison of their ECD curves (Figure 5.6) with that of chaetochromin A (**5.2**). The shape of the ECD curve shown earlier (Figure 5.3) for the original sample of **5.7** (now known to be a mixture of **5.9** and **5.10**) was similar to that of **5.10** and was consistent with the presence of higher amounts of **5.10** in the mixture.

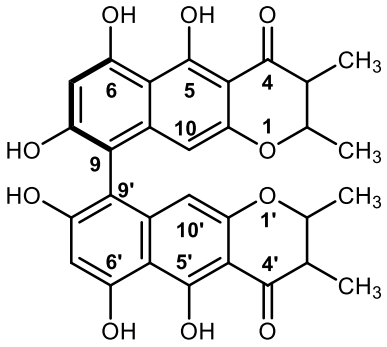

5.9

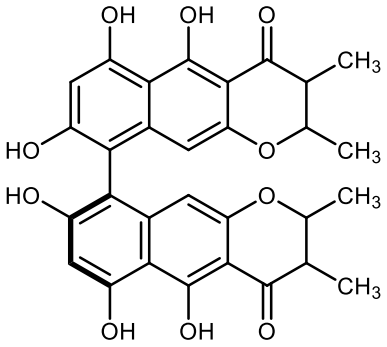

5.10

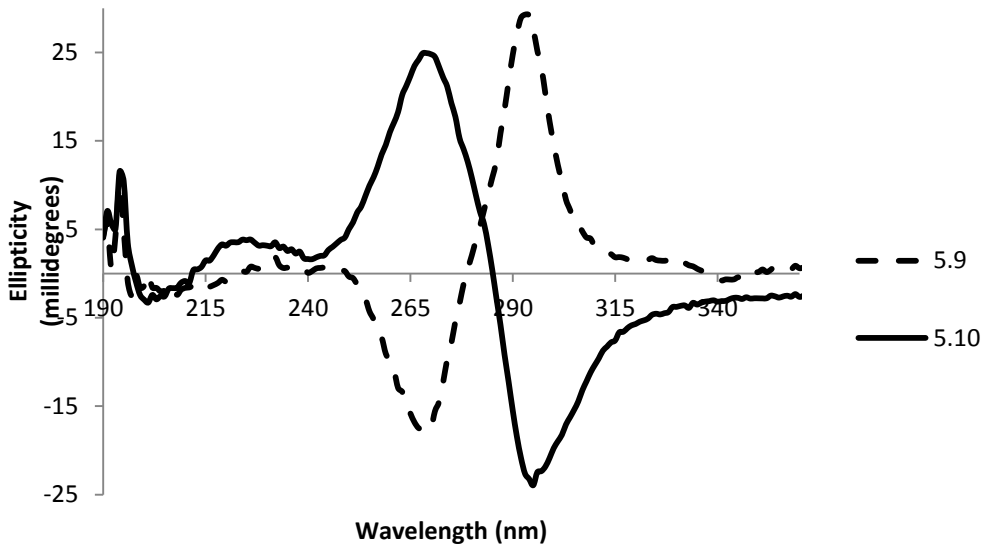

Figure 5.6. ECD curves for **5.9** and **5.10** in CH_3OH

Table 5.2. ^{13}C NMR data for **5.9** and **5.10** in $CDCl_3$ (125 MHz) (10 mg/mL concentration

	δ_C	δ_C		δ_C	δ_C
Position	**5.9**	**5.10**	Position	**5.10**	**5.9**
2, 2'	78.4	78.4	7, 7'	99.8	99.9
	75.6	75.6		102	102
3, 3'	46.1	46.1	8, 8'	159.5	159.7
	44.4	43.4		158.4	158.7
4, 4'	200.7	200.7	9, 9'	141.3	141.3
	202.2	202.2		142.6	142.6
4a, 4a'	102.2	102.5	9a, 9a'	100.04	100.1
	101.5	101.4		102.2	102.5
5, 5'	164.7	164.6	10, 10'	99	99.1
	165.6	165.5		101.4	102
5a, 5a'	105.6	105.6	10a, 10a'	156.1	156.2
	105.1	105		155.5	155.4
6, 6'	161.2	161.1	2, 2'-CH_3	16.6	16.5
	158.3	158.2		19.6	19.6
			3, 3'-CH_3	9.7	9.9
				10.1	9.6

Table 5.3. ^{1}H NMR data for **5.9** and **5.10** in $CDCl_3$ at 1.2 mg/mL concentration

Position	δ_H (mult; *J* in Hz)	δ_H (mult; *J* in Hz)
	5.9	**5.10**
2, 2'	4.15 (dq, 6.4, 11)	4.12 (dq, 6.1, 11)
	4.62 (dq, 3.2, 6.4)	4.60 (dq, 3.3, 6.5)
3, 3'	2.64 (dq, 7.1, 11)	2.65 (dq, 7.0, 11)
	2.73 (dq, 3.2, 7.3)	2.72 (dq, 3.3, 7.3)
7, 7'	6.53 (s)	6.54 (s)
	6.55 (s)	6.55 (s)
10, 10'	6.13 (s)	6.11 (s)
	6.72 (s)	6.72 (s)
2, 2'-CH_3	1.42 (d, 6.4)	1.41 (d, 6.1)
	1.42 (d, 6.4)	1.42 (d, 6.5)
3, 3'-CH_3	1.23 (d, 7.1)	1.22 (d, 7.0)
	1.24 (d, 7.3)	1.24 (d, 7.3)
5, 5'-OH	15.4 (s)	15.4 (s)
	15.5 (s)	15.5 (s)
6, 6'-OH	9.9 (s)	9.93 (s)
	9.75 (s)	9.75 (s)
8, 8'-OH	5.42 (s)	5.51 (s)
	5.20 (s)	5.20 (s)
$CDCl_3$, 400 MHz		

Both **5.9** and **5.10** showed the same gross structural features, including the relative configuration at C-2/C-3 and C-2'/C-3'. In each case, the presence of one *trans* unit and one *cis* unit was recognized based on the coupling constants between H-2/H-2' and H-3/H-3' of 11 and 3.2 Hz, respectively.

To assign the absolute configuration definitively at the sp^3 centers would almost certainly require an X-ray crystal structure. Unfortunately, extensive efforts to crystallize these two isomers were unsuccessful. Efforts to prepare *p*-bromobenzoate derivatives

(using the much larger available sample of **5.7** with the intention of separating after derivatization) resulted in very complex mixtures of products with different numbers of benzoyl groups, even with exhaustive treatment using excess reagents. Efforts to prepare 2,4-dinitrophenylhydrazone derivatives also resulted in complex mixtures of products. Six chaetochromin analogues having the same gross structure, including chaetochromin A (**5.2**), chaetochromin B, ustilaginoidin D, isochaetochromin A_1, B_1, and B_2 have been reported in literature.[114-117] Chaetochromin A (**5.2**) absolute stereochemistry was determined by X-ray crystallography of a *p*-bromobenzoate derivative.[109] However, the absolute stereochemistry of the remaining five isomers has not been established. This would indicate the general challenged faced in crystallizing these compounds or derivatizing them to obtain crystals of derivatives.

Because of the structural similarity of **5.6** (cephalochromin) with **5.9** and **5.10**, and because of the availability of a large sample of **5.6**, it was used as a model compound to further explore possible synthetic modifications. Compound **5.6** was acylated using *p*-bromobenzoyl chloride to obtain a mixture of tribenzoates and a symmetrical dibenzoate (**5.11**). This mixture was further purified to obtain a pure sample of **5.11**. Compound **5.6** was also acetylated using acetic anhydride and pyridine to obtain hexacetate **5.12**. Efforts to crystallize these products are ongoing. It is not clear why similar reactions of **5.7**, **5.9**, and **5.10** do not proceed as cleanly, in spite of repeated attempts using the same conditions. Efforts to co-crystallize **5.6** with 1,2-bis(4-pyridyl)ethane (**5.13**) and trans-1,2-bis(4-pyridyl)ethylene (**5.14**) by forming hydrogen bonds between O-H groups of **5.6** and nitrogen atom of **5.13** and **5.14** were also explored, but did not succeed.[118]

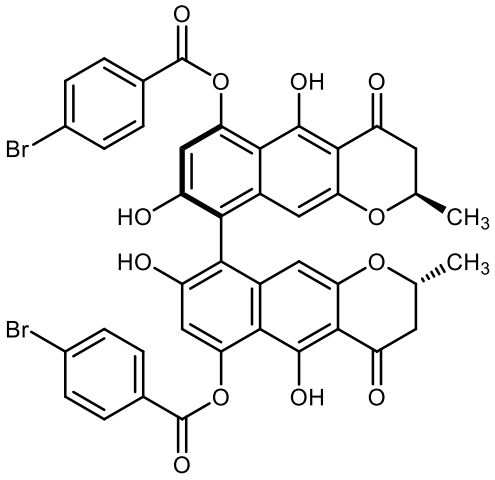

5.11

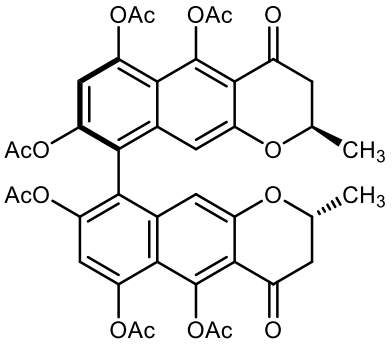

5.12

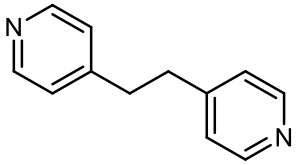

5.13

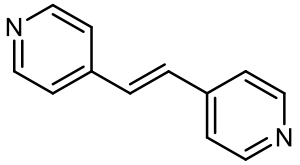

5.14

Two new fungal bis-naphthopyrones **5.9** and **5.10** were isolated from an extract of *A. cavaraeanum.* The absolute stereochemistry of both bis-naphthopyrones remains unassigned and can be established by X-ray crystallization. Both these compounds inhibited the protease activity of the BONTs and could potentially find application as inhibitors of this toxin.

CHAPTER 6

CHEMICAL INVESTIGATION OF AN ENDOPHYTIC ISOLATE OF *PHOMA* SP.

During an investigation of a small collection of fungal endophytes found in prairie grasses, a culture of *Phoma* sp. (ENDO 3417 = NRRL 54108) was isolated from a seed of *Bromus kalmii* obtained from a nursery in Winona, Minnesota. A subculture was deposited in the culture collection at the USDA National Center for Agricultural Utilization Research and assigned the accession number NRRL 54108. The culture was subjected to partial sequence analysis of the internal transcribed spacer region (ITS) and domains D1 and D2 of the nuclear large subunit (28S) rDNA gene using ITS5 and NL4 as polymerase chain reaction and sequencing primers. Sequence data were deposited in GenBank with the accession number HM751088. A nucleotide-to-nucleotide BLAST query of the GenBank database found this isolate to be a close (99%) match with an unnamed *Phoma* sp. isolated from the marine sponge *Tethya aurantium* as well as a few other *Phoma* isolates.[119] Several *Phoma* spp. are often phytopathogenic and cause necrotic lesions on leaves, stems, and fruits.[120-122] There have been several reports of isolation of phytotoxic metabolites from *Phoma* spp., with examples including phomalirazine, epoxydon, altertoxins, putaminoxins, and herbarumins.[120-124]

The ethyl acetate extract of solid state fermentation cultures of ENDO-3417 showed antifungal activity against *Fusarium verticillioides*. Chemical studies of this extract (Scheme 6.1) afforded three new herbarumin analogues that we named herbarumin IV (**6.1**/**6.2**), herbarumin V (**6.3**), and 7-epi-herbarumin V (**6.4**), along with four known compounds that were identified as herbarumin I (**6.5**), herbarumin II (**6.6**), pinolide (**6.7**), and 7-epi-herbarumin III (**6.8**).[120,122,123,125] All of the known compounds encountered had been reported from other *Phoma* spp. isolates except for 7-epi-herbarumin III, which was previously known only as a synthetic product. These known

compounds were identified based on comparison of their NMR and MS data with reported literature values. Several other related nonenolides, including putaminoxin and other herbarumins, have been previously reported from *Phoma* spp.[120-123,126]

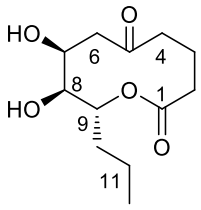

6.1

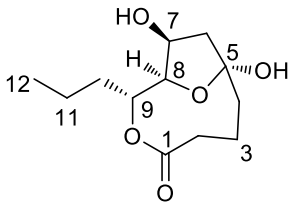

6.2

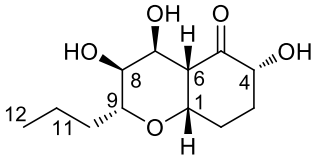

6.3

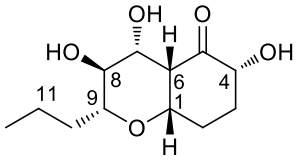

6.4

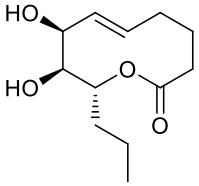

6.5

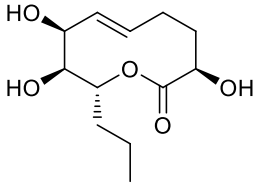

6.6

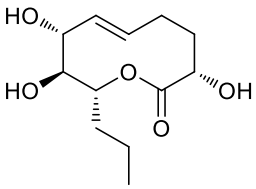

6.7

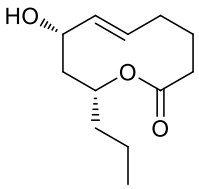

6.8

The EtOAc extract of the *Phoma* sp. solid-substrate fermentation cultures was partitioned between CH_3CN and hexanes and the CH_3CN fraction was further separated by silica gel chromatography, followed by Sephadex LH-20, and reversed phase HPLC to obtain **6.1** – **6.8** (Scheme 6.1).

Scheme 6.1. Isolation of metabolites from *Phoma* sp. (ENDO 3417).

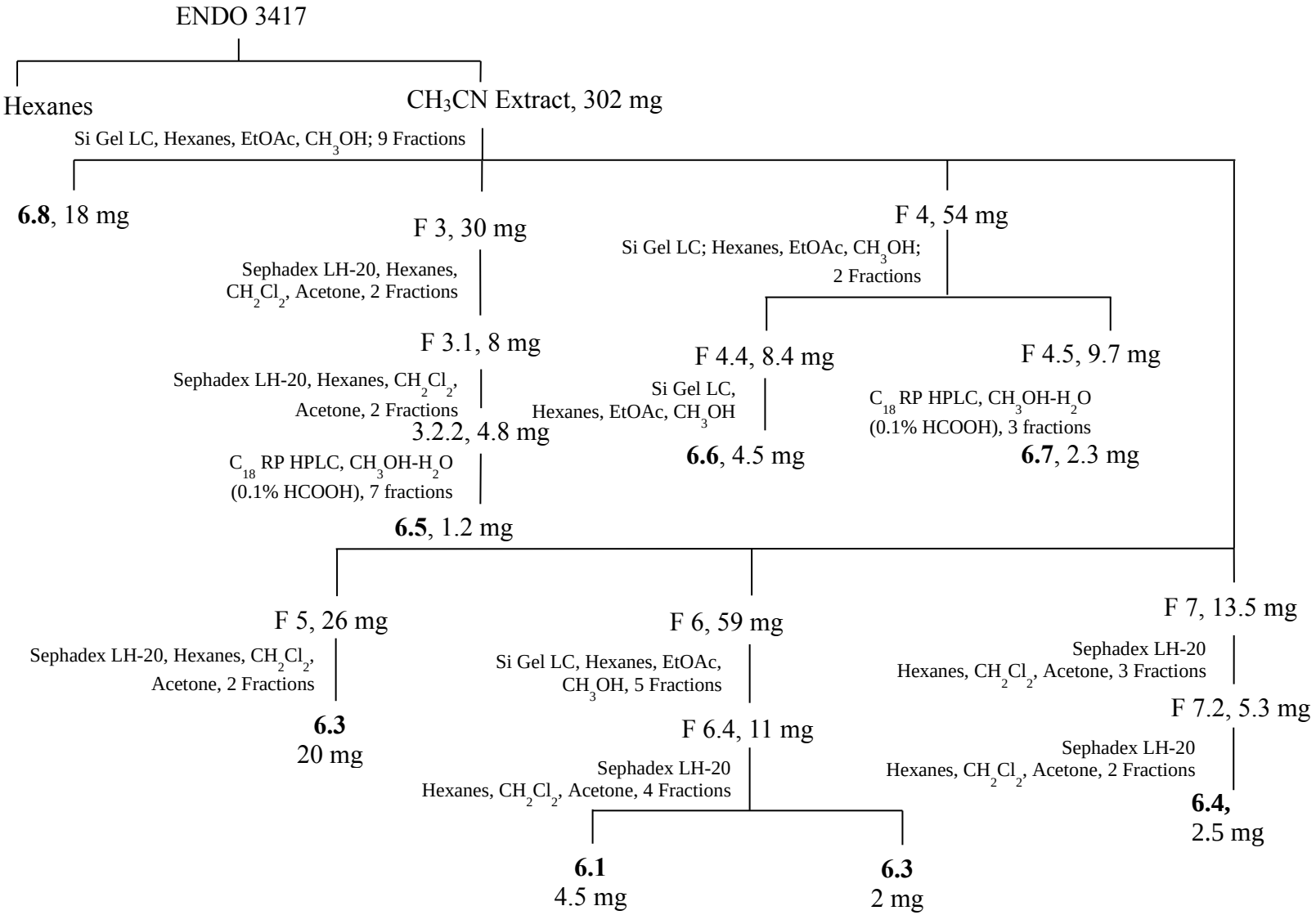

Structure elucidation of Herbarumin IV

Compound **6.1** was obtained as a 6:1 mixture of **6.1** and a related, but minor component (**6.2**). Attempts to separate them were unsuccessful and their ratio remained unchanged through multiple separation steps. Conformational equilibration between two species giving rise to doubled NMR signals in $CDCl_3$ has previously been reported for herbarumin II (**6.5**).[122] However, this doubling was reportedly not observed in CD_3OD because of preference for one conformer in CD_3OD. In the case of our mixture, doubled signals were seen in $CDCl_3$ and CD_3OD, albeit in different ratios. Once the structure and relative configuration has been assigned (see below), conformational analysis of **6.1** was carried out using Spartan 10® employing molecular mechanics MMFF methods. Unlike the results reported for **6.5**, the data indicated that herbarumin IV should exist predominantly in a twist-boat-chair conformer (Figure 6.2) but only a 73% expected abundance.[122] In any event, the cause of the signal doubling in this case was not clear, and was not restricted to a conformational equilibrium.

The molecular formula of the major component of this mixture which we later named herbarumin IV (**6.1**), was determined to be $C_{12}H_{20}O_5$ based on HRESITOFMS [*m/z* 267.1189 $(M+Na)^+$ Δ -1.8 mDa] and NMR data. The NMR and MS data suggested that herbarumin IV is a member of the nonenolide class i.e., a group of fungal polyketides that contain ten-membered lactone rings). The ^1H NMR data (Table 6.1) showed the presence of a methyl triplet along with oxygenated methine resonances similar to those observed in many of the known nonenolides.[120-123] The presence of the methyl triplet and the molecular formula suggested a hexaketide biogenetic origin, along with other structural features commonly found in other nonenolides previously named as herbarumins.[120,122]

Table 6.1. ^{1}H and ^{13}C NMR data for 6.1 and 6.2 in CD_3OD[a]

	6.1		**6.2**	
position	δ_C	δ_H, mult (*J* in Hz)	δ_C	δ_H, mult (*J* in Hz)
1	173.4		177.8	
2a	44.7	2.58 (ov)	38.3	2.34 (ov)
2b		2.4, (ov)		1.96 (ov)
3	22.2	1.9-2.1 (ov)	21	1.8 (ov)
4	36.0	2.4-2.5 (ov)	39.9	1.88 (ov)
				1.8 (ov)
5	212.6		107.6	
6a	44.9	3.28, dd (10, 16)	47.3	2.34 (ov)
6b		2.29, dd (2.6, 16)		1.96 (ov)
7	68.7	4.38, dt (2.0, 10)	70.8	4.48, dt (7.0, 9.2)
8	74.9	3.82, dd (2.0, 4.7)	85.6	3.87, dd (3.7, 7.0)
9	76.9	4.86, dt (4.7, 6.3)	76.6	5.19, dt (3.7, 10)
10	34.3	1.57 (ov)	31.2	1.60-1.70 (ov)
11	19.4	1.31 (ov)	20.4	1.37-1.51 (ov)
12	14.3	0.92, t (7.3)	14.1	0.98, t (7.4)

note. [a] ^{13}C NMR data were recorded at 150 MHz and ^{1}H NMR data were recorded at 400 MHz; ov - overlap

The absence of resonances for *trans* olefinic proton signals indicated that **6.1** was different from known herbarumins. The ^{13}C NMR data showed resonances for a methyl groups, six methylenes, and three oxygenated methines, along with carbonyl resonances for an ester and a ketone. The H-6 – H_2-12 and H_2-4 – H_2-2 spin systems were established as shown in **6.1** based on COSY correlations. The δ-value for C-9 (76.9) and HMBC correlations from H_2-2 and H-9 to C-1 located the ester unit and indicated that the oxygen atom at C-9 was acylated. HMBC correlations from H-7, H-6, and H-4 to the ketone carbonyl (C-5) connected the two spin systems through the ketone, completing the macrolactone structure (Figure 6.1).

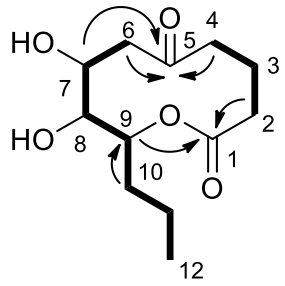

Figure 6.1. Key HMBC (→) and COSY (▬) correlations for **6.1**

The relative configuration was determined by evaluating the coupling constants in conjunction with the generalized Karplus curve and NOESY data (Figure 6.2). A coupling constant of 10.4 Hz between H-6a and H-7 indicated a pseudo axial-axial relationship. H-8 was placed pseudoequatorial to H-7 based on the $J_{H7\text{-}H8}$ value of 2.0 Hz. A NOESY correlation between H-10a and H-7 indicated their proximity in space and was used to determine the relative configuration at C-9. Conformational analysis of the two possible epimers at C-9 (H-8 – H-9 *trans* and H-8 – H-9 *cis*) carried out using Spartan 10®, indicated that the lowest energy conformer of **6.1** in the *trans* epimer is a twist-boat-chair conformation (Figure 6.2), while the *cis* epimer would prefer a chair-boat conformer. In these two lowest energy conformers, the distance between H-10a (the nearest C-10 hydrogen atom to H-7 in the model) and H-7 was calculated as 2.318 Å in the H-8 – H-9 *trans* epimer and as 4.373 Å in the H-8 – H-9 *cis* epimer. Thus, the relative configuration at C-9 could not be determined with certainty on this basis alone because both possible C-9 epimers would place H-7 and H-10a within the ~ 4 - 5 Å limit of the standard NOESY experiment.

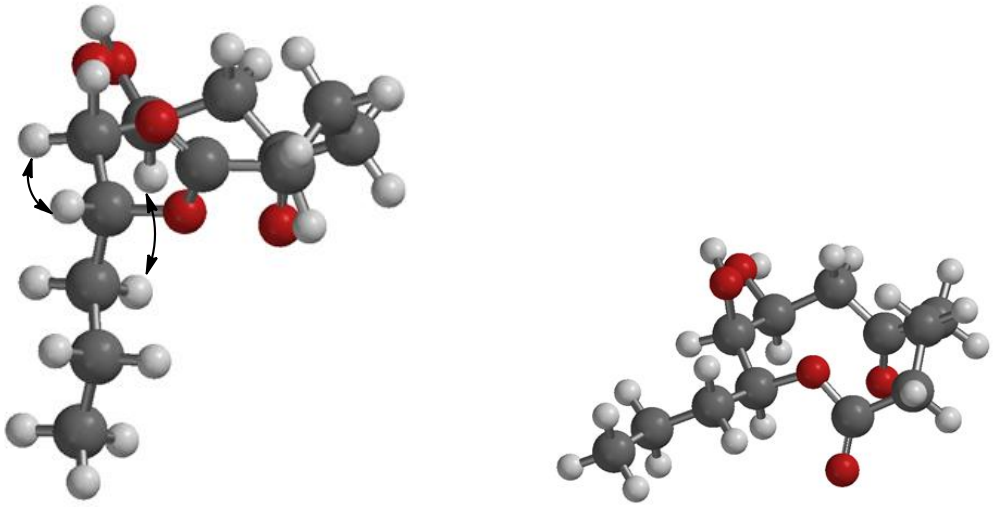

a **b**

Figure 6.2. Energy-minimized model of **6.1** (Spartan 10) – **a**. H-8 – H-9 *trans* (key NOESY correlations) **b**. H-8 – H-9 *cis*

To better approximate the distance between H-10a and H-7 in the natural product, a series of NOESY experiments was performed using different mixing times. The volumes of the cross peaks between H-10a – H-7 and H-6a – H-6b (corresponding to intensities) were measured for each mixing time (Figure 6.3). As can been seen from the chart, the NOE initially increases with increasing mixing time, but eventually plateaus. The distance between methylene protons H-6a and H-6b was determined to be 1.8 Å using an energy minimized model of **6.1** and was used as a standard for calculation. Using the equation,[127]

$$r(H7 - H10a) = \sqrt[6]{\frac{NOE\,(H6a-H6b)}{NOE\,(H7-H10a)} * r(H6a - H6b)^6}$$

the distance between H-10a and H-7 was estimated to be 2.29 Å (Table 6.2). On the basis of the energy minimized conformers of **6.1** and its C-9 epimer, this distance was in much better agreement with a H-8 – H-9 *trans* arrangement.

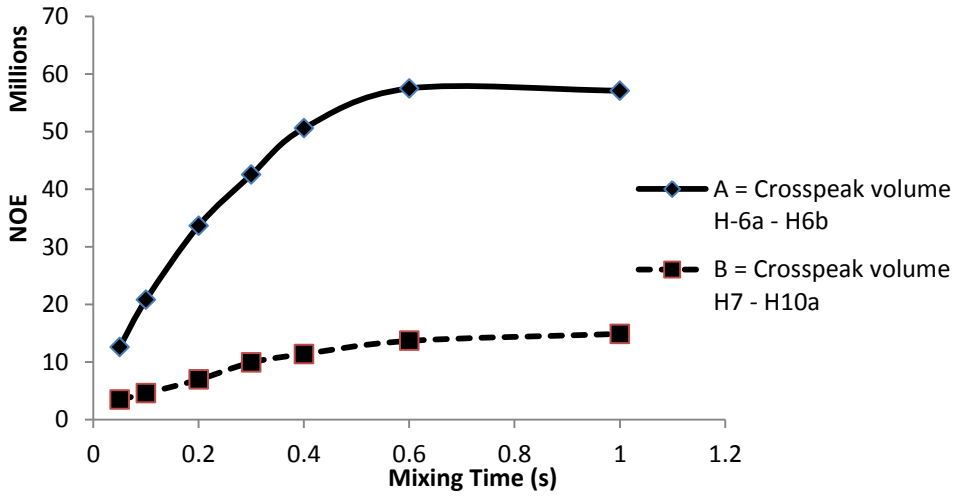

Figure 6.3. Development of NOE with mixing time

Table 6.2. Distance measurement using NOE

Mixing Time	A = NOE (H-6a - H6b)	B = NOE (H7 - H10a)	C = A/B	D = C*1.8^6	*r* (H7 - H10a) = $D^{1/6}$
0.05	1.26E+07	3.47E+06	3.63	123.45	2.23
0.1	2.08E+07	4.56E+06	4.56	155.07	2.32
0.2	3.37E+07	6.95E+06	4.84	164.77	2.34
0.3	4.25E+07	9.92E+06	4.29	145.79	2.29
0.4	5.06E+07	1.14E+07	4.45	151.20	2.31
0.6	5.75E+07	1.37E+07	4.21	143.06	2.29
1	5.71E+07	1.49E+07	3.84	130.51	2.25
				Average	2.29

In an effort to determine the absolute configuration of **6.1**, a sample was treated with *p*-bromobenzoyl chloride. The reaction mixture was then purified by HPLC to obtain pure di-benzoate product **6.9**. Conformational analysis carried out using Spartan 10® employing molecular mechanics MMFF calculations indicated that **6.9** should exist predominantly in a twist boat chair conformer (Figure 6.5).

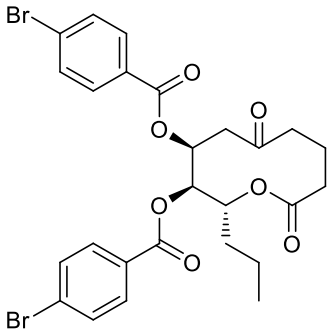

6.9

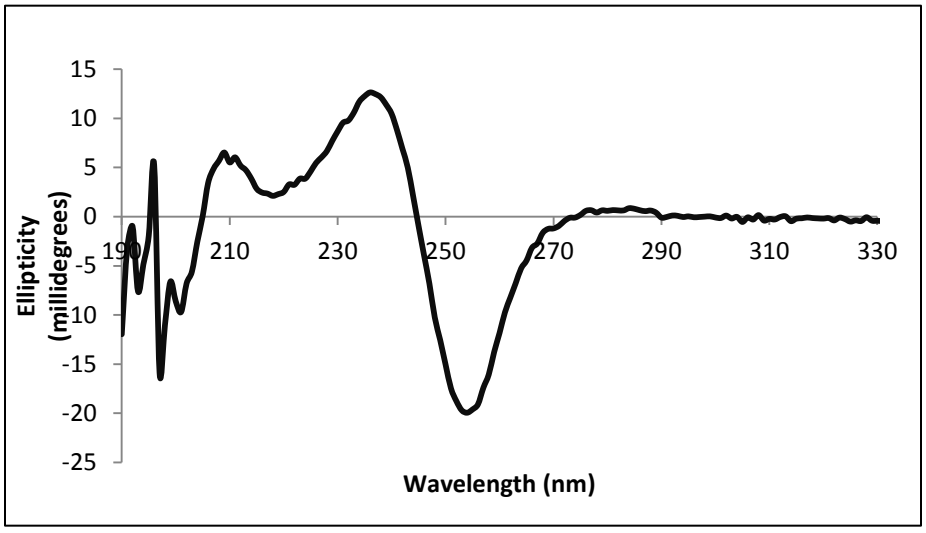

Figure 6.4. ECD spectrum of dibromobenzoate derivative **6.9**

A bisignate electronic circular dichroism (ECD) curve would be expected for **6.9** due to exciton coupling of the two chromophores.[128] The shape of the curve would correspond to the spatial arrangement of the two bromobenzoyl groups, which would be directly related to the absolute configuration. The ECD spectrum of **6.9** was recorded (Figure 6.4), and showed a negative bisignate cotton effect. This result implied a counterclockwise spatial arrangement of the two chromophores (Figure 6.5), thereby enabling assignment of the 7*S*, 8*S*, 9*R* absolute configuration based on the exciton chirality rule.

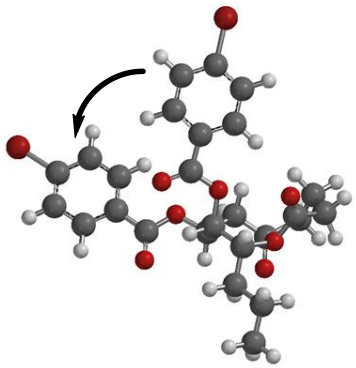

Figure 6.5. Spatial arrangement of the two interacting benzoate groups in dibromobenzoate derivative **6.9**

As noted earlier, all attempts to separate the minor component **6.2** from **6.1** were unsuccessful. The structure of **6.2** was therefore assigned by 2D NMR analysis of the mixture once major component **6.1** had been identified. NMR resonances for the minor component (**6.2)** were similar to those of herbarumin IV except for the replacement of the ketone resonance with a non-protonated carbon at δ 107.6, but with no partner signal in the sp^2 region suggestive of an olefin. This observation suggested that the ketone had

been converted to an acetal-type unit. An HMBC correlation from H-8 to C-5 was consistent with a C-8/C-5 linkage via an oxygen atom to form a hemiacetal structure. The remainder of the structure matched that of **6.1** based on 2D NMR analysis. The relative configuration of **6.2** was proposed by analogy to **6.1**. The 5-OH group was proposed to be anti to OH-7 based on the lowest energy conformer of **6.1** and the corresponding likely preferred face for attack by the bridging oxygen. The ratio of **6.1** to **6.2** changed from 6:1 in CD_3OD to 12:1 in $CDCl_3$. This could mean that **6.1** and **6.2** are in equilibrium with each other, with **6.1** being the preferred form.

Structure elucidation of herbarumin V (**6.3**) and 7-epi-herbarumin V (**6.4**)

Herbarumin V (**6.3**) was assigned a molecular formula of $C_{12}H_{20}O_5$ based on NMR and HRESITOFMS [*m/z* 267.1193 $[M+Na]^+$] data. NMR data for **6.3** (Table 6.3) resembled those of the other herbarumins, but showed a few key differences, most notably the absence of an ester carbonyl group. Based on the HRESITOFMS-derived formula and the presence of a ketone ^{13}C NMR signal corresponding to the only sp^2 carbon, the structure was determined to be bicyclic. ^{13}C NMR data also showed resonances for six methines, four methylenes, and one methyl group. The single spin-system present was assembled based on COSY data. HMBC correlations from H-6, H-7, H-1 and H-4 to ketone carbon C-5 linked C-6 to C-4 via the ketone unit. An HMBC correlation from H-1 to C-9 established a C-1-O-C-9 ether linkage (Figure 6.6).

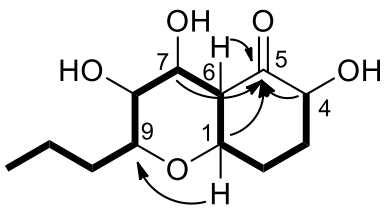

Figure 6.6. COSY (▬) and HMBC (→) correlations for herbarumin V (**6.3**)

The relative configuration of **6.3** was determined based on ^{1}H NMR and NOESY data. A large (>9 Hz) coupling between H-9 and H-8 indicated a *trans* diaxial relationship between them. A 3.0-Hz coupling between H-7 and H-8 placed these protons *cis* with respect to each other. A 1.2-Hz coupling between H-1 and H-6 established a *cis* ring junction, which was supported by a NOESY correlation between the corresponding signals. A NOESY correlation between H-4 and H-6 located these protons 1,3-diaxial with respect to each other (Figure 6.7). Conformational analysis performed using Spartan 10® and molecular mechanics MMFF methods indicated that the lowest energy conformer of **6.3** is a near chair-chair conformation (Figure 6.7).

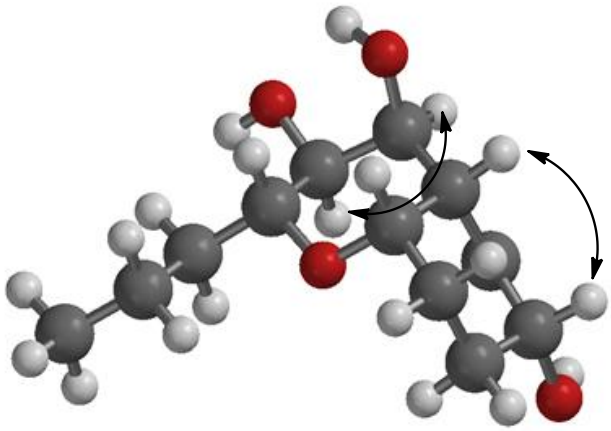

Figure 6.7. Energy-minimized model (Spartan 10) of herbarumin V (**6.3**) showing key NOESY correlations

A positive ECD cotton effect for **6.3** in the n→π* ketone absorption region (Figure 6.8) enabled assignment of the 4*R*, 7*S*, 8*R*, 9*R* absolute configuration based on the octant rule (Figure 6.9).[129] The relative configurations at C-7, C-8, and C-9 are consistent with those seen in **6.1**. This would support a possible mechanism of formation of **6.3** from **6.1** that could be envisioned to involve an aldol-type condensation to link carbons C-1 and C-6.

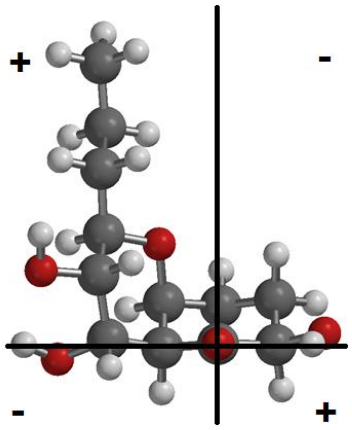

Figure 6.8. Spatial arrangement of energy-minimized conformer of herbarumin V (**6.3**) displayed on the four relevant octants (as viewed along the C=O unit)

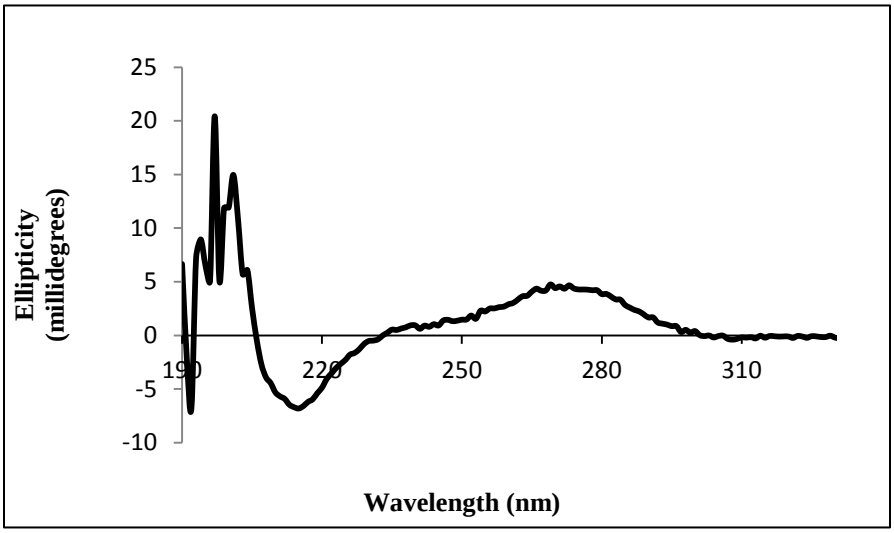

Figure 6.9. ECD spectrum of herbarumin V (**6.3**).

7-Epi-herbarumin V (**6.4**) was identified by an analogous process. The key difference in this case was a 9.2-Hz coupling between H-8 and H-7, placing these protons *trans* diaxial with respect to each other. All other *J*-values and NOESY correlations were similar to those of **6.3 (**Figure 6.10**)**. As was the case with **6.3**, a positive ECD cotton

effect for **6.4** in the n→π* ketone absorption region (Figure 6.11) enabled independent assignment of the 4*R*, 7*R*, 8*R*, 9*R* absolute configuration based on the octant rule.

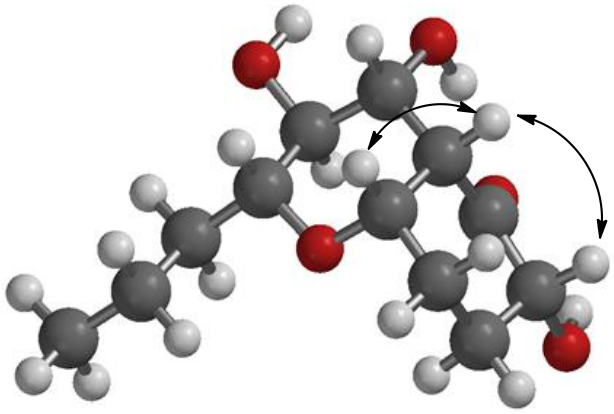

Figure 6.10. Energy-minimized model (Spartan 10) of 7-epi-herbarumin V (**6.4)** showing key NOESY correlations

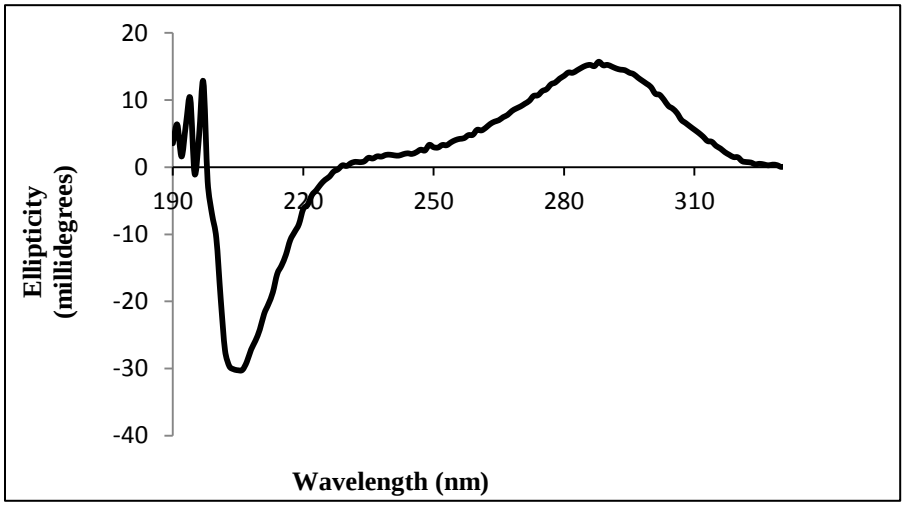

Figure 6.11. ECD spectrum of 7-epi-herbarumin (**6.4**)

Table 6.3. ^{1}H and ^{13}C NMR data for herbarumin V (**6.3**) and 7-epi-herbarumin V (**6.4**) in CD_3OD[a]

	6.3		**6.4**	
position	δ_C	δ_H, mult (*J* in Hz)	δ_C	δ_H, mult (*J* in Hz)
1	74.5	4.27 (m)	79.2	3.95, ddd (1.2, 2.7, 6.2)
2	28.8	1.91-2.05 (m)	29.1	1.98-2.04 (m)
3	32	2.05-2.15 (m)	32.6	2.12 (m)
		1.86-1.91 (m)		1.90 (ov)
4	76.2	4.21, dd (1.2, 7.2)	76.3	4.21, ddd (1.2, 6.6, 12)
5	210.8		212.2	
6	56.1	2.85, dt (1.2, 3.0)	55	3.12,ddd (1.0, 2.7, 5.1)
7	67.5	4.34, t (3.0)	75.4	3.46, dd (5.1, 9.3)
8	69.6	3.39 dd, (3.0, 9.9)	72.5	3.60, t (9.3)
9	77.1	3.49, ddd (2.5, 7.8, 9.9)	81.7	3.06, ddd (2.7, 7.9, 9.3)
10	35.3	1.2-1.4 (m)	35.1	1.73-1.82 (m)
		1.7 (m)		1.36-1.43 (m)
11	19.3	1.2-1.4 (m)	19.5	1.27-1.34 (m)
				1.44-1.53 (m)
12	14.5	0.9, t (7.2)	14.5	0.90, t (7.2)

[a] ^{13}C NMR data were recorded at 150 MHz and ^{1}H NMR data were recorded at 400 MHz; ov - overlap

New analogues **6.1**, **6.3**, and **6.4** did not show activity in standard disk assays against *Staphylococcus aureus* (ATCC 29213), *Bacillus subtilis* (ATCC 6051), *Escherichia coli* (ATCC 25922), or *Candida albicans* (ATCC 10231) at 200 μg/disk. These new analogues along with the known herbarumins were also inactive in antifungal assays against *A. flavus*, and *F. verticillioides.*[120,122] The compounds responsible for the original antifungal activity were probably not recovered during the extensive separation steps.

CHAPTER 7

SUMMARY AND CONCLUSIONS

The research described in this thesis focused on isolation and structure elucidation of metabolites from fungicolous, mycoparasitic, and endophytic fungi. Fungicolous and mycoparasitic fungal isolates were collected from host fungi in Hawaii, whereas endophytic fungi were obtained from healthy crop plants in Illinois and Minnesota. Fermentation extracts produced using individual fungal isolates were generally selected for chemical investigation based on their antifungal activity against two pathogens of corn, *Aspergillus flavus* and *Fusarium verticillioides*, and/or antiinsectan activity against *Spodoptera frugiperda*, an economically important insect crop pest. Chemical investigation of several such fungicolous and endophytic fungal isolates led to the isolation and/or identification of 32 known and 14 new secondary metabolites. In all 18 fungicolous and 14 endophytic isolates were studied that resulted in isolation of 18 and 28 secondary metabolites respectively. Studies on fungicolous fungi resulted in isolation of more new secondary metabolites as compared to endophytic fungi. Details of the isolation and structure elucidation of these metabolites are presented in this thesis.

Along with the known metabolites that were described in chapter 2, several other known fungal metabolites were isolated in course of this work, including rasfonin, mycophenolic acid, tenuazonic acid, secalonic acid, cytochalasin E, and epoxydon were encountered. Of the new compounds that were isolated, two new cyclic glycopeptide analogues were isolated from *Phaeoacremonium* sp. (chapter 4). As reviewed in chapter 1, non-ribosomally synthesized peptides contain many unique structural features and exhibit broad range of activities that are attributed to their structural diversity. *Phaeoacremonium* is a relatively unexplored genus from a chemical standpoint and this was the first report of a peptide-type natural product from a member of this genus. Apart from the pentose unit attached to the carbon skeleton, one of the analogues

phaeoacreamide B **4.2** contained an unusual homoisoleucine unit. There have been only two previous report of this amino acid unit in a peptide from a fungal isolate. Structure elucidation of this peptide was particularly challenging because of extensive overlap in the NMR spectrum, and required chemical derivatization and NMR and MS analysis of the derivatized peptide. The absolute configuration of both the pentose unit and the homoIle unit could not be determined because unavailability of issues described in this thesis. Isolation of these peptides on a larger scale could certainly help in assigning these stereochemical issues.

Three other fugal cyclic peptides (sesquilarins A – C) were isolated from a fungicolous Hawaiian isolate of *Sesquicillium microspora*. This was the first report of cyclic peptides from a member of this genus. Their structures were determined using conventional techniques such as NMR and MS, and were later verified by X-ray crystallography of sesquilarin C.

Fungal bis-naphthopyrones were identified as potential inhibitors of Botulinum neurotoxins (BONTs). Chaetochromin A previously reported from *Chaetomium* sp. and also isolated from prior work in our group, was found to be an effective inhibitor. Further screening of several other fungal bis-naphthopyrones that had been isolated in our research led to recognition of talaroderxines and another pair of chaetochromin analogues as effective inhibitors. Talaroderxines had been isolated from a coprophilous *Delitschia* sp. while the pair of chaetochromin analogues had been isolated from a fungicolous isolate of *Acremonium cavaraeanum*. Further attempts to purify the later two analogues ultimately led to their isolation. Both were found to be potent inhibitors BONTs, but while their stereostructure were partially assigned through work described here, their complete stereochemical assignment proved to be very challenging and still awaits final solution.

While the majority of compounds isolated from endophytic fungal extracts in these studies were previously reported in the literature, some were also found to be new

and have been described in chapter 6. Three new herbarumin analogues, herbarumin IV, V, and 7-epi-herbarumin V were isolated from a *Phoma* sp along with four previously known compounds. Stereochemical assignment of herbarumin IV in particular was challenging because of its conformational flexibility. The stereochemistry was assigned by analysis of NOESY and ECD spectra of its bromobenzoate derivative in conjunction with molecular modelling. The known compounds have been reported to exhibit phytotoxic activity against seedlings of the plant *Amaranthus hypochondriacus*; Such activity might not be expected from metabolites from endophytic isolated, but it was not an objective of our study.

These results show that fungicolous and endophytic fungi are excellent source of structurally diverse and biologically active secondary metabolites. Determination of the structures of these metabolites provided several different kinds of challenges, only some of which were overcome. The known and the new metabolites described in this thesis represent a number of structural classes, including terpenoid, polyketide, peptide, and mixed biogenetic origins, and demonstrate the broad structural diversity of biologically active metabolites that can be found through studies from these targeted niche groups.

CHAPTER 8

EXPERIMENTAL

General Experimental Procedures

Solvents and Reagents

Reagent grade solvents were used for partitioning as well as for column chromatography, and HPLC grade solventswere used for HPLC separations employed during the course of this research. Both were purchased from Fisher Scientific. Distilled water for HPLC applications was purified using a SYBRON/Barnstead NANOpure system with a pre-treatment cartridge (catalog number D0835), two ultrapure cartridges (D0809), and a 0.2-µm hollow fiber filter (D3750). Reagents and deuterated solvents were purchased either from Sigma-Aldrich Chemical Company or Fisher Scientific.

Weight Measurements

Weights of reagents, crude extracts, and fractions obtained after separation techniques were measured using a Mettler AR 160 balance.

Chromatography

Normal-phase TLC separations were performed using pre-coated plastic sheets (Alltech, 0.25-mm thickness silica gel with fluorescent indicator, 40 x 80 mm), whereas, normal phase preparative TLC separations were done using Analtech Uniplate TLC plates (20 x 20 cm, 250 μ). Reversed phase preparative TLC separations were done using Analtech Uniplate TLC plates (10 x 20 cm, 250 μ). TLC spots were visualized by exposure to UV light at 254 nm or by exposure to iodine vapor.

Silica gel column chromatography was carried out using silica gel (63-200-µm particles) from SA Scientific Adsorbents. Sephadex LH-20 (Sigma) was used for performing gel filtration chromatography.

One of the following three Beckman Instruments systems were used for semi-preparative reversed-phase HPLC separations: (**1**) System Gold 127 solvent delivery

module with model 166 photodiode array detector, both controlled by System Gold 32 Karat software using an IBM 300PL PC; (**2**) System Gold 127P solvent delivery module with a model 166P variable wavelength UV detector, both controlled with system Gold software (version 5.1); or (**3**) System Gold 127 solvent delivery module with a model 166 variable wavelength UV detector. All three HPLC systems employed Rheodyne model 7725 injectors. These separations were conducted using Alltech Altima C18 (5-μm particle size, 10.0 mm x 250 mm) or Alltech Apollo C18 (5-μm particle size, 10.0 mm x 250 mm) columns employing a flow rate of 2.0 mL/min unless otherwise noted. Semi-preparative HPLC chromatograms were recorded using a Linear model 1200 chart recorder, and were monitored at selected wavelengths between 210-290 nm.

Spectroscopic Instrumentation

Optical rotations were measured using a Rudolph Research Autopol III automatic polarimeter. UV spectra were recorded using a Varian Cary 100 Bio UV-visible spectrophotometer. Low-resolution EI mass spectra, including those obtained by GC-MS, were acquired at 70 eV on a Finnigan Voyager quadrupole mass spectrometer. Low-resolution ESIMS data, including LC-MSMS data, were obtained using a ThermoFinnigan LCQ ion trap instrument unless otherwise indicated. High resolution EI and ESI mass spectra were recorded using a Micromass Autospec or QTOF Premier mass spectrometer. Tandem mass spectrometry (MS^n) data were obtained using the Q-TOF premier mass spectrometer. Most ^1H NMR data were recorded on Bruker AVANCE-600, DRX-400, or AVANCE-300 spectrometers (5-mm probes) at room temperature. Some ^1H NMR data were recorded on a second Bruker AVANCE-600 spectrometer using a 1.7-mm probe. ^{13}C NMR, DEPT, and homonuclear decoupling experiments were performed on the DRX-400 instrument. All spectrometers used XWINNMR 3.1 or Topspin 1.3 software. The AVANCE-600 operates at ^1H and ^{13}C frequencies of 600.1422 and 150.9203 MHz, respectively. A second AVANCE-600 spectrometer (acquired later) was equipped with a 1.7-mm microprobe. The Bruker DRX-400

spectrometer operated at a ^{1}H frequency of 400.1355 MHz and a ^{13}C frequency of 100.6230 MHz, and used a 5-mm proton-carbon-fluorine-phosphorous (HCFP) probe. The AVANCE-300 spectrometer operated at a ^{1}H frequency of 300.1675 MHz and a ^{13}C frequency of 75.4768 MHz, and used a 5-mm Quadra Nuclei probe (QNP) that detects proton, carbon, fluorine, and phosphorus nuclei. All NMR spectra were recorded in the deuterated equivalents of benzene, chloroform, acetone, methanol, dimethylsulfoxide, acetonitrile, or pyridine, and the chemical shifts are reported in ppm downfield from tetramethylsilane (TMS), with the appropriate residual solvent peaks used as internal reference standards (δ_H/δ_C, 7.16/128.1, 7.24/77.0, 2.05/29.8, 3.31/49.0, 2.50/39.5, 1.94/118.3, and 8.74, 7.58, 7.22/150.4, 135.9, 123.9, respectively). NOESY experiments were conducted on the DRX-400 or AVANCE-600 spectrometers (5-mm and 1.7-mm probes). HMQC, HMBC, TOCSY, COSY, and ROESY experiments were conducted on the AVANCE-600 spectrometers (5-mm and 1.7-mm probes). 1D NMR data were processed using the NUTS program (Acorn NMR Inc., version 5.02). 2D-NMR data were processed using XWINNMR 3.1 on a Silicon Graphics workstation (SGI O2), or TopSpin 1.3, or TopSpin 3.0 on Windows PC. Five-mm 535-pp and 5-mm 528-J4-7 NMR sample tubes were purchased from Wilmad Glass Company, and 1.7-mm sample tubes were purchased from Bruker.

General Procedures for NMR Experiments

DEPT Experiment

DEPT experiments were used to establish carbon multiplicities. Data were recorded on the DRX-400 spectrometer using a file size of 16 K and a suitable receiver gain (RG) for a ^{13}C NMR spectrum. The experiment gives CH and CH_3 carbon signals as positive signals, and CH_2 signals as negative signals in the spectrum. Non-protonated carbon signals do not appear. The experimental parameters were set for the DRX-400 instrument (Bruker software, version 3.1) in the program DEPT135. Once the program

was loaded, a suitable number of scans were entered and the experiment was started by typing zg.

Homonuclear Decoupling Experiment

Homonuclear decoupling experiments were used to determine which protons in a compound are mutually coupled and/or to help obtain ^{1}H-^{1}H coupling constants for individual signals. These experiments were carried out on the DRX-400 spectrometer. A ^{1}H NMR spectrum was first obtained with a suitable number of scans, and saved as a file, entering "1" in the cell labeled as EXPO. The frequencies (O2 values in Hz) of all proton signals to be irradiated were recorded. Different files were created equivalent to the number of protons to be irradiated, and saved with the numbers "2", "3", etc. in the cell labeled EXPO. The decoupling power P24 was set between 50 and 70, usually at 55, and the frequency to be irradiated (O2 value) was then entered for each EXPO experiment. The number of scans for each experiment was equivalent to the number of scans in EXPO 1. The EXPO 2 file was recalled by typing re 2. The acquisition was started by typing multizg and entering the number of experiments into the dialog box. The resulting data were processed using NUTS software.

Homonuclear COSY Experiment

This two-dimensional NMR technique was used to identify proton spin-systems. COSY experiments were conducted using the AVANCE-600 spectrometer. The procedure began with a well-shimmed proton spectrum that was obtained after carefully tuning the probe. Suitable SW and O2 values were calculated from the proton spectrum. A proton pulse calibration was carried out using the pulse program "zg", from which the parameters P0 (90º pulse), P1 (90º pulse), and P2 (180º pulse) were determined. For the 5-mm inverse detection probe, the following parameters were set with the COSYPH pulse program: D1 = 4, TD = 2K, NS = 16 (multiples of 16), DS = 16. DW was automatically set, IN0 = 2 x DW, ND0 = 1, parameter mode was set to 2D, SFO1 = SFO2, SW = SW2 = the desired spectrum window of the ^{1}H NMR spectrum, SW 1 = ½

(SW) = center of the desired spectrum window in Hz, SR = SR1 = SR2 = reference for the ^{1}H NMR spectrum (in Hz). With TD1 = 256, acquisition was started by typing zg. For the 1.7-mm microprobe, the following parameters were set with the COSY pulse program: D1 = 20, NS = multiples of 8, DS = 0, DW was automatically set, IN0 = 2 x DW, ND0 = 1, parameter mode was set to 2D, SFO1 = SFO2, SW = SW2 = the desired ^{1}H NMR spectrum window, O1P = ½ (SW) = center of the desired spectrum window in Hz. After verifying that SW in F1 was the same as SW in F2 and TD = 256 or 512 in F1, acquisition was started by typing zg. When using the AVANCE III-600 (1.7-mm probe), all parameters were preset for this experiment by the Bruker TopSpin 3.0 software pulse program.

TOCSY Experiment

This 2D NMR technique is similar to COSY, except that the second 90º pulse is replaced by a spin-lock stage, and correlations can be observed for all protons within a spin-system, and not just those directly coupled to one another. TOCSY experiments were conducted using the AVANCE-600 spectrometer. The procedure began with a well-shimmed proton spectrum that was obtained after carefully tuning the probe. Suitable SW and O2 values were calculated from the proton spectrum. For the 5-mm inverse detection probe, a proton pulse calibration was carried out using the pulse program "zg", from which the parameters P0 (90º pulse), P1 (90º pulse), and P2 (180º pulse) were determined. The following parameters were set with the "clmlevphpr" pulse program: D1 = 4, TD = 2K, NS = 16 (multiples of 16), DS = 16. DW was automatically set, IN0 = 2 x DW, ND0 = 1, parameter mode was set to 2D, SFO1 = SFO2, SW = SW2 = the desired spectrum window of the ^{1}H NMR spectrum, SW 1 = ½ (SW) with TD1 = 256 = center of the desired spectrum window in Hz, SR = SR1 = SR2 = reference for the ^{1}H NMR spectrum (in Hz). Acquisition was started by typing zg. For the 1.7-mm microprobe, a proton pulse calibration was carried out using the pulse program "zg," from which the parameters P0 (90° pulse), P1 (90° pulse), and P2 (180° pulse) were

determined at the power level -8.30 dB (PLW1). A second proton pulse calibration was also carried out using the pulse program "zg," from which the P6 value was determined (P1/4) at the power level 6.02 dB (PLW10). The following parameters were set with the "clmlevphpr" pulse program: D1 = 4, TD = 2K, NS = 16 (multiples of 16), DS = 16. DW was automatically set, IN0 = 2 x DW, ND0 = 1, parameter mode was set to 2D, SFO1 = SFO2, SW = SW2 = the desired ^{1}H NMR spectrum window, O1P = ½ (SW) = center of the desired spectrum window in Hz, SR = SR1 = SR2 = reference for the ^{1}H NMR spectrum (in Hz). After verifying that SW in F1 was the same as SW in F2 and TD = 256 or 512 in F1, acquisition was started by typing zg.

NOESY Experiment

The relative configuration of certain compounds could sometimes be determined based on the results of NOESY experiments. This type of experiment provides through-space ^{1}H-^{1}H correlations based on the nuclear Overhauser effect. The AVANCE-600 spectrometer was used to carry out NOESY experiments. The procedure began by tuning the probe, followed by obtaining a well-shimmed ^{1}H NMR spectrum. Suitable SW and O2 values were calculated from the ^{1}H NMR spectrum. A proton pulse calibration was carried out using the pulse program "zg", from which the parameters P0 (90º pulse), P1 (90º pulse), and P2 (180º pulse) were determined. A second pulse calibration was created by using the pulse program "t1ir1d" to determine the mixing time by varying the parameter D7 until all peaks in the sample were positive or null. Then d8, the mixing time, was set (D7/0.7). For both the 1.7- and 5-mm inverse detection probes, the following parameters were set with the "noesygpph" pulse program: D1 (relaxation delay) = 4, D8 = (value determined by pulse calibration), TD = 2k or 4k, NS = 8 (multiples of 8), DS = 16. The DW parameter was automatically set and the IN0 parameter was entered as double the value of DW. The parameter mode was set to 2D, ND0 = 1, and FnMODE = TPPI. After verifying that SW in F1 was the same as SW in F2 and TD = 256 or 512 in F1, acquisition was started by typing zg.

ROESY Experiment

ROESY is similar to NOESY, since both experiments provide through-space ^{1}H - ^{1}H correlations based on the nuclear Overhauser effect. ROESY is used primarily for intermediate and high molecular weight compounds that have a small or zero NOE for all distances and mixing times. For the 1.7-mm microprobe, the procedure began with a well-shimmed ^{1}H NMR spectrum that was obtained after carefully tuning the probe. Suitable SW and O2 values were calculated from the ^{1}H NMR spectrum. A proton pulse calibration was carried out using the pulse program "zg," from which the parameters P0 (90° pulse), P1 (90° pulse), and P2 (180° pulse) were determined at the power level -8.30 dB (PLW1). A second proton pulse calibration was also carried out using the pulse program "zg," from which the P25 value was determined at the power level 10.19 dB (PLW27). The following parameters were set with the "roesyph.2" pulse program: D1 (relaxation delay) = 4, D12 (value determined by pulse calibration), TD = 2K or 4K, NS = 8, 16, or 32, DS = 128. The DW parameter was automatically set and the IN0 parameter entered as double the value of DW. The parameter mode was set to 2D, ND0 = 1, and FnMODE = TPPI. After verifying that SW in F1 was the same as SW in F2, and TD = 512 in F1, acquisition was started by typing zg.

HMQC Experiment

The HMQC experiment was used to provide one-bond proton-carbon correlations. This method relies on indirect detection of ^{13}C nuclei by observing their effect on the more sensitive ^{1}H nuclei to which they are coupled (inverse detection). HMQC experiments were conducted on the AVANCE-600 spectrometer. The procedure began by tuning the probe, followed by obtaining a well-shimmed ^{1}H NMR spectrum. Suitable SW and O2 values were calculated from the ^{1}H NMR spectrum. The proton pulse calibration was carried out using the pulse program "zg," from which the parameters P0 (90° pulse), P1 (90° pulse), and P2 (180° pulse) were determined. The following parameters were set with the pulse program "hmqcgpnd1d": D1 = 4 sec, D2 [1/(2xJXH)]

= 3.3 msec (if the experiment is optimized for J = 150 Hz), D13 = 3 μsec, DS = 4, NS = 16, TD = 8K. After the acquisition, the commands FT and MC were entered in order to observe signals for protons bound to ^{13}C atoms and to determine signal intensity to predict the number of scans required for the HMQC experiment. The HMQC experiment was then conducted using the pulse program "hmqcgpqf" with the following parameters: DS = 96, TD = 2K, NS = multiple of 8, RG = 16K, TD (F1 dimension) = 256 or 512, SI = 1K, SFO1 (F1 dimension) = 150.92 MHz, ND0 = 2, IN0 = 15 μsec, O2P = 80. The parameter mode was set to 2D and the acquisition was initiated by typing zg. When using the AVANCE III-600 NMR (1.7 mm probe), all parameters were preset by the Bruker TopSpin 3.0 software pulse program.

HMBC Experiment

Long-range (two- and three-bond) ^{1}H-^{13}C correlations were obtained from this type of experiment. The experiment was conducted on the AVANCE-600 spectrometer using a 5-mm inverse detection probe and the pulse program "hmbcgplpndqf". The parameters and procedures were nearly identical to those used for HMQC, with the exception that IN0 = 13 μsec, and O2P = 100. The D6 parameter was used to optimize the experiment for the desired *J*-value. In most cases, a typical value of 8 Hz was used, which corresponds to a D6 value of 60 msec. As with the HMQC parameters and pulse calibrations, the Avance III-600 NMR (1.7 mm probe), controlled by Bruker TopSpin 3.0, had many of these parameters preset in the selected program simply named HMBC.

Electronic Circular Dichroism (ECD) Analysis

ECD analysis was carried out on an Olis Cary 17 instrument. Samples analyzed on the ECD instrument were prepared in such a way that the maximum UV absorbance was *ca.* one absorbance unit (AU).

General Procedures for Collection and Refinement of X-Ray Data

Procedures for collection and refinement of X-ray data for individual compounds are included in Appendix A. Crystallographic data have been deposited with the Cambridge Crystallographic Data Centre (CCDC). Copies of the data can be obtained, free of charge, on application to the Director, CCDC, 12 Union Road, Cambridge CB2 1EZ, UK (fax: +44-(0) 1223-336033 or email: deposit@ccdc.cam.ak.uk).

GCMS Conditions for Amino Acid Derivative Analysis

A Thermo Voyager single quadrupole mass spectrometer interfaced with a Trace2000 GC equipped with an Agilent Technologies DB-1701 capillary column (30 m x 0.25 mm ID; 0.25 μm film) was used for GCMS analysis. The GC temperature program started at 70°C for one minute, then ramped up at 10°C/min to 280°C and was held there for 18 minutes. Helium was used as the GC carrier gas (1 mL/min flow rate). The GC inlet temperature was set at 280°C. The attached autosampler was set to inject 1 μL for each sample and standard. EIMS data (70 eV) were collected over the mass range 50-700 Da. Thermo's Xcalibur 1.4 software was used for data acquisition and processing.

General Procedures for Isolation of Fungal Species from Wood-Decay Fungi

Collection of wood-decay fungi was carried out by Dr. Donald T. Wicklow of the Bacterial Foodborne Pathogens and Mycology Research Unit, Agricultural Research Service, National Center for Agricultural Utilization Research (NCAUR), United States Department of Agriculture in Peoria, Illinois. Samples of wood-decay fungi were returned to the laboratory in Peoria in plastic bags and placed in a freezer (-7 ºC). In order to isolate microfungal colonies from these host fungi, direct plating of filings from the surface of the samples was accomplished by sprinkling a small portion (100-200 mg)

of the powders over the surface of each of two plates of dextrose-peptone-yeast extract agar (DPYA) containing streptomycin (25 mg/L) and tetracycline (1.25 mg/L). Plates were incubated in the dark at 25 ºC for five days, and representative cultures were isolated from each colony type showing distinctive morphology on DPYA. After 7-12 days of incubation, tube cultures isolated were segregated into groups of presumptive species and maintained for solid-substrate fermentation and potential identification.

General Procedures for Solid-Substrate Fermentations

Fermentation of mycoparasitic/fungicolous/endophytic fungi was conducted in the laboratory of Dr. Donald T. Wicklow of the NCAUR. Fungal strains were cultured on slants of potato dextrose agar (PDA) at 25 ºC for 14 days. Spore inoculum was suspended in sterile distilled H_2O to give a final spore/cell suspension of 1 x 10^6/mL. Fermentation was carried out in 500-mL Erlenmeyer flasks each containing 50 g of rice (Botan Brand; J.F.C. International). Distilled H_2O (50 mL) was added to each flask and the contents were soaked overnight before autoclaving at 15 lb/in^2 for 30 min. After cooling to room temperature, each was inoculated with 1.0 mL of a selected fungal spore inoculum and incubated at 25 ºC for 15-30 days. After incubation, the fermented substrate was mechanically fragmented and extracted with EtOAc (3 x 50 mL). The combined EtOAc extracts were filtered and concentrated under vacuum to give a crude extract. In cases where additional material was needed, this process was scaled up using the number of flasks expected to give the desired amount of crude extract for a given species.

General Procedures for Antifungal Assays

Antifungal assays against *Aspergillus flavus* (NRRL 6541) and *Fusarium verticillioides* (NRRL 25457) were conducted in the laboratory of Dr. Donald T. Wicklow of the NCAUR. A portion of the EtOAc extract of each solid-substrate fermentation culture (approximately 6 mg) was redissolved in EtOAc. One-mg and 0.5-

mg equivalents of extractable residue were pipetted onto individual analytical grade filter paper disks (12.5 mm diameter), which were then placed in individual Petri dish lids and dried for 30 min in a laminar flow hood. After each disk was allowed to dry, up to four disks were placed equidistant from one another on the surface of freshly poured and solidified PDA that was seeded with a spore suspension of *A. flavus* conidia to give a final spore suspension of 1×10^2 cells per mL. These bioassay plates were incubated at 25 ºC for four days and examined for inhibition of *A. flavus* at two and four days as indicated by the presence of a clear or mottled zone around the disk, which is evidence of the inhibition of germination and a measure of fungistatic activity. An analogous procedure was employed for the assay against *F. verticillioides*. Solvent used for extract transfer was used as a negative control. Positive control disks were not used for testing of crude extracts, but were used for later testing of pure compounds. Antifungal assays against *Candida albicans* (ATCC 14053) were conducted in our own laboratory. *C. albicans* test plates were prepared as needed. One *C. albicans* pellet (BioMerieux) was dissolved in 1 mL of sterile H_2O, and 250 μL of the inoculum suspension was transferred to warm agar and mixed thoroughly by gentle swirling. The agar was poured into Petri plates (100 x 15 mm; 5 mL each) which were stored in the refrigerator at 4 ºC. In conducting the disk diffusion assay, each filter paper disk (6.25-mm in diameter) was impregnated with the sample to be tested (typically 100 or 200 μg/disk). After evaporation of the solvent, the disk was placed on the agar surface and incubated at room temperature for 24-72 h. Activity was reported by measuring the diameter (in mm) of the inhibition zone around each disk. Stock solutions of the control antifungal agents filipin or nystatin (Sigma Chemical Co.) at 25 μg/disk were used as positive controls.

General Procedures for Antiinsectan Assays

Antiinsectan assays were developed and conducted by Dr. Patrick F. Dowd, also of the NCAUR.[130] Selection of crude extracts for chemical investigation in search of

antiinsectan metabolites was based on bioactivity against the fall armyworm (*Spodoptera frugiperda*).

S. frugiperda larvae were maintained on a standard pinto bean diet, consisting of the following ingredients: 120 g dried pinto beans, 43 g wheat germ, 28 g brewer's yeast, 8 g Vanderzant's vitamin mix, 2.8 g ascorbic acid, 1.75 g methylparaben, 0.9 g sorbic acid, 12 g sugar, 2 mL formaldehyde (39%), 1.5 mL propionic-phosphoric acid solution (4.2% phosphoric acid), and 550 mL of H_2O. For screening purposes, crude extracts were incorporated into the diet at levels of atleast 200 ppm. Column fractions and pure compounds were tested at levels of up to 1000 ppm or more (wet weight). The samples were added in 125 μL of acetone to test tubes (100 x 16 mm) containing 5-mL aliquots of molten diet (60 ºC). The mixture was then blended with a vortex mixer for 20 seconds. The diets were dispensed into Petri plates, allowed to cool to room temperature, and placed in a fume hood for ca. 20 min to remove residual solvent. The diet was cut into equal blocks (ca. 250 mg). Each block was placed into a single well of a 24-well immunoassay plate, and then a single neonate S. frugiperda larva was added to each well. To prevent dessication of the diet, the plate was covered by a sheet of Parafilm, a sheet of cardboard, and a plastic cover. The cover was secured by two rubber bands. Bioassays were conducted at 27 ºC for seven days at 40% humidity with a 14:10 (light:dark) photoperiod. The insects were inspected at two, four, and seven days for mortality, and seven-day survivors were weighed. A solvent blank was used as a control. Each sample was tested on a total of 40 neonate larvae. Antiinsectan activity was measured by comparison of the test larval weights relative to those of controls. Data were reported as percent reduction in weight gain relative to controls. Percent mortality was recorded in cases where mortality was also observed.

General Procedures for Antibacterial Assays

Bacillus subtilis

In assays using *Bacillus subtilis* (ATCC 6051), one *B. subtilis* pellet (BioMerieux), was dissolved in 1 mL of sterile H_2O, and 250 μL of the inoculum suspension was transferred to warm Penassay seed agar (Difco) and mixed thoroughly by gentle swirling. The agar was poured into Petri plates (100 x 15 mm; 5 mL each) which were stored in the refrigerator at 4 ºC. The antibiotic agent gentamycin (Sigma Chemical Co.) was used as a positive control at a level of 25 μg/disk.

Staphylococcus aureus

In assays using *Staphylococcus aureus* (ATCC 29213) pellets (BioMerieux), one pellet was dissolved in 1 mL of sterile H_2O, and 250 μL of the inoculum suspension was transferred to warm agar and mixed thoroughly by gentle swirling. The agar was poured into Petri plates (100 x 15 mm; 5 mL each) which were stored in the refrigerator at 4 ºC. The antibiotic gentamycin (Sigma Chemical Co.) was again used as a positive control at 25 μg/disk.

Escherichia coli

In assays using *Escherichia coli* (ATCC 25922) pellets (BioMerieux), one pellet was dissolved in 1 mL of sterile H_2O, and 250 μL of the inoculum suspension was transferred to warm agar and mixed thoroughly by gentle swirling. The agar was poured into Petri plates (100 x 15 mm; 5 mL each) which were stored in the refrigerator at 4 ºC. The gentamycin (Sigma Chemical Co.) was used as a positive control at 25 μg/disk.

In conducting all of the above disk diffusion assays, the filter paper disks (6.25-mm in diameter) were impregnated with the sample to be tested (200 μg/disk). After evaporation of the solvent, the disk was placed on the agar surface of a *B. subtilis*, *S. aureus*, or *E. coli* petri plate, and the plate was then incubated at room temperature for 24-48 hr. The antimicrobial activity of the sample was reported by measuring the

diameter (in mm) of the inhibition zone around the disk in which no growth of the test organism was observed.

Procedures for Isolation and Characterization of Metabolites from *Sesquicillium microspora* (MYC-1881)

A fungal isolate (MYC-1881) was obtained from a basidioma of *Phellinus gilvus* found growing on a dead branch in a lowland wet forest, Lava Tree State Park, Puna District, Hawaii. The culture was subjected to partial sequence analysis of the internal transcribed spacer region (ITS) and domains D1 and D2 of the nuclear large subunit (28S) rDNA gene using ITS5 and NL4 as polymerase chain reaction and sequencing primers. A nucleotide-to-nucleotide BLAST query of the GenBank database (http://www.ncbi.nlm.nih.gov/BLAST) identified the isolate as *Sesquicillium microspora. S. microspora* was grown on 6 x 50 g of autoclaved rice for 30 days at 25 °C. The resulting culture material was then extracted with EtOAc, affording 800 mg of crude extract upon evaporation of the resulting filtered solution.

Extraction and Isolation. The crude extract was partitioned between hexanes and CH_3CN. The CH_3CN-soluble fraction (147 mg) was subjected to silica gel column chromatography using a hexanes/EtOAc/CH_3OH step gradient (hexanes; hexanes/EtOAc, 90:10, 75:25; 50:50; 25:75, v/v; EtOAc; EtOAc/CH_3OH, 90:10, 75:25, 25:75, v/v; CH_3OH) to yield eleven 100-mL crude fractions. Fraction 10 (28 mg), which eluted with 1:1-EtoAc/ CH_3OH was subjected to C_{18} RP HPLC (gradient elution using CH_3CN in H_2O (0.1% HCOOH): 60 - 100% for 20 min, 100% CH_3CN for 5 mins; λ=232 nm) to afford sesquilarins A (**3.4**; 4.7 mg), B (**3.5**; 3.6 mg), and C (**3.6**; 1.8 mg). Fraction 11 (13 mg), which eluted with 1:3-EtoAc/CH_3OH was subjected to C_{18} reveresed phase (RP) HPLC (gradient elution using CH_3CN in H_2O (0.1% HCOOH): 60 - 100% for 20 min,

100% CH_3CN for 5 mins; λ=232 nm) to afford additional, but impure sample of sesquilarins A (1.2 mg), B (0.9 mg), and C (1.0 mg).

Chiral Amino Acid Analysis. Samples of **3.4**, **3.5**, and **3.6** (0.2 mg each) were dissolved in 0.5 mL 6N HCl and heated at 110 °C for 24 h in separate vacuum-sealed hydrolysis tubes. In each case, the mixture was then cooled and dried down directly under air flow. The resulting hydrolyzate of **3.4** was dissolved in ~ 1 mL of (+)-*S*-2-butanolic HCl (produced by combining 1 mL (+)-*S*-2-butanol + 35 µL acetyl chloride) and heated at 110 °C for 30 min in a vacuum-sealed hydrolysis tube. After evaporation, the resulting residue was dissolved in 1 mL CH_2Cl_2 and 500 µL of trifluoroacetic anhydride and heated at 150 °C for 5 min. This solution was cooled, dried to near completion under air, diluted with CH_2Cl_2 and subjected to GCMS analysis. The hydrolyzates of **3.5** and **3.6** were subjected to the same protocol.

Derivatives of standard amino acids (1.0 mg each) were prepared in a manner analogous to that described above for the peptide hydrolyzates. GC retention times of each of the trifluoroacetyl (+)-*S*-2-butyl esters of the amino acids were: D-Val (t_R = 11.53), L-Val (t_R = 11.66), D-Ile (t_R = 12.72), L-Ile (t_R = 12.84), D-*allo* Ile (t_R = 12.60), L-*allo* Ile (t_R = 12.72), D-Thr (t_R = 14.22), L-Thr (t_R = 14.33), D-*allo* Thr (t_R = 12.94), L-*allo* Thr (t_R = 13.05), D-Phe (t_R = 17.21), L-Phe (t_R = 17.29), D-MeAla (t_R =11.49), L-MeAla (t_R = 11.49), D-MePhe (t_R =18.08), and L-MePhe (t_R =18.04). Comparison of the retention times and MS data, as well as co-injection of the trifluoroacetyl (±)-2-butyl ester derivatives of the standards with the trifluoroacetyl (+)-*S*-2-butyl ester derivative mixtures prepared from the hydrolyzates of compounds **3.4 – 3.6** allowed identification of the amino acids in each of these peptides.

Sesquilarin A (**3.4**): white powder; $[\alpha]^{25}_D$ -1.008 (*c* 0.1, CH_3OH); UV (*c* 0.1, CH_3OH) λ_{max} (log ε) 207 (4.37) nm; ^1H and ^{13}C NMR data see Table 3.1; key ROESY data (600 MHz; $CDCl_3$) NH (Gly-1) ↔ NH (Val-1), α-H (Val-1) ↔ NH (Thr), α-H (Thr) ↔ NH (Ile), α-H (Ile) ↔ NCH_3 (NMeAla), α-H (NMeAla) ↔ NH (Gly-2), NH (Gly-2)

↔ NH (Phe), α-H (NMeThr) ↔ NH (Val-2), NH (Val-2) ↔ NCH_3 (NMePhe); α-H (NMePhe) ↔ NH(Gly-1); (HRESITOFMS *m/z* 1035.5887 $[M+H]^+$, calcd for $C_{52}H_{78}N_{10}O_{12}$, 1035.5879. HRESITOFMSMS *m/z* 320.1592 (Gly – Phe – N-MeThr, $C_{16}H_{22}N_3O_4$, calcd. 320.1610), 456.2806 (Val-1 – Thr – Ile – N-MeAla – Gly-2, $C_{21}H_{38}N_5O_6$, calcd. 456.2781), 580.3084 (Phe – N-MeThr – Val-2 – N-MePhe – Gly-1, $C_{31}H_{42}N_5O_6$, calcd. 580.3135), 716.4347 (peptide minus Gly-2 – Phe – N-MeThr, $C_{36}H_{58}N_7O_8$, calcd. 716.4347).

Sesquilarin B (**3.5**): white powder; $[\alpha]^{25}_D$ -0.817 (*c* 0.1, CH_3OH); UV (*c* 0.1, CH_3OH) λ_{max} (log ε) 206 (4.35) nm; ^1H and ^{13}C NMR data see Table 3.2; key ROESY data (600 MHz; $CDCl_3$) NH (Gly-1) ↔ NH (Ile-1), α-H (Ile-1) ↔ NH (Thr), α-H (Thr) ↔ NH (Ile-2), α-H (Ile-2) ↔ NCH_3 (NMeAla), α-H (NMeAla) ↔ NH (Gly-2), NH (Gly-2) ↔ NH (Phe), α-H (NMeThr) ↔ NH(Val), NH(Val) ↔ NCH_3 (NMePhe); α-H (NMePhe) ↔ NH(Gly-1); HRESITOFMS *m/z* 1049.6050 $[M+H]^+$, calcd for $C_{53}H_{80}N_{10}O_{12}$, 1049.6035. HRESITOFMSMS *m/z* 320.1606 (Gly – Phe – N-MeThr, $C_{16}H_{22}N_3O_4$, calcd. 320.1610), 470.2975 (Ile-1 – Thr – Ile-2 – N-MeAla – Gly-2, $C_{22}H_{40}N_5O_6$, calcd. 470.2979), 580.3136 (Phe – N-MeThr – Val-2 – N-MePhe – Gly-1, $C_{31}H_{42}N_5O_6$, calcd. 580.3135), 730.4507 (peptide minus Gly-2 – Phe – N-MeThr, $C_{37}H_{60}N_7O_8$, calcd. 730.4503).

Sesquilarin C (**3.6**): white powder; $[\alpha]^{25}_D$ -0.38 (*c* 0.1, CH_3OH); UV (*c* 0.1, CH_3OH) λ_{max} (log ε) 205 (4.08) nm; ^1H and ^{13}C NMR data see Table 3.3; key ROESY data (600 MHz; $CDCl_3$) NH (Gly-1) ↔ NH (Ile-1), α-H (Ile-1) ↔ NH (Thr), α-H (Thr) ↔ NH (Ile-2), α-H (Ile-2) ↔ NCH_3 (NMeAla), α-H (NMeAla) ↔ NH (Gly-2), NH (Gly-2) ↔ NH (Phe), α-H (NMeThr) ↔ NH(Ile-3), NH(Ile-3) ↔ NCH_3 (NMePhe); α-H (NMePhe) ↔ NH(Gly-1); HRESITOFMS *m/z* 1063.6204 $[M+H]^+$, calcd for $C_{54}H_{82}N_{10}O_{12}$, 1063.6192. HRESITOFMSMS *m/z* 320.1602 (Gly – Phe – N-MeThr, $C_{16}H_{22}N_3O_4$, calcd. 320.1610), 470.2975 (Ile-1 – Thr – Ile-2 – N-MeAla – Gly-2, $C_{22}H_{40}N_5O_6$, calcd. 470.2979), 594.3290 (Phe – N-MeThr – Ile-3 – N-MePhe – Gly-1,

$C_{32}H_{44}N_5O_6$, calcd. 594.3292), 744.4667 (peptide minus Gly-2 – Phe – N-MeThr, $C_{38}H_{62}N_7O_8$, calcd. 744.4660).

X-ray Crystallographic Analysis of sesquilarin C (3.3). Crystal was obtained from CH_2Cl_2 (5% hexanes). A colorless plate (0.15 x 0.10 x 0.02 mm) was isolated from the sample and mounted with grease on the tip of a nitrile polymer mount wrapped around a stainless steel pin epoxied to a brass pin and placed on the diffractometer with the long crystal dimension (unit cell a-axis) approximately parallel to the diffractometer phi axis. Intensity data were collected at **150K** on a D8 goniostat equipped with a Bruker APEXII CCD detector at Beamline 11.3.1 at the Advanced Light Source (Lawrence Berkeley National Laboratory) using synchrotron radiation tuned to λ=0.77490Å. For data collection ,frames were measured for a duration of 2-s at 0.3^o intervals of ω with a maximum 2θ value of ~60^o. The data frames were collected using the program APEX2 and processed using the program SAINT routine within APEX2. The data were corrected for absorption and beam corrections based on the multi-scan technique as implemented in SADABS. (Appendix B)

Procedures for Isolation and Characterization of Metabolites from *Phaeoacremonium* sp. (MYC-2025)

Fungal Material. A fungal isolate (MYC-2025) was obtained from black stromata of a pyrenomycete found on a dead hardwood branch in a Hawaiian lowland wet forest, Mackenzie State Park, Puna District, Hawaii. A subculture was deposited in the culture collection at the USDA NCAUR and assigned the accession number NRRL 54515. The culture was subjected to partial sequence analysis of the internal transcribed spacer region (ITS) and domains D1 and D2 of the nuclear large subunit (28S) rDNA gene using ITS5 and NL4 as polymerase chain reaction and sequencing primers. A nucleotide-to-nucleotide BLAST query of the GenBank database (http://www.ncbi.nlm.nih.gov/BLAST) identified the isolate as *Phaeoacremonium* sp.

Phaeoacremonium sp. was grown on 6 x 50 g of autoclaved rice for 30 days at 25 °C. The resulting culture material was then extracted with EtOAc, affording 570 mg of crude extract upon evaporation of the resulting filtered solution.

Extraction and Isolation. The crude extract was partitioned between hexanes and CH_3CN. The CH_3CN soluble fraction (571 mg) was subjected to silica gel column chromatography using a hexanes/CH_2Cl_2/CH_3OH step gradient (hexanes; hexanes/CH_2Cl_2, 75:25; 50:50; 25:75, v/v; CH_2Cl_2; CH_2Cl_2/CH_3OH, 95:5, 90:10, 80:20, 70:30, 50:50, 25:75, v/v; CH_3OH) to yield twelve 100-mL crude fractions. Fraction 8 (24 mg), which eluted with 80:20, CH_2Cl_2/CH_3OH was subjected to RP HPLC (isocratic elution using 100% CH_3CN for 20 mins; λ=216 nm) to afford phaeoacreamide A (**4.1**; 0.9 mg) and B (**4.2**, 0.5 mg). Fraction 9 (20 mg), which eluted with 70:30 - CH_2Cl_2/ CH_3OH was subjected further to RP HPLC (isocratic elution using 100% CH_3OH for 20 mins; λ=216 nm) to afford impure sample of phaeoacreamides A (1.0 mg) and B (0.6 mg).

Acetylation of phaeoacreamides A (4.1) and B (4.2). A solution of **4.1** or **4.2** (0.4 mg) in dry pyridine (2 mL) was treated with excess of acetic anhydride. The mixture was stirred for 48 hrs under N_2. The crude mixture was washed with CH_2Cl_2 (10 mL) and H_2O (10 mL). The organic layer was separated and again washed with CH_2Cl_2 (10 mL) and H_2O (10 mL). The organic layer was separated and dried to obtain the pentaacetate. ^{1}H and ^{13}C NMR data see Table 4.2 and Table 4.4.

Chiral Amino Acid Analysis. Samples of **4.1** and **4.2,** (0.2 mg each) were dissolved in 0.5 mL 6N HCl and heated at 110 °C for 24 h in separate vacuum-sealed hydrolysis tubes. In each case, the mixture was then cooled and dried down directly under air flow. The resulting hydrolyzate of **4.1** was dissolved in ~ 1 mL of (+)-*S*-2-butanolic HCl (1 mL (+)-*S*-2-butanol + 35 µL acetyl chloride) and heated at 110 °C for 30 mins in a vacuum-sealed hydrolysis tube. After evaporation, resulting residue was dissolved in 1 mL CH_2Cl_2 and 500 µL of trifluoroacetic anhydride and heated at 150 °C for 5 min. This solution was cooled, dried to near completion under air, diluted with

CH_2Cl_2 and subjected to GCMS analysis. The hydrolyzate of **4.2** was subjected to the same protocol.

Derivatives of standard amino acids (1.0 mg each) were prepared in a manner analogous to that as described above for the peptide hydrolyzates. A mixture of diastereomers prepared from a mixture of enantiomers of each amino acids was co-injected with derivatized enantiopure amino acid to determine the retention time. Retention times of each of the trifluoroacetyl (+)-*S*-2-butyl esters of the amino acids were: D-Val (t_R = 11.53), L-Val (t_R = 11.66), D-Ile (t_R = 12.72), L-Ile (t_R = 12.84), D-alloIle (t_R = 12.60), L-alloIle (t_R = 12.72), D-MeVal (t_R =), L-MeVal (t_R =), D-Ser (t_R =), L-Ser (t_R =). Comparison of the retention times and MS data of the trifluoroacetyl (±)-2-butyl ester derivatives of the standards with the trifluoroacetyl (+)-*S*-2-butyl ester derivative mixtures prepared from the hydrolyzates of compounds **4.1** and **4.2** allowed identification of the amino acids in each of these peptides.

Preparation of D-ribono-1,4-lactone.[96] A solution of D-ribose (5.0 mg) in H_2O (1 mL) was treated with bromine (1 mL), and the mixture was stirred in dark at RT for 4 days in a vial. Excess bromine was removed under pressure. The resulting solution was neutralized by treatment with silver carbonate. The precipitate was removed by filtration and the filtrate was concentrated under air to obtain D-ribono-1,4-lactone. ^{1}H NMR ($CDCl_3$, 400 MHz) δ 4.58 (d, 5.5 Hz, H-2), 4.29 (dd, 5.5, 0.8 Hz, H-3), 4.36 (t, 3.0 Hz, H-4), 3.79 (dd, 3.0, 12.5 Hz, H-5a), 3.72 (dd, 3.0, 12.5 Hz, H-5b).

Preparation of D-xylono-1,4-lactone.[96] This product was prepared by using D-xylose using in a manner analogous to that described previously. ^{1}H NMR ($CDCl_3$, 400 MHz) δ 4.46 (d, 7.5 Hz, H-2), 4.37 (t, 7.5 Hz, H-3), 4.50 (ddd, 3.6, 3.6, 7.5 Hz, H-4), 3.90 (dd, 3.6, 12.5 Hz, H-5a), 3.82 (dd, 3.0, 12.5 Hz, H-5b).

Preparation of D-arabino-1,4-lactone.[96] This product was prepared by using D-arabinose using in a manner analogous to that described above. ^{1}H NMR ($CDCl_3$, 400

MHz) δ 4.35 (d, 8.0 Hz, H-2), 4.16 (t, 8.0 Hz, H-3), 4.13 (ov, H-4), 3.90 (dd, 1.9, 13 Hz, H-5a), 3.69 (dd, 4.0, 13 Hz, H-5b).

Phaeoacreamide A (**4.1**): white powder; $[\alpha]_D^{25}$ -0.68 (*c* 0.05, CH_3OH); ^1H and ^{13}C NMR data see Table 4.3; HRESITOFMS, 1128.7151 $[M+H]^+$, calcd for $C_{54}H_{98}N_9O_{16}$. HRESITOFMSMS *m/z* 342.2350 N-MeThr-Ile-N-MeVal ($C_{17}H_{32}N_3O_4$, calcd. 342.2393), *m/z* 472.2600 N-MeLeu-THPA-Val1-N-MeThr minus H_2O ($C_{21}H_{34}N_3O_9$, calcd. 472.2295), *m/z* 716.4399 Ile3-N-MeLeu-THPA-Val1-N-MeThr-Ile1 ($C_{34}H_{62}N_5O_{11}$, 716.4446).

Phaeoacreamide B (**4.2**): white powder; $[\alpha]_D^{25}$ -0.56 (*c* 0.05, CH_3OH); ^1H and ^{13}C NMR data see Table 4.1; key HMBC and ROESY data (600 MHz; $CDCl_3$) See Figure 4.2. HRESITOFMS *m/z* 1142.7301 $[M+H]^+$, calcd for $C_{55}H_{100}N_9O_{16}$. HRESITOFMSMS *m/z* 342.2353 N-MeThr-Ile-N-MeVal ($C_{17}H_{32}N_3O_4$, calcd. 342.2393), *m/z* 486.2805 N-MeHomoIle-THPA-Val1-N-MeThr minus H_2O ($C_{22}H_{36}N_3O_9$, calcd. 486.2452), *m/z* 730.4586 Ile3-N-MeHomoIle-THPA-Val1-N-MeThr-Ile1 ($C_{35}H_{64}N_5O_{11}$, calcd. 730.4602).

Pentaacetate phaeoacreamide A (**4.3**): ^1H and ^{13}C NMR data see Table 4.4. HRESITOFMS *m/z* 1338.7690 $[M+H]^+$, calcd for $C_{64}H_{108}N_9O_{21}$ (calcd. 1338.7660).

Pentaacetate phaeoacreamide B (**4.4**): ^1H and ^{13}C NMR data see Table 4.2. HRESITOFMS *m/z* 1374.7672 $[M+Na]^+$, calcd for $C_{65}H_{109}N_9O_{21}Na$ (calcd. 1374.7636).

Procedures for Isolation and Characterization of Metabolites from *Acremonium cavaraeanum.* (NRRL 29884)

Fungal Material. A subculture of MYC 1150 = NRRL 29884 deposited in the culture collection at the USDA NCAUR was regrown on 6 x 50 g of autoclaved rice for 30 days at 25 °C. The resulting culture material was then extracted with EtOAc,

affording aprroximately 3 g of the crude extract upon evaporation of the resulting filtered solution.

Extraction and Isolation. The crude extract was partitioned between hexanes and CH_3CN. A portion (580 mg) of the total CH_3CN fraction was separated by sephadex LH-20 chromatography using isocratic $CHCl_3/CH_3OH/ H_2O$ (9:1:0.1) to give 3 fractions. Sub-fraction 2 was further separated by sephadex LH-20 chromatography using isocratic $CHCl_3/CH_3OH/H_2O$ (9:0.5:0.05) to give 3 fractions. A portion of sub-fraction 2.2 from sephadex LH-20 (35 mg) was separated by sephadex LH-20 chromatography using isocratic $CHCl_3$ to give three fractions including fraction 2.2 A. Another portion of sub-fraction 2.2 (30 mg) was separated by C_{18}RP column chromatography using 80% CH_3OH in H_2O (0.2 % TFA) to give fraction 2.2 B. Sub-fractions 2.2 A and 2.2 B were combined with original fraction 2.2. The combined sample (Fraction 2.2) was then subjected to RP HPLC with gradient elution using 50% CH_3CN in H_2O (0.1 % HCOOH) for 15 mins, 50 – 100% in 25 mins, isocratic CH_3OH for 10 mins; 286 nm) to afford two fractions 1 and 2. Fraction 1 was further purified by RP HPLC gradient elution using (30% CH_3CN in H_2O (0.1 % HCOOH) for 15 mins, 30 – 100% in 15 mins, isocratic CH_3OH for 15 mins; 254 nm) to afford **5.9** (1.0 mg) and **5.10** (5.5 mg). Fraction 2 was further purified by RP HPLC (gradient elution using 30% CH_3CN in H_2O (0.1 % HCOOH) for 15 mins, 30 – 100% in 15 mins, isocratic CH_3OH for 15 mins; 254 nm) to afford **5.9** (3.7 mg) and **5.10** (1.0 mg).

Compound **5.9**: UV (CH_3OH) λ_{max} (log ε) 235 (4.06), 290 (4.32), 420 (3.58) nm; CD (31 μM, CH_3OH) λ_{max} ($\Delta\varepsilon$) 269 (−17.78), 293 (+29.28) nm; ^{1}H and ^{13}C NMR data see Table 5.2 and 5.3.

Compound **5.10**: UV (CH_3OH) λ_{max} (log ε) 235 (4.07), 290 (4.33), 420 (3.57) nm; CD (31 μM, CH_3OH) λ_{max} ($\Delta\varepsilon$) 269 (24.92), 295 (-23.94) nm; ^{1}H and ^{13}C NMR data see Table 5.2 and 5.3.

Preparation of bromobenzoyl esters of cephalochromin (5.6). To a stirred solution of **5.6** (10 mg, 0.20 mmol) and 4-bromobenzoyl chloride (40 mg) in pyridine (10 mL) was added 4-(dimethylamino) pyridine (20 mg). The reaction mixture was stirred at room temperature under N_2 for 60 hrs. The crude mixture was diluted with CH_2Cl_2, washed with 1 N HCl (10 mL), then washed with $NaHCO_3$ (10 mL), and water (10 mL), dried over anhydrous Na_2SO_4, and evaporated to dryness. The dry residue was then purified by silica gel chromatography using a hexanes/EtOAc/CH_3OH gradient; (hexanes/EtOAc, 50:50, v/v; EtOAc; EtOAc/CH_3OH, 50:50, v/v; CH_3OH) to afford four fractions. Sub-fractions two, three, and four were combined together and further purified by preparative silica gel TLC using 30:70 hexanes/EtOAc to obtain dibromobenzoate **5.11** (2.1 mg).

Cephalochromin dibromobenzoate (**5.11**): ^{1}H NMR (600 MHz, $CDCl_3$) δ 13.55 (s, 2H), 7.85 (d, 8.7, 4H), 742 (d, 8.7, 4H), 7.0 (s, 2H), 6.97 (s, 2H), 5.99 (s, 2H), 4.18 (m, 2H), 2.41 (m, 4H), 1.13 (d, 6.2 Hz, 6H).

Preparation of bromobenzoyl esters of 5.9 and 5.10. A Procedure analogous to one described above was followed in efforts to derivatize **5.9** and **5.10**. A complex mixture containing multiple derivatives was obtained. Attempts to separate the mixture were unsuccessful.

Preparation of cephalochromin hexaacetate (5.12). A solution of cephalochromin (**5.6**; 4.1 mg) in dry pyridine (10 mL) was treated with excess of acetic anhydride. The mixture was stirred for 36 hrs under N_2. Pyridine was evaporated under air and the crude mixture was washed with CH_2Cl_2 (10 mL) and H_2O (10 mL). The organic layer was separated and the aqueous layer was again washed with CH_2Cl_2 (10 mL) and H_2O (10 mL). The organic layer was separated and dried to obtain cephalochromin hexaaacetate (**5.12**, 2 mg).

Cephalochromin hexaacetate (**5.12**): ^{1}H NMR (600 MHz, $CDCl_3$) δ 7.0 (s, 2H), 6.61 (s, 2H), 4.51 (m, 2H), 2.34 – 2.57 (m), 2.53 (s, 3H), 2.43 (s, 3H), 1.92 (s, 3H), 1.39 (d, 6.1 Hz, 6H); ESITOFMS, 793.20 $[M+Na]^+$.

Preparation of acetates of 5.9 and 5.10. Procedure analogues to one described above was followed to derivatize **5.9** and **5.10**. A complex mixture containing multiple derivatives was obtained. Attempts to separate the mixture were unsuccessful.

Preparation of 2,4-dinitrophenylhydrazine derivatives of 5.9 and 5.10.[131] 2,4-dinitrophenylhydrazine in CH_3OH (8.1 mmol) was added to a solution of **5.9** (1.0 mg, 1.8 μmol) in CH_3OH:H_2O (1:1). The mixture was acidified with a drop of H_2SO_4. This mixture was stirred at room temperature for 75 mins. The crude mixture was washed with $NaHCO_3$ (10 mL), was diluted with CH_2Cl_2 (10 mL) and water (10 mL). The organic layer was separated and dried over anhydrous Na_2SO_4. The filtrate was evaporated to dryness.

Procedures for Isolation and Characterization of Metabolites from *Phoma* sp. (ENDO-3417)

Fungal Material. A fungal isolate (ENDO-3417) was obtained from a seed of *Bromus kalmii* obtained from a nursery in Winona, Minnesota. A subculture was deposited in the culture collection at the USDA NCAUR and assigned the accession number NRRL 54108. The culture was subjected to partial sequence analysis of the internal transcribed spacer region (ITS) and domains D1 and D2 of the nuclear large subunit (28S) rDNA gene using ITS5 and NL4 as polymerase chain reaction and sequencing primers. A nucleotide-to-nucleotide BLAST query of the GenBank database (http://www.ncbi.nlm.nih.gov/BLAST) identified the isolate as a *Phoma* sp. This *Phoma* sp. was grown on 6 x 50 g of autoclaved rice for 30 days at 25 °C. The resulting culture material was then extracted with EtOAc to give the crude extract upon evaporation of the resulting filtered solution.

Extraction and Isolation. The crude extract was partitioned between hexanes and CH_3CN. The resulting CH_3CN fraction (302 mg) was fractionated by silica gel chromatography using a hexanes/EtOAc/CH_3OH step gradient; (hexanes/EtOAc, 75:25, 50:50, 30:70, 10:90, v/v; EtOAc; EtOAc/CH_3OH, 95:5, 85:15, 75:25, 60:40, 30:70, v/v; CH_3OH) to yield eleven 100-mL crude fractions. These fractions were later combined into 9 fractions based on silica gel TLC analysis. Fraction 6 (59 mg), which eluted with 19:1 EtOAc/CH_3OH, was further separated by silica gel chromatography using hexanes/EtOAc/CH_3OH step gradient (hexanes/EtOAc, 50:50, 25:75, v/v; EtOAc; EtOAc/CH_3OH, 98:2, 95:5, v/v; CH_3OH) to afford 6 fractions. Fraction 6.4 (11 mg), which eluted with 3:1 EtOAc/hexanes was further purified by Sephadex LH-20 chromatography using a hexanes/CH_2Cl_2/acetone gradient (hexanes:CH_2Cl_2, 20:80 v/v; CH_2Cl_2:acetone, 60:40 v/v; CH_2Cl_2:acetone, 20:80 v/v) to give compounds herbarumin IV mixture (**6.1,** 4.5 mg) and herbarumin V (**6.3,** 2.0 mg). Fraction 7 (13 mg) which eluted with 3:1 EtOAc/CH_3OH was further purified by Sephadex LH-20 chromatography using hexanes/CH_2Cl_2/acetone gradient (hexanes:CH_2Cl_2, 20:80 v/v; CH_2Cl_2:acetone, 60:40 v/v; CH_2Cl_2:acetone, 20:80 v/v) to yield 3 fractions. Fraction 7.2 (5.3 mg) which eluted with 1:4 hexanes/CH_2Cl_2 was further separated by sephadex LH-20 chromatography using hexanes/CH_2Cl_2/acetone step gradient; (hexanes:CH_2Cl_2,50:50, 1:2, 25:75, 20:80 v/v; CH_2Cl_2:acetone, 60:40 v/v; CH_2Cl_2:acetone, 20:80 v/v) to give compound 7-epi-herbarumin V (**6.4**, 2.5 mg). Fraction 4 (54 mg) which eluted with 9:1 EtOAc/hexanes was subjected to silica gel chromatography (22 mg) using hexanes/EtOAc/CH_3OH gradient (hexanes/EtOAc, 75:25, 50:50, 25:75, v/v; EtOAc; EtOAc/CH_3OH, 50:50, v/v; CH_3OH) to afford 9 fractions. Fraction 4.4 (8.4 mg) which eluted with 1:1 hexanes/EtOAc was further purified by silica gel chromatography using hexanes/EtOAc/CH_3OH (hexanes/EtOAc, 75:25, 50:50, 25:75, v/v; EtOAc) to give herbarumin II (**6.6**, 4.5 mg). Fraction 4.5 (9.7 mg) which eluted with 1:3 Hexanes/EtOAc was further separated by C_{18} RP HPLC gradient elution using 70% CH_3OH in H_2O (0.1

% HCOOH) for 10 mins, 70 – 100% in 5 mins, isocratic CH_3OH for 5 mins; 260 nm to afford Pinolide (**6.7**, 2.0 mg).[b] Fraction 3 (30 mg) which eluted with 3:7 hexanes/EtOAc was further subjected to Sephadex LH-20 chromatography using hexanes/CH_2Cl_2/Acetone step gradient (hexanes:CH_2Cl_2, 1:2, 25:75, 20:80 v/v; CH_2Cl_2:Acetone, 60:40 v/v; CH_2Cl_2:Acetone, 20:80 v/v) to yield 7 fractions. Fraction 3.2 (8 mg) was subjected to Sephadex LH-20 chromatography using hexanes/CH_2Cl_2/acetone step gradient (hexanes:CH_2Cl_2, 75:25, 50:50, 25:75, 20:80; v/v) gradient to give 2 fractions. Fraction 3.2.2 (4.8 mg) was further purified by C_{18} RP HPLC gradient elution using (50% CH_3OH in H_2O (0.1 % HCOOH) for 10 mins, 50 – 100% in 5 mins, isocratic CH_3OH for 10 mins; 262 nm) to afford herbarumin I (**6.5**, 1.2 mg).

Preparation of bromobenzoate esters of herbarumin IV (6.1). To a stirred solution of **6.1** (1 mg) and 4-bromobenzoyl chloride (2 mg) in CH_2Cl_2 (3 mL), was added 4-(dimethylamino) pyridine (0.5 mg) and Et_3N (1.25 µL). The reaction mixture was stirred at room temperature under N_2 for 48 hrs. The crude mixture was diluted with CH_2Cl_2, washed successively with 1 N HCl (10 mL), washed with saturated. $NaHCO_3$ (10 mL), and water (10 mL), dried over anhydrous Na_2SO_4, and evaporated to dryness. The reaction mixture was purified by RP-HPLC with gradient elution using 90% CH_3CN in H_2O (0.1 % HCOOH) for 5 mins, 90 – 100% in 5 mins, isocratic CH_3CN for 15 mins; 248 nm to yield herbarumin IV dibromobenzoate (**6.9**)

Herbarumin IV (**6.1**): $[\alpha]^{25}_D$ -1.33 (*c* 0.45, CH_3OH); ^1H and ^{13}C NMR data see Table 6.1; key HMBC (600 MHz; CD_3OD) H_2-10 → C-8, C-9, C-11, C-12; H_2-6 → C-4, C-5, C-7, C-8; H_2-2 → C-1, C-3, C-4, see Figures 6.1 and NOESY (600 MHz; CD_3OD) H-7 ↔ H_a-10; H-9 ↔ H-8, see Figure 6.2 HRESITOFMS, 267.1189 $[M+Na]^+$, calcd for $C_{12}H_{20}O_5Na$.

Herbarumin V (**6.3**): $[\alpha]^{25}_D$ +22 (*c* 0.2, CH_3OH); CD (CH_3OH) λ_{max} ($\Delta\varepsilon$) 215 (−6.8), 233 (0), 269 (+4.75) nm; ^1H and ^{13}C NMR data see Table 6.3; key HMBC (600

MHz; CD_3OD) H-1 → C-9, C-5; H-4,H-6, H-7 → C-5, see Figure 6.6 and NOESY data (600 MHz; CD_3OD) H-7 ↔ H_{-8}; H-6 ↔ H-1; H-6 ↔ H4, Figure 6.7; HRESITOFMS, 267.1193 $[M+Na]^+$, calcd for $C_{12}H_{20}O_5Na$.

7-Epi-herbarumin V (**6.4**): $[\alpha]^{25}_D$ +4 (*c* 0.25, CH_3OH); CD (CH_3OH) λ_{max} ($\Delta\varepsilon$) 205 (−30.25), 288 (+15.71) nm; ^1H and ^{13}C NMR data see Table 6.3; key NOESY data (600 MHz; CD_3OD) H-6 ↔ H-1; H-6 ↔ H4, see Figure 6.10; HRESITOFMS, 267.1193 $[M+Na]^+$, calcd for $C_{12}H_{20}O_5Na$.

Herbarumin IV dibromobenzoate (**6.9)**: UV (CH_3OH) λ_{max} (log ε) 204 (3.83), 245 (3.88) nm; CD (328 μM, CH_3OH) λ_{max} ($\Delta\varepsilon$) 205 (−30.25), 288 (+15.71) nm; ^1H NMR data ($CDCl_3$, 600 MHz) δ 7.90 (d, 8.3 Hz, 2H), 7.80 (d, 8.3 Hz, 2H), 7.65 (d, 8.3 Hz, 2H), 7.56 (d, 8.3 Hz, 2H), 6.11 (d, 10.3 Hz, 1H), 5.65 (br s, 1H), 5.21 (dt, 6.9 Hz, 3.1 Hz, 1H), 3.65 (dd, 15.2 Hz, 11 Hz, 1H), 2.61 (m, 2H), 2.57 (m, 2H), 2.52 (d, 15.5 Hz, 1H), 2.18 (p, 5.6 Hz, 2H), 1.80 (dd, 7.2 Hz, 6.1 Hz, 1H), 1.79 (dd, 7.2 Hz, 5.1 Hz, 1H), 1.43 (m, 2H), 0.97 (t, 7.2, 3H); HRESITOFMS, 609.0121 $[M+H]^+$, calcd for $C_{26}H_{27}O_7Br_2$

Herbarumin I (**6.5**): Identified by comparison of NMR data with literature values.[122] HRESITOFMS, 251.1250 $[M+Na]^+$, calcd for $C_{12}H_{20}O_4Na$ (calcd. 251.1259)

Herbarumin II (**6.6**): Identified by comparison of NMR data with literature values.[122] HRESITOFMS, 267.1185 $[M+Na]^+$, calcd for $C_{12}H_{20}O_5Na$ (calcd. 267.1208)

Pinolide (**6.7**): Identified by comparison of NMR data with literature values.[123] HRESITOFMS, 267.1190 $[M+Na]^+$, calcd for $C_{12}H_{20}O_5Na$ (calcd. 267.1208).

APPENDIX A

SELECTED NMR SPECTRA

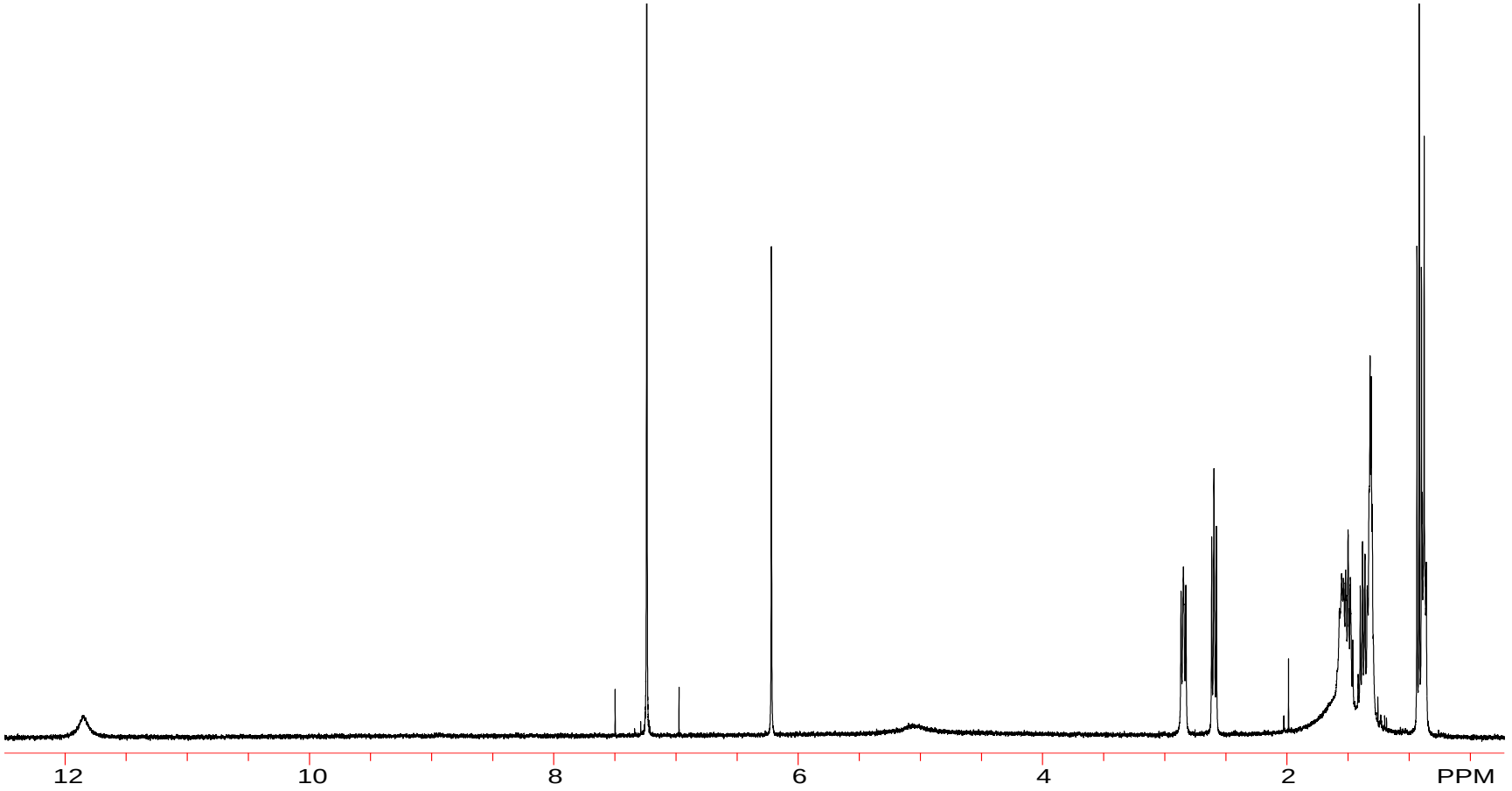

Figure A.1. ^{1}H NMR Spectra of **2.3** ($CDCl_3$, 400 MHz)

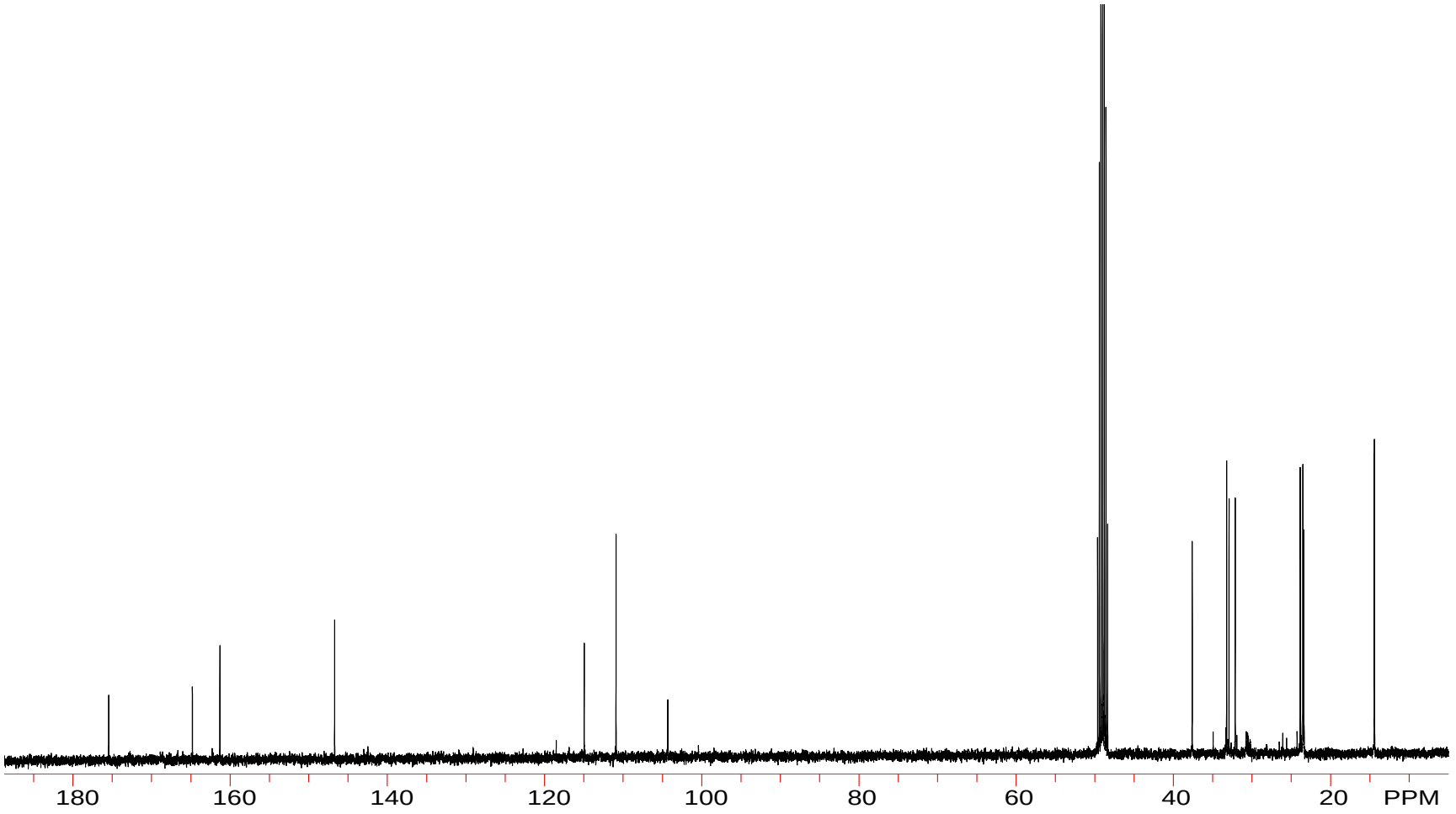

Figure A.2. ^{13}C NMR Spectra of **2.3** (CD_3OD, 100 MHz)

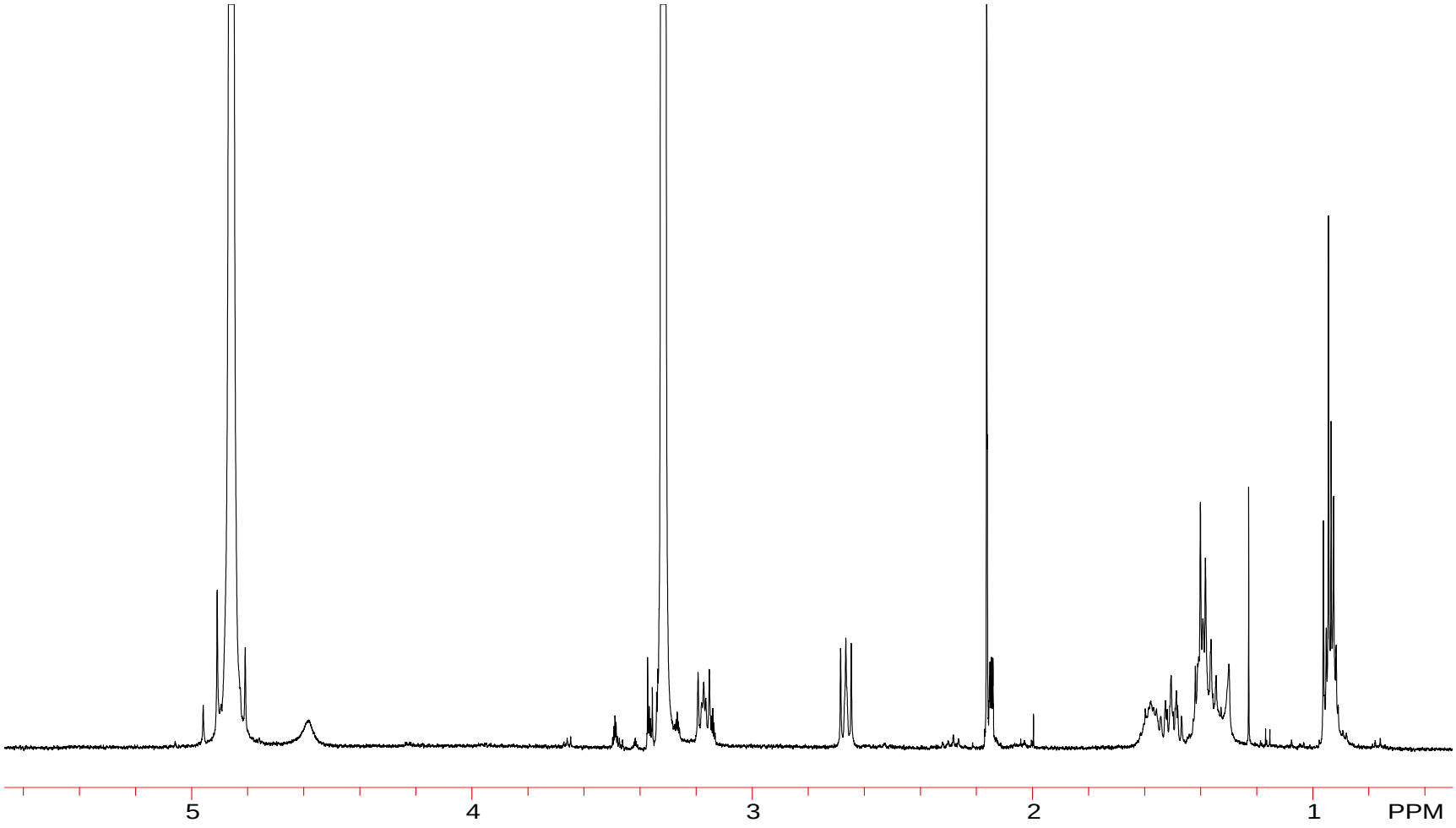

Figure A.3. ^{1}H NMR Spectra of **2.4** (CD_3OD, 400 MHz)

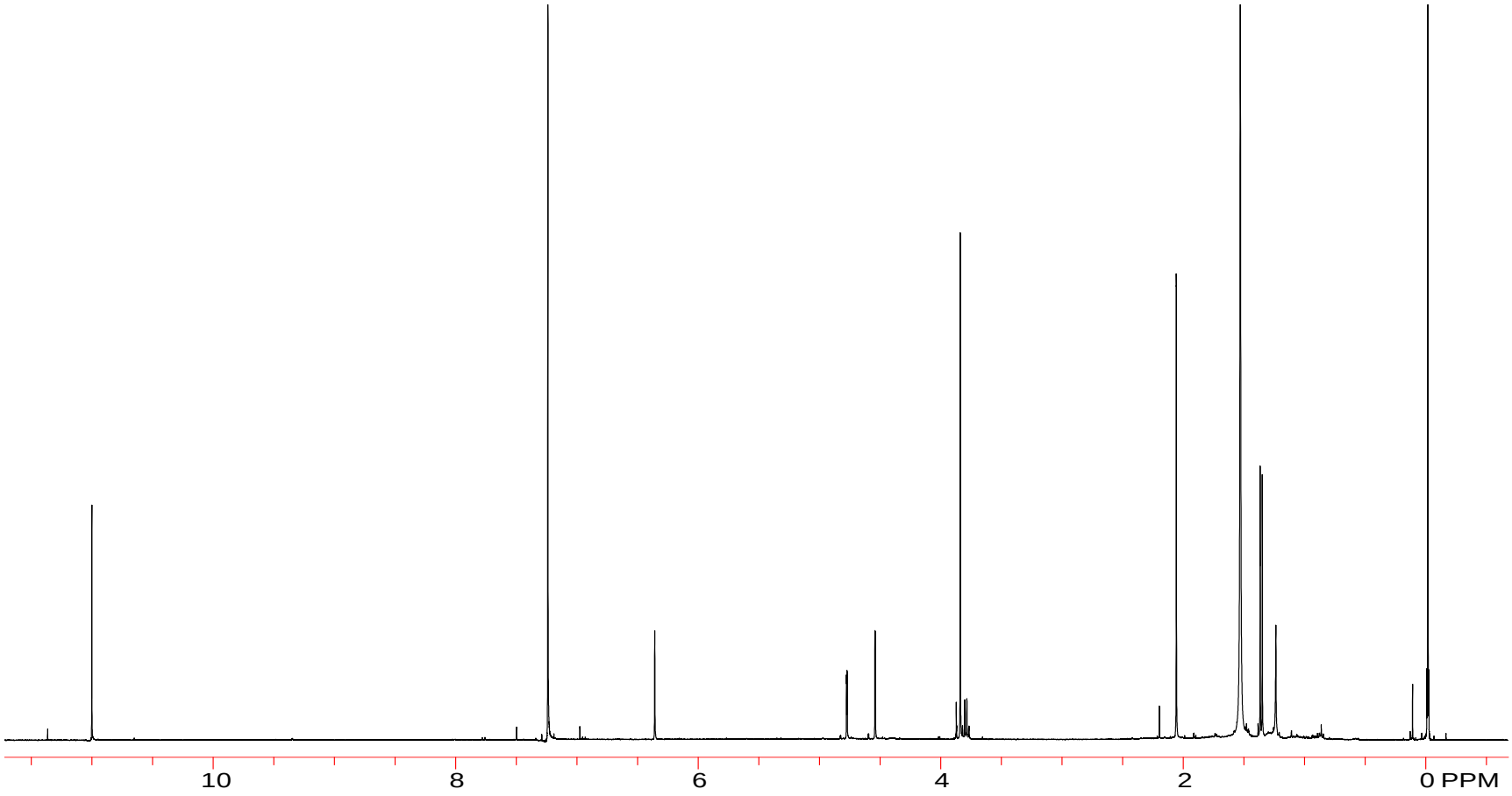

Figure A.4. ^{1}H NMR Spectra of **2.8** ($CDCl_3$, 400 MHz)

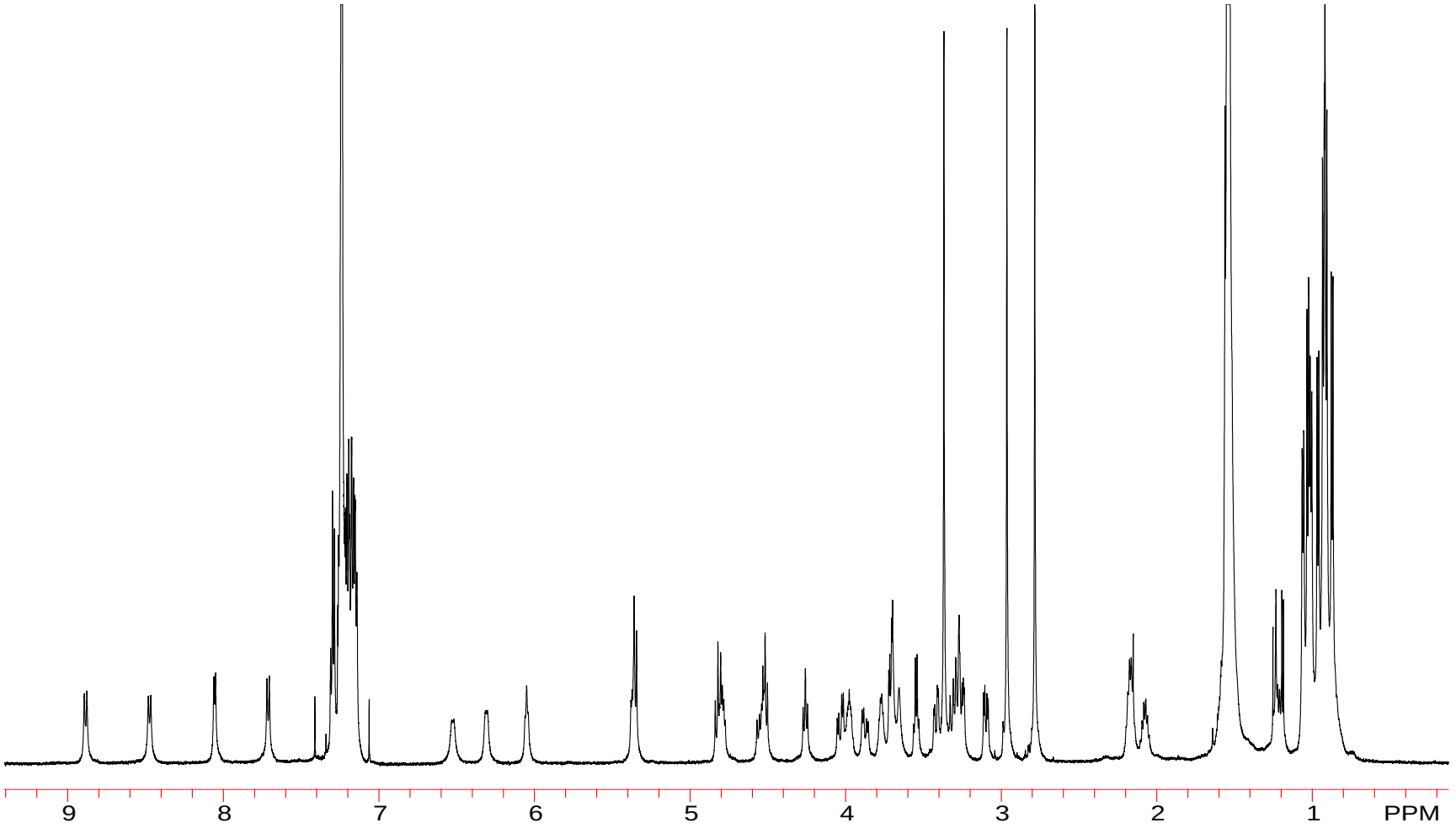

Figure A.5. ^{1}H NMR Spectra of sesquilarin A (3.4, $CDCl_3$, 600 MHz)

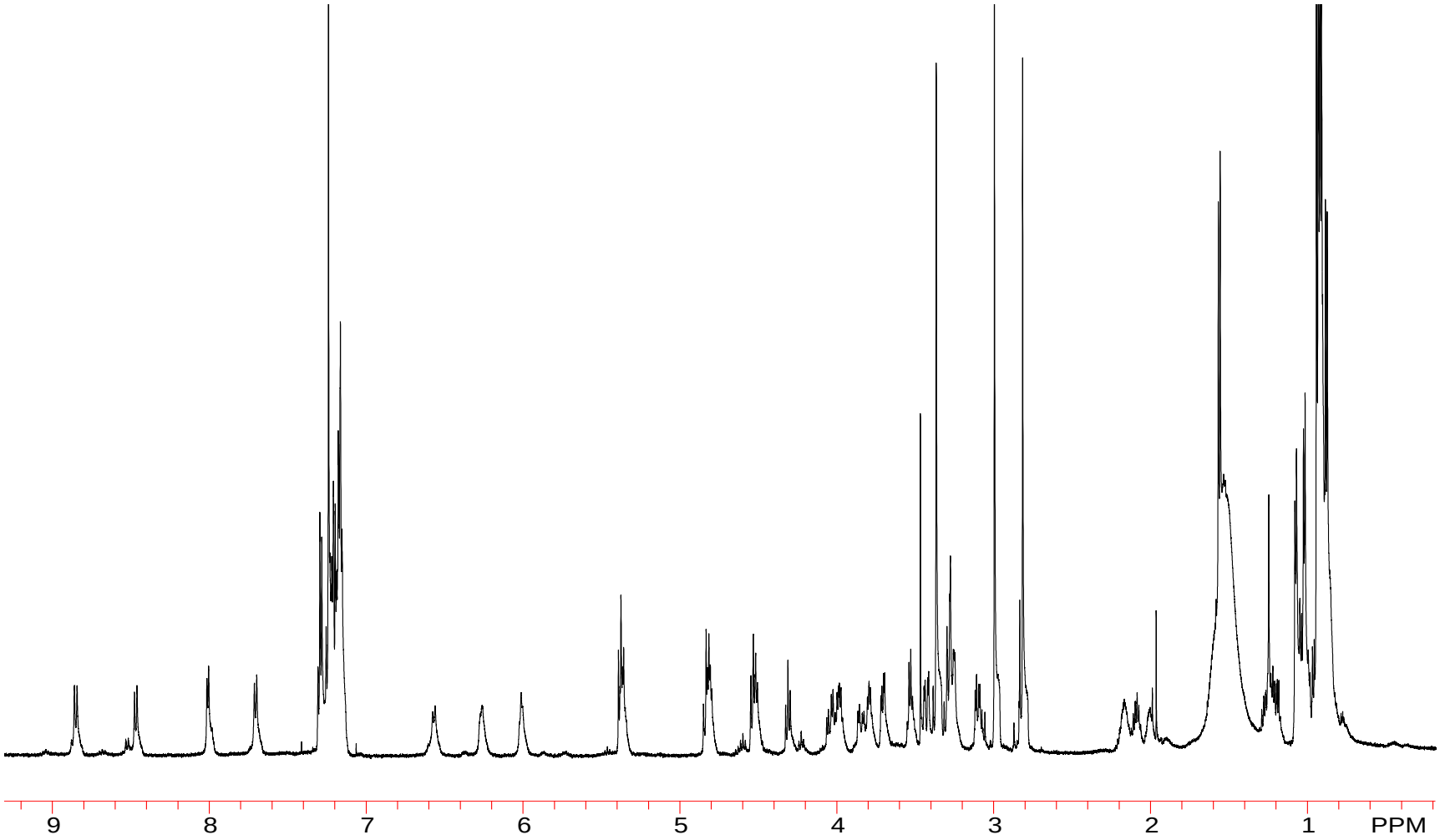

Figure A.6. ^{1}H NMR spectra of sesquilarin B (3.5, $CDCl_3$, 600 MHz)

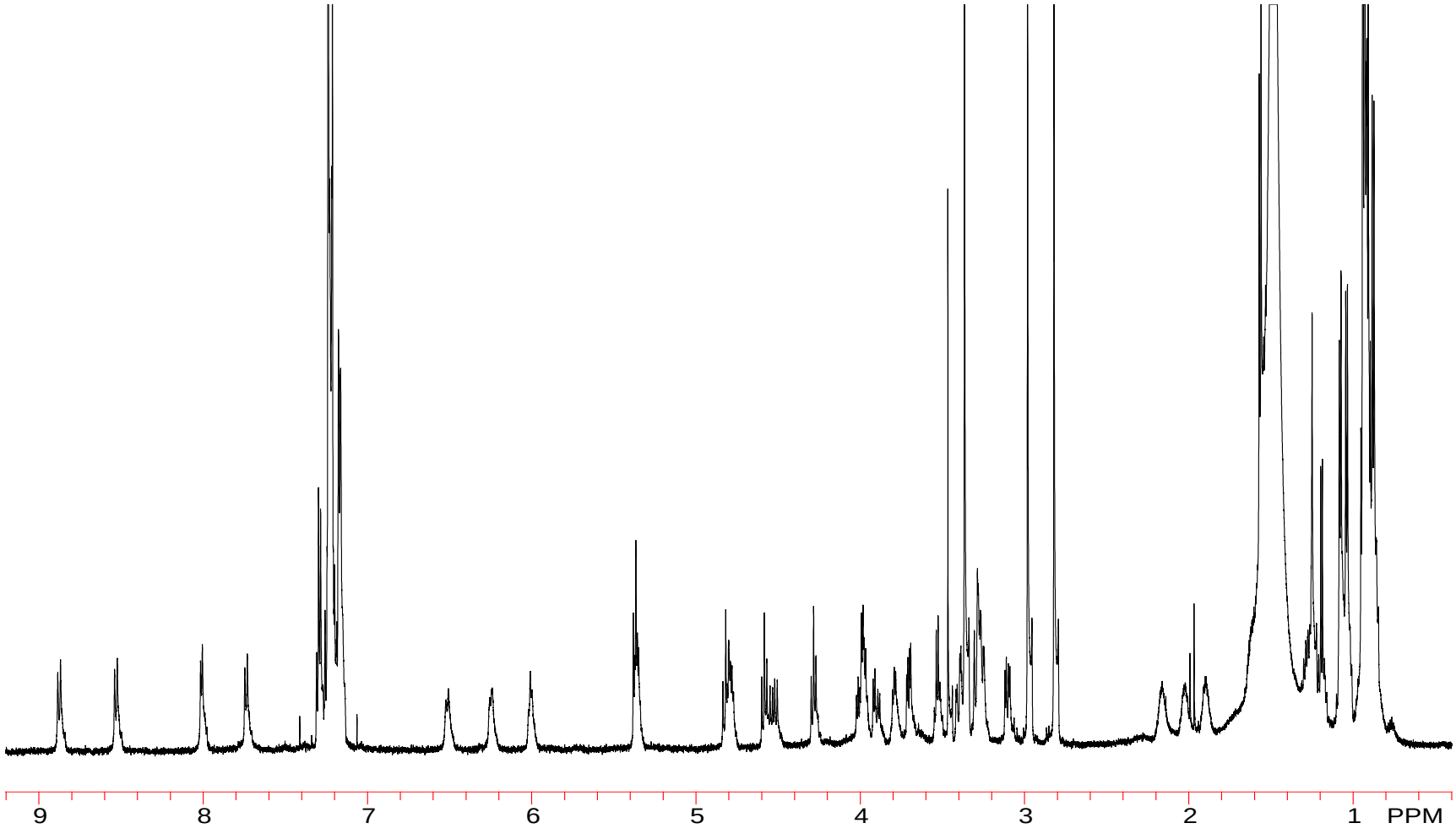

Figure A.7. ^{1}H NMR spectra of sesquilarin C (**3.6**, $CDCl_3$, 600 MHz)

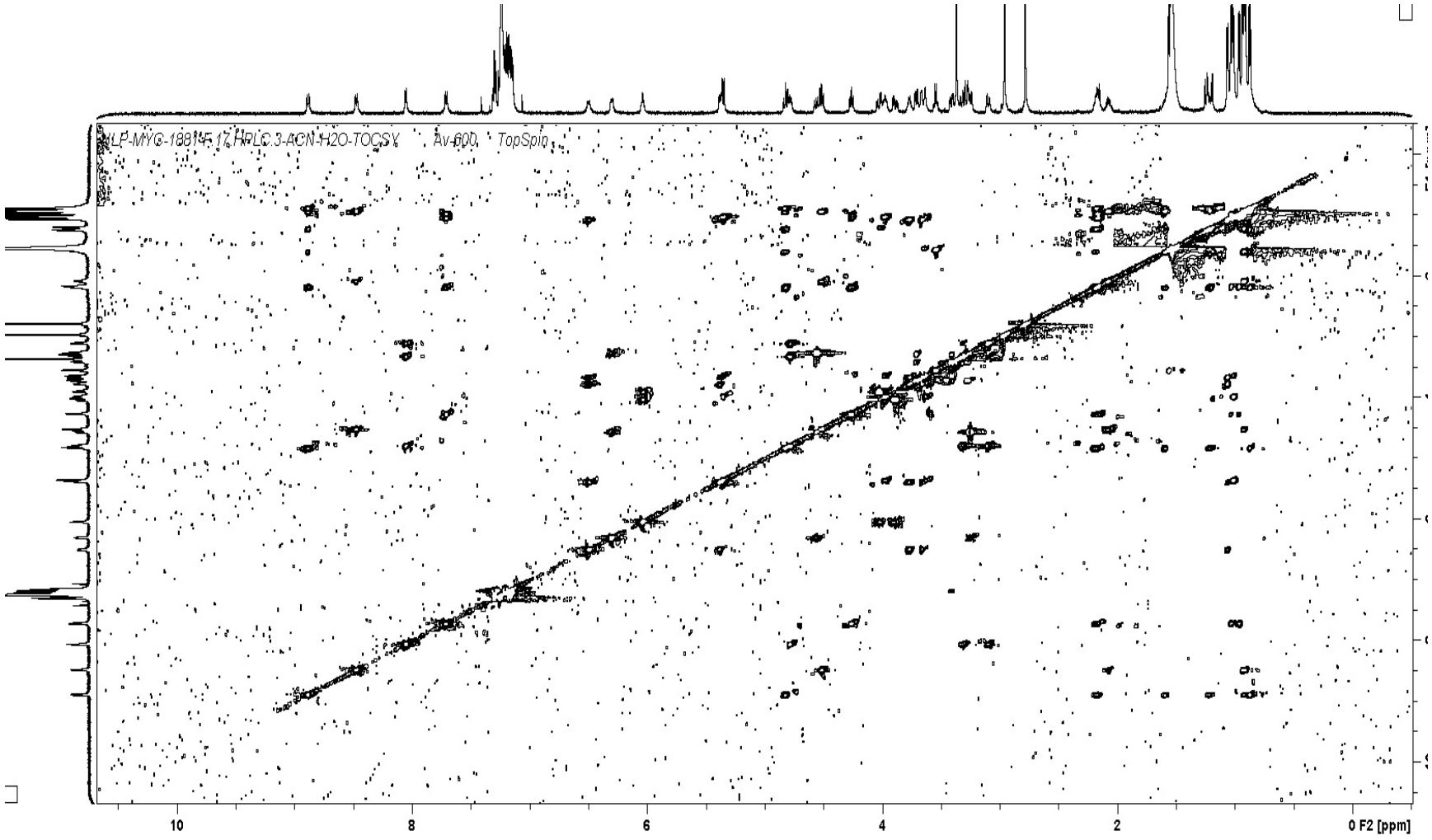

Figure A.8. TOCSY Spectra of sesquilarin A (**3.4**, $CDCl_3$, 600 MHz)

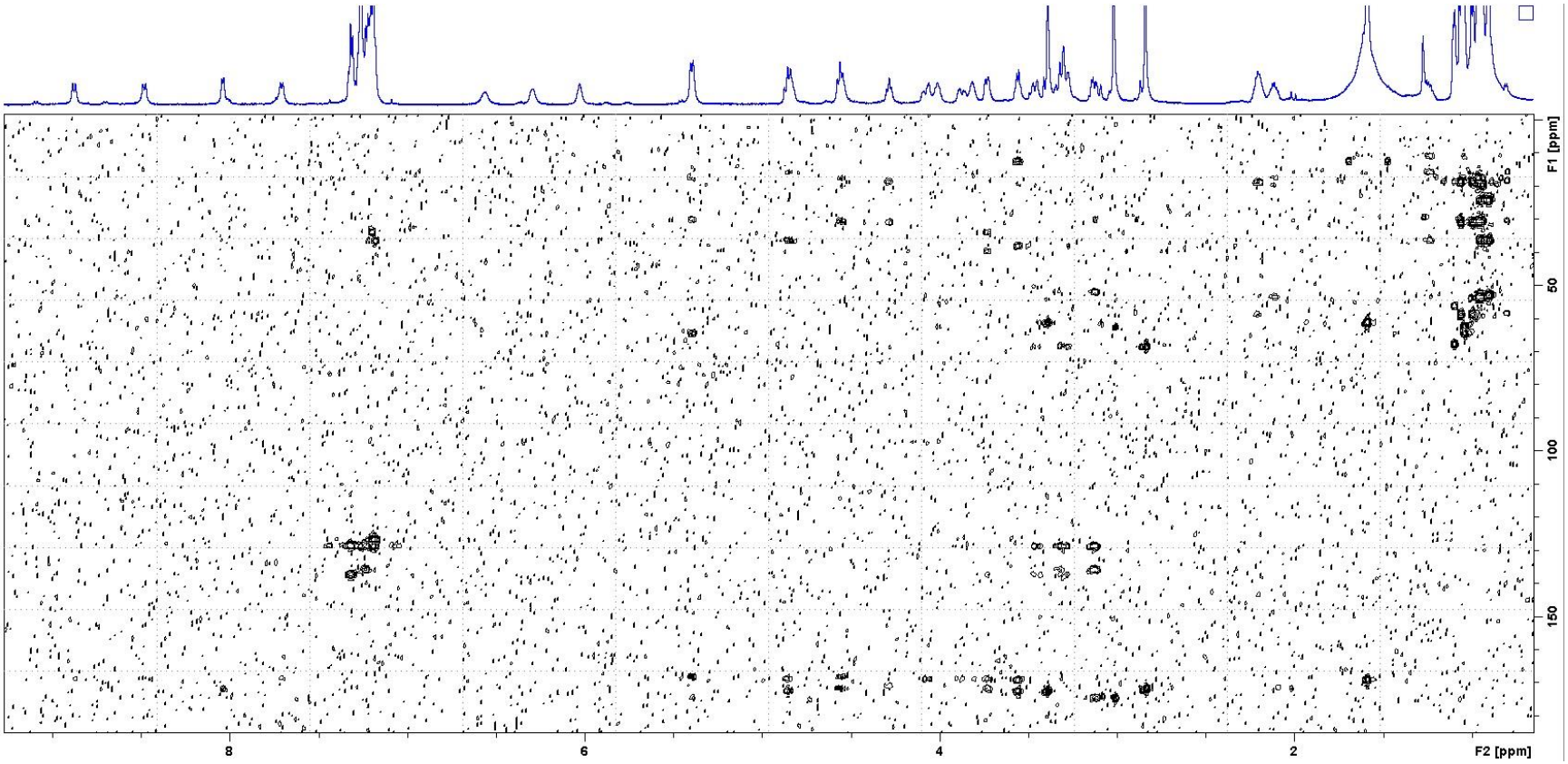

Figure A.9. HMBC Spectra of sesquilarin A (**3.4**, $CDCl_3$, 600 MHz)

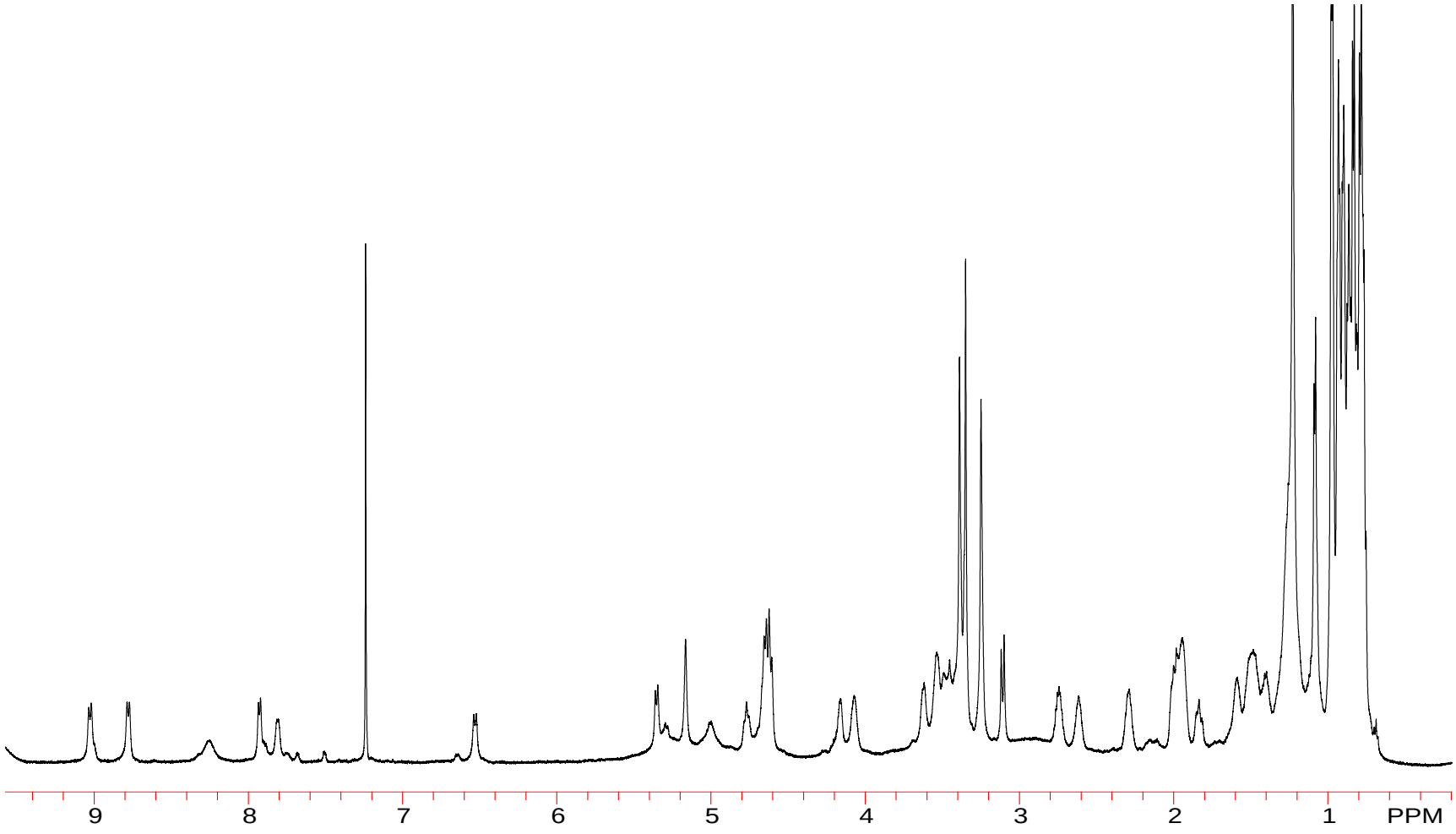

Figure A.10. ^{1}H NMR spectra of phaeoacremonium A (**4.1**, $CDCl_3$, 600 MHz)

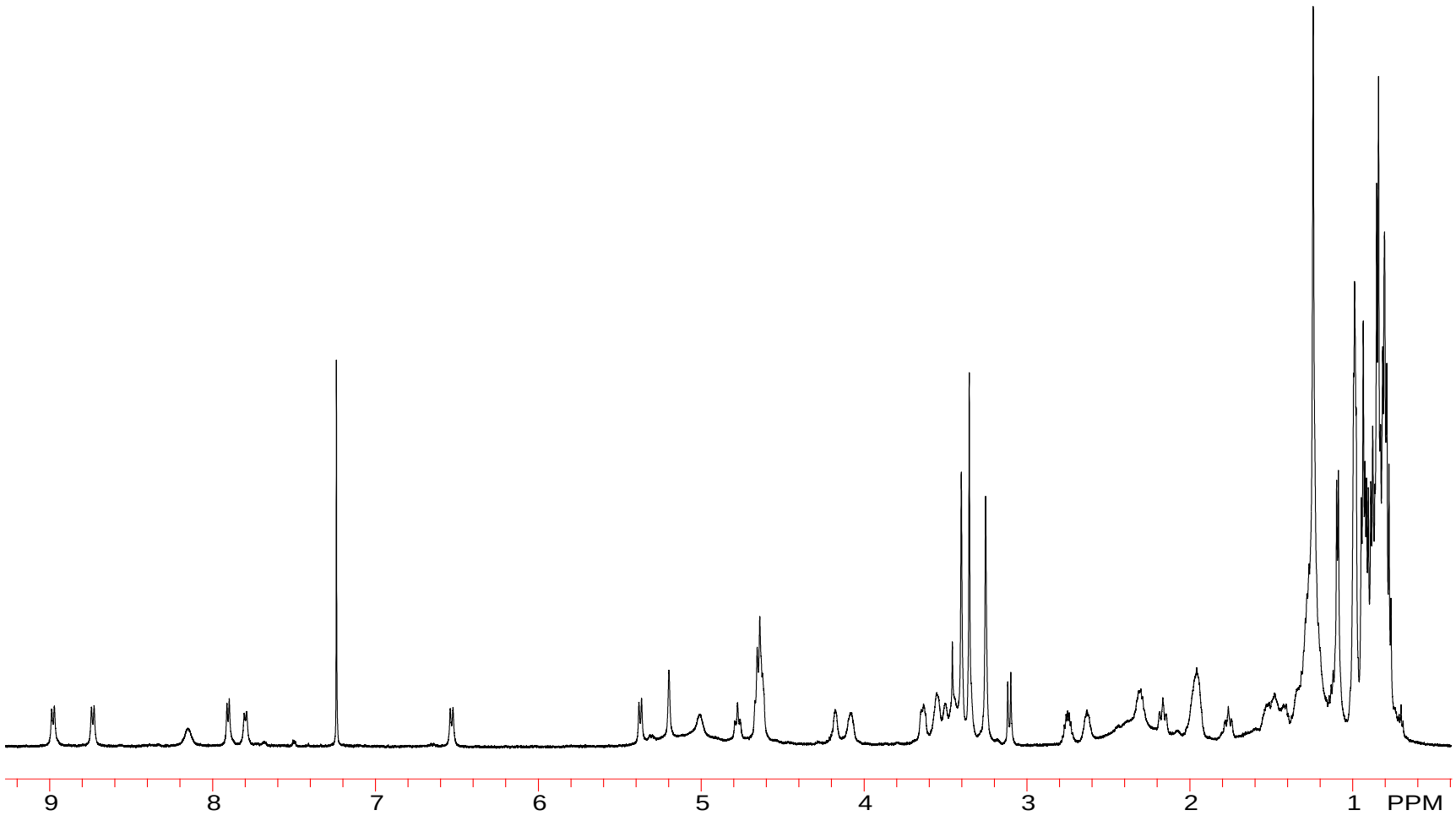

Figure A.11. ^{1}H NMR spectra of phaeoacremonium B (**4.2**, $CDCl_3$, 600 MHz)

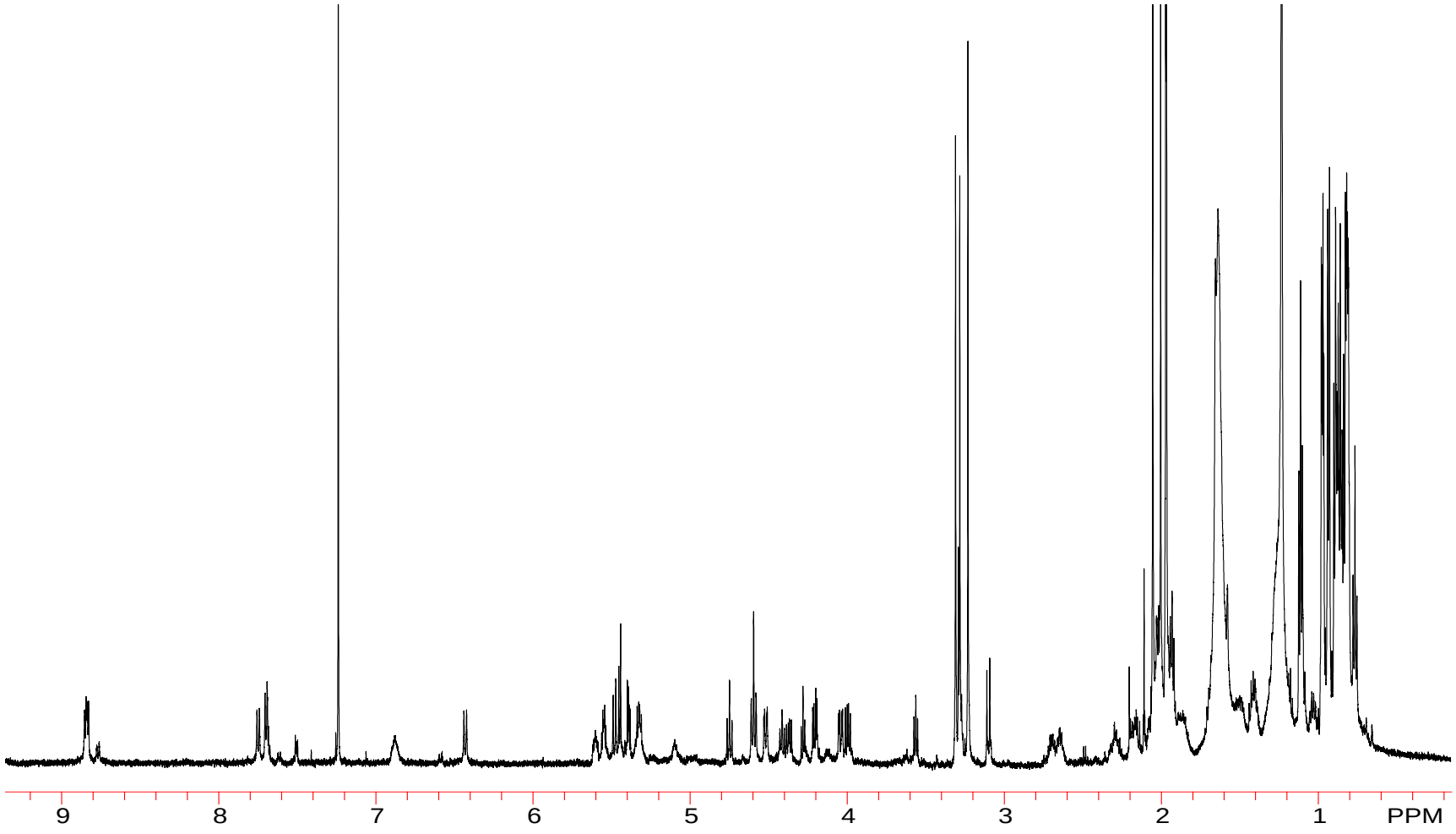

Figure A.12. ^{1}H NMR spectra of acetylated phaeoacremonium A (**4.3**, $CDCl_3$, 600 MHz)

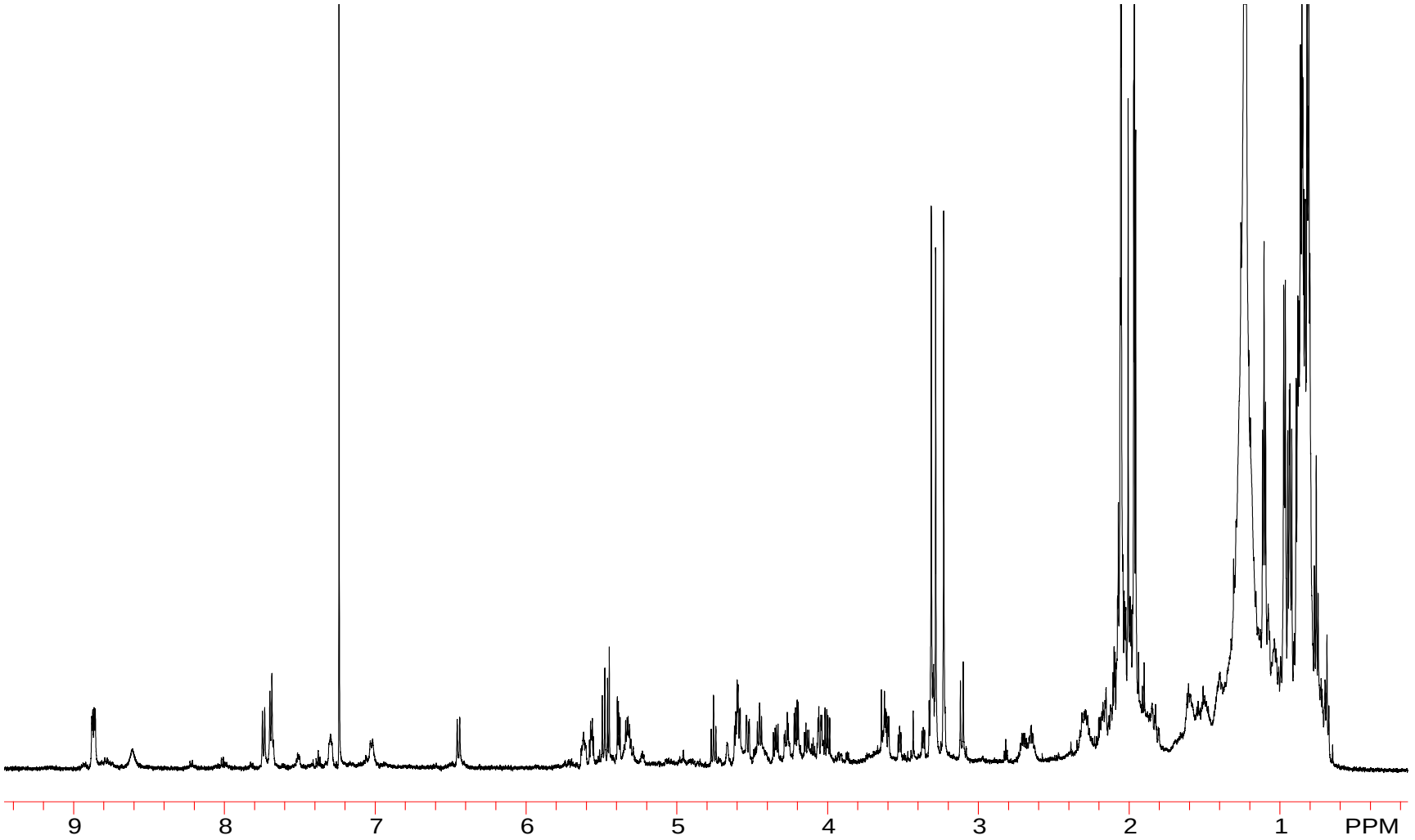

Figure A.13. ^{1}H NMR spectra of acetylated phaeoacremonium B (**4.4**, $CDCl_3$, 600 MHz)

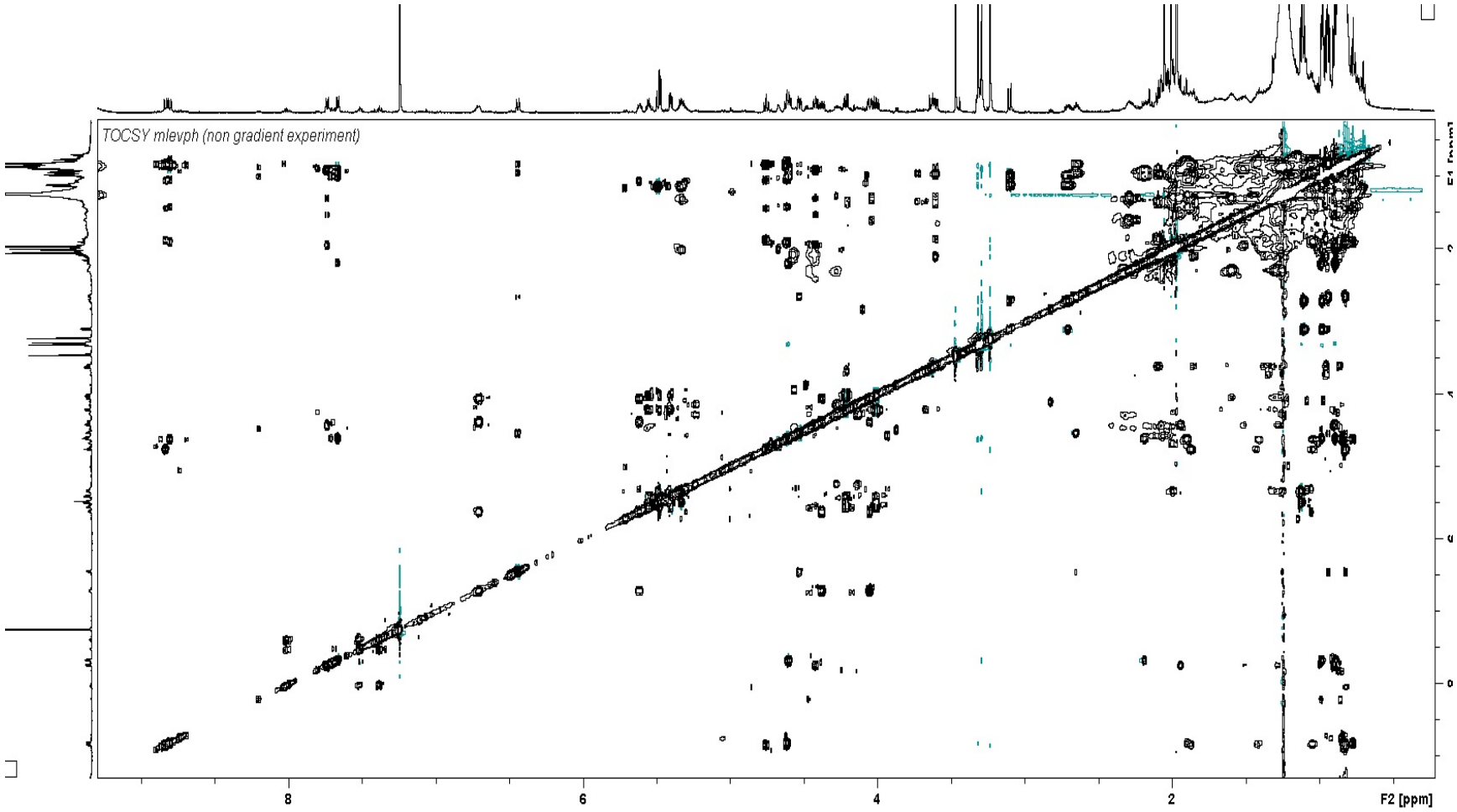

Figure A.14. TOCSY spectra of acetylated phaeoacremonium B (**4.4**, $CDCl_3$, 600 MHz)

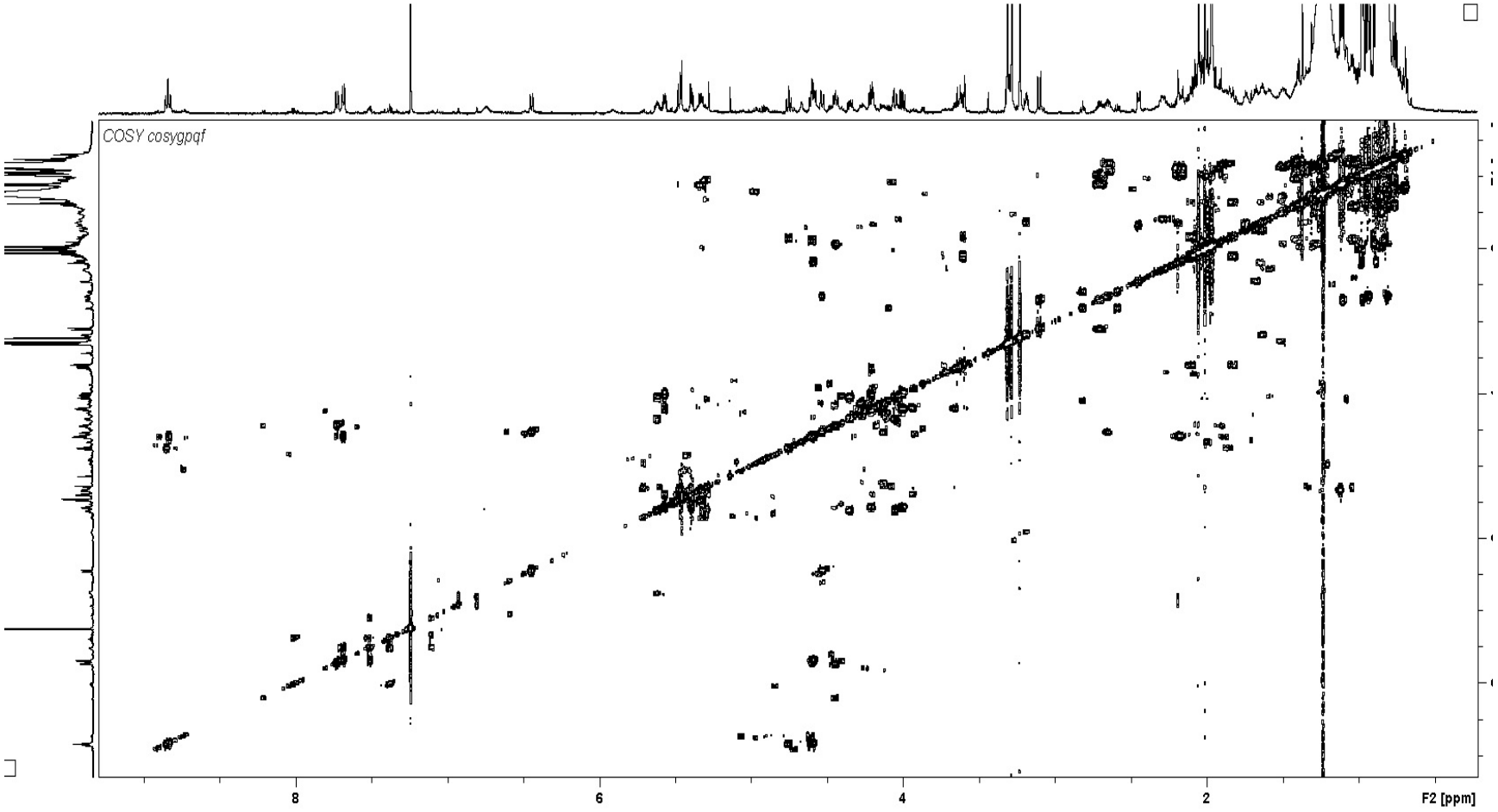

Figure A.15. COSY spectra of acetylated phaeoacremonium B (**4.4**, $CDCl_3$, 600 MHz)

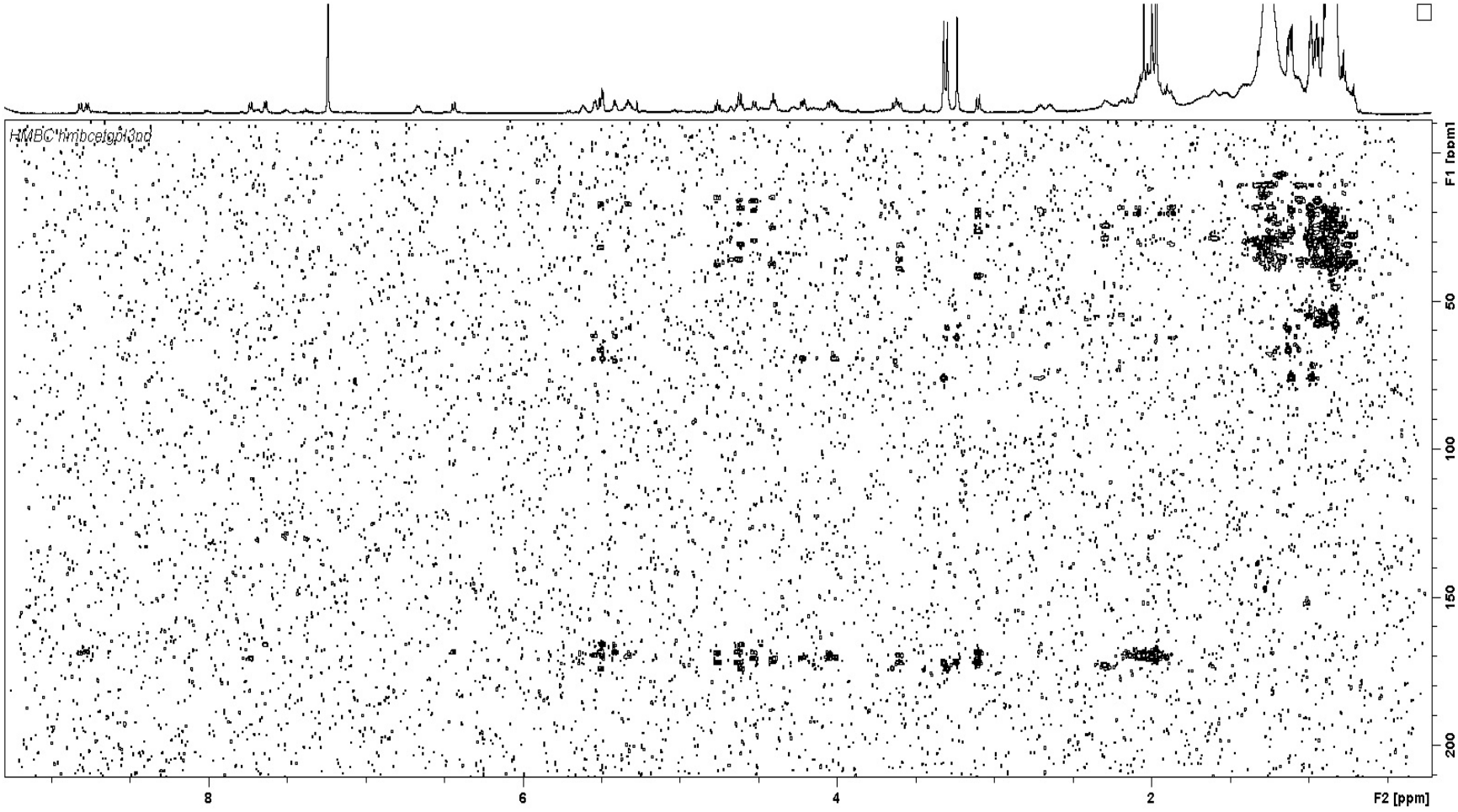

Figure A.16. HMBC spectra of acetylated phaeoacremonium B (**4.4**, $CDCl_3$, 600 MHz)

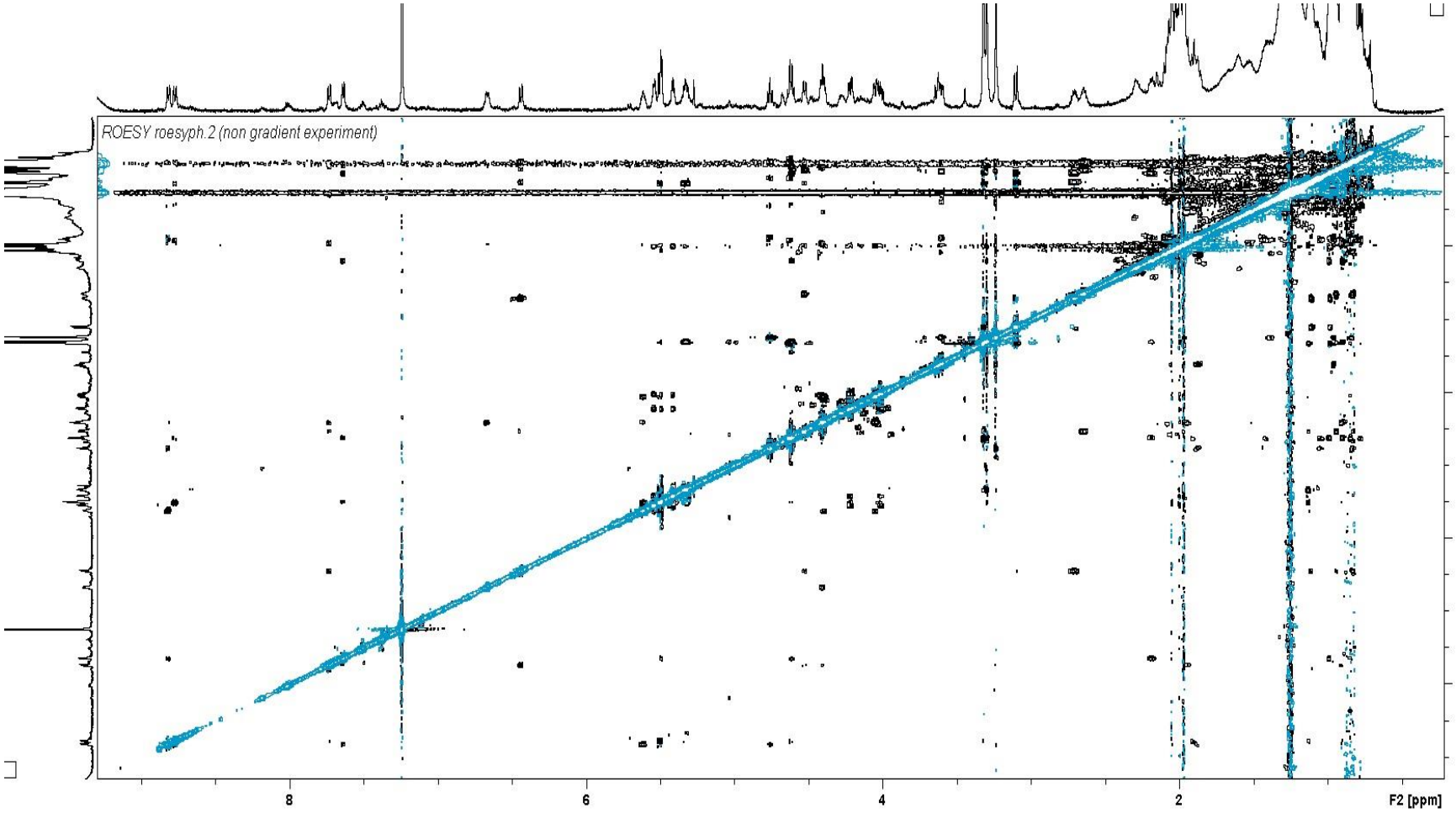

Figure A.17. ROESY spectra of acetylated phaeoacremonium B (**4.4**, $CDCl_3$, 600 MHz)

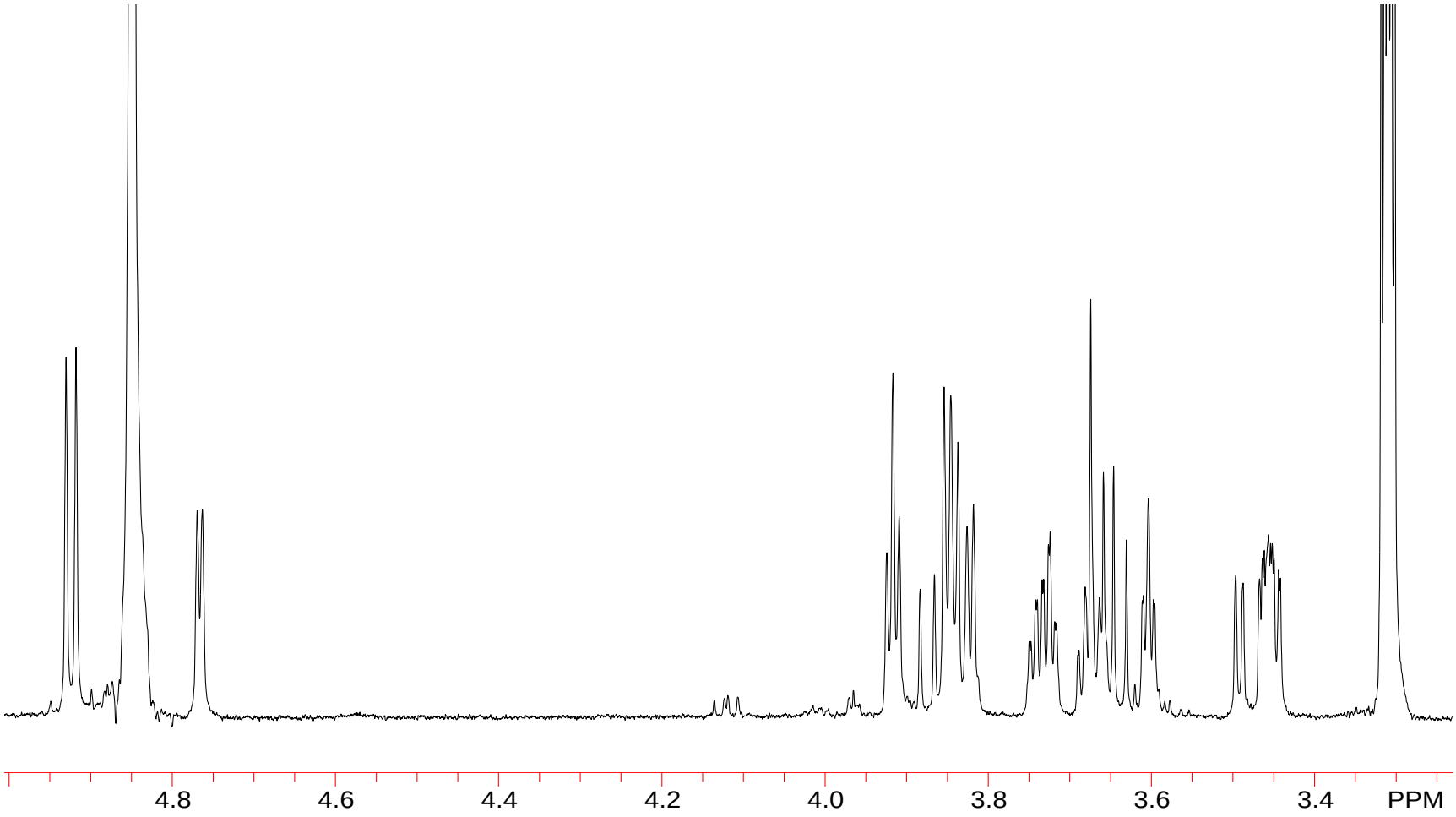

Figure A.18. ^{1}H NMR spectra of d-ribose (CD_3OD, 400 MHz)

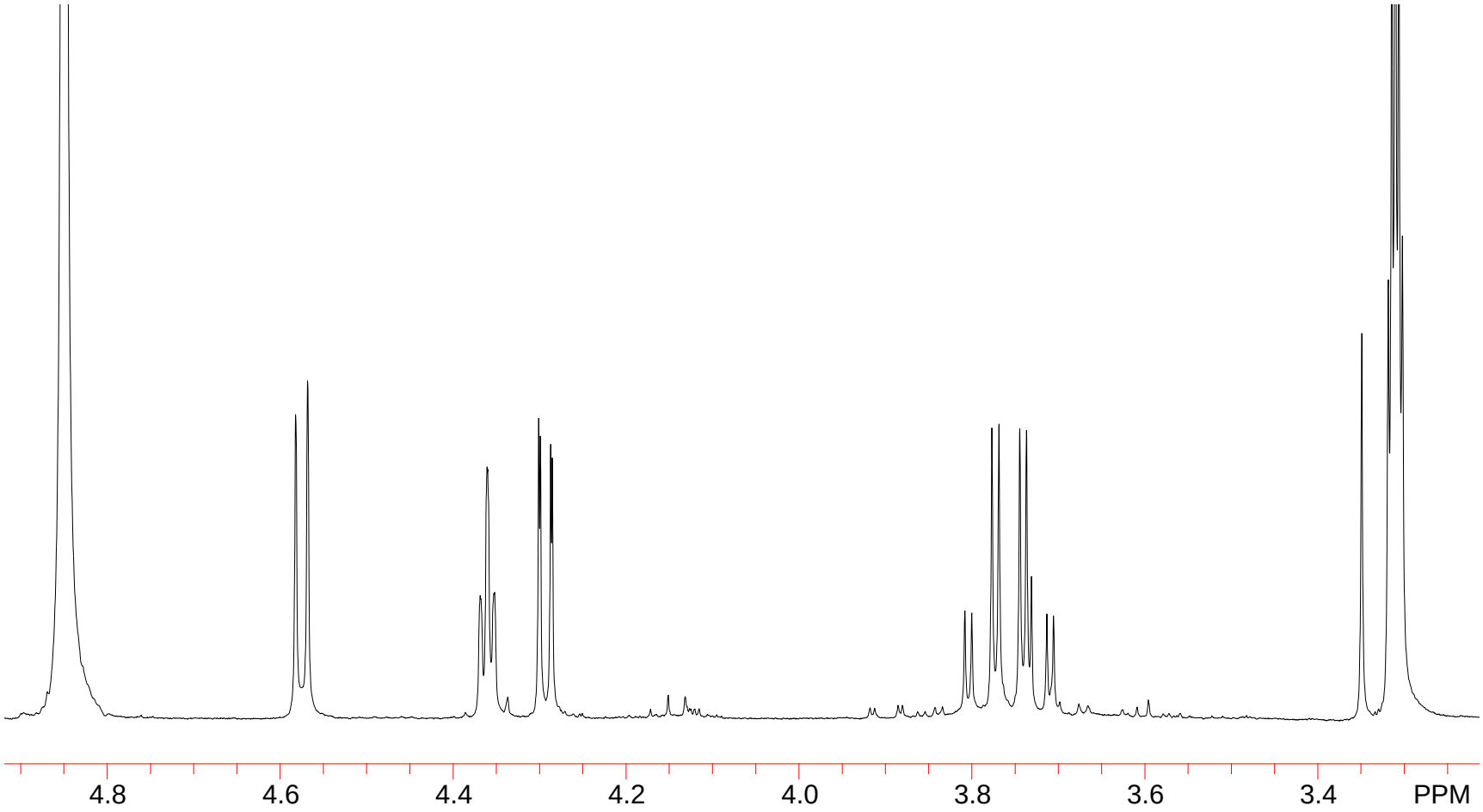

Figure A.19 ^{1}H NMR spectra of D-ribono-1,4-lactone (CD_3OD, 400 MHz)

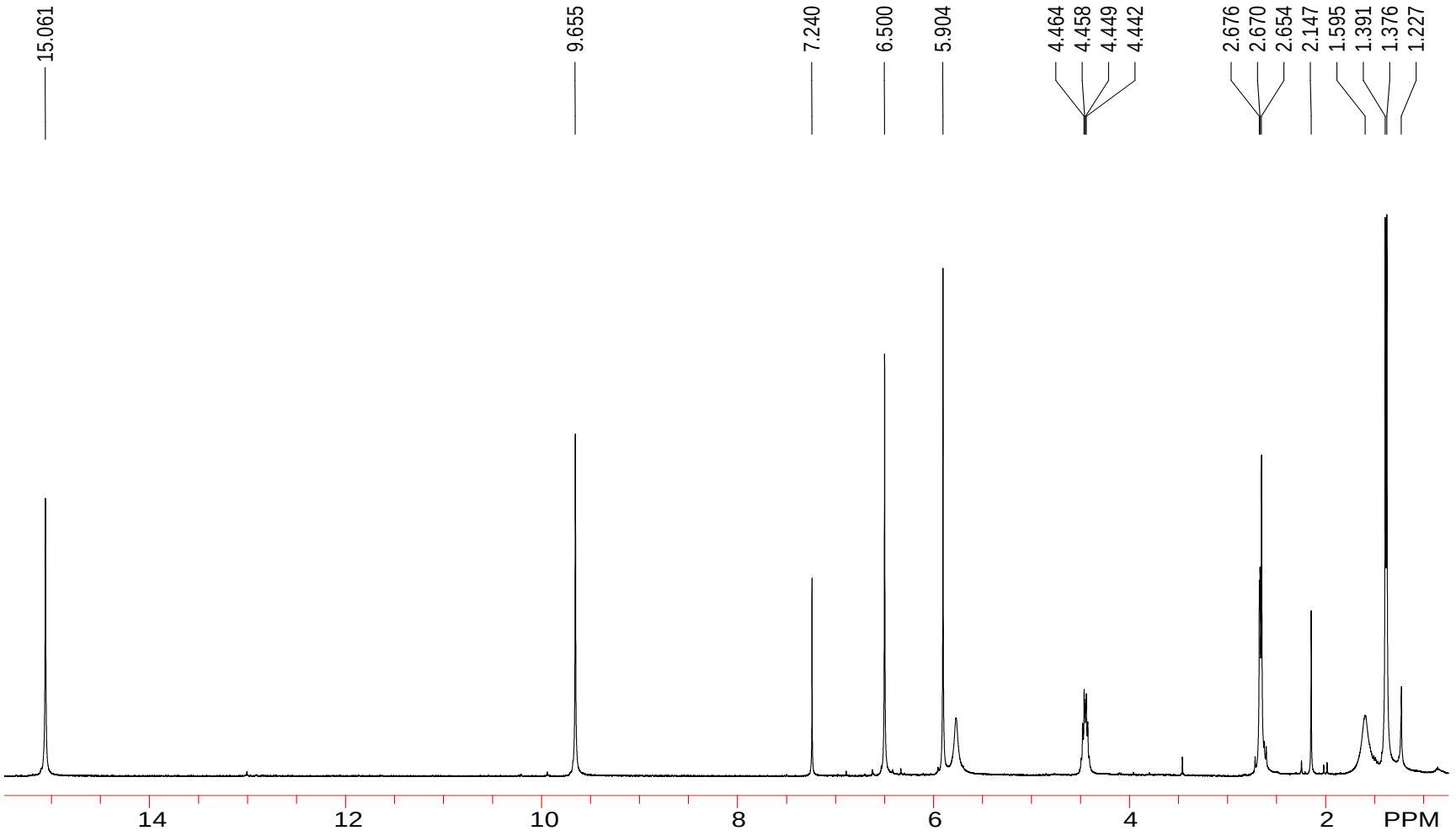

Figure A.20. ^{1}H NMR Spectrum of cephalochromin (**5.6**, $CDCl_3$, 400 MHz)

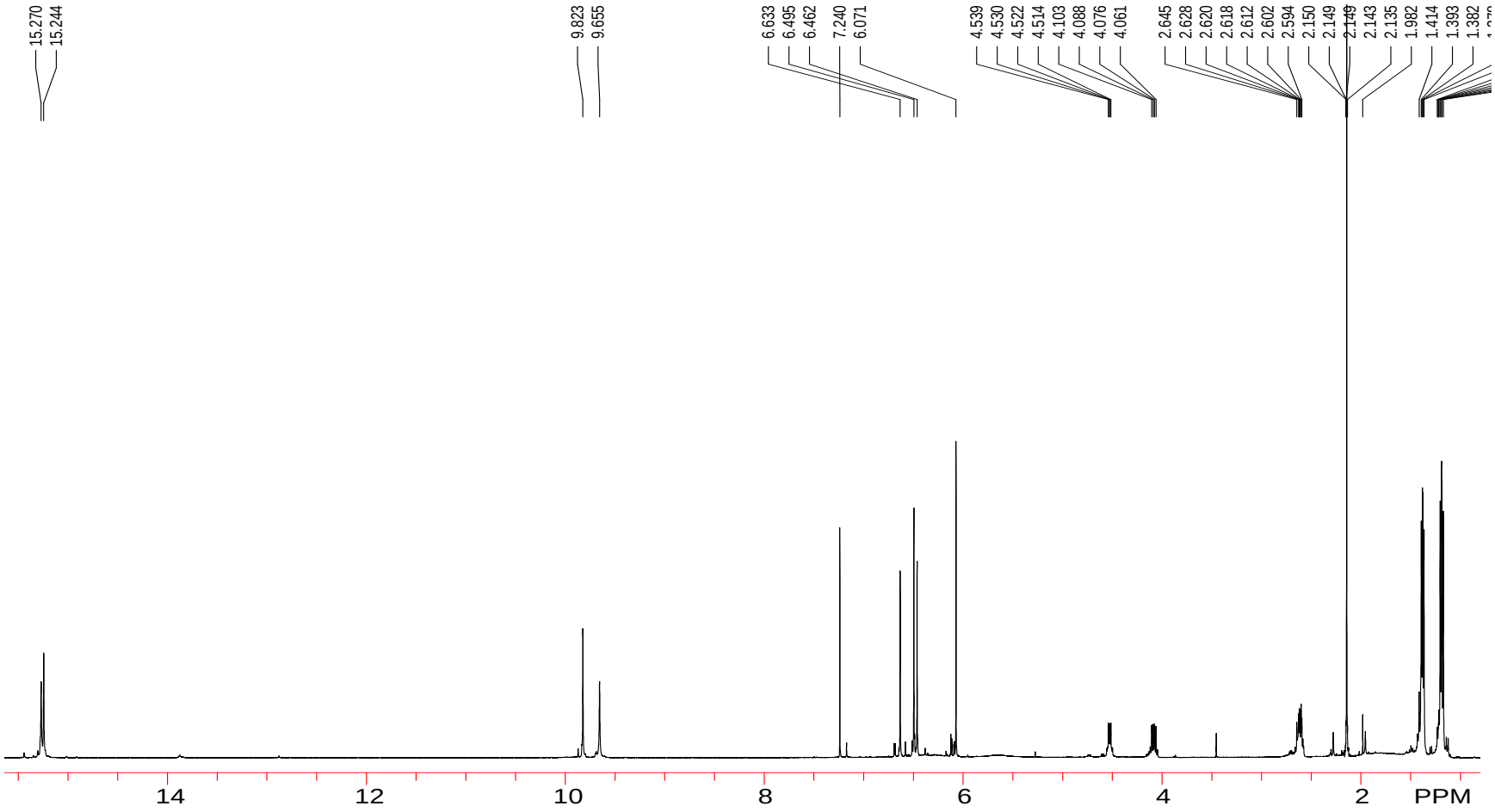

Figure A.21. ^{1}H NMR spectra of **5.7** at 100 mg/mL ($CDCl_3$, 400 MHz)

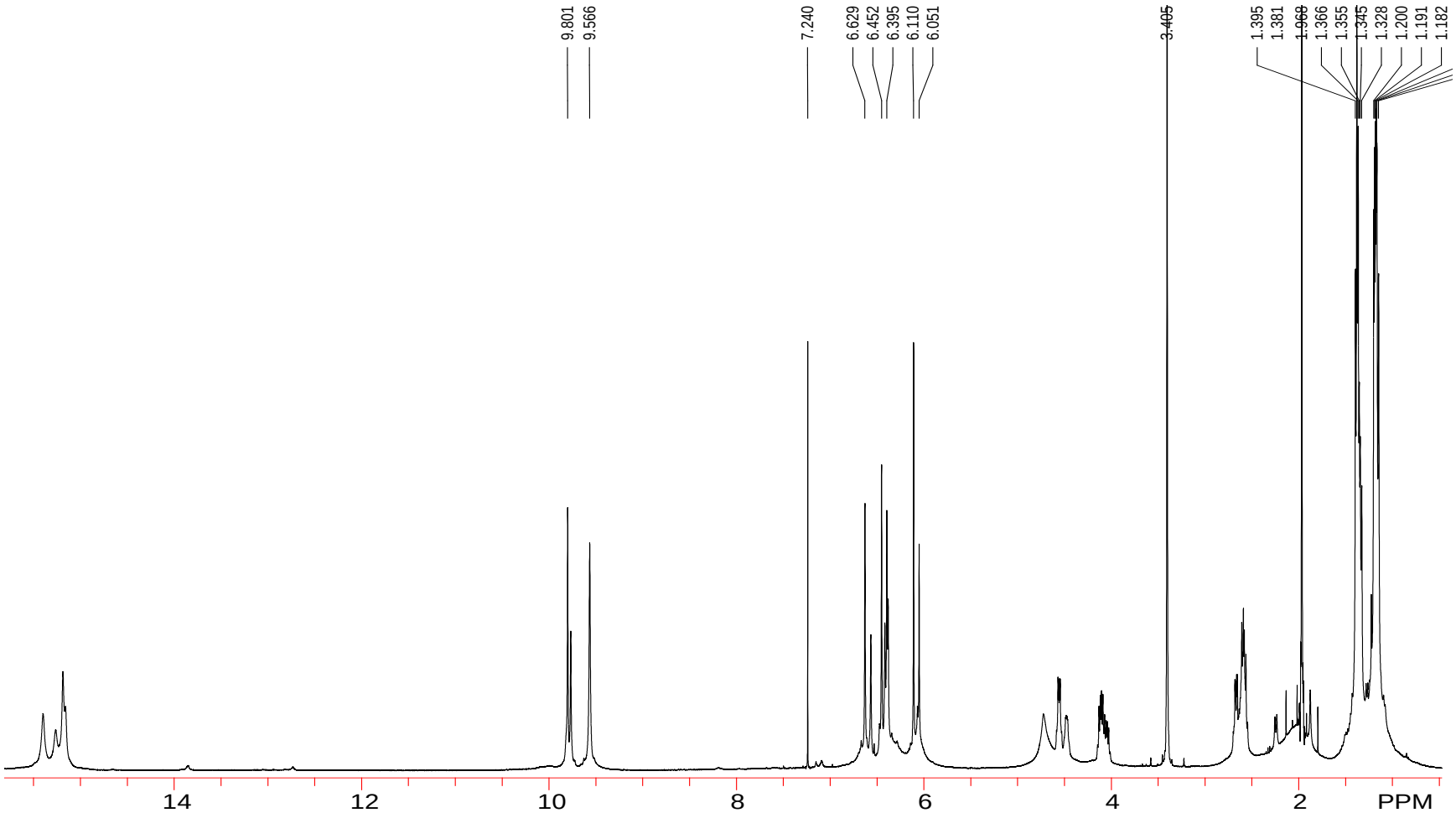

Figure A.22. ^{1}H NMR spectra of **5.7** at 75 mg/mL ($CDCl_3$, 400 MHz)

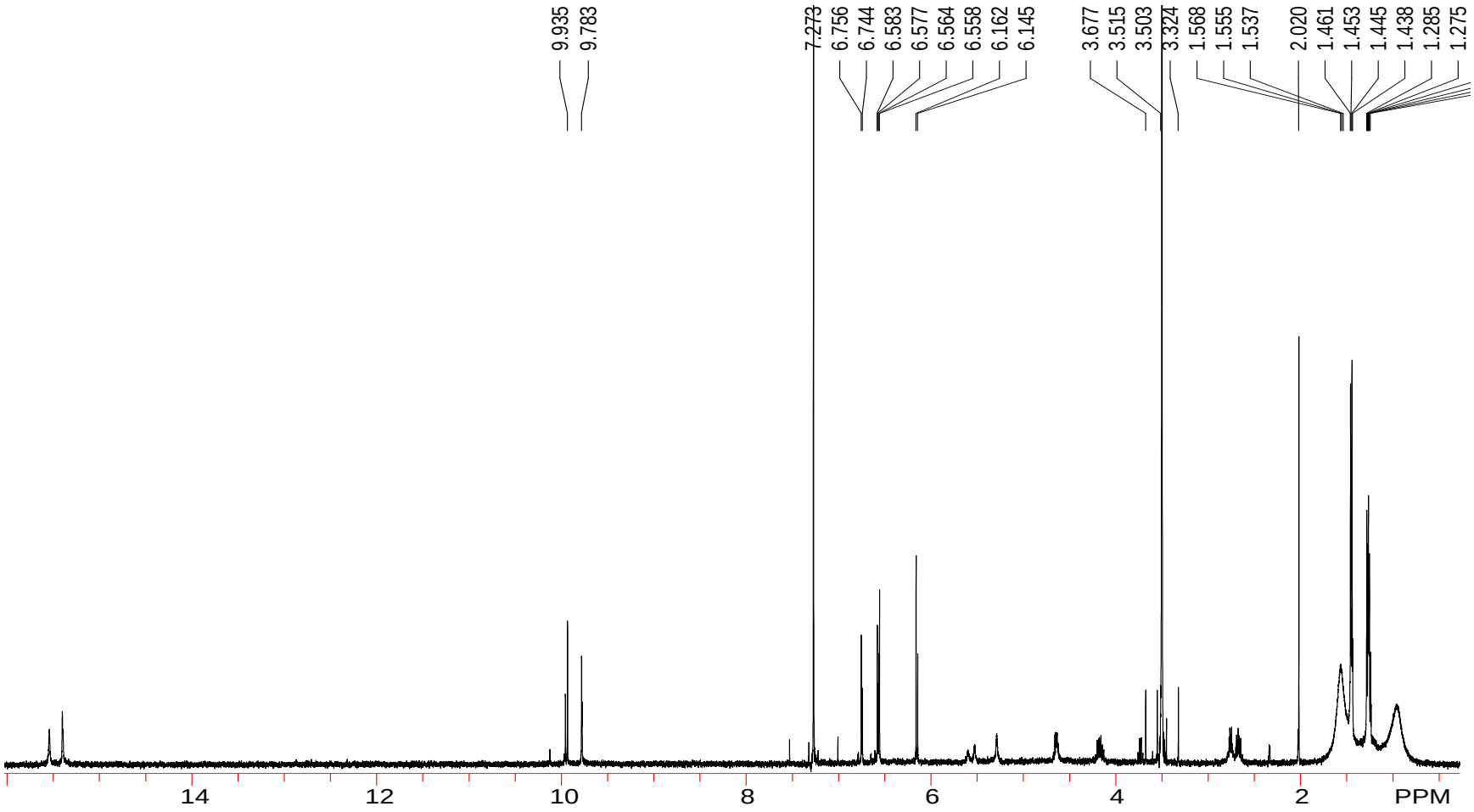

Figure A.23. ^{1}H NMR spectra of **5.7** at 1.2 mg/mL ($CDCl_3$, 400 MHz)

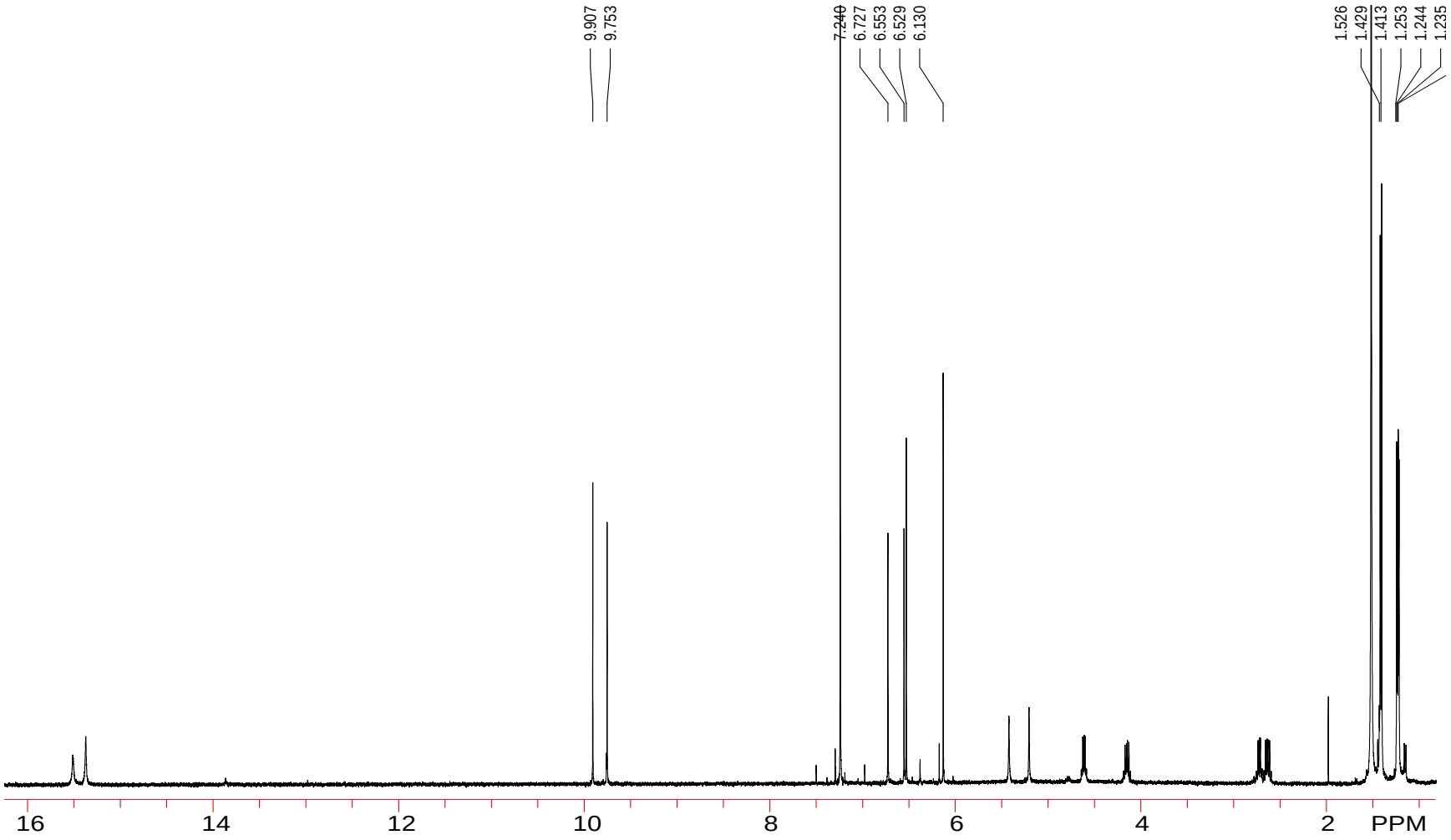

Figure A.24. ^{1}H NMR spectra of **5.9** ($CDCl_3$, 400 MHz)

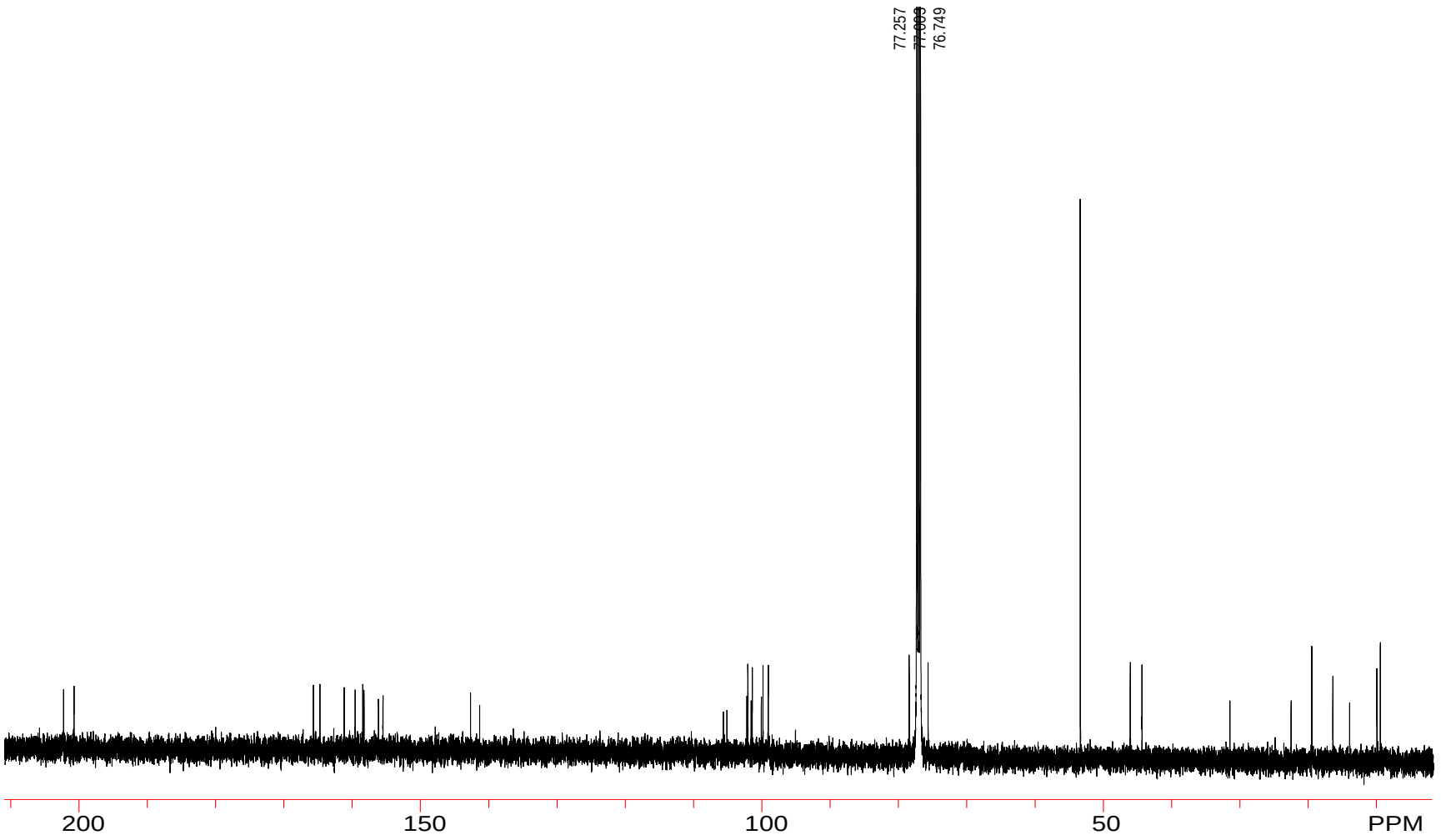

Figure A.25. ^{13}C NMR data for **5.9** ($CDCl_3$, 125 MHz)

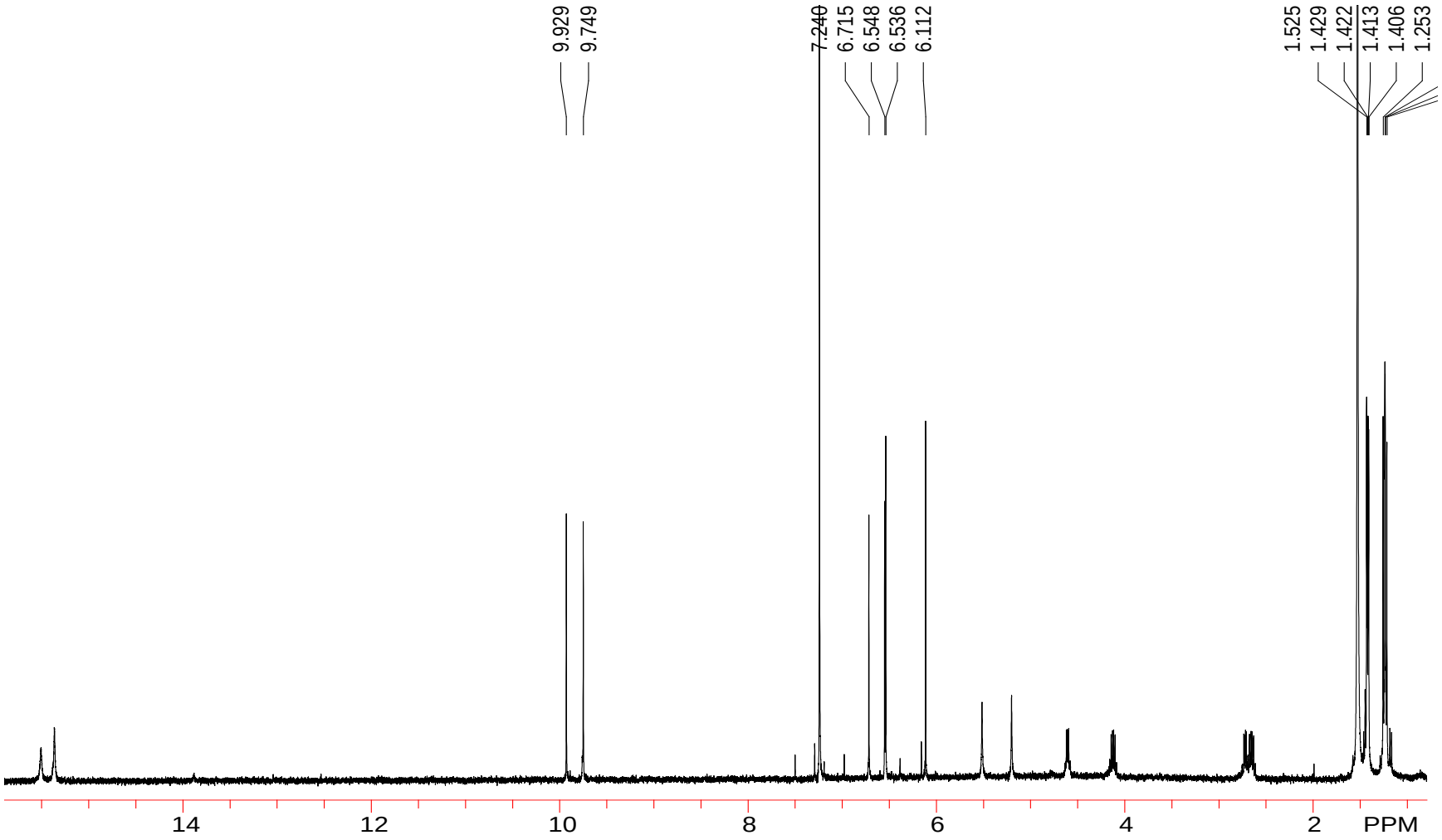

Figure A.26. ^{1}H NMR spectra of **5.10** ($CDCl_3$, 400 MHz)

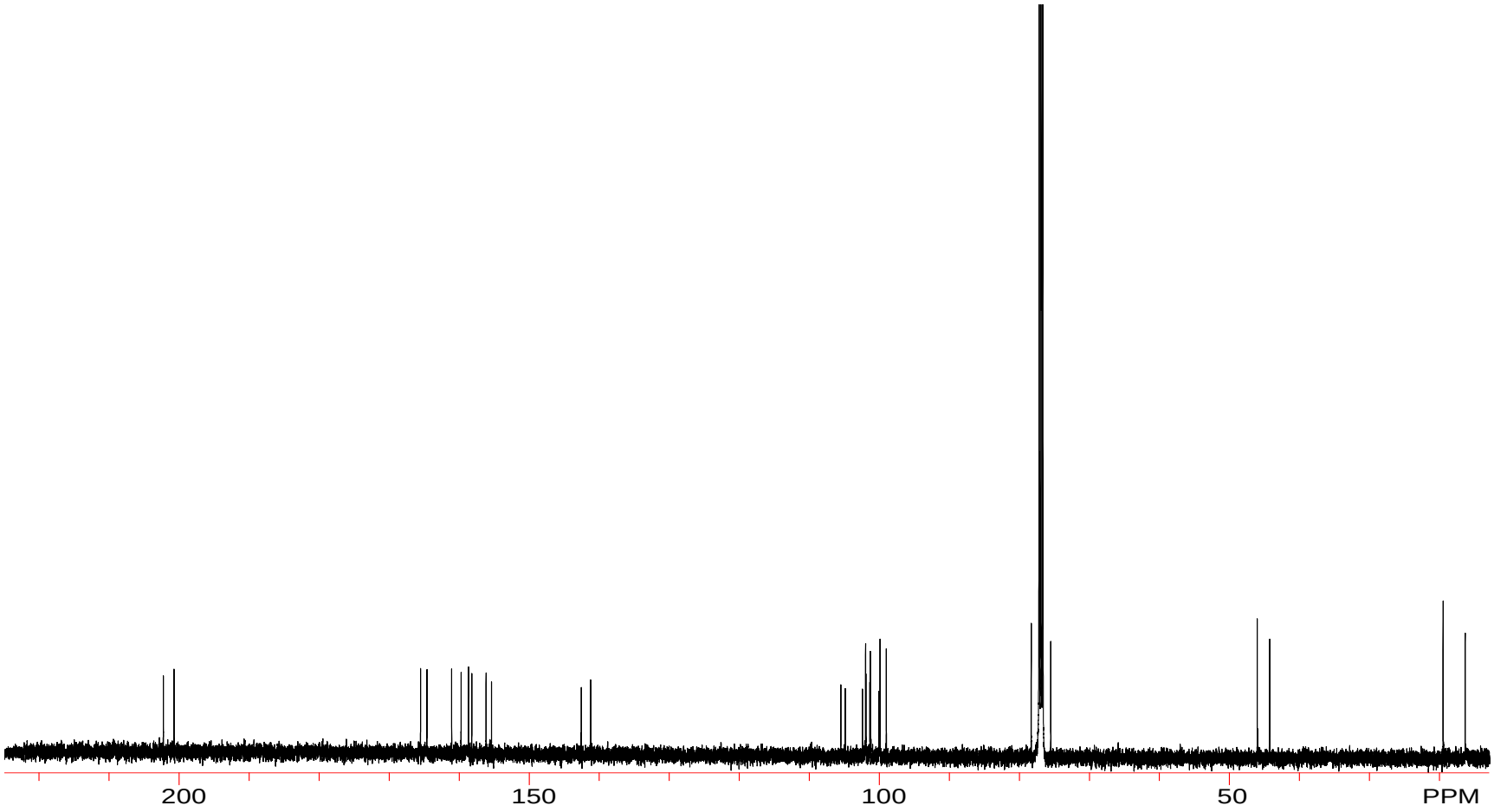

Figure A.27. ^{13}C NMR spectra for **5.10** ($CDCl_3$, 500 MHz)

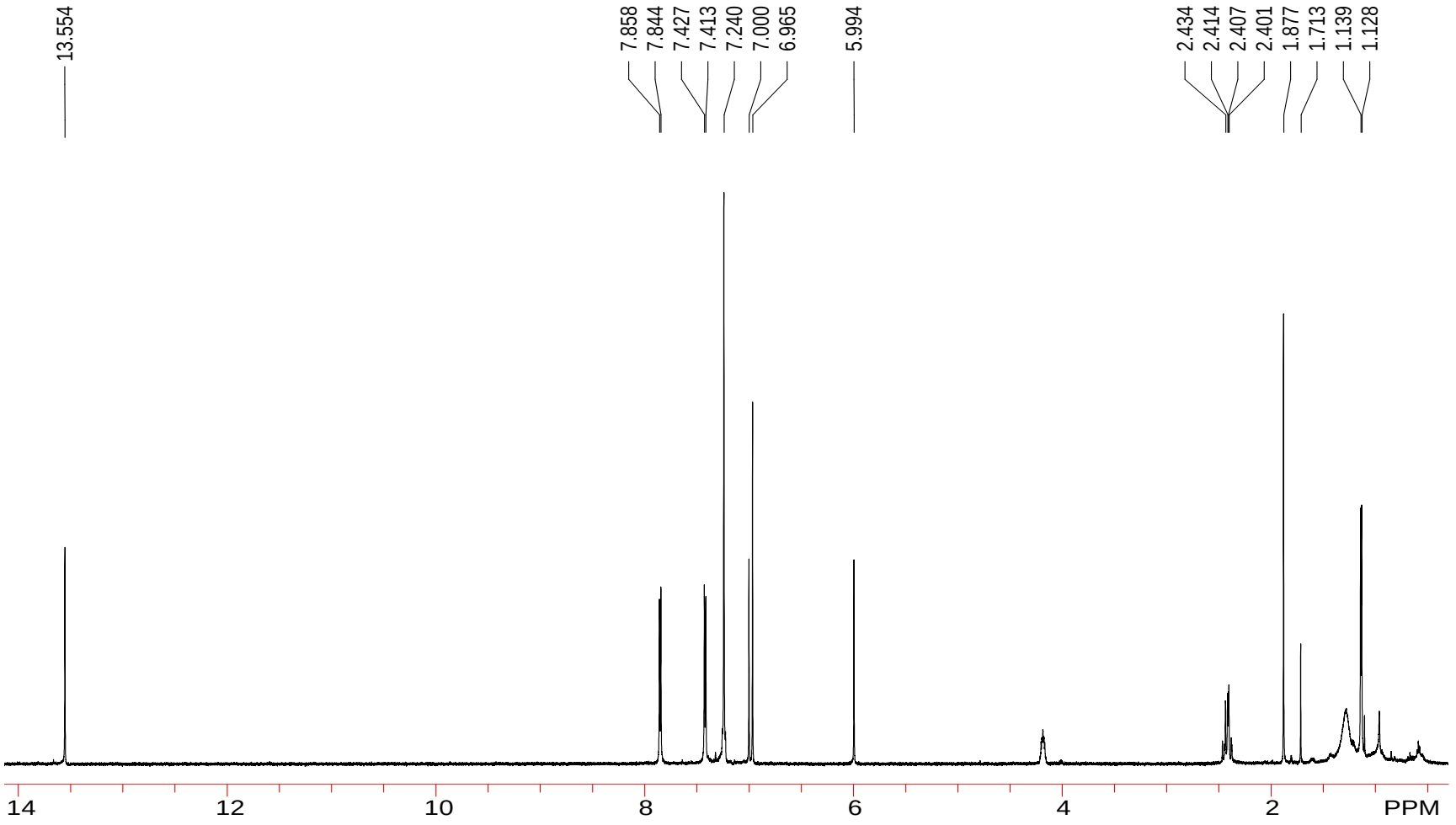

Figure A.28. ^{1}H NMR spectrum of **5.11** ($CDCl_3$, 600 MHz)

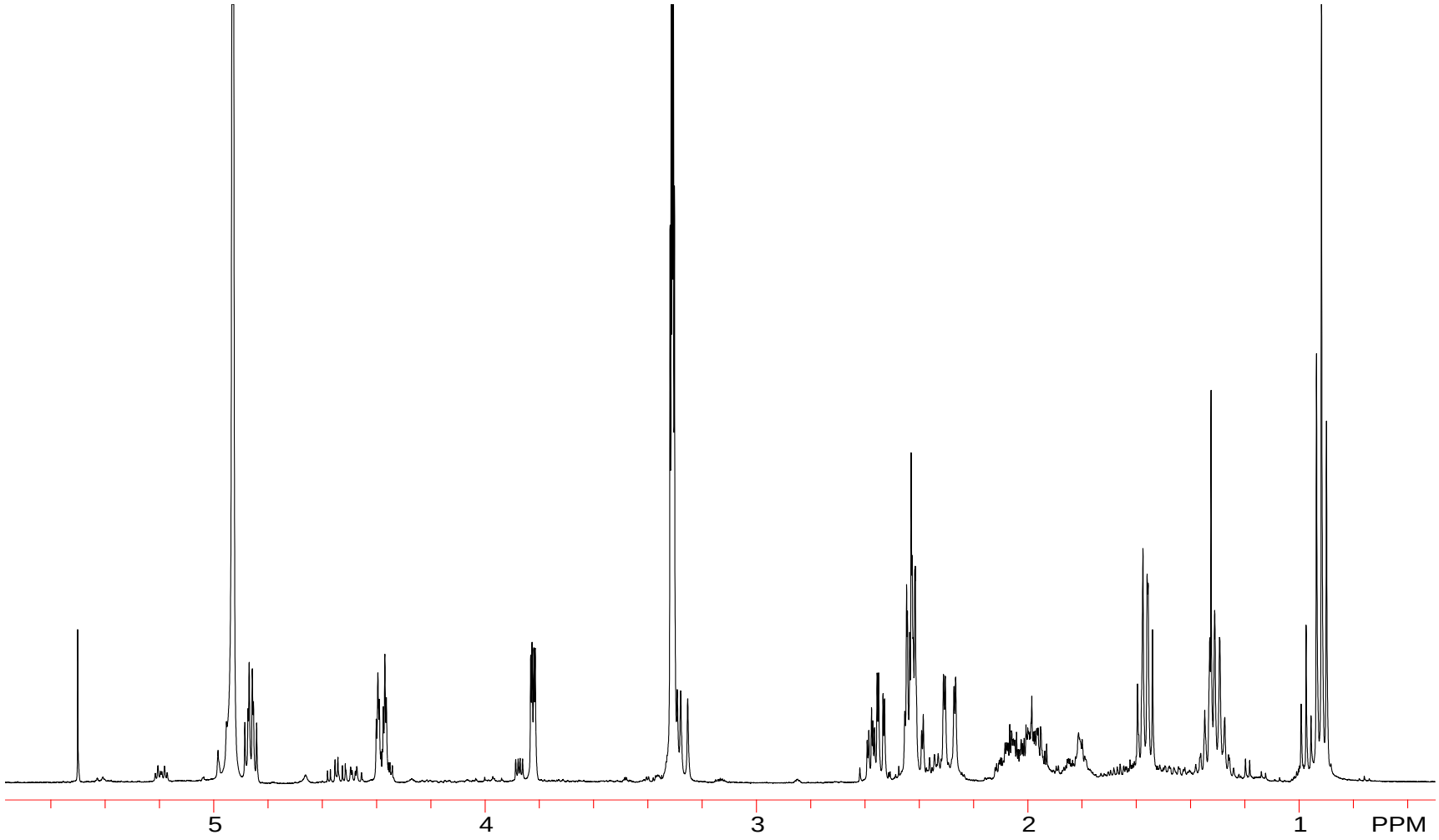

Figure A.29. ^{1}H NMR spectra for herbarumin IV (**6.1**, CD_3OD, 400 MHz)

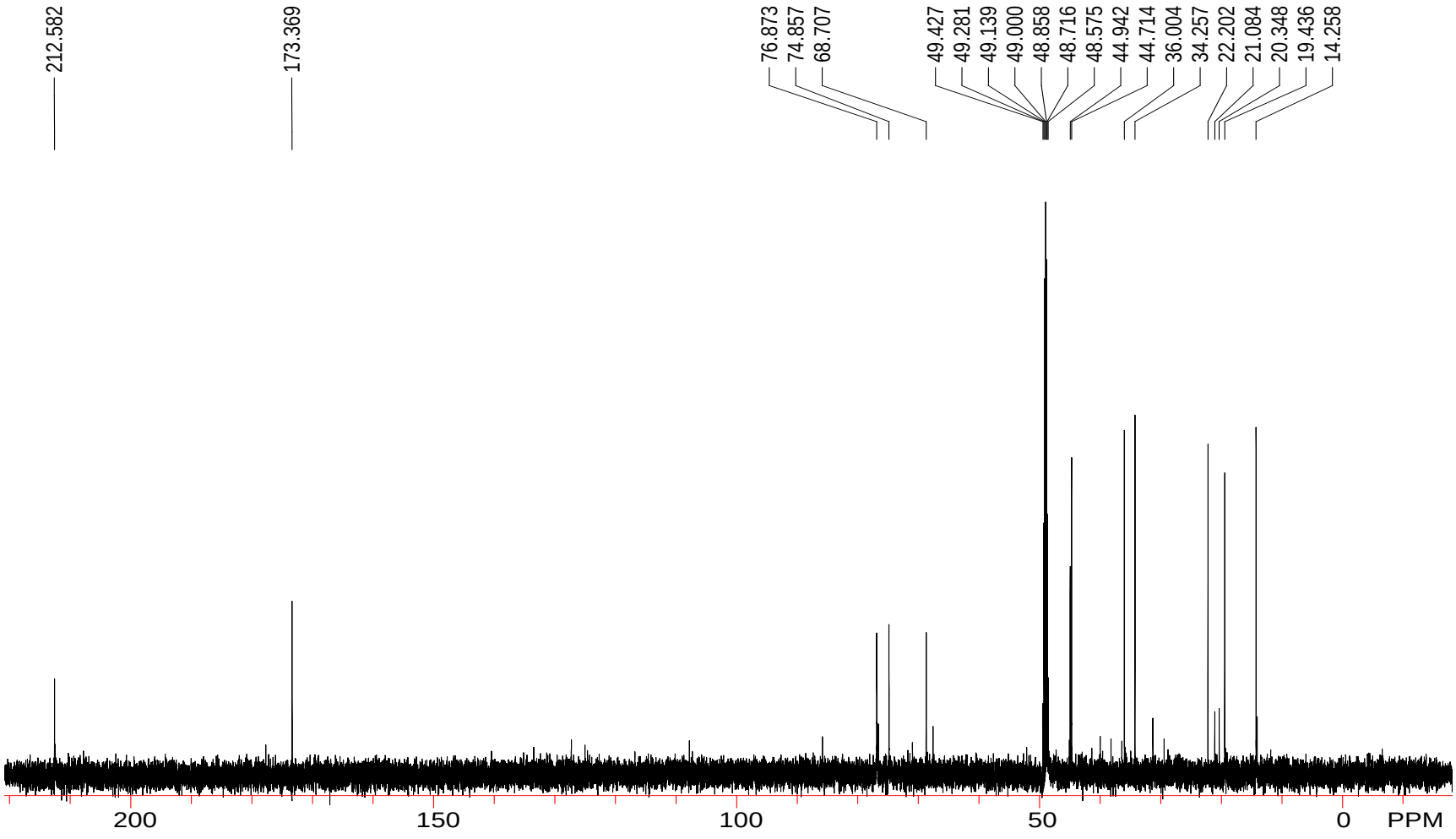

Figure A.30. ^{13}C NMR spectra for herbarumin IV (**6.1**, CD_3OD, 100 MHz)

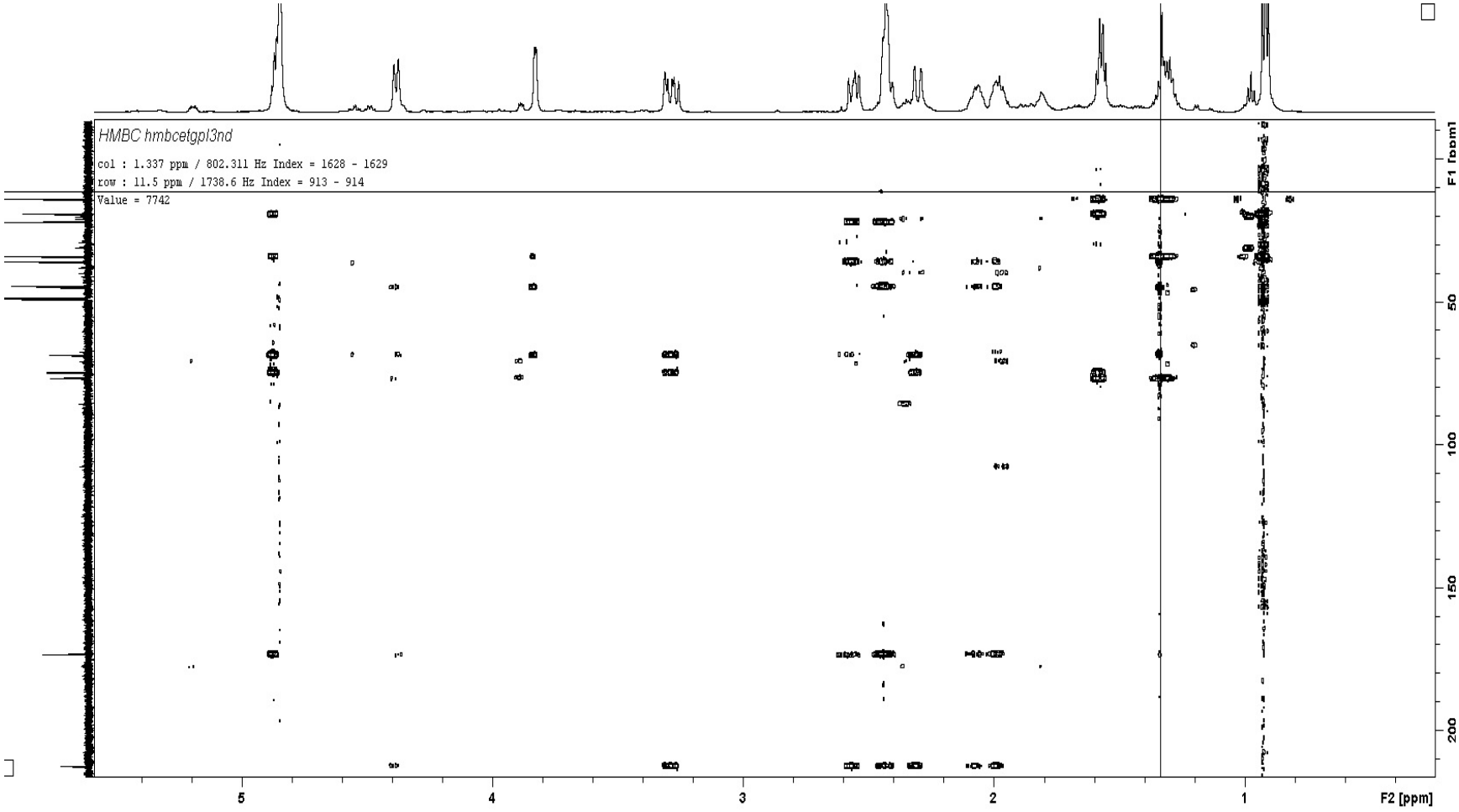

Figure A.31. HMBC spectra for herbarumin IV (**6.1**, CD_3OD, 100 MHz)

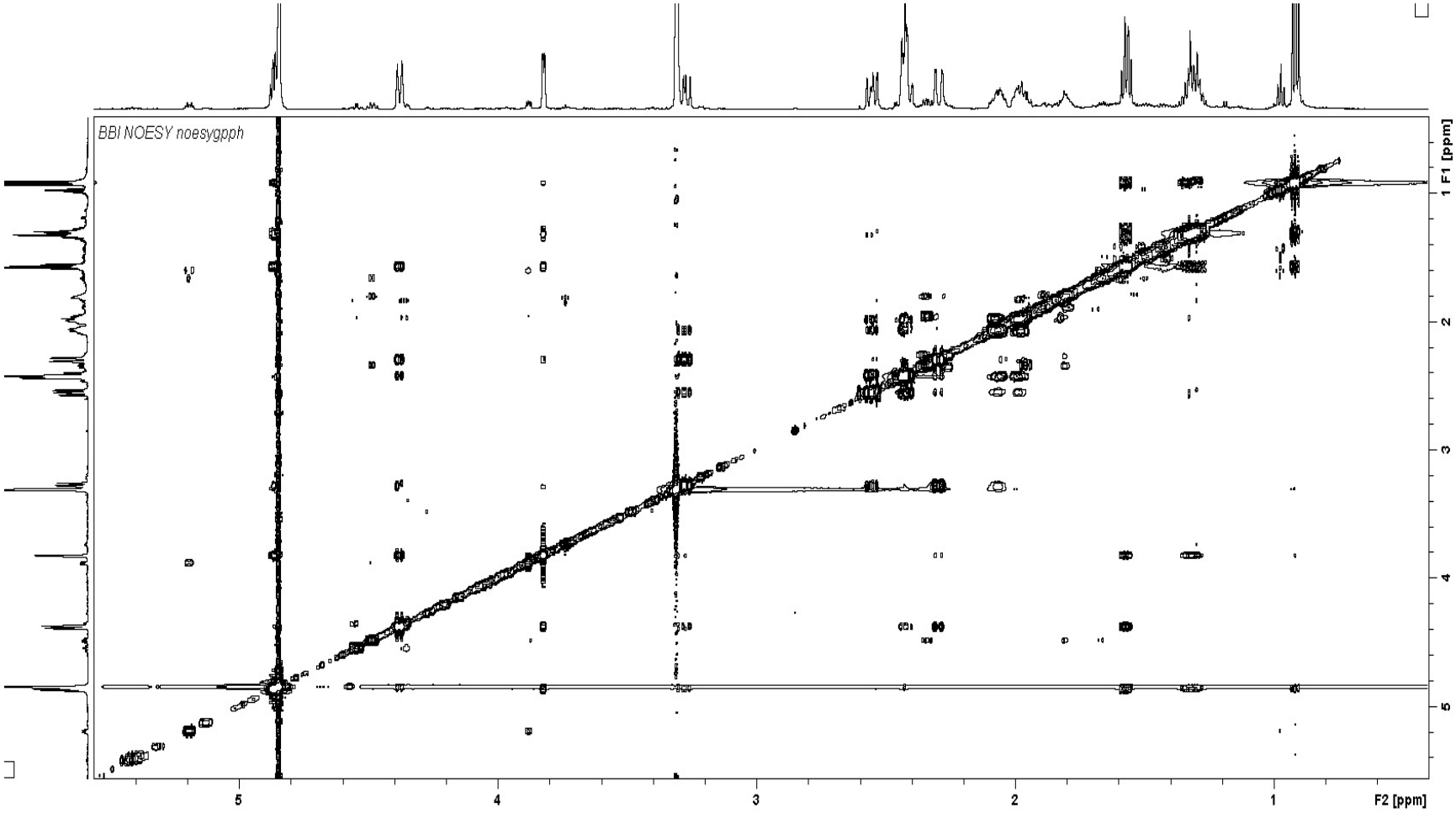

Figure A.32. NOESY spectra for herbarumin IV (**6.1**, CD_3OD, 100 MHz)

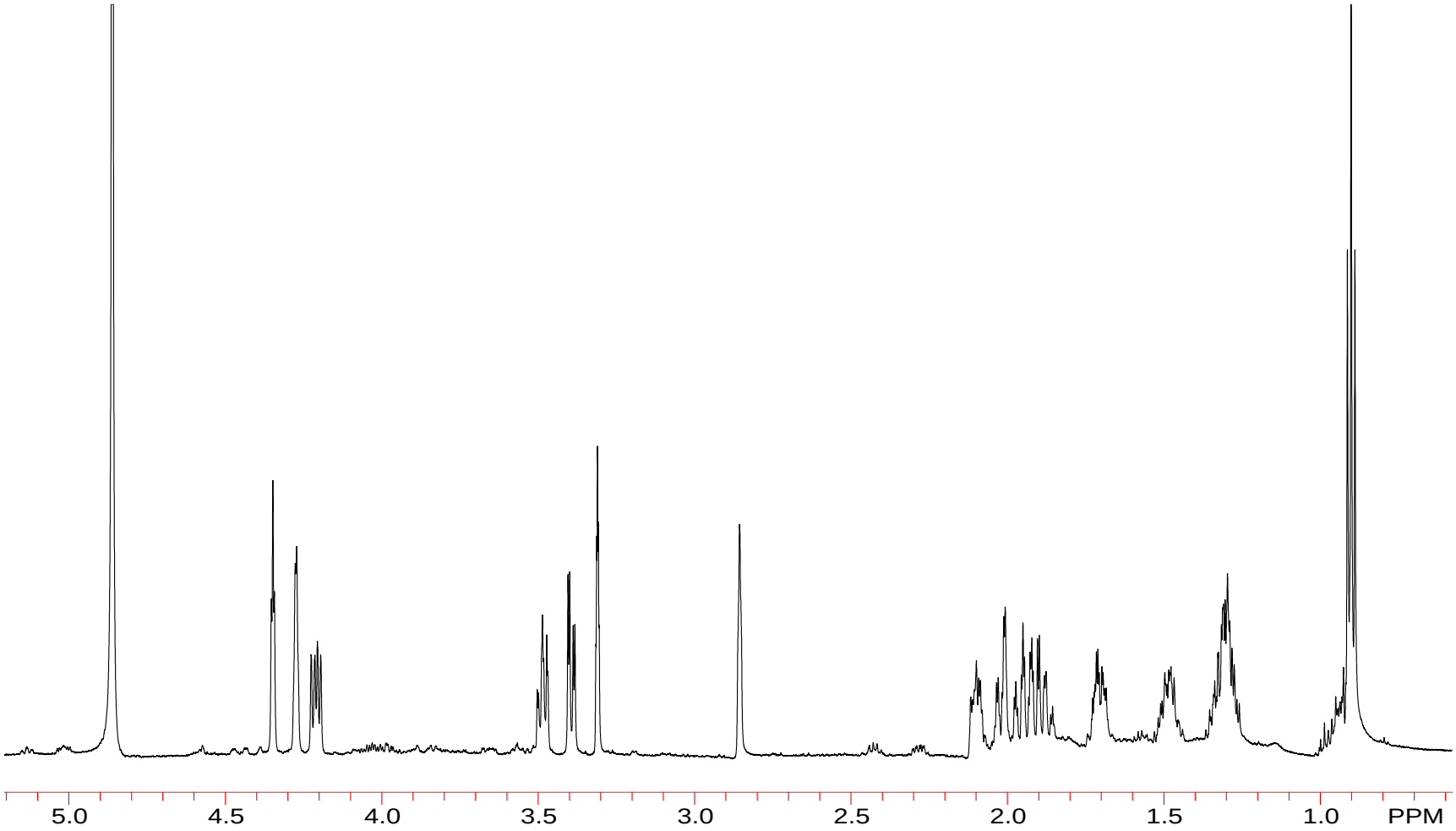

Figure A.33. ^{1}H NMR spectra of herbarumin V (**6.3**, CD_3OD, 600 MHz)

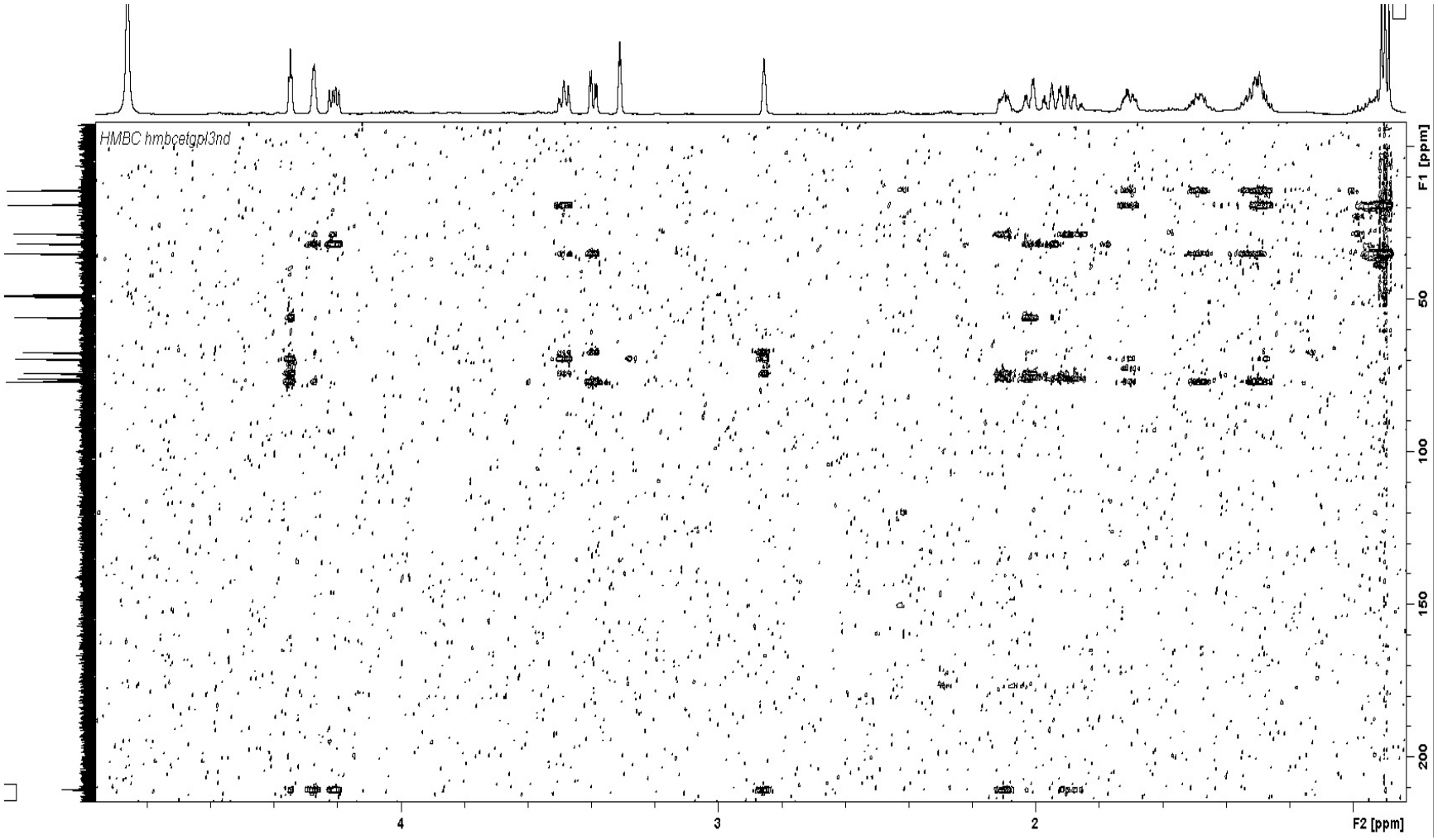

Figure A. 34. HMBC spectra of herbarumin V (**6.3**, CD_3OD, 600 MHz)

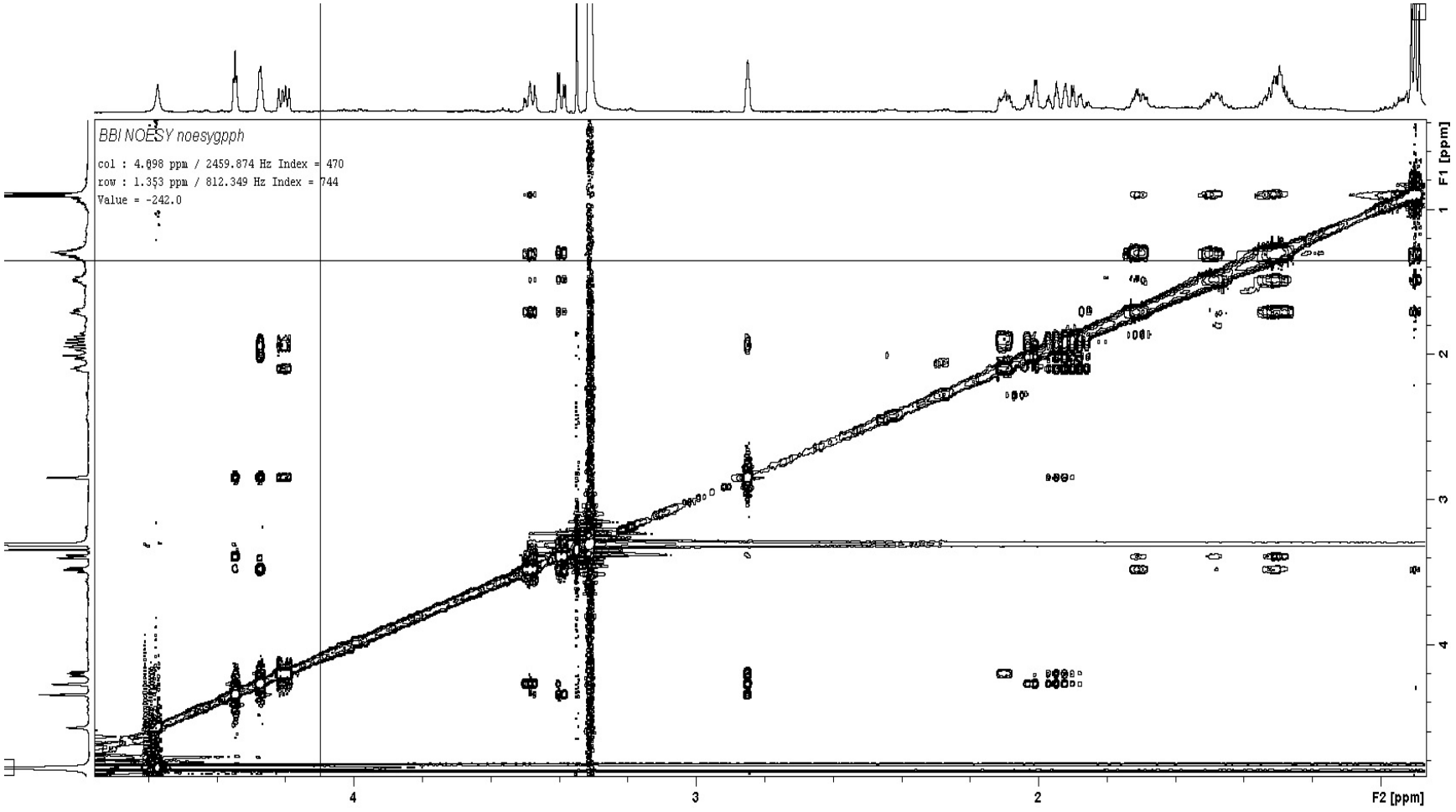

Figure A.35. NOESY spectra of herbarumin V (**6.3**, CD_3OD, 600 MHz)

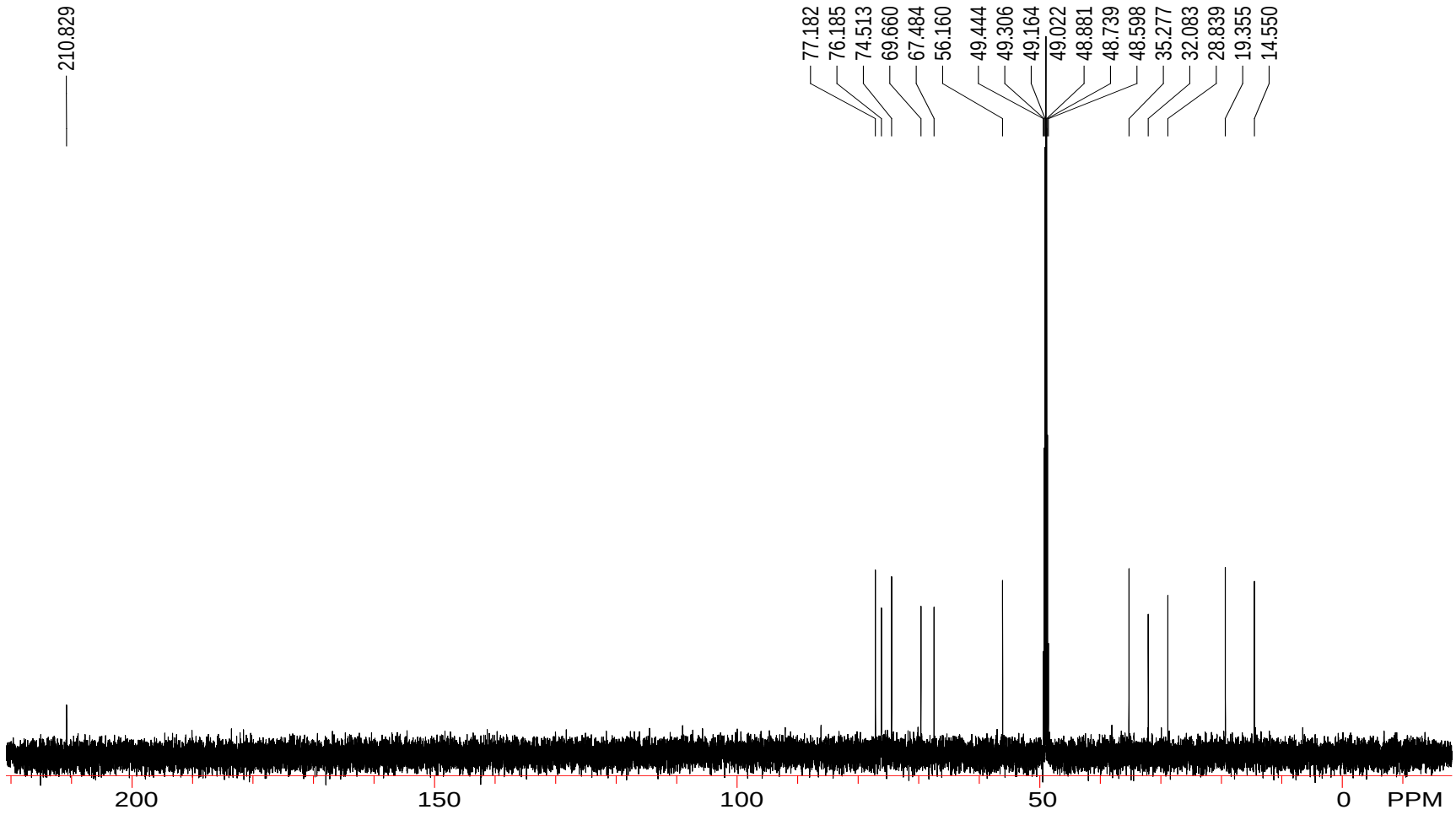

Figure A.36. ^{13}C NMR spectra of herbarumin V (**6.3**, CD_3OD, 150 MHz)

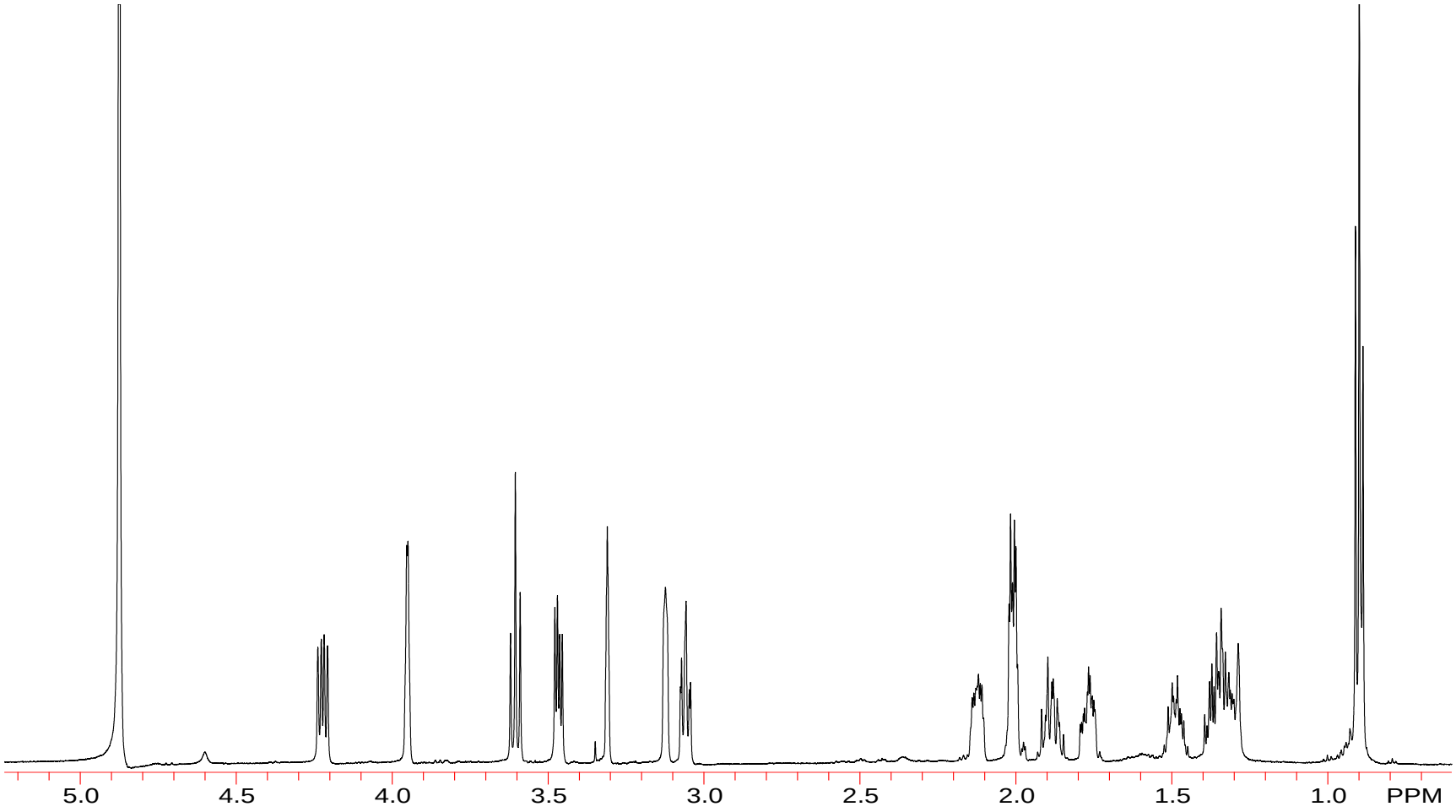

Figure A.37. ^{1}H NMR spectra of 7-epi-herbarumin V (**6.4**, CD_3OD, 600 MHz)

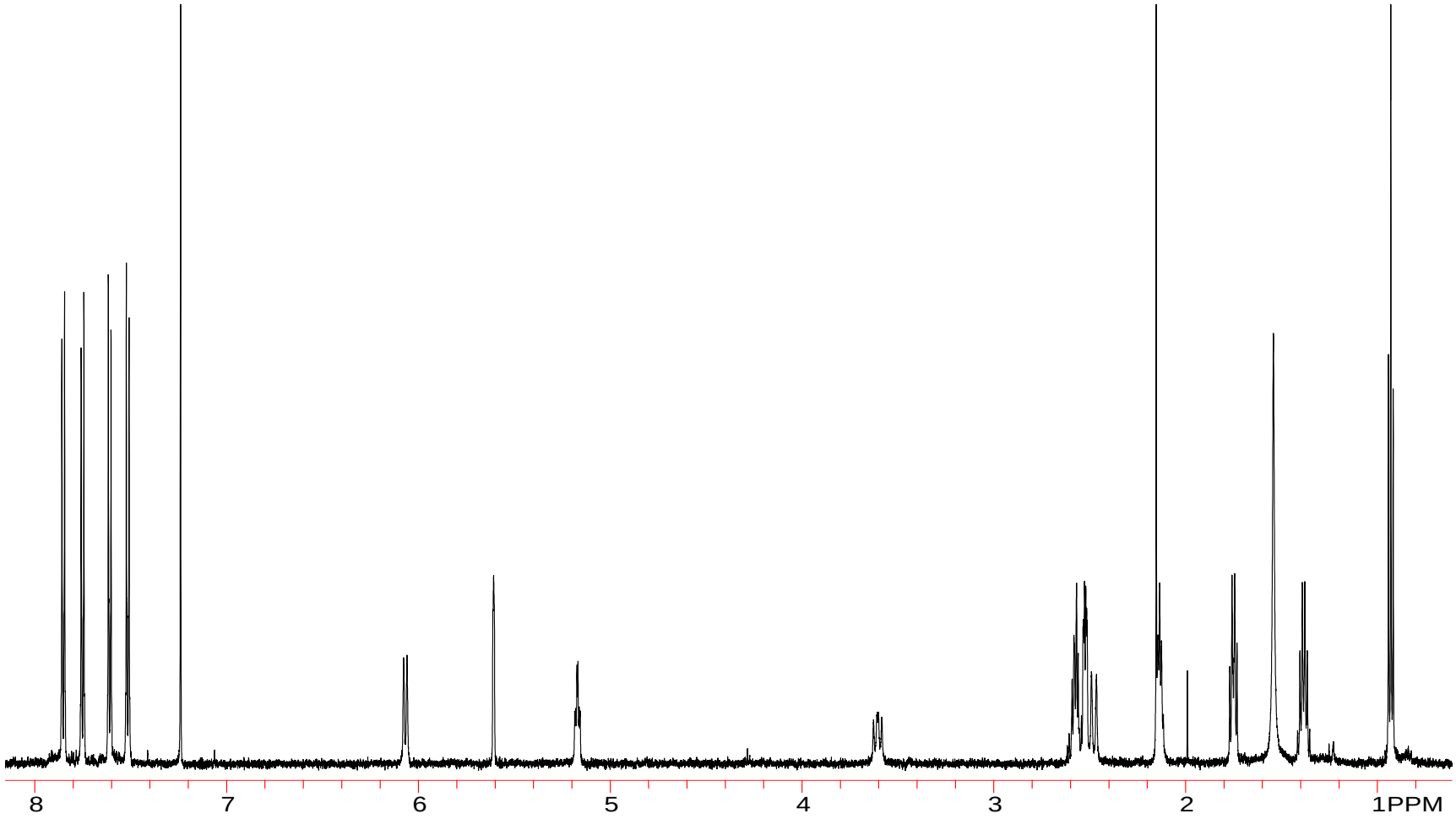

Figure A.38. ^{1}H NMR spectra of **6.9** ($CDCl_3$, 600 MHz)

APPENDIX B

SUPPLEMENTARY X-RAY DATA

Table B.1. Crystal data and structure refinement for **3.6**

Identification code	Peptide 2
Empirical formula	C54 H85.57 N10 O13.89
Formula weight	1097.20
Temperature	150(2) K
Wavelength	0.77490 A
Crystal system, space group	Orthorhombic, P 21 21 21
Unit cell dimensions	a = 18.784(3) A alpha = 90 deg.
	b = 22.671(4)A beta = 90deg
	c = 27.890(5) A gamma = 90 deg
Volume	11877(4) A^3
Z, Calculated density	8, 1.227 Mg/m^3
Absorption coefficient	0.107 mm^-1
F(000)	4726
Crystal size	0.15 x 0.10 x 0.02 mm
Theta range for data collection	2.49 to 28.99 deg.
Limiting indices	-23<=h<=23,-28<=k<=28,34<=l<=34
Reflections collected / unique	129780 / 24290 [R(int)=0.0774]
Completeness to theta = 28.99	99.7 %
Absorption correction	Semi-empirical from equivalents
Max. and min. transmission	0.9979 and 0.9842
Refinement method	Full-matrix least-squares on F^2
Data / restraints / parameters	24290 / 291 / 1538
Goodness-of-fit on F^2	1.018
Final R indices [I>2sigma(I)]	R1 = 0.0474, wR2 = 0.1200
R indices (all data)	R1 = 0.0611, wR2 = 0.1283
Absolute structure parameter	0.0(4)
Largest diff. peak and hole	0.508 and -0.187 e.A^-3

Table B.2. Atomic coordinates (x 10^4) and equivalent isotropic displacement parameters (A^2 x 10^3) for **3.6**[1]

	x	y	z	U(eq)
C(1A)	3814(1)	2196(1)	818(1)	30(1)
O(1A)	3969(1)	1755(1)	1054(1)	37(1)
C(2A)	3087(1)	2489(1)	875(1)	30(1)
N(1A)	2542(1)	2052(1)	760(1)	30(1)
C(7A)	2209(1)	2035(1)	339(1)	29(1)
O(2A)	2324(1)	2377(1)	5(1)	39(1)
C(8A)	1638(1)	1563(1)	270(1)	31(1)
N(2A)	1568(1)	1134(1)	652(1)	29(1)
C(9A)	1184(1)	1256(1)	1052(1)	31(1)
O(3A)	900(1)	1731(1)	1119(1)	43(1)
C(10A)	1106(1)	734(1)	1398(1)	32(1)
N(3A)	1777(1)	402(1)	1453(1)	30(1)
C(19A)	2373(1)	710(1)	1556(1)	31(1)
O(4A)	2358(1)	1253(1)	1594(1)	36(1)
C(20A)	3089(1)	395(1)	1601(1)	35(1)
N(4A)	3517(1)	564(1)	1186(1)	33(1)
C(25A)	3782(1)	176(1)	871(1)	31(1)
O(5A)	3651(1)	-355(1)	873(1)	39(1)
C(26A)	4280(1)	454(1)	499(1)	29(1)
N(5A)	4969(1)	143(1)	502(1)	33(1)
C(30A)	5536(1)	441(1)	660(1)	31(1)
O(7A)	5496(1)	955(1)	805(1)	46(1)
C(31A)	6257(1)	136(1)	700(1)	31(1)
N(6A)	6796(1)	533(1)	509(1)	28(1)
C(39A)	7022(1)	502(1)	62(1)	31(1)
O(8A)	6847(1)	115(1)	-226(1)	44(1)
C(40A)	7533(1)	981(1)	-110(1)	36(1)
N(7A)	7740(1)	1428(1)	236(1)	36(1)

1 . U(eq) is defined as one third of the trace of the orthogonalized Uij tensor.

Table B.2 contd.

C(41A)	8200(1)	1304(1)	592(1)	38(1)
O(9A)	8465(1)	814(1)	636(1)	44(1)
C(42A)	8399(1)	1808(1)	932(1)	51(1)
N(8A)	7792(1)	2205(1)	1027(1)	37(1)
C(45A)	7171(1)	1970(1)	1158(1)	32(1)
O(10A)	7096(1)	1431(1)	1188(1)	39(1)
C(46A)	6537(1)	2372(1)	1257(1)	40(1)
N(9A)	5939(1)	2150(1)	974(1)	34(1)
C(51A)	5532(1)	2498(1)	706(1)	31(1)
O(11A)	5596(1)	3040(1)	690(1)	39(1)
C(52A)	4957(1)	2183(1)	409(1)	32(1)
N(10A)	4265(1)	2443(1)	506(1)	34(1)
C(3A)	2986(1)	2727(1)	1387(1)	35(1)
C(4A)	3613(2)	3123(1)	1521(1)	54(1)
C(5A)	2270(1)	3050(1)	1423(1)	47(1)
C(6A)	2115(2)	3298(1)	1918(1)	58(1)
C(11A)	788(1)	926(1)	1881(1)	43(1)
C(12A)	542(1)	407(1)	2178(1)	40(1)
C(13A)	-98(2)	125(1)	2076(1)	54(1)
C(14A)	-325(2)	-356(1)	2340(1)	61(1)
C(15A)	85(2)	-575(1)	2709(1)	54(1)
C(16A)	716(2)	-306(1)	2812(1)	53(1)
C(17A)	939(1)	185(1)	2552(1)	48(1)
C(18A)	1738(1)	-244(1)	1411(1)	40(1)
C(21A)	3475(1)	576(1)	2068(1)	46(1)
C(22A)	3008(2)	436(2)	2502(1)	64(1)
C(23A)	4216(2)	294(2)	2099(1)	69(1)
C(24A)	4242(2)	-380(2)	2080(1)	86(1)
C(27A)	3950(1)	493(1)	-3(1)	33(1)
O(6A)	4471(1)	754(1)	-309(1)	41(1)
C(28A)	3289(1)	869(1)	7(1)	41(1)
C(29A)	5017(1)	-454(1)	302(1)	49(1)
C(32A)	6365(1)	19(1)	1240(1)	39(1)
C(33A)	6976(1)	-370(1)	1379(1)	40(1)

Table B.2 contd.

C(34A)	6842(2)	-881(1)	1641(1)	58(1)
C(35A)	7383(2)	-1217(1)	1813(1)	71(1)
C(36A)	8077(2)	-1070(1)	1719(1)	72(1)
C(37A)	8227(2)	-576(2)	1447(1)	70(1)
C(38A)	7673(2)	-218(1)	1282(1)	53(1)
C(43A)	8722(2)	1577(2)	1400(2)	86(1)
C(44A)	7963(2)	2839(1)	1052(1)	54(1)
C(47A)	6403(2)	2495(1)	1798(1)	40(1)
C(48A)	6321(2)	1929(2)	2093(1)	54(1)
C(49A)	5691(2)	1545(2)	1984(1)	57(1)
C(50A)	5787(3)	2918(2)	1871(2)	54(1)
C(47C)	6355(4)	2092(4)	1783(2)	48(2)
C(48C)	5666(4)	2375(4)	1973(4)	54(2)
C(49C)	5659(8)	3036(4)	2001(5)	54(1)
C(50C)	6975(4)	2183(5)	2127(4)	59(3)
C(53A)	5129(1)	2215(1)	-131(1)	35(1)
O(12A)	4548(1)	1987(1)	-403(1)	43(1)
C(54A)	5813(1)	1890(1)	-247(1)	44(1)
C(1B)	5499(1)	5391(1)	710(1)	27(1)
O(1B)	5456(1)	5846(1)	951(1)	39(1)
C(2B)	6206(1)	5071(1)	661(1)	29(1)
N(1B)	6712(1)	5489(1)	455(1)	28(1)
C(7B)	6964(1)	5449(1)	13(1)	27(1)
O(2B)	6800(1)	5053(1)	-268(1)	41(1)
C(8B)	7473(1)	5930(1)	-154(1)	28(1)
N(2B)	7666(1)	6363(1)	207(1)	28(1)
C(9B)	8166(1)	6250(1)	535(1)	30(1)
O(3B)	8469(1)	5772(1)	557(1)	39(1)
C(10B)	8364(1)	6764(1)	867(1)	32(1)
N(3B)	7731(1)	7112(1)	1000(1)	28(1)
C(19B)	7173(1)	6826(1)	1192(1)	31(1)
O(4B)	7182(1)	6282(1)	1237(1)	36(1)
C(20B)	6501(1)	7163(1)	1338(1)	35(1)
N(4B)	5948(1)	7027(1)	989(1)	35(1)

Table B.2 contd.

C(25B)	5611(1)	7430(1)	724(1)	36(1)
O(5B)	5785(1)	7953(1)	699(1)	47(1)
C(26B)	4962(1)	7193(1)	450(1)	36(1)
N(5B)	4311(1)	7489(1)	623(1)	39(1)
C(30B)	3829(1)	7168(1)	856(1)	34(1)
O(7B)	3926(1)	6645(1)	960(1)	42(1)
C(31B)	3126(1)	7443(1)	1030(1)	42(1)
N(6B)	2545(1)	7065(1)	874(1)	39(1)
C(39B)	2257(1)	7116(1)	442(1)	39(1)
O(8B)	2406(1)	7519(1)	163(1)	54(1)
C(40B)	1724(1)	6653(1)	267(1)	42(1)
N(7B)	1580(1)	6172(1)	594(1)	36(1)
C(41B)	1134(1)	6250(1)	963(1)	42(1)
O(9B)	811(1)	6711(1)	1029(1)	61(1)
C(42B)	1015(1)	5715(1)	1293(1)	42(1)
N(8B)	1660(1)	5347(1)	1347(1)	38(1)
C(45B)	2271(1)	5611(1)	1481(1)	35(1)
O(10B)	2302(1)	6151(1)	1535(1)	38(1)
C(46B)	2966(1)	5269(1)	1552(1)	37(1)
N(9B)	3451(1)	5470(1)	1175(1)	34(1)
C(51B)	3777(1)	5119(1)	862(1)	29(1)
O(11B)	3719(1)	4574(1)	856(1)	33(1)
C(52B)	4246(1)	5439(1)	499(1)	29(1)
N(10B)	4944(1)	5159(1)	483(1)	32(1)
C(3B)	6467(1)	4844(1)	1148(1)	34(1)
C(4B)	5885(2)	4491(1)	1394(1)	51(1)
C(5B)	7148(1)	4489(1)	1072(1)	46(1)
C(6B)	7543(2)	4332(1)	1529(1)	67(1)
C(11B)	8795(1)	6539(1)	1294(1)	47(1)
C(12B)	9021(1)	7004(1)	1655(1)	44(1)
C(13B)	8841(2)	6945(1)	2127(1)	55(1)
C(14B)	9089(2)	7341(1)	2470(1)	61(1)
C(15B)	9510(2)	7804(1)	2332(1)	64(1)
C(16B)	9686(2)	7876(2)	1857(1)	64(1)

Table B.2 contd.

C(17B)	9446(1)	7473(1)	1517(1)	51(1)
C(18B)	7777(1)	7754(1)	926(1)	40(1)
C(21B)	6259(2)	6965(1)	1845(1)	51(1)
C(22B)	6820(2)	7110(2)	2215(1)	69(1)
C(23B)	5521(2)	7225(2)	1972(1)	71(1)
C(24B)	5477(2)	7899(2)	1967(1)	85(1)
C(27B)	5044(1)	7238(1)	-99(1)	45(1)
O(6B)	4409(1)	7042(1)	-326(1)	56(1)
C(28B)	5686(1)	6889(1)	-269(1)	51(1)
C(29B)	4202(1)	8114(1)	511(1)	54(1)
C(32B)	3190(1)	7468(1)	1579(1)	49(1)
C(33B)	2593(3)	7735(3)	1875(2)	53(2)
C(34B)	2026(3)	7408(2)	2047(2)	61(1)
C(35B)	1496(3)	7658(2)	2332(2)	68(1)
C(36B)	1551(3)	8240(2)	2464(2)	64(2)
C(37B)	2106(4)	8566(3)	2300(4)	67(2)
C(38B)	2636(4)	8325(4)	2002(5)	57(2)
C(33C)	2610(5)	7819(6)	1801(4)	59(4)
C(34C)	1944(6)	7559(5)	1815(5)	58(3)
C(35C)	1387(6)	7810(6)	2077(6)	76(3)
C(36C)	1474(7)	8365(6)	2267(6)	73(4)
C(37C)	2104(9)	8648(7)	2214(11)	69(5)
C(38C)	2688(9)	8383(8)	1983(14)	60(4)
C(43B)	712(2)	5905(1)	1776(1)	58(1)
C(44B)	1548(2)	4707(1)	1331(1)	47(1)
C(47B)	3258(2)	5412(1)	2057(1)	49(1)
C(48B)	3996(2)	5144(1)	2148(1)	56(1)
C(49B)	4034(2)	4477(1)	2106(1)	57(1)
C(50B)	2706(2)	5242(2)	2437(1)	70(1)
O(12B)	4410(1)	5711(1)	-328(1)	40(1)
O(12C)	4291(6)	5930(4)	-278(5)	40(1)
C(53B)	3906(2)	5456(2)	-3(1)	33(1)
C(52C)	4246(1)	5439(1)	499(1)	29(1)
C(53C)	3926(4)	5485(5)	-7(2)	33(1)

Table B.2 contd.

C(54C)	3221(1)	5805(1)	-4(1)	40(1)
C(54B)	3221(1)	5805(1)	-4(1)	40(1)
O(61)	9432(1)	5080(1)	1022(1)	58(1)
O(62)	4630(1)	3811(1)	290(1)	63(1)
O(63)	4870(1)	4504(1)	-605(1)	66(1)
O(63')	5430(5)	5245(4)	-688(4)	66
O(64)	4995(2)	2236(2)	-1416(1)	84(1)

Table B.3. Bond lengths [A] and angles [deg] for **3.6**

C(1A)-O(1A)	1.233(3)	C(5A)-C(3A)-H(3AA)	108.3
C(1A)-N(10A)	1.337(3)	C(2A)-C(3A)-H(3AA)	108.3
C(1A)-C(2A)	1.526(3)	C(3A)-C(4A)-H(4AA)	109.5
C(2A)-N(1A)	1.459(2)	C(3A)-C(4A)-H(4AB)	109.5
C(2A)-C(3A)	1.538(3)	H(4AA)-C(4A)-H(4AB)	109.5
C(2A)-H(2AA)	1	C(3A)-C(4A)-H(4AC)	109.5
N(1A)-C(7A)	1.333(3)	H(4AA)-C(4A)-H(4AC)	109.5
N(1A)-H(1AN)	0.88	H(4AB)-C(4A)-H(4AC)	109.5
C(7A)-O(2A)	1.229(3)	C(6A)-C(5A)-C(3A)	113.9(2)
C(7A)-C(8A)	1.527(3)	C(6A)-C(5A)-H(5AA)	108.8
C(8A)-N(2A)	1.447(3)	C(3A)-C(5A)-H(5AA)	108.8
C(8A)-H(8AA)	0.99	C(6A)-C(5A)-H(5AB)	108.8
C(8A)-H(8AB)	0.99	C(3A)-C(5A)-H(5AB)	108.8
N(2A)-C(9A)	1.357(3)	H(5AA)-C(5A)-H(5AB)	107.7
N(2A)-H(2AN)	0.88	C(5A)-C(6A)-H(6AA)	109.5
C(9A)-O(3A)	1.217(3)	C(5A)-C(6A)-H(6AB)	109.5
C(9A)-C(10A)	1.534(3)	H(6AA)-C(6A)-H(6AB)	109.5
C(10A)-N(3A)	1.476(3)	C(5A)-C(6A)-H(6AC)	109.5
C(10A)-C(11A)	1.537(3)	H(6AA)-C(6A)-H(6AC)	109.5
C(10A)-H(10C)	1	H(6AB)-C(6A)-H(6AC)	109.5
N(3A)-C(19A)	1.349(3)	C(12A)-C(11A)-C(10A)	112.23(19)
N(3A)-C(18A)	1.472(3)	C(12A)-C(11A)-H(11A)	109.2
C(19A)-O(4A)	1.237(3)	C(10A)-C(11A)-H(11A)	109.2
C(19A)-C(20A)	1.529(3)	C(12A)-C(11A)-H(11B)	109.2
C(20A)-N(4A)	1.460(3)	C(10A)-C(11A)-H(11B)	109.2
C(20A)-C(21A)	1.544(3)	H(11A)-C(11A)-H(11B)	107.9
C(20A)-H(20A)	1	C(17A)-C(12A)-C(13A)	117.0(2)
N(4A)-C(25A)	1.340(3)	C(17A)-C(12A)-C(11A)	122.4(2)
N(4A)-H(4AN)	0.88	C(13A)-C(12A)-C(11A)	120.6(2)
C(25A)-O(5A)	1.228(2)	C(14A)-C(13A)-C(12A)	121.3(3)
C(25A)-C(26A)	1.532(3)	C(14A)-C(13A)-H(13A)	119.3
C(26A)-N(5A)	1.474(3)	C(12A)-C(13A)-H(13A)	119.3
C(26A)-C(27A)	1.534(3)	C(15A)-C(14A)-C(13A)	120.6(3)

Table B.3 contd.

C(26A)-H(26A)	1	C(15A)-C(14A)-H(14A)	119.7
N(5A)-C(30A)	1.335(3)	C(13A)-C(14A)-H(14A)	119.7
N(5A)-C(29A)	1.467(3)	C(16A)-C(15A)-C(14A)	118.9(3)
C(30A)-O(7A)	1.236(2)	C(16A)-C(15A)-H(15A)	120.5
C(30A)-C(31A)	1.525(3)	C(14A)-C(15A)-H(15A)	120.5
C(31A)-N(6A)	1.455(3)	C(15A)-C(16A)-C(17A)	120.5(3)
C(31A)-C(32A)	1.543(3)	C(15A)-C(16A)-H(16A)	119.8
C(31A)-H(31A)	1	C(17A)-C(16A)-H(16A)	119.8
N(6A)-C(39A)	1.318(3)	C(12A)-C(17A)-C(16A)	121.6(3)
N(6A)-H(6AN)	0.88	C(12A)-C(17A)-H(17A)	119.2
C(39A)-O(8A)	1.235(3)	C(16A)-C(17A)-H(17A)	119.2
C(39A)-C(40A)	1.526(3)	N(3A)-C(18A)-H(18A)	109.5
C(40A)-N(7A)	1.453(3)	N(3A)-C(18A)-H(18B)	109.5
C(40A)-H(40A)	0.99	H(18A)-C(18A)-H(18B)	109.5
C(40A)-H(40D)	0.99	N(3A)-C(18A)-H(18C)	109.5
N(7A)-C(41A)	1.344(3)	H(18A)-C(18A)-H(18C)	109.5
N(7A)-H(7AN)	0.88	H(18B)-C(18A)-H(18C)	109.5
C(41A)-O(9A)	1.223(3)	C(22A)-C(21A)-C(23A)	112.9(2)
C(41A)-C(42A)	1.532(3)	C(22A)-C(21A)-C(20A)	110.1(2)
C(42A)-N(8A)	1.476(3)	C(23A)-C(21A)-C(20A)	111.2(2)
C(42A)-C(43A)	1.531(5)	C(22A)-C(21A)-H(21A)	107.5
C(42A)-H(42A)	1	C(23A)-C(21A)-H(21A)	107.5
N(8A)-C(45A)	1.335(3)	C(20A)-C(21A)-H(21A)	107.5
N(8A)-C(44A)	1.474(3)	C(21A)-C(22A)-H(22A)	109.5
C(45A)-O(10A)	1.232(3)	C(21A)-C(22A)-H(22B)	109.5
C(45A)-C(46A)	1.524(3)	H(22A)-C(22A)-H(22B)	109.5
C(46A)-N(9A)	1.462(3)	C(21A)-C(22A)-H(22C)	109.5
C(46A)-C(47A)	1.556(4)	H(22A)-C(22A)-H(22C)	109.5
C(46A)-C(47C)	1.635(8)	H(22B)-C(22A)-H(22C)	109.5
C(46A)-H(46A)	1	C(24A)-C(23A)-C(21A)	116.4(3)
N(9A)-C(51A)	1.331(3)	C(24A)-C(23A)-H(23A)	108.2
N(9A)-H(9AN)	0.88	C(21A)-C(23A)-H(23A)	108.2
C(51A)-O(11A)	1.234(2)	C(24A)-C(23A)-H(23B)	108.2
C(51A)-C(52A)	1.537(3)	C(21A)-C(23A)-H(23B)	108.2

Table B.3 contd.

C(52A)-N(10A)	1.454(3)	H(23A)-C(23A)-H(23B)	107.3
C(52A)-C(53A)	1.542(3)	C(23A)-C(24A)-H(24A)	109.5
C(52A)-H(52A)	1	C(23A)-C(24A)-H(24B)	109.5
N(10A)-H(10A)	0.88	H(24A)-C(24A)-H(24B)	109.5
C(3A)-C(4A)	1.527(3)	C(23A)-C(24A)-H(24C)	109.5
C(3A)-C(5A)	1.535(3)	H(24A)-C(24A)-H(24C)	109.5
C(3A)-H(3AA)	1	H(24B)-C(24A)-H(24C)	109.5
C(4A)-H(4AA)	0.98	O(6A)-C(27A)-C(28A)	109.99(18)
C(4A)-H(4AB)	0.98	O(6A)-C(27A)-C(26A)	106.97(16)
C(4A)-H(4AC)	0.98	C(28A)-C(27A)-C(26A)	110.49(17)
C(5A)-C(6A)	1.519(4)	O(6A)-C(27A)-H(27A)	109.8
C(5A)-H(5AA)	0.99	C(28A)-C(27A)-H(27A)	109.8
C(5A)-H(5AB)	0.99	C(26A)-C(27A)-H(27A)	109.8
C(6A)-H(6AA)	0.98	C(27A)-O(6A)-H(6A)	109.5
C(6A)-H(6AB)	0.98	C(27A)-C(28A)-H(28A)	109.5
C(6A)-H(6AC)	0.98	C(27A)-C(28A)-H(28B)	109.5
C(11A)-C(12A)	1.512(4)	H(28A)-C(28A)-H(28B)	109.5
C(11A)-H(11A)	0.99	C(27A)-C(28A)-H(28C)	109.5
C(11A)-H(11B)	0.99	H(28A)-C(28A)-H(28C)	109.5
C(12A)-C(17A)	1.377(4)	H(28B)-C(28A)-H(28C)	109.5
C(12A)-C(13A)	1.392(4)	N(5A)-C(29A)-H(29A)	109.5
C(13A)-C(14A)	1.382(4)	N(5A)-C(29A)-H(29B)	109.5
C(13A)-H(13A)	0.95	H(29A)-C(29A)-H(29B)	109.5
C(14A)-C(15A)	1.376(5)	N(5A)-C(29A)-H(29C)	109.5
C(14A)-H(14A)	0.95	H(29A)-C(29A)-H(29C)	109.5
C(15A)-C(16A)	1.363(4)	H(29B)-C(29A)-H(29C)	109.5
C(15A)-H(15A)	0.95	C(33A)-C(32A)-C(31A)	117.07(19)
C(16A)-C(17A)	1.393(4)	C(33A)-C(32A)-H(32A)	108
C(16A)-H(16A)	0.95	C(31A)-C(32A)-H(32A)	108
C(17A)-H(17A)	0.95	C(33A)-C(32A)-H(32B)	108
C(18A)-H(18A)	0.98	C(31A)-C(32A)-H(32B)	108
C(18A)-H(18B)	0.98	H(32A)-C(32A)-H(32B)	107.3
C(18A)-H(18C)	0.98	C(38A)-C(33A)-C(34A)	118.9(3)
C(21A)-C(22A)	1.529(4)	C(38A)-C(33A)-C(32A)	121.9(2)

Table B.3 contd.

C(21A)-C(23A)	1.534(4)	C(34A)-C(33A)-C(32A)	119.1(2)
C(21A)-H(21A)	1	C(35A)-C(34A)-C(33A)	121.2(3)
C(22A)-H(22A)	0.98	C(35A)-C(34A)-H(34A)	119.4
C(22A)-H(22B)	0.98	C(33A)-C(34A)-H(34A)	119.4
C(22A)-H(22C)	0.98	C(34A)-C(35A)-C(36A)	120.4(3)
C(23A)-C(24A)	1.530(5)	C(34A)-C(35A)-H(35A)	119.8
C(23A)-H(23A)	0.99	C(36A)-C(35A)-H(35A)	119.8
C(23A)-H(23B)	0.99	C(35A)-C(36A)-C(37A)	119.8(3)
C(24A)-H(24A)	0.98	C(35A)-C(36A)-H(36A)	120.1
C(24A)-H(24B)	0.98	C(37A)-C(36A)-H(36A)	120.1
C(24A)-H(24C)	0.98	C(36A)-C(37A)-C(38A)	119.9(3)
C(27A)-O(6A)	1.428(3)	C(36A)-C(37A)-H(37A)	120
C(27A)-C(28A)	1.506(3)	C(38A)-C(37A)-H(37A)	120
C(27A)-H(27A)	1	C(33A)-C(38A)-C(37A)	119.8(3)
O(6A)-H(6A)	0.84	C(33A)-C(38A)-H(38A)	120.1
C(28A)-H(28A)	0.98	C(37A)-C(38A)-H(38A)	120.1
C(28A)-H(28B)	0.98	C(42A)-C(43A)-H(43A)	109.5
C(28A)-H(28C)	0.98	C(42A)-C(43A)-H(43B)	109.5
C(29A)-H(29A)	0.98	H(43A)-C(43A)-H(43B)	109.5
C(29A)-H(29B)	0.98	C(42A)-C(43A)-H(43C)	109.5
C(29A)-H(29C)	0.98	H(43A)-C(43A)-H(43C)	109.5
C(32A)-C(33A)	1.500(3)	H(43B)-C(43A)-H(43C)	109.5
C(32A)-H(32A)	0.99	N(8A)-C(44A)-H(44A)	109.5
C(32A)-H(32B)	0.99	N(8A)-C(44A)-H(44B)	109.5
C(33A)-C(38A)	1.380(4)	H(44A)-C(44A)-H(44B)	109.5
C(33A)-C(34A)	1.392(3)	N(8A)-C(44A)-H(44C)	109.5
C(34A)-C(35A)	1.357(4)	H(44A)-C(44A)-H(44C)	109.5
C(34A)-H(34A)	0.95	H(44B)-C(44A)-H(44C)	109.5
C(35A)-C(36A)	1.372(5)	C(50A)-C(47A)-C(48A)	112.4(3)
C(35A)-H(35A)	0.95	C(50A)-C(47A)-C(46A)	111.5(3)
C(36A)-C(37A)	1.382(5)	C(48A)-C(47A)-C(46A)	112.7(3)
C(36A)-H(36A)	0.95	C(50A)-C(47A)-H(47A)	106.6
C(37A)-C(38A)	1.397(4)	C(48A)-C(47A)-H(47A)	106.6
C(37A)-H(37A)	0.95	C(46A)-C(47A)-H(47A)	106.6

Table B.3 contd.

C(38A)-H(38A)	0.95	C(49A)-C(48A)-C(47A)	117.2(3)
C(43A)-H(43A)	0.98	C(49A)-C(48A)-H(48A)	108
C(43A)-H(43B)	0.98	C(47A)-C(48A)-H(48A)	108
C(43A)-H(43C)	0.98	C(49A)-C(48A)-H(48B)	108
C(44A)-H(44A)	0.98	C(47A)-C(48A)-H(48B)	108
C(44A)-H(44B)	0.98	H(48A)-C(48A)-H(48B)	107.2
C(44A)-H(44C)	0.98	C(50C)-C(47C)-C(48C)	111.7(5)
C(47A)-C(50A)	1.518(6)	C(50C)-C(47C)-C(46A)	110.8(6)
C(47A)-C(48A)	1.532(5)	C(48C)-C(47C)-C(46A)	108.9(5)
C(47A)-H(47A)	1	C(50C)-C(47C)-H(47C)	108.5
C(48A)-C(49A)	1.500(6)	C(48C)-C(47C)-H(47C)	108.5
C(48A)-H(48A)	0.99	C(46A)-C(47C)-H(47C)	108.5
C(48A)-H(48B)	0.99	C(49C)-C(48C)-C(47C)	116.2(5)
C(49A)-H(49A)	0.98	C(49C)-C(48C)-H(48E)	108.2
C(49A)-H(49B)	0.98	C(47C)-C(48C)-H(48E)	108.2
C(49A)-H(49C)	0.98	C(49C)-C(48C)-H(48F)	108.2
C(50A)-H(50A)	0.98	C(47C)-C(48C)-H(48F)	108.2
C(50A)-H(50B)	0.98	H(48E)-C(48C)-H(48F)	107.4
C(50A)-H(50C)	0.98	C(48C)-C(49C)-H(49G)	109.5
C(47C)-C(50C)	1.523(7)	C(48C)-C(49C)-H(49H)	109.5
C(47C)-C(48C)	1.538(6)	H(49G)-C(49C)-H(49H)	109.5
C(47C)-H(47C)	1	C(48C)-C(49C)-H(49I)	109.5
C(48C)-C(49C)	1.502(7)	H(49G)-C(49C)-H(49I)	109.5
C(48C)-H(48E)	0.99	H(49H)-C(49C)-H(49I)	109.5
C(48C)-H(48F)	0.99	C(47C)-C(50C)-H(50D)	109.5
C(49C)-H(49G)	0.98	C(47C)-C(50C)-H(50E)	109.5
C(49C)-H(49H)	0.98	H(50D)-C(50C)-H(50E)	109.5
C(49C)-H(49I)	0.98	C(47C)-C(50C)-H(50F)	109.5
C(50C)-H(50D)	0.98	H(50D)-C(50C)-H(50F)	109.5
C(50C)-H(50E)	0.98	H(50E)-C(50C)-H(50F)	109.5
C(50C)-H(50F)	0.98	O(12A)-C(53A)-C(54A)	111.10(19)
C(53A)-O(12A)	1.425(3)	O(12A)-C(53A)-C(52A)	110.00(17)
C(53A)-C(54A)	1.517(3)	C(54A)-C(53A)-C(52A)	111.18(19)
C(53A)-H(53A)	1	O(12A)-C(53A)-H(53A)	108.1

Table B.3 contd.

O(12A)-H(12A)	0.84	C(54A)-C(53A)-H(53A)	108.1
C(54A)-H(54A)	0.98	C(52A)-C(53A)-H(53A)	108.1
C(54A)-H(54B)	0.98	C(53A)-O(12A)-H(12A)	109.5
C(54A)-H(54C)	0.98	C(53A)-C(54A)-H(54A)	109.5
C(1B)-O(1B)	1.232(2)	C(53A)-C(54A)-H(54B)	109.5
C(1B)-N(10B)	1.329(3)	H(54A)-C(54A)-H(54B)	109.5
C(1B)-C(2B)	1.520(3)	C(53A)-C(54A)-H(54C)	109.5
C(2B)-N(1B)	1.458(3)	H(54A)-C(54A)-H(54C)	109.5
C(2B)-C(3B)	1.534(3)	H(54B)-C(54A)-H(54C)	109.5
C(2B)-H(2BA)	1	O(1B)-C(1B)-N(10B)	122.65(19)
N(1B)-C(7B)	1.325(3)	O(1B)-C(1B)-C(2B)	120.37(18)
N(1B)-H(1BN)	0.88	N(10B)-C(1B)-C(2B)	116.98(17)
C(7B)-O(2B)	1.231(2)	N(1B)-C(2B)-C(1B)	107.19(15)
C(7B)-C(8B)	1.522(3)	N(1B)-C(2B)-C(3B)	111.06(17)
C(8B)-N(2B)	1.452(3)	C(1B)-C(2B)-C(3B)	111.05(17)
C(8B)-H(8BA)	0.99	N(1B)-C(2B)-H(2BA)	109.2
C(8B)-H(8BB)	0.99	C(1B)-C(2B)-H(2BA)	109.2
N(2B)-C(9B)	1.336(3)	C(3B)-C(2B)-H(2BA)	109.2
N(2B)-H(2BN)	0.88	C(7B)-N(1B)-C(2B)	123.72(16)
C(9B)-O(3B)	1.226(2)	C(7B)-N(1B)-H(1BN)	118.1
C(9B)-C(10B)	1.534(3)	C(2B)-N(1B)-H(1BN)	118.1
C(10B)-N(3B)	1.475(3)	O(2B)-C(7B)-N(1B)	123.57(19)
C(10B)-C(11B)	1.529(3)	O(2B)-C(7B)-C(8B)	119.05(18)
C(10B)-H(10D)	1	N(1B)-C(7B)-C(8B)	117.37(17)
N(3B)-C(19B)	1.344(3)	N(2B)-C(8B)-C(7B)	115.49(16)
N(3B)-C(18B)	1.474(3)	N(2B)-C(8B)-H(8BA)	108.4
C(19B)-O(4B)	1.240(2)	C(7B)-C(8B)-H(8BA)	108.4
C(19B)-C(20B)	1.530(3)	N(2B)-C(8B)-H(8BB)	108.4
C(20B)-N(4B)	1.458(3)	C(7B)-C(8B)-H(8BB)	108.4
C(20B)-C(21B)	1.552(3)	H(8BA)-C(8B)-H(8BB)	107.5
C(20B)-H(20B)	1	C(9B)-N(2B)-C(8B)	121.27(17)
N(4B)-C(25B)	1.336(3)	C(9B)-N(2B)-H(2BN)	119.4
N(4B)-H(4BN)	0.88	C(8B)-N(2B)-H(2BN)	119.4
C(25B)-O(5B)	1.231(3)	O(3B)-C(9B)-N(2B)	122.01(19)

Table B.3 contd.

C(25B)-C(26B)	1.535(3)	O(3B)-C(9B)-C(10B)	122.00(18)
C(26B)-N(5B)	1.477(3)	N(2B)-C(9B)-C(10B)	115.92(17)
C(26B)-C(27B)	1.540(4)	N(3B)-C(10B)-C(11B)	114.13(19)
C(26B)-H(26B)	1	N(3B)-C(10B)-C(9B)	111.31(16)
N(5B)-C(30B)	1.332(3)	C(11B)-C(10B)-C(9B)	110.18(17)
N(5B)-C(29B)	1.463(3)	N(3B)-C(10B)-H(10D)	106.9
C(30B)-O(7B)	1.234(3)	C(11B)-C(10B)-H(10D)	106.9
C(30B)-C(31B)	1.539(3)	C(9B)-C(10B)-H(10D)	106.9
C(31B)-N(6B)	1.455(3)	C(19B)-N(3B)-C(18B)	125.42(18)
C(31B)-C(32B)	1.536(4)	C(19B)-N(3B)-C(10B)	118.10(16)
C(31B)-H(31B)	1	C(18B)-N(3B)-C(10B)	116.44(17)
N(6B)-C(39B)	1.326(3)	O(4B)-C(19B)-N(3B)	120.7(2)
N(6B)-H(6BN)	0.88	O(4B)-C(19B)-C(20B)	118.79(19)
C(39B)-O(8B)	1.232(3)	N(3B)-C(19B)-C(20B)	120.49(17)
C(39B)-C(40B)	1.533(3)	N(4B)-C(20B)-C(19B)	107.74(16)
C(40B)-N(7B)	1.446(3)	N(4B)-C(20B)-C(21B)	109.78(18)
C(40B)-H(40B)	0.99	C(19B)-C(20B)-C(21B)	109.9(2)
C(40B)-H(40C)	0.99	N(4B)-C(20B)-H(20B)	109.8
N(7B)-C(41B)	1.341(3)	C(19B)-C(20B)-H(20B)	109.8
N(7B)-H(7BN)	0.88	C(21B)-C(20B)-H(20B)	109.8
C(41B)-O(9B)	1.223(3)	C(25B)-N(4B)-C(20B)	124.35(18)
C(41B)-C(42B)	1.538(3)	C(25B)-N(4B)-H(4BN)	117.8
C(42B)-N(8B)	1.477(3)	C(20B)-N(4B)-H(4BN)	117.8
C(42B)-C(43B)	1.524(4)	O(5B)-C(25B)-N(4B)	124.3(2)
C(42B)-H(42B)	1	O(5B)-C(25B)-C(26B)	121.4(2)
N(8B)-C(45B)	1.348(3)	N(4B)-C(25B)-C(26B)	114.32(18)
N(8B)-C(44B)	1.467(3)	N(5B)-C(26B)-C(25B)	109.60(19)
C(45B)-O(10B)	1.235(3)	N(5B)-C(26B)-C(27B)	112.10(19)
C(45B)-C(46B)	1.531(3)	C(25B)-C(26B)-C(27B)	113.08(18)
C(46B)-N(9B)	1.465(3)	N(5B)-C(26B)-H(26B)	107.3
C(46B)-C(47B)	1.547(4)	C(25B)-C(26B)-H(26B)	107.3
C(46B)-H(46B)	1	C(27B)-C(26B)-H(26B)	107.3
N(9B)-C(51B)	1.331(3)	C(30B)-N(5B)-C(29B)	122.5(2)
N(9B)-H(9BN)	0.88	C(30B)-N(5B)-C(26B)	118.28(17)

Table B.3 contd.

C(51B)-O(11B)	1.240(2)	C(29B)-N(5B)-C(26B)	119.12(19)
C(51B)-C(52B)	1.525(3)	O(7B)-C(30B)-N(5B)	122.7(2)
C(52B)-N(10B)	1.457(3)	O(7B)-C(30B)-C(31B)	116.20(19)
C(52B)-C(53B)	1.539(3)	N(5B)-C(30B)-C(31B)	121.09(18)
C(52B)-H(52B)	1	N(6B)-C(31B)-C(32B)	112.3(2)
N(10B)-H(10B)	0.88	N(6B)-C(31B)-C(30B)	108.12(18)
C(3B)-C(4B)	1.519(3)	C(32B)-C(31B)-C(30B)	105.19(19)
C(3B)-C(5B)	1.527(3)	N(6B)-C(31B)-H(31B)	110.3
C(3B)-H(3BA)	1	C(32B)-C(31B)-H(31B)	110.3
C(4B)-H(4BA)	0.98	C(30B)-C(31B)-H(31B)	110.3
C(4B)-H(4BB)	0.98	C(39B)-N(6B)-C(31B)	121.80(19)
C(4B)-H(4BC)	0.98	C(39B)-N(6B)-H(6BN)	119.1
C(5B)-C(6B)	1.516(4)	C(31B)-N(6B)-H(6BN)	119.1
C(5B)-H(5BA)	0.99	O(8B)-C(39B)-N(6B)	123.2(2)
C(5B)-H(5BB)	0.99	O(8B)-C(39B)-C(40B)	117.1(2)
C(6B)-H(6BA)	0.98	N(6B)-C(39B)-C(40B)	119.73(19)
C(6B)-H(6BB)	0.98	N(7B)-C(40B)-C(39B)	115.9(2)
C(6B)-H(6BC)	0.98	N(7B)-C(40B)-H(40B)	108.3
C(11B)-C(12B)	1.517(3)	C(39B)-C(40B)-H(40B)	108.3
C(11B)-H(11C)	0.99	N(7B)-C(40B)-H(40C)	108.3
C(11B)-H(11D)	0.99	C(39B)-C(40B)-H(40C)	108.3
C(12B)-C(13B)	1.368(4)	H(40B)-C(40B)-H(40C)	107.4
C(12B)-C(17B)	1.384(4)	C(41B)-N(7B)-C(40B)	120.20(19)
C(13B)-C(14B)	1.390(4)	C(41B)-N(7B)-H(7BN)	119.9
C(13B)-H(13B)	0.95	C(40B)-N(7B)-H(7BN)	119.9
C(14B)-C(15B)	1.370(5)	O(9B)-C(41B)-N(7B)	122.5(2)
C(14B)-H(14B)	0.95	O(9B)-C(41B)-C(42B)	120.8(2)
C(15B)-C(16B)	1.374(5)	N(7B)-C(41B)-C(42B)	116.6(2)
C(15B)-H(15B)	0.95	N(8B)-C(42B)-C(43B)	112.1(2)
C(16B)-C(17B)	1.392(4)	N(8B)-C(42B)-C(41B)	112.74(18)
C(16B)-H(16B)	0.95	C(43B)-C(42B)-C(41B)	111.0(2)
C(17B)-H(17B)	0.95	N(8B)-C(42B)-H(42B)	106.8
C(18B)-H(18D)	0.98	C(43B)-C(42B)-H(42B)	106.8
C(18B)-H(18E)	0.98	C(41B)-C(42B)-H(42B)	106.8

Table B.3 contd.

C(18B)-H(18F)	0.98	C(45B)-N(8B)-C(44B)	124.64(19)
C(21B)-C(22B)	1.511(4)	C(45B)-N(8B)-C(42B)	118.46(18)
C(21B)-C(23B)	1.546(4)	C(44B)-N(8B)-C(42B)	115.97(19)
C(21B)-H(21B)	1	O(10B)-C(45B)-N(8B)	120.9(2)
C(22B)-H(22D)	0.98	O(10B)-C(45B)-C(46B)	116.6(2)
C(22B)-H(22E)	0.98	N(8B)-C(45B)-C(46B)	122.48(19)
C(22B)-H(22F)	0.98	N(9B)-C(46B)-C(45B)	106.19(17)
C(23B)-C(24B)	1.529(5)	N(9B)-C(46B)-C(47B)	111.61(19)
C(23B)-H(23C)	0.99	C(45B)-C(46B)-C(47B)	108.26(19)
C(23B)-H(23D)	0.99	N(9B)-C(46B)-H(46B)	110.2
C(24B)-H(24D)	0.98	C(45B)-C(46B)-H(46B)	110.2
C(24B)-H(24E)	0.98	C(47B)-C(46B)-H(46B)	110.2
C(24B)-H(24F)	0.98	C(51B)-N(9B)-C(46B)	124.85(18)
C(27B)-O(6B)	1.421(3)	C(51B)-N(9B)-H(9BN)	117.6
C(27B)-C(28B)	1.518(4)	C(46B)-N(9B)-H(9BN)	117.6
C(27B)-H(27B)	1	O(11B)-C(51B)-N(9B)	124.21(19)
O(6B)-H(6BO)	0.84	O(11B)-C(51B)-C(52B)	121.14(19)
C(28B)-H(28D)	0.98	N(9B)-C(51B)-C(52B)	114.64(17)
C(28B)-H(28E)	0.98	N(10B)-C(52B)-C(51B)	109.41(16)
C(28B)-H(28F)	0.98	N(10B)-C(52B)-C(53B)	110.87(17)
C(29B)-H(29D)	0.98	C(51B)-C(52B)-C(53B)	112.07(19)
C(29B)-H(29E)	0.98	N(10B)-C(52B)-H(52B)	108.1
C(29B)-H(29F)	0.98	C(51B)-C(52B)-H(52B)	108.1
C(32B)-C(33C)	1.484(8)	C(53B)-C(52B)-H(52B)	108.1
C(32B)-C(33B)	1.520(5)	C(1B)-N(10B)-C(52B)	121.22(16)
C(32B)-H(32C)	0.99	C(1B)-N(10B)-H(10B)	119.4
C(32B)-H(32D)	0.99	C(52B)-N(10B)-H(10B)	119.4
C(33B)-C(34B)	1.383(6)	C(4B)-C(3B)-C(5B)	112.9(2)
C(33B)-C(38B)	1.385(5)	C(4B)-C(3B)-C(2B)	110.38(19)
C(34B)-C(35B)	1.394(5)	C(5B)-C(3B)-C(2B)	108.81(18)
C(34B)-H(34B)	0.95	C(4B)-C(3B)-H(3BA)	108.2
C(35B)-C(36B)	1.374(6)	C(5B)-C(3B)-H(3BA)	108.2
C(35B)-H(35B)	0.95	C(2B)-C(3B)-H(3BA)	108.2
C(36B)-C(37B)	1.356(7)	C(3B)-C(4B)-H(4BA)	109.5

Table B.3 contd.

C(36B)-H(36B)	0.95	C(3B)-C(4B)-H(4BB)	109.5
C(37B)-C(38B)	1.406(5)	H(4BA)-C(4B)-H(4BB)	109.5
C(37B)-H(37B)	0.95	C(3B)-C(4B)-H(4BC)	109.5
C(38B)-H(38B)	0.95	H(4BA)-C(4B)-H(4BC)	109.5
C(33C)-C(34C)	1.382(6)	H(4BB)-C(4B)-H(4BC)	109.5
C(33C)-C(38C)	1.384(6)	C(6B)-C(5B)-C(3B)	114.7(2)
C(34C)-C(35C)	1.398(6)	C(6B)-C(5B)-H(5BA)	108.6
C(34C)-H(34C)	0.95	C(3B)-C(5B)-H(5BA)	108.6
C(35C)-C(36C)	1.374(7)	C(6B)-C(5B)-H(5BB)	108.6
C(35C)-H(35C)	0.95	C(3B)-C(5B)-H(5BB)	108.6
C(36C)-C(37C)	1.355(7)	H(5BA)-C(5B)-H(5BB)	107.6
C(36C)-H(36C)	0.95	C(5B)-C(6B)-H(6BA)	109.5
C(37C)-C(38C)	1.408(6)	C(5B)-C(6B)-H(6BB)	109.5
C(37C)-H(37C)	0.95	H(6BA)-C(6B)-H(6BB)	109.5
C(38C)-H(38C)	0.95	C(5B)-C(6B)-H(6BC)	109.5
C(43B)-H(43D)	0.98	H(6BA)-C(6B)-H(6BC)	109.5
C(43B)-H(43E)	0.98	H(6BB)-C(6B)-H(6BC)	109.5
C(43B)-H(43F)	0.98	C(12B)-C(11B)-C(10B)	115.65(19)
C(44B)-H(44D)	0.98	C(12B)-C(11B)-H(11C)	108.4
C(44B)-H(44E)	0.98	C(10B)-C(11B)-H(11C)	108.4
C(44B)-H(44F)	0.98	C(12B)-C(11B)-H(11D)	108.4
C(47B)-C(50B)	1.531(4)	C(10B)-C(11B)-H(11D)	108.4
C(47B)-C(48B)	1.536(4)	H(11C)-C(11B)-H(11D)	107.4
C(47B)-H(47B)	1	C(13B)-C(12B)-C(17B)	119.0(2)
C(48B)-C(49B)	1.517(4)	C(13B)-C(12B)-C(11B)	120.1(3)
C(48B)-H(48C)	0.99	C(17B)-C(12B)-C(11B)	120.8(2)
C(48B)-H(48D)	0.99	C(12B)-C(13B)-C(14B)	121.1(3)
C(49B)-H(49D)	0.98	C(12B)-C(13B)-H(13B)	119.4
C(49B)-H(49E)	0.98	C(14B)-C(13B)-H(13B)	119.4
C(49B)-H(49F)	0.98	C(15B)-C(14B)-C(13B)	119.7(3)
C(50B)-H(50G)	0.98	C(15B)-C(14B)-H(14B)	120.1
C(50B)-H(50H)	0.98	C(13B)-C(14B)-H(14B)	120.1
C(50B)-H(50I)	0.98	C(14B)-C(15B)-C(16B)	120.0(3)
O(12B)-C(53B)	1.433(3)	C(14B)-C(15B)-H(15B)	120

Table B.3 contd.

O(12B)-H(12B)	0.84	C(16B)-C(15B)-H(15B)	120
O(12C)-C(53C)	1.433(5)	C(15B)-C(16B)-C(17B)	120.1(3)
O(12C)-H(12C)	0.84	C(15B)-C(16B)-H(16B)	119.9
C(53B)-H(53B)	1	C(17B)-C(16B)-H(16B)	119.9
C(53C)-C(54C)	1.510(5)	C(12B)-C(17B)-C(16B)	120.1(3)
C(53C)-H(53C)	1	C(12B)-C(17B)-H(17B)	119.9
O(61)-H(61A)	0.858(10)	C(16B)-C(17B)-H(17B)	119.9
O(61)-H(61B)	0.863(10)	N(3B)-C(18B)-H(18D)	109.5
O(62)-H(62A)	0.858(10)	N(3B)-C(18B)-H(18E)	109.5
O(62)-H(62B)	0.855(10)	H(18D)-C(18B)-H(18E)	109.5
O(63)-H(63A)	0.866(10)	N(3B)-C(18B)-H(18F)	109.5
O(63)-H(63B)	0.851(10)	H(18D)-C(18B)-H(18F)	109.5
O(64)-H(64A)	0.850(10)	H(18E)-C(18B)-H(18F)	109.5
O(64)-H(64B)	0.849(10)	C(22B)-C(21B)-C(23B)	112.7(3)
O(1A)-C(1A)-N(10A)	122.6(2)	C(22B)-C(21B)-C(20B)	110.8(2)
O(1A)-C(1A)-C(2A)	120.56(19)	C(23B)-C(21B)-C(20B)	111.1(2)
N(10A)-C(1A)-C(2A)	116.87(18)	C(22B)-C(21B)-H(21B)	107.3
N(1A)-C(2A)-C(1A)	108.06(15)	C(23B)-C(21B)-H(21B)	107.3
N(1A)-C(2A)-C(3A)	110.79(17)	C(20B)-C(21B)-H(21B)	107.3
C(1A)-C(2A)-C(3A)	111.04(17)	C(21B)-C(22B)-H(22D)	109.5
N(1A)-C(2A)-H(2AA)	109	C(21B)-C(22B)-H(22E)	109.5
C(1A)-C(2A)-H(2AA)	109	H(22D)-C(22B)-H(22E)	109.5
C(3A)-C(2A)-H(2AA)	109	C(21B)-C(22B)-H(22F)	109.5
C(7A)-N(1A)-C(2A)	122.80(17)	H(22D)-C(22B)-H(22F)	109.5
C(7A)-N(1A)-H(1AN)	118.6	H(22E)-C(22B)-H(22F)	109.5
C(2A)-N(1A)-H(1AN)	118.6	C(24B)-C(23B)-C(21B)	115.3(3)
O(2A)-C(7A)-N(1A)	124.51(19)	C(24B)-C(23B)-H(23C)	108.5
O(2A)-C(7A)-C(8A)	118.05(18)	C(21B)-C(23B)-H(23C)	108.5
N(1A)-C(7A)-C(8A)	117.44(18)	C(24B)-C(23B)-H(23D)	108.5
N(2A)-C(8A)-C(7A)	116.22(17)	C(21B)-C(23B)-H(23D)	108.5
N(2A)-C(8A)-H(8AA)	108.2	H(23C)-C(23B)-H(23D)	107.5
C(7A)-C(8A)-H(8AA)	108.2	C(23B)-C(24B)-H(24D)	109.5
N(2A)-C(8A)-H(8AB)	108.2	C(23B)-C(24B)-H(24E)	109.5
C(7A)-C(8A)-H(8AB)	108.2	H(24D)-C(24B)-H(24E)	109.5

Table B.3 contd.

H(8AA)-C(8A)-H(8AB)	107.4	C(23B)-C(24B)-H(24F)	109.5
C(9A)-N(2A)-C(8A)	121.15(17)	H(24D)-C(24B)-H(24F)	109.5
C(9A)-N(2A)-H(2AN)	119.4	H(24E)-C(24B)-H(24F)	109.5
C(8A)-N(2A)-H(2AN)	119.4	O(6B)-C(27B)-C(28B)	111.4(2)
O(3A)-C(9A)-N(2A)	122.7(2)	O(6B)-C(27B)-C(26B)	109.84(19)
O(3A)-C(9A)-C(10A)	122.9(2)	C(28B)-C(27B)-C(26B)	110.8(2)
N(2A)-C(9A)-C(10A)	114.30(17)	O(6B)-C(27B)-H(27B)	108.2
N(3A)-C(10A)-C(9A)	112.18(16)	C(28B)-C(27B)-H(27B)	108.2
N(3A)-C(10A)-C(11A)	112.67(19)	C(26B)-C(27B)-H(27B)	108.2
C(9A)-C(10A)-C(11A)	111.68(18)	C(27B)-O(6B)-H(6BO)	109.5
N(3A)-C(10A)-H(10C)	106.6	C(27B)-C(28B)-H(28D)	109.5
C(9A)-C(10A)-H(10C)	106.6	C(27B)-C(28B)-H(28E)	109.5
C(11A)-C(10A)-H(10C)	106.6	H(28D)-C(28B)-H(28E)	109.5
C(19A)-N(3A)-C(18A)	124.97(18)	C(27B)-C(28B)-H(28F)	109.5
C(19A)-N(3A)-C(10A)	117.85(16)	H(28D)-C(28B)-H(28F)	109.5
C(18A)-N(3A)-C(10A)	117.13(17)	H(28E)-C(28B)-H(28F)	109.5
O(4A)-C(19A)-N(3A)	120.94(19)	N(5B)-C(29B)-H(29D)	109.5
O(4A)-C(19A)-C(20A)	118.60(19)	N(5B)-C(29B)-H(29E)	109.5
N(3A)-C(19A)-C(20A)	120.38(18)	H(29D)-C(29B)-H(29E)	109.5
N(4A)-C(20A)-C(19A)	107.24(17)	N(5B)-C(29B)-H(29F)	109.5
N(4A)-C(20A)-C(21A)	109.85(18)	H(29D)-C(29B)-H(29F)	109.5
C(19A)-C(20A)-C(21A)	110.96(19)	H(29E)-C(29B)-H(29F)	109.5
N(4A)-C(20A)-H(20A)	109.6	C(33C)-C(32B)-C(31B)	112.2(5)
C(19A)-C(20A)-H(20A)	109.6	C(33B)-C(32B)-C(31B)	119.9(3)
C(21A)-C(20A)-H(20A)	109.6	C(33C)-C(32B)-H(32C)	117.8
C(25A)-N(4A)-C(20A)	123.58(18)	C(33B)-C(32B)-H(32C)	107.3
C(25A)-N(4A)-H(4AN)	118.2	C(31B)-C(32B)-H(32C)	107.3
C(20A)-N(4A)-H(4AN)	118.2	C(33C)-C(32B)-H(32D)	104.6
O(5A)-C(25A)-N(4A)	124.4(2)	C(33B)-C(32B)-H(32D)	107.3
O(5A)-C(25A)-C(26A)	121.9(2)	C(31B)-C(32B)-H(32D)	107.3
N(4A)-C(25A)-C(26A)	113.70(17)	H(32C)-C(32B)-H(32D)	106.9
N(5A)-C(26A)-C(25A)	109.63(17)	C(34B)-C(33B)-C(38B)	118.3(3)
N(5A)-C(26A)-C(27A)	112.84(17)	C(34B)-C(33B)-C(32B)	122.9(4)
C(25A)-C(26A)-C(27A)	113.16(16)	C(38B)-C(33B)-C(32B)	118.7(5)

Table B.3 contd.

N(5A)-C(26A)-H(26A)	106.9	C(35B)-C(34B)-C(33B)	121.9(3)
C(25A)-C(26A)-H(26A)	106.9	C(35B)-C(34B)-H(34B)	119.1
C(27A)-C(26A)-H(26A)	106.9	C(33B)-C(34B)-H(34B)	119.1
C(30A)-N(5A)-C(29A)	122.89(18)	C(36B)-C(35B)-C(34B)	119.3(4)
C(30A)-N(5A)-C(26A)	117.36(16)	C(36B)-C(35B)-H(35B)	120.3
C(29A)-N(5A)-C(26A)	119.58(17)	C(34B)-C(35B)-H(35B)	120.3
O(7A)-C(30A)-N(5A)	122.44(19)	C(37B)-C(36B)-C(35B)	119.3(4)
O(7A)-C(30A)-C(31A)	117.20(18)	C(37B)-C(36B)-H(36B)	120.3
N(5A)-C(30A)-C(31A)	120.24(17)	C(35B)-C(36B)-H(36B)	120.3
N(6A)-C(31A)-C(30A)	108.20(16)	C(36B)-C(37B)-C(38B)	122.1(4)
N(6A)-C(31A)-C(32A)	111.87(17)	C(36B)-C(37B)-H(37B)	118.9
C(30A)-C(31A)-C(32A)	105.37(17)	C(38B)-C(37B)-H(37B)	118.9
N(6A)-C(31A)-H(31A)	110.4	C(33B)-C(38B)-C(37B)	118.9(5)
C(30A)-C(31A)-H(31A)	110.4	C(33B)-C(38B)-H(38B)	120.5
C(32A)-C(31A)-H(31A)	110.4	C(37B)-C(38B)-H(38B)	120.5
C(39A)-N(6A)-C(31A)	122.52(17)	C(34C)-C(33C)-C(38C)	118.7(5)
C(39A)-N(6A)-H(6AN)	118.7	C(34C)-C(33C)-C(32B)	116.6(9)
C(31A)-N(6A)-H(6AN)	118.7	C(38C)-C(33C)-C(32B)	124.7(9)
O(8A)-C(39A)-N(6A)	124.5(2)	C(33C)-C(34C)-C(35C)	121.3(5)
O(8A)-C(39A)-C(40A)	117.94(19)	C(33C)-C(34C)-H(34C)	119.4
N(6A)-C(39A)-C(40A)	117.54(19)	C(35C)-C(34C)-H(34C)	119.4
N(7A)-C(40A)-C(39A)	117.13(18)	C(36C)-C(35C)-C(34C)	119.0(5)
N(7A)-C(40A)-H(40A)	108	C(36C)-C(35C)-H(35C)	120.5
C(39A)-C(40A)-H(40A)	108	C(34C)-C(35C)-H(35C)	120.5
N(7A)-C(40A)-H(40D)	108	C(37C)-C(36C)-C(35C)	119.7(5)
C(39A)-C(40A)-H(40D)	108	C(37C)-C(36C)-H(36C)	120.1
H(40A)-C(40A)-H(40D)	107.3	C(35C)-C(36C)-H(36C)	120.1
C(41A)-N(7A)-C(40A)	121.10(18)	C(36C)-C(37C)-C(38C)	121.9(5)
C(41A)-N(7A)-H(7AN)	119.5	C(36C)-C(37C)-H(37C)	119
C(40A)-N(7A)-H(7AN)	119.5	C(38C)-C(37C)-H(37C)	119
O(9A)-C(41A)-N(7A)	121.7(2)	C(33C)-C(38C)-C(37C)	118.6(5)
O(9A)-C(41A)-C(42A)	121.0(2)	C(33C)-C(38C)-H(38C)	120.7
N(7A)-C(41A)-C(42A)	117.23(19)	C(37C)-C(38C)-H(38C)	120.7
N(8A)-C(42A)-C(41A)	112.24(19)	C(42B)-C(43B)-H(43D)	109.5

Table B.3 contd.

N(8A)-C(42A)-C(43A)	111.1(2)	C(42B)-C(43B)-H(43E)	109.5
C(41A)-C(42A)-C(43A)	111.7(2)	H(43D)-C(43B)-H(43E)	109.5
N(8A)-C(42A)-H(42A)	107.1	C(42B)-C(43B)-H(43F)	109.5
C(41A)-C(42A)-H(42A)	107.1	H(43D)-C(43B)-H(43F)	109.5
C(43A)-C(42A)-H(42A)	107.1	H(43E)-C(43B)-H(43F)	109.5
C(45A)-N(8A)-C(44A)	124.55(19)	N(8B)-C(44B)-H(44D)	109.5
C(45A)-N(8A)-C(42A)	118.70(18)	N(8B)-C(44B)-H(44E)	109.5
C(44A)-N(8A)-C(42A)	115.83(18)	H(44D)-C(44B)-H(44E)	109.5
O(10A)-C(45A)-N(8A)	121.0(2)	N(8B)-C(44B)-H(44F)	109.5
O(10A)-C(45A)-C(46A)	119.4(2)	H(44D)-C(44B)-H(44F)	109.5
N(8A)-C(45A)-C(46A)	119.56(19)	H(44E)-C(44B)-H(44F)	109.5
N(9A)-C(46A)-C(45A)	107.28(18)	C(50B)-C(47B)-C(48B)	113.4(2)
N(9A)-C(46A)-C(47A)	117.4(2)	C(50B)-C(47B)-C(46B)	109.7(2)
C(45A)-C(46A)-C(47A)	114.1(2)	C(48B)-C(47B)-C(46B)	112.8(2)
N(9A)-C(46A)-C(47C)	100.9(3)	C(50B)-C(47B)-H(47B)	106.8
C(45A)-C(46A)-C(47C)	95.4(3)	C(48B)-C(47B)-H(47B)	106.8
N(9A)-C(46A)-H(46A)	105.7	C(46B)-C(47B)-H(47B)	106.8
C(45A)-C(46A)-H(46A)	105.7	C(49B)-C(48B)-C(47B)	115.1(3)
C(47A)-C(46A)-H(46A)	105.7	C(49B)-C(48B)-H(48C)	108.5
C(47C)-C(46A)-H(46A)	138.9	C(47B)-C(48B)-H(48C)	108.5
C(51A)-N(9A)-C(46A)	122.74(19)	C(49B)-C(48B)-H(48D)	108.5
C(51A)-N(9A)-H(9AN)	118.6	C(47B)-C(48B)-H(48D)	108.5
C(46A)-N(9A)-H(9AN)	118.6	H(48C)-C(48B)-H(48D)	107.5
O(11A)-C(51A)-N(9A)	123.70(19)	C(48B)-C(49B)-H(49D)	109.5
O(11A)-C(51A)-C(52A)	120.82(19)	C(48B)-C(49B)-H(49E)	109.5
N(9A)-C(51A)-C(52A)	115.48(18)	H(49D)-C(49B)-H(49E)	109.5
N(10A)-C(52A)-C(51A)	109.77(17)	C(48B)-C(49B)-H(49F)	109.5
N(10A)-C(52A)-C(53A)	110.50(18)	H(49D)-C(49B)-H(49F)	109.5
C(51A)-C(52A)-C(53A)	110.92(16)	H(49E)-C(49B)-H(49F)	109.5
N(10A)-C(52A)-H(52A)	108.5	C(47B)-C(50B)-H(50G)	109.5
C(51A)-C(52A)-H(52A)	108.5	C(47B)-C(50B)-H(50H)	109.5
C(53A)-C(52A)-H(52A)	108.5	H(50G)-C(50B)-H(50H)	109.5
C(1A)-N(10A)-C(52A)	121.17(18)	C(47B)-C(50B)-H(50I)	109.5
C(1A)-N(10A)-H(10A)	119.4	H(50G)-C(50B)-H(50I)	109.5

Table B.3 contd.

C(52A)-N(10A)-H(10A)	119.4	H(50H)-C(50B)-H(50I)	109.5
C(4A)-C(3A)-C(5A)	112.2(2)	C(53B)-O(12B)-H(12B)	109.5
C(4A)-C(3A)-C(2A)	109.86(19)	C(53C)-O(12C)-H(12C)	109.5
C(5A)-C(3A)-C(2A)	109.72(19)	O(12B)-C(53B)-C(52B)	108.2(2)
C(4A)-C(3A)-H(3AA)	108.3	O(12B)-C(53B)-H(53B)	108.8
H(61A)-O(61)-H(61B)	111.2(17)	C(52B)-C(53B)-H(53B)	108.8
H(62A)-O(62)-H(62B)	111.8(17)	O(12C)-C(53C)-C(54C)	94.9(7)
H(63A)-O(63)-H(63B)	109.1(17)	O(12C)-C(53C)-H(53C)	113
H(64A)-O(64)-H(64B)	113.0(19)	C(54C)-C(53C)-H(53C)	113

Table B.4. Anisotropic displacement parameters (A^2 x 10^3) for **3.6**[2]

	U11	U22	U33	U23	U13	U12
C(1A)	28(1)	22(1)	40(1)	-2(1)	-2(1)	-6(1)
O(1A)	30(1)	32(1)	49(1)	8(1)	2(1)	0(1)
C(2A)	25(1)	23(1)	43(1)	3(1)	-1(1)	-2(1)
N(1A)	25(1)	25(1)	40(1)	2(1)	-1(1)	-3(1)
C(7A)	23(1)	23(1)	42(1)	1(1)	-1(1)	4(1)
O(2A)	40(1)	30(1)	48(1)	11(1)	-5(1)	-6(1)
C(8A)	28(1)	26(1)	39(1)	2(1)	-5(1)	-2(1)
N(2A)	26(1)	21(1)	39(1)	0(1)	-2(1)	2(1)
C(9A)	22(1)	28(1)	43(1)	-6(1)	-3(1)	-1(1)
O(3A)	39(1)	33(1)	58(1)	-7(1)	5(1)	9(1)
C(10A)	24(1)	31(1)	41(1)	-4(1)	4(1)	-4(1)
N(3A)	29(1)	29(1)	33(1)	0(1)	2(1)	-2(1)
C(19A)	32(1)	35(1)	27(1)	4(1)	1(1)	-6(1)
O(4A)	37(1)	32(1)	40(1)	-3(1)	-5(1)	-6(1)
C(20A)	29(1)	38(1)	37(1)	8(1)	-2(1)	-7(1)
N(4A)	32(1)	29(1)	39(1)	5(1)	2(1)	-4(1)
C(25A)	23(1)	31(1)	39(1)	2(1)	-8(1)	-5(1)
O(5A)	41(1)	29(1)	49(1)	1(1)	-6(1)	-13(1)
C(26A)	25(1)	23(1)	39(1)	-2(1)	-1(1)	-5(1)
N(5A)	31(1)	22(1)	46(1)	-5(1)	0(1)	-4(1)
C(30A)	28(1)	24(1)	40(1)	-2(1)	-1(1)	0(1)
O(7A)	27(1)	30(1)	80(1)	-20(1)	-10(1)	1(1)
C(31A)	28(1)	24(1)	39(1)	-2(1)	0(1)	-2(1)
N(6A)	26(1)	25(1)	32(1)	-2(1)	-4(1)	0(1)
C(39A)	31(1)	27(1)	34(1)	2(1)	-2(1)	10(1)
O(8A)	58(1)	37(1)	39(1)	-7(1)	-1(1)	5(1)
C(40A)	36(1)	33(1)	39(1)	4(1)	9(1)	9(1)
N(7A)	34(1)	23(1)	50(1)	5(1)	7(1)	6(1)
C(41A)	22(1)	31(1)	62(2)	0(1)	5(1)	1(1)

2. The anisotropic displacement factor exponent takes the form:-2 pi^2 [h^2 a*^2 U11 + ... + 2 h k a* b* U12]

Table B.4 contd.

O(9A)	31(1)	29(1)	71(1)	-2(1)	-5(1)	6(1)
C(42A)	26(1)	34(1)	92(2)	-13(1)	-1(1)	1(1)
N(8A)	27(1)	26(1)	59(1)	-1(1)	2(1)	1(1)
C(45A)	30(1)	36(1)	30(1)	2(1)	-7(1)	-5(1)
O(10A)	49(1)	34(1)	35(1)	1(1)	-4(1)	-12(1)
C(46A)	27(1)	54(1)	38(1)	-9(1)	1(1)	0(1)
N(9A)	27(1)	34(1)	41(1)	1(1)	-2(1)	-6(1)
C(51A)	23(1)	31(1)	38(1)	2(1)	2(1)	-6(1)
O(11A)	36(1)	30(1)	51(1)	1(1)	0(1)	-7(1)
C(52A)	24(1)	26(1)	47(1)	4(1)	-1(1)	-4(1)
N(10A)	24(1)	26(1)	51(1)	7(1)	-1(1)	-2(1)
C(3A)	34(1)	28(1)	44(1)	1(1)	0(1)	-3(1)
C(4A)	52(2)	49(2)	61(2)	-20(1)	4(1)	-15(1)
C(5A)	50(1)	47(1)	44(1)	3(1)	4(1)	12(1)
C(6A)	63(2)	58(2)	53(2)	6(1)	12(1)	16(1)
C(11A)	43(1)	40(1)	45(1)	-10(1)	12(1)	1(1)
C(12A)	37(1)	46(1)	37(1)	-8(1)	11(1)	3(1)
C(13A)	48(2)	68(2)	45(1)	1(1)	-3(1)	-11(1)
C(14A)	60(2)	67(2)	54(2)	-2(1)	1(1)	-21(2)
C(15A)	57(2)	48(2)	56(2)	-5(1)	14(1)	-3(1)
C(16A)	56(2)	55(2)	48(2)	0(1)	4(1)	10(1)
C(17A)	36(1)	57(2)	51(2)	-7(1)	4(1)	-4(1)
C(18A)	40(1)	29(1)	50(1)	3(1)	6(1)	-1(1)
C(21A)	39(1)	58(2)	40(1)	9(1)	-10(1)	-11(1)
C(22A)	60(2)	96(2)	36(1)	12(1)	-9(1)	-23(2)
C(23A)	49(2)	96(3)	61(2)	14(2)	-22(1)	-6(2)
C(24A)	77(2)	101(3)	79(2)	13(2)	-28(2)	28(2)
C(27A)	33(1)	30(1)	35(1)	-2(1)	0(1)	-10(1)
O(6A)	44(1)	37(1)	44(1)	-5(1)	5(1)	-14(1)
C(28A)	34(1)	48(1)	40(1)	2(1)	-8(1)	-6(1)
C(29A)	35(1)	26(1)	84(2)	-15(1)	-6(1)	-3(1)
C(32A)	42(1)	35(1)	41(1)	5(1)	7(1)	-2(1)
C(33A)	57(2)	32(1)	30(1)	-1(1)	-3(1)	5(1)
C(34A)	91(2)	34(1)	48(2)	4(1)	-11(2)	1(1)

Table B.4 contd.

C(35A)	110(3)	38(1)	64(2)	3(1)	-29(2)	7(2)
C(36A)	110(3)	46(2)	60(2)	-13(1)	-44(2)	37(2)
C(37A)	64(2)	88(2)	58(2)	-13(2)	-20(2)	26(2)
C(38A)	55(2)	60(2)	44(1)	6(1)	-11(1)	13(1)
C(43A)	69(2)	68(2)	122(3)	-39(2)	-59(2)	31(2)
C(44A)	47(2)	31(1)	85(2)	-5(1)	17(1)	-6(1)
C(47A)	46(2)	36(2)	37(2)	-8(1)	2(1)	-5(1)
C(48A)	68(3)	53(2)	42(2)	2(2)	1(2)	9(2)
C(49A)	86(3)	37(2)	47(2)	3(2)	15(2)	-3(2)
C(50A)	78(3)	41(2)	44(3)	-8(2)	23(2)	11(2)
C(49C)	78(3)	41(2)	44(3)	-8(2)	23(2)	11(2)
C(53A)	28(1)	32(1)	44(1)	2(1)	-5(1)	-8(1)
O(12A)	39(1)	38(1)	53(1)	2(1)	-10(1)	-9(1)
C(54A)	36(1)	49(1)	46(1)	-2(1)	4(1)	-4(1)
C(1B)	27(1)	22(1)	32(1)	-1(1)	3(1)	-5(1)
O(1B)	30(1)	30(1)	57(1)	-15(1)	-2(1)	-1(1)
C(2B)	27(1)	24(1)	35(1)	-5(1)	1(1)	-6(1)
N(1B)	27(1)	24(1)	35(1)	-8(1)	0(1)	-7(1)
C(7B)	26(1)	26(1)	29(1)	-4(1)	-3(1)	3(1)
O(2B)	54(1)	33(1)	36(1)	-11(1)	0(1)	-10(1)
C(8B)	30(1)	28(1)	28(1)	-3(1)	1(1)	1(1)
N(2B)	29(1)	21(1)	32(1)	-1(1)	-2(1)	0(1)
C(9B)	26(1)	29(1)	35(1)	-2(1)	-1(1)	0(1)
O(3B)	40(1)	30(1)	47(1)	-9(1)	-13(1)	11(1)
C(10B)	27(1)	26(1)	42(1)	-5(1)	-7(1)	-1(1)
N(3B)	28(1)	24(1)	33(1)	-4(1)	-3(1)	-2(1)
C(19B)	35(1)	31(1)	26(1)	-3(1)	-6(1)	-5(1)
O(4B)	48(1)	26(1)	35(1)	0(1)	-3(1)	-8(1)
C(20B)	33(1)	32(1)	38(1)	-7(1)	2(1)	-9(1)
N(4B)	33(1)	25(1)	46(1)	-2(1)	-3(1)	-6(1)
C(25B)	32(1)	30(1)	46(1)	2(1)	4(1)	-8(1)
O(5B)	47(1)	29(1)	64(1)	7(1)	2(1)	-14(1)
C(26B)	31(1)	28(1)	50(1)	9(1)	-2(1)	-7(1)
N(5B)	33(1)	23(1)	60(1)	10(1)	-4(1)	-3(1)

Table B.4 contd.

C(30B)	33(1)	26(1)	43(1)	2(1)	0(1)	-3(1)
O(7B)	44(1)	22(1)	61(1)	6(1)	17(1)	1(1)
C(31B)	36(1)	23(1)	67(2)	2(1)	1(1)	1(1)
N(6B)	34(1)	27(1)	56(1)	11(1)	-2(1)	-2(1)
C(39B)	31(1)	27(1)	61(2)	10(1)	1(1)	3(1)
O(8B)	56(1)	35(1)	71(1)	19(1)	2(1)	-4(1)
C(40B)	32(1)	36(1)	56(2)	14(1)	-4(1)	1(1)
N(7B)	29(1)	27(1)	51(1)	7(1)	1(1)	4(1)
C(41B)	30(1)	36(1)	59(2)	5(1)	1(1)	5(1)
O(9B)	54(1)	42(1)	88(2)	9(1)	19(1)	20(1)
C(42B)	31(1)	39(1)	56(2)	8(1)	7(1)	-1(1)
N(8B)	35(1)	30(1)	49(1)	8(1)	7(1)	2(1)
C(45B)	38(1)	32(1)	36(1)	6(1)	10(1)	2(1)
O(10B)	42(1)	29(1)	44(1)	4(1)	6(1)	3(1)
C(46B)	38(1)	32(1)	41(1)	7(1)	7(1)	-1(1)
N(9B)	35(1)	24(1)	42(1)	2(1)	7(1)	0(1)
C(51B)	23(1)	26(1)	36(1)	1(1)	-4(1)	-2(1)
O(11B)	35(1)	22(1)	42(1)	0(1)	-2(1)	-3(1)
C(52B)	26(1)	22(1)	40(1)	-4(1)	1(1)	-3(1)
N(10B)	28(1)	25(1)	44(1)	-10(1)	2(1)	-2(1)
C(3B)	37(1)	26(1)	37(1)	-3(1)	-3(1)	-1(1)
C(4B)	60(2)	43(1)	51(2)	13(1)	-2(1)	-11(1)
C(5B)	51(2)	40(1)	47(1)	-8(1)	-7(1)	16(1)
C(6B)	72(2)	66(2)	64(2)	-19(2)	-27(2)	28(2)
C(11B)	46(1)	35(1)	60(2)	-10(1)	-22(1)	8(1)
C(12B)	39(1)	40(1)	51(2)	-7(1)	-18(1)	10(1)
C(13B)	72(2)	42(1)	51(2)	6(1)	-20(1)	0(1)
C(14B)	78(2)	53(2)	53(2)	-7(1)	-18(2)	9(2)
C(15B)	72(2)	54(2)	65(2)	-24(1)	-21(2)	6(2)
C(16B)	49(2)	67(2)	76(2)	-19(2)	-6(2)	-19(1)
C(17B)	37(1)	60(2)	56(2)	-18(1)	-5(1)	-7(1)
C(18B)	38(1)	24(1)	59(2)	-4(1)	7(1)	-2(1)
C(21B)	58(2)	56(2)	39(1)	-2(1)	9(1)	-15(1)
C(22B)	85(2)	84(2)	37(1)	-3(1)	-2(1)	-24(2)

Table B.4 contd.

C(23B)	64(2)	91(2)	59(2)	-6(2)	26(2)	-15(2)
C(24B)	81(2)	91(3)	83(2)	-18(2)	39(2)	5(2)
C(27B)	34(1)	46(1)	55(2)	14(1)	-5(1)	-14(1)
O(6B)	44(1)	66(1)	57(1)	15(1)	-13(1)	-17(1)
C(28B)	43(1)	60(2)	49(2)	2(1)	2(1)	-16(1)
C(29B)	41(1)	28(1)	94(2)	22(1)	1(1)	-4(1)
C(32B)	36(1)	44(1)	67(2)	-12(1)	0(1)	-1(1)
C(33B)	53(3)	40(3)	65(3)	-16(2)	5(2)	8(2)
C(34B)	49(3)	41(2)	91(4)	-14(2)	17(3)	5(2)
C(35B)	57(3)	59(3)	89(4)	-13(3)	22(3)	7(2)
C(36B)	67(3)	64(3)	62(3)	-8(2)	3(2)	31(2)
C(37B)	102(4)	41(3)	58(4)	-20(3)	-10(3)	22(3)
C(38B)	70(3)	45(4)	57(3)	-12(3)	-5(3)	-4(3)
C(33C)	47(7)	38(6)	92(8)	-19(6)	4(6)	-2(5)
C(34C)	42(5)	44(6)	89(8)	-19(6)	1(6)	12(5)
C(35C)	68(6)	71(7)	89(7)	-9(6)	16(6)	19(6)
C(36C)	75(7)	63(7)	80(8)	-17(6)	8(7)	29(6)
C(37C)	99(8)	37(6)	70(9)	-10(6)	-3(7)	21(6)
C(38C)	81(8)	28(6)	71(8)	-17(6)	-14(7)	19(6)
C(43B)	44(2)	64(2)	65(2)	13(1)	18(1)	12(1)
C(44B)	49(1)	32(1)	60(2)	8(1)	6(1)	-5(1)
C(47B)	56(2)	48(1)	44(1)	4(1)	-4(1)	7(1)
C(48B)	62(2)	55(2)	50(2)	2(1)	-15(1)	3(1)
C(49B)	63(2)	53(2)	55(2)	1(1)	-11(1)	4(1)
C(50B)	83(2)	86(2)	42(2)	17(2)	6(2)	27(2)
O(12B)	31(1)	40(2)	49(1)	8(1)	8(1)	0(1)
O(12C)	31(1)	40(2)	49(1)	8(1)	8(1)	0(1)
C(53B)	29(1)	32(1)	39(1)	-1(1)	-1	-5(1)
C(52C)	26(1)	22(1)	40(1)	-4(1)	1(1)	-3(1)
C(53C)	29(1)	32(1)	39(1)	-1(1)	3(1)	-5(1)
C(54C)	35(1)	40(1)	46(1)	2(1)	-5(1)	2(1)
C(54B)	35(1)	40(1)	46(1)	2(1)	-5(1)	2(1)
O(61)	68(1)	55(1)	51(1)	-8(1)	-18(1)	13(1)
O(62)	62(1)	52(1)	74(1)	-14(1)	-13(1)	25(1)

Table B.4 contd.

O(63)	21(1)	113(2)	64(2)	-37(2)	14(1)	-4(1)
O(64)	102(2)	101(2)	49(2)	6(2)	-5(2)	-45(2)

Table B.5. Hydrogen coordinates (x 10^4) and isotropic displacement parameters (A^2 x 10^3) for **3.6**

	x	y	z	U(eq)
H(2AA)	3050	2823	643	36
H(1AN)	2429	1788	979	36
H(8AA)	1174	1762	228	37
H(8AB)	1742	1348	-31	37
H(2AN)	1778	789	624	34
H(10C)	756	457	1249	38
H(20A)	3013	-42	1599	42
H(4AN)	3606	941	1141	40
H(26A)	4375	868	607	35
H(31A)	6255	-244	517	37
H(6AN)	6978	803	699	33
H(40A)	7970	786	-228	43
H(40D)	7311	1183	-387	43
H(7AN)	7563	1786	212	43
H(42A)	8774	2047	768	61
H(46A)	6664	2762	1112	48
H(9AN)	5844	1770	982	40
H(52A)	4944	1758	507	39
H(10A)	4140	2770	357	40
H(3AA)	2977	2385	1612	42
H(4AA)	4059	2905	1478	81
H(4AB)	3568	3244	1857	81
H(4AC)	3614	3473	1315	81
H(5AA)	2266	3378	1188	56
H(5AB)	1885	2773	1334	56
H(6AA)	1618	3426	1934	87
H(6AB)	2428	3636	1980	87
H(6AC)	2200	2993	2160	87
H(11A)	1149	1151	2063	51
H(11B)	378	1191	1821	51
H(13A)	-385	265	1820	64

Table B.5 contd.

H(14A)	-767	-537	2267	73
H(15A)	-70	-907	2889	65
H(16A)	1006	-456	3064	64
H(17A)	1375	371	2635	57
H(18A)	2191	-395	1287	60
H(18B)	1352	-351	1191	60
H(18C)	1645	-416	1727	60
H(21A)	3543	1013	2058	55
H(22A)	3252	562	2795	96
H(22B)	2919	11	2516	96
H(22C)	2554	647	2473	96
H(23A)	4508	449	1832	82
H(23B)	4441	423	2402	82
H(24A)	4737	-513	2109	128
H(24B)	4045	-517	1774	128
H(24C)	3961	-544	2344	128
H(27A)	3829	89	-121	39
H(6A)	4506	555	-562	62
H(28A)	3100	909	-319	61
H(28B)	3406	1261	134	61
H(28C)	2930	683	212	61
H(29A)	5214	-722	543	73
H(29B)	5328	-449	19	73
H(29C)	4541	-589	208	73
H(32A)	6427	404	1402	47
H(32B)	5922	-160	1367	47
H(34A)	6364	-995	1701	69
H(35A)	7279	-1557	2000	85
H(36A)	8453	-1306	1840	87
H(37A)	8706	-479	1372	84
H(38A)	7775	129	1103	64
H(43A)	8837	1910	1610	129
H(43B)	9156	1354	1329	129
H(43C)	8378	1319	1561	129

Table B.5 contd.

H(44A)	7706	3018	1321	81
H(44B)	7819	3031	752	81
H(44C)	8476	2889	1099	81
H(47A)	6838	2699	1921	48
H(48A)	6757	1689	2048	65
H(48B)	6298	2040	2436	65
H(49A)	5600	1283	2257	85
H(49B)	5790	1307	1698	85
H(49C)	5272	1792	1927	85
H(50A)	5761	3032	2210	82
H(50B)	5341	2725	1777	82
H(50C)	5859	3271	1674	82
H(47C)	6274	1659	1745	57
H(48E)	5268	2249	1764	65
H(48F)	5572	2216	2297	65
H(49G)	5197	3169	2124	82
H(49H)	5736	3202	1681	82
H(49I)	6038	3169	2217	82
H(50D)	7404	1998	1995	89
H(50E)	6861	2002	2437	89
H(50F)	7058	2606	2171	89
H(53A)	5194	2639	-220	42
H(12A)	4532	1618	-372	65
H(54A)	5913	1922	-590	66
H(54B)	5763	1473	-160	66
H(54C)	6207	2064	-64	66
H(2BA)	6147	4731	437	34
H(1BN)	6857	5784	635	34
H(8BA)	7915	5740	-271	34
H(8BB)	7254	6138	-428	34
H(2BN)	7449	6707	210	33
H(10D)	8683	7031	680	38
H(20B)	6600	7596	1338	41
H(4BN)	5827	6655	951	41

Table B.5 contd.

H(26B)	4916	6765	531	43
H(31B)	3068	7849	896	50
H(6BN)	2380	6795	1071	47
H(40B)	1268	6854	194	50
H(40C)	1904	6484	-38	50
H(7BN)	1786	5828	550	43
H(42B)	646	5463	1136	50
H(46B)	2878	4835	1520	44
H(9BN)	3532	5851	1154	40
H(52B)	4311	5855	611	35
H(10B)	4999	4830	320	39
H(3BA)	6582	5192	1354	40
H(4BA)	5473	4746	1454	77
H(4BB)	6064	4337	1700	77
H(4BC)	5742	4161	1188	77
H(5BA)	7027	4120	902	55
H(5BB)	7471	4718	863	55
H(6BA)	7974	4109	1449	101
H(6BB)	7235	4092	1735	101
H(6BC)	7676	4694	1699	101
H(11C)	8508	6238	1464	56
H(11D)	9227	6340	1171	56
H(13B)	8541	6629	2223	66
H(14B)	8967	7290	2798	73
H(15B)	9680	8076	2565	76
H(16B)	9972	8200	1762	77
H(17B)	9573	7521	1190	61
H(18D)	7300	7914	872	61
H(18E)	8078	7836	647	61
H(18F)	7985	7939	1212	61
H(21B)	6208	6526	1838	61
H(22D)	7272	6927	2123	103
H(22E)	6670	6959	2529	103
H(22F)	6881	7539	2234	103

Table B.5 contd.

H(23C)	5168	7069	1741	85
H(23D)	5384	7083	2294	85
H(24D)	4990	8022	2044	127
H(24E)	5608	8046	1649	127
H(24F)	5806	8060	2207	127
H(27B)	5119	7661	-183	54
H(6BO)	4354	6680	-276	83
H(28D)	5638	6477	-168	76
H(28E)	6119	7058	-129	76
H(28F)	5715	6908	-619	76
H(29D)	4109	8332	808	81
H(29E)	3794	8155	295	81
H(29F)	4630	8272	356	81
H(32C)	3262	7059	1694	59
H(32D)	3630	7689	1655	59
H(34B)	1996	7001	1968	73
H(35B)	1102	7428	2434	82
H(36B)	1203	8413	2667	77
H(37B)	2139	8969	2390	80
H(38B)	3017	8563	1890	68
H(34C)	1865	7203	1644	70
H(35C)	954	7601	2122	91
H(36C)	1094	8548	2435	87
H(37C)	2152	9037	2336	83
H(38C)	3127	8588	1952	72
H(43D)	574	5556	1960	87
H(43E)	294	6156	1724	87
H(43F)	1074	6127	1953	87
H(44D)	2001	4510	1261	70
H(44E)	1202	4612	1080	70
H(44F)	1368	4572	1642	70
H(47B)	3315	5850	2074	59
H(48C)	4336	5318	1917	67
H(48D)	4153	5257	2474	67

Table B.5 contd.

H(49D)	4517	4344	2183	85
H(49E)	3913	4359	1777	85
H(49F)	3695	4298	2330	85
H(50G)	2890	5339	2757	105
H(50H)	2611	4817	2419	105
H(50I)	2264	5460	2380	105
H(12B)	4731	5464	-388	60
H(12C)	4672	5790	-387	60
H(53B)	3802	5043	-107	40
H(53C)	3904	5097	-177	40
H(54D)	3040	5835	-332	60
H(54E)	3310	6201	124	60
H(54F)	2868	5605	198	60
H(61A)	9090(20)	5290(20)	914(14)	180(30)
H(61B)	9400(20)	5034(17)	1328(4)	97(14)
H(62A)	4922(14)	3564(12)	415(10)	79(11)
H(62B)	4372(18)	3979(16)	502(9)	111(15)
H(63A)	4930(20)	4183(14)	-442(17)	100
H(63B)	4457(13)	4496(19)	-731(16)	100
H(64A)	4900(30)	2062(19)	-1153(10)	126
H(64B)	5100(30)	2597(9)	-1379(17)	126

Table B.6. Torsion angles [deg] for **3.6**

O(1A)-C(1A)-C(2A)-N(1A)	-58.6(3)
N(10A)-C(1A)-C(2A)-N(1A)	121.78(19)
O(1A)-C(1A)-C(2A)-C(3A)	63.1(2)
N(10A)-C(1A)-C(2A)-C(3A)	-116.5(2)
C(1A)-C(2A)-N(1A)-C(7A)	-100.7(2)
C(3A)-C(2A)-N(1A)-C(7A)	137.46(19)
C(2A)-N(1A)-C(7A)-O(2A)	0.4(3)
C(2A)-N(1A)-C(7A)-C(8A)	-178.74(17)
O(2A)-C(7A)-C(8A)-N(2A)	174.16(18)
N(1A)-C(7A)-C(8A)-N(2A)	-6.7(3)
C(7A)-C(8A)-N(2A)-C(9A)	82.4(2)
C(8A)-N(2A)-C(9A)-O(3A)	-2.4(3)
C(8A)-N(2A)-C(9A)-C(10A)	174.48(17)
O(3A)-C(9A)-C(10A)-N(3A)	-141.0(2)
N(2A)-C(9A)-C(10A)-N(3A)	42.1(2)
O(3A)-C(9A)-C(10A)-C(11A)	-13.4(3)
N(2A)-C(9A)-C(10A)-C(11A)	169.69(18)
C(9A)-C(10A)-N(3A)-C(19A)	50.5(2)
C(11A)-C(10A)-N(3A)-C(19A)	-76.6(2)
C(9A)-C(10A)-N(3A)-C(18A)	-131.87(19)
C(11A)-C(10A)-N(3A)-C(18A)	101.1(2)
C(18A)-N(3A)-C(19A)-O(4A)	-178.6(2)
C(10A)-N(3A)-C(19A)-O(4A)	-1.2(3)
C(18A)-N(3A)-C(19A)-C(20A)	4.7(3)
C(10A)-N(3A)-C(19A)-C(20A)	-177.89(18)
O(4A)-C(19A)-C(20A)-N(4A)	-67.3(2)
N(3A)-C(19A)-C(20A)-N(4A)	109.4(2)
O(4A)-C(19A)-C(20A)-C(21A)	52.6(3)
N(3A)-C(19A)-C(20A)-C(21A)	-130.6(2)
C(19A)-C(20A)-N(4A)-C(25A)	-121.5(2)
C(21A)-C(20A)-N(4A)-C(25A)	117.9(2)
C(20A)-N(4A)-C(25A)-O(5A)	5.8(3)
C(20A)-N(4A)-C(25A)-C(26A)	-173.55(18)

Table B.6 contd.

O(5A)-C(25A)-C(26A)-N(5A)	-53.9(3)
N(4A)-C(25A)-C(26A)-N(5A)	125.53(19)
O(5A)-C(25A)-C(26A)-C(27A)	73.1(2)
N(4A)-C(25A)-C(26A)-C(27A)	-107.5(2)
C(25A)-C(26A)-N(5A)-C(30A)	-112.3(2)
C(27A)-C(26A)-N(5A)-C(30A)	120.6(2)
C(25A)-C(26A)-N(5A)-C(29A)	72.3(3)
C(27A)-C(26A)-N(5A)-C(29A)	-54.9(3)
C(29A)-N(5A)-C(30A)-O(7A)	176.0(2)
C(26A)-N(5A)-C(30A)-O(7A)	0.7(3)
C(29A)-N(5A)-C(30A)-C(31A)	-8.1(3)
C(26A)-N(5A)-C(30A)-C(31A)	176.59(18)
O(7A)-C(30A)-C(31A)-N(6A)	-48.1(3)
N(5A)-C(30A)-C(31A)-N(6A)	135.8(2)
O(7A)-C(30A)-C(31A)-C(32A)	71.7(2)
N(5A)-C(30A)-C(31A)-C(32A)	-104.4(2)
C(30A)-C(31A)-N(6A)-C(39A)	-95.3(2)
C(32A)-C(31A)-N(6A)-C(39A)	149.07(19)
C(31A)-N(6A)-C(39A)-O(8A)	-5.8(3)
C(31A)-N(6A)-C(39A)-C(40A)	173.96(17)
O(8A)-C(39A)-C(40A)-N(7A)	-179.11(19)
N(6A)-C(39A)-C(40A)-N(7A)	1.1(3)
C(39A)-C(40A)-N(7A)-C(41A)	73.8(3)
C(40A)-N(7A)-C(41A)-O(9A)	0.7(3)
C(40A)-N(7A)-C(41A)-C(42A)	178.7(2)
O(9A)-C(41A)-C(42A)-N(8A)	-145.7(2)
N(7A)-C(41A)-C(42A)-N(8A)	36.3(3)
O(9A)-C(41A)-C(42A)-C(43A)	-20.0(4)
N(7A)-C(41A)-C(42A)-C(43A)	161.9(2)
C(41A)-C(42A)-N(8A)-C(45A)	49.8(3)
C(43A)-C(42A)-N(8A)-C(45A)	-76.1(3)
C(41A)-C(42A)-N(8A)-C(44A)	-140.7(2)
C(43A)-C(42A)-N(8A)-C(44A)	93.4(3)
C(44A)-N(8A)-C(45A)-O(10A)	-170.3(2)

Table B.6 contd.

C(42A)-N(8A)-C(45A)-O(10A)	-1.8(3)
C(44A)-N(8A)-C(45A)-C(46A)	11.6(3)
C(42A)-N(8A)-C(45A)-C(46A)	-179.8(2)
O(10A)-C(45A)-C(46A)-N(9A)	-49.6(3)
N(8A)-C(45A)-C(46A)-N(9A)	128.5(2)
O(10A)-C(45A)-C(46A)-C(47A)	82.3(3)
N(8A)-C(45A)-C(46A)-C(47A)	-99.7(3)
O(10A)-C(45A)-C(46A)-C(47C)	53.6(4)
N(8A)-C(45A)-C(46A)-C(47C)	-128.3(4)
C(45A)-C(46A)-N(9A)-C(51A)	-132.4(2)
C(47A)-C(46A)-N(9A)-C(51A)	97.6(3)
C(47C)-C(46A)-N(9A)-C(51A)	128.4(3)
C(46A)-N(9A)-C(51A)-O(11A)	-4.0(3)
C(46A)-N(9A)-C(51A)-C(52A)	176.30(18)
O(11A)-C(51A)-C(52A)-N(10A)	-53.2(3)
N(9A)-C(51A)-C(52A)-N(10A)	126.4(2)
O(11A)-C(51A)-C(52A)-C(53A)	69.1(3)
N(9A)-C(51A)-C(52A)-C(53A)	-111.2(2)
O(1A)-C(1A)-N(10A)-C(52A)	3.4(3)
C(2A)-C(1A)-N(10A)-C(52A)	-177.02(18)
C(51A)-C(52A)-N(10A)-C(1A)	-98.2(2)
C(53A)-C(52A)-N(10A)-C(1A)	139.1(2)
N(1A)-C(2A)-C(3A)-C(4A)	172.89(19)
C(1A)-C(2A)-C(3A)-C(4A)	52.8(2)
N(1A)-C(2A)-C(3A)-C(5A)	-63.3(2)
C(1A)-C(2A)-C(3A)-C(5A)	176.63(18)
C(4A)-C(3A)-C(5A)-C(6A)	-58.2(3)
C(2A)-C(3A)-C(5A)-C(6A)	179.4(2)
N(3A)-C(10A)-C(11A)-C(12A)	-66.5(3)
C(9A)-C(10A)-C(11A)-C(12A)	166.14(19)
C(10A)-C(11A)-C(12A)-C(17A)	100.8(3)
C(10A)-C(11A)-C(12A)-C(13A)	-78.1(3)
C(17A)-C(12A)-C(13A)-C(14A)	0.1(4)
C(11A)-C(12A)-C(13A)-C(14A)	179.0(3)

Table B.6 contd.

C(12A)-C(13A)-C(14A)-C(15A)	-0.9(5)
C(13A)-C(14A)-C(15A)-C(16A)	0.5(4)
C(14A)-C(15A)-C(16A)-C(17A)	0.7(4)
C(13A)-C(12A)-C(17A)-C(16A)	1.1(4)
C(11A)-C(12A)-C(17A)-C(16A)	-177.8(2)
C(15A)-C(16A)-C(17A)-C(12A)	-1.5(4)
N(4A)-C(20A)-C(21A)-C(22A)	176.3(2)
C(19A)-C(20A)-C(21A)-C(22A)	57.9(3)
N(4A)-C(20A)-C(21A)-C(23A)	-57.8(3)
C(19A)-C(20A)-C(21A)-C(23A)	-176.2(2)
C(22A)-C(21A)-C(23A)-C(24A)	66.2(4)
C(20A)-C(21A)-C(23A)-C(24A)	-58.2(3)
N(5A)-C(26A)-C(27A)-O(6A)	-54.3(2)
C(25A)-C(26A)-C(27A)-O(6A)	-179.55(16)
N(5A)-C(26A)-C(27A)-C(28A)	-174.04(17)
C(25A)-C(26A)-C(27A)-C(28A)	60.7(2)
N(6A)-C(31A)-C(32A)-C(33A)	-72.8(2)
C(30A)-C(31A)-C(32A)-C(33A)	169.85(18)
C(31A)-C(32A)-C(33A)-C(38A)	62.3(3)
C(31A)-C(32A)-C(33A)-C(34A)	-121.9(2)
C(38A)-C(33A)-C(34A)-C(35A)	2.0(4)
C(32A)-C(33A)-C(34A)-C(35A)	-173.9(3)
C(33A)-C(34A)-C(35A)-C(36A)	-2.0(4)
C(34A)-C(35A)-C(36A)-C(37A)	0.0(5)
C(35A)-C(36A)-C(37A)-C(38A)	2.0(5)
C(34A)-C(33A)-C(38A)-C(37A)	0.0(4)
C(32A)-C(33A)-C(38A)-C(37A)	175.8(2)
C(36A)-C(37A)-C(38A)-C(33A)	-2.0(4)
N(9A)-C(46A)-C(47A)-C(50A)	-55.7(4)
C(45A)-C(46A)-C(47A)-C(50A)	177.5(3)
C(47C)-C(46A)-C(47A)-C(50A)	-122.1(6)
N(9A)-C(46A)-C(47A)-C(48A)	71.9(3)
C(45A)-C(46A)-C(47A)-C(48A)	-54.9(3)
C(47C)-C(46A)-C(47A)-C(48A)	5.4(5)

Table B.6 contd.

C(50A)-C(47A)-C(48A)-C(49A)	62.3(4)
C(46A)-C(47A)-C(48A)-C(49A)	-64.8(4)
N(9A)-C(46A)-C(47C)-C(50C)	170.9(5)
C(45A)-C(46A)-C(47C)-C(50C)	62.1(6)
C(47A)-C(46A)-C(47C)-C(50C)	-65.1(7)
N(9A)-C(46A)-C(47C)-C(48C)	-65.8(5)
C(45A)-C(46A)-C(47C)-C(48C)	-174.6(5)
C(47A)-C(46A)-C(47C)-C(48C)	58.2(5)
C(50C)-C(47C)-C(48C)-C(49C)	67.1(12)
C(46A)-C(47C)-C(48C)-C(49C)	-55.6(10)
N(10A)-C(52A)-C(53A)-O(12A)	-50.7(2)
C(51A)-C(52A)-C(53A)-O(12A)	-172.67(17)
N(10A)-C(52A)-C(53A)-C(54A)	-174.21(17)
C(51A)-C(52A)-C(53A)-C(54A)	63.8(2)
O(1B)-C(1B)-C(2B)-N(1B)	-58.2(2)
N(10B)-C(1B)-C(2B)-N(1B)	121.64(19)
O(1B)-C(1B)-C(2B)-C(3B)	63.3(2)
N(10B)-C(1B)-C(2B)-C(3B)	-116.9(2)
C(1B)-C(2B)-N(1B)-C(7B)	-109.5(2)
C(3B)-C(2B)-N(1B)-C(7B)	129.0(2)
C(2B)-N(1B)-C(7B)-O(2B)	-0.5(3)
C(2B)-N(1B)-C(7B)-C(8B)	178.37(17)
O(2B)-C(7B)-C(8B)-N(2B)	-177.05(18)
N(1B)-C(7B)-C(8B)-N(2B)	4.0(3)
C(7B)-C(8B)-N(2B)-C(9B)	80.5(2)
C(8B)-N(2B)-C(9B)-O(3B)	-2.2(3)
C(8B)-N(2B)-C(9B)-C(10B)	174.86(18)
O(3B)-C(9B)-C(10B)-N(3B)	-144.4(2)
N(2B)-C(9B)-C(10B)-N(3B)	38.5(3)
O(3B)-C(9B)-C(10B)-C(11B)	-16.8(3)
N(2B)-C(9B)-C(10B)-C(11B)	166.1(2)
C(11B)-C(10B)-N(3B)-C(19B)	-71.8(2)
C(9B)-C(10B)-N(3B)-C(19B)	53.7(2)
C(11B)-C(10B)-N(3B)-C(18B)	106.0(2)

Table B.6 contd.

C(9B)-C(10B)-N(3B)-C(18B)	-128.5(2)
C(18B)-N(3B)-C(19B)-O(4B)	179.5(2)
C(10B)-N(3B)-C(19B)-O(4B)	-2.9(3)
C(18B)-N(3B)-C(19B)-C(20B)	2.3(3)
C(10B)-N(3B)-C(19B)-C(20B)	179.92(17)
O(4B)-C(19B)-C(20B)-N(4B)	-70.4(2)
N(3B)-C(19B)-C(20B)-N(4B)	106.8(2)
O(4B)-C(19B)-C(20B)-C(21B)	49.2(3)
N(3B)-C(19B)-C(20B)-C(21B)	-133.6(2)
C(19B)-C(20B)-N(4B)-C(25B)	-121.7(2)
C(21B)-C(20B)-N(4B)-C(25B)	118.7(2)
C(20B)-N(4B)-C(25B)-O(5B)	9.2(4)
C(20B)-N(4B)-C(25B)-C(26B)	-169.6(2)
O(5B)-C(25B)-C(26B)-N(5B)	-62.3(3)
N(4B)-C(25B)-C(26B)-N(5B)	116.6(2)
O(5B)-C(25B)-C(26B)-C(27B)	63.6(3)
N(4B)-C(25B)-C(26B)-C(27B)	-117.5(2)
C(25B)-C(26B)-N(5B)-C(30B)	-113.4(2)
C(27B)-C(26B)-N(5B)-C(30B)	120.2(2)
C(25B)-C(26B)-N(5B)-C(29B)	69.7(3)
C(27B)-C(26B)-N(5B)-C(29B)	-56.8(3)
C(29B)-N(5B)-C(30B)-O(7B)	-178.4(2)
C(26B)-N(5B)-C(30B)-O(7B)	4.7(3)
C(29B)-N(5B)-C(30B)-C(31B)	-0.9(4)
C(26B)-N(5B)-C(30B)-C(31B)	-177.7(2)
O(7B)-C(30B)-C(31B)-N(6B)	-52.2(3)
N(5B)-C(30B)-C(31B)-N(6B)	130.1(2)
O(7B)-C(30B)-C(31B)-C(32B)	68.0(3)
N(5B)-C(30B)-C(31B)-C(32B)	-109.7(2)
C(32B)-C(31B)-N(6B)-C(39B)	159.0(2)
C(30B)-C(31B)-N(6B)-C(39B)	-85.4(2)
C(31B)-N(6B)-C(39B)-O(8B)	-7.6(4)
C(31B)-N(6B)-C(39B)-C(40B)	171.1(2)
O(8B)-C(39B)-C(40B)-N(7B)	177.7(2)

Table B.6 contd.

N(6B)-C(39B)-C(40B)-N(7B)	-1.1(3)
C(39B)-C(40B)-N(7B)-C(41B)	79.2(3)
C(40B)-N(7B)-C(41B)-O(9B)	3.0(4)
C(40B)-N(7B)-C(41B)-C(42B)	-179.8(2)
O(9B)-C(41B)-C(42B)-N(8B)	-148.5(2)
N(7B)-C(41B)-C(42B)-N(8B)	34.3(3)
O(9B)-C(41B)-C(42B)-C(43B)	-21.7(4)
N(7B)-C(41B)-C(42B)-C(43B)	161.1(2)
C(43B)-C(42B)-N(8B)-C(45B)	-73.4(3)
C(41B)-C(42B)-N(8B)-C(45B)	52.8(3)
C(43B)-C(42B)-N(8B)-C(44B)	96.0(3)
C(41B)-C(42B)-N(8B)-C(44B)	-137.8(2)
C(44B)-N(8B)-C(45B)-O(10B)	-172.1(2)
C(42B)-N(8B)-C(45B)-O(10B)	-3.6(3)
C(44B)-N(8B)-C(45B)-C(46B)	10.9(3)
C(42B)-N(8B)-C(45B)-C(46B)	179.31(19)
O(10B)-C(45B)-C(46B)-N(9B)	-64.1(2)
N(8B)-C(45B)-C(46B)-N(9B)	113.1(2)
O(10B)-C(45B)-C(46B)-C(47B)	55.9(3)
N(8B)-C(45B)-C(46B)-C(47B)	-126.9(2)
C(45B)-C(46B)-N(9B)-C(51B)	-125.0(2)
C(47B)-C(46B)-N(9B)-C(51B)	117.2(2)
C(46B)-N(9B)-C(51B)-O(11B)	-1.1(3)
C(46B)-N(9B)-C(51B)-C(52B)	179.05(19)
O(11B)-C(51B)-C(52B)-N(10B)	-49.3(3)
N(9B)-C(51B)-C(52B)-N(10B)	130.51(18)
O(11B)-C(51B)-C(52B)-C(53B)	74.1(3)
N(9B)-C(51B)-C(52B)-C(53B)	-106.1(2)
O(1B)-C(1B)-N(10B)-C(52B)	1.2(3)
C(2B)-C(1B)-N(10B)-C(52B)	-178.62(18)
C(51B)-C(52B)-N(10B)-C(1B)	-100.9(2)
C(53B)-C(52B)-N(10B)-C(1B)	134.9(2)
N(1B)-C(2B)-C(3B)-C(4B)	170.72(18)
C(1B)-C(2B)-C(3B)-C(4B)	51.6(2)

Table B.6 contd.

N(1B)-C(2B)-C(3B)-C(5B)	-64.9(2)
C(1B)-C(2B)-C(3B)-C(5B)	175.91(17)
C(4B)-C(3B)-C(5B)-C(6B)	-68.0(3)
C(2B)-C(3B)-C(5B)-C(6B)	169.1(2)
N(3B)-C(10B)-C(11B)-C(12B)	-53.5(3)
C(9B)-C(10B)-C(11B)-C(12B)	-179.6(2)
C(10B)-C(11B)-C(12B)-C(13B)	124.0(3)
C(10B)-C(11B)-C(12B)-C(17B)	-59.7(3)
C(17B)-C(12B)-C(13B)-C(14B)	-1.4(4)
C(11B)-C(12B)-C(13B)-C(14B)	174.9(3)
C(12B)-C(13B)-C(14B)-C(15B)	1.3(5)
C(13B)-C(14B)-C(15B)-C(16B)	-0.1(5)
C(14B)-C(15B)-C(16B)-C(17B)	-0.9(5)
C(13B)-C(12B)-C(17B)-C(16B)	0.4(4)
C(11B)-C(12B)-C(17B)-C(16B)	-176.0(3)
C(15B)-C(16B)-C(17B)-C(12B)	0.8(5)
N(4B)-C(20B)-C(21B)-C(22B)	-179.1(2)
C(19B)-C(20B)-C(21B)-C(22B)	62.6(3)
N(4B)-C(20B)-C(21B)-C(23B)	-53.0(3)
C(19B)-C(20B)-C(21B)-C(23B)	-171.3(2)
C(22B)-C(21B)-C(23B)-C(24B)	66.0(4)
C(20B)-C(21B)-C(23B)-C(24B)	-59.1(4)
N(5B)-C(26B)-C(27B)-O(6B)	-52.1(3)
C(25B)-C(26B)-C(27B)-O(6B)	-176.61(19)
N(5B)-C(26B)-C(27B)-C(28B)	-175.64(18)
C(25B)-C(26B)-C(27B)-C(28B)	59.8(3)
N(6B)-C(31B)-C(32B)-C(33C)	-72.7(6)
C(30B)-C(31B)-C(32B)-C(33C)	169.9(6)
N(6B)-C(31B)-C(32B)-C(33B)	-64.5(4)
C(30B)-C(31B)-C(32B)-C(33B)	178.1(3)
C(33C)-C(32B)-C(33B)-C(34B)	135(4)
C(31B)-C(32B)-C(33B)-C(34B)	89.5(6)
C(33C)-C(32B)-C(33B)-C(38B)	-48(4)
C(31B)-C(32B)-C(33B)-C(38B)	-94.2(8)

Table B.6 contd.

C(38B)-C(33B)-C(34B)-C(35B)	1.4(10)
C(32B)-C(33B)-C(34B)-C(35B)	177.7(5)
C(33B)-C(34B)-C(35B)-C(36B)	-2.7(9)
C(34B)-C(35B)-C(36B)-C(37B)	2.2(10)
C(35B)-C(36B)-C(37B)-C(38B)	-0.6(13)
C(34B)-C(33B)-C(38B)-C(37B)	0.3(15)
C(32B)-C(33B)-C(38B)-C(37B)	-176.2(9)
C(36B)-C(37B)-C(38B)-C(33B)	-0.7(17)
C(33B)-C(32B)-C(33C)-C(34C)	-64(4)
C(31B)-C(32B)-C(33C)-C(34C)	74.0(11)
C(33B)-C(32B)-C(33C)-C(38C)	118(4)
C(31B)-C(32B)-C(33C)-C(38C)	-105(2)
C(38C)-C(33C)-C(34C)-C(35C)	-11(2)
C(32B)-C(33C)-C(34C)-C(35C)	170.5(12)
C(33C)-C(34C)-C(35C)-C(36C)	9(2)
C(34C)-C(35C)-C(36C)-C(37C)	-2(3)
C(35C)-C(36C)-C(37C)-C(38C)	-2(4)
C(34C)-C(33C)-C(38C)-C(37C)	6(4)
C(32B)-C(33C)-C(38C)-C(37C)	-176(2)
C(36C)-C(37C)-C(38C)-C(33C)	1(5)
N(9B)-C(46B)-C(47B)-C(50B)	175.2(2)
C(45B)-C(46B)-C(47B)-C(50B)	58.7(3)
N(9B)-C(46B)-C(47B)-C(48B)	-57.4(3)
C(45B)-C(46B)-C(47B)-C(48B)	-173.9(2)
C(50B)-C(47B)-C(48B)-C(49B)	66.3(3)
C(46B)-C(47B)-C(48B)-C(49B)	-59.2(3)
N(10B)-C(52B)-C(53B)-O(12B)	-51.8(3)
C(51B)-C(52B)-C(53B)-O(12B)	-174.4(2)

Table B.7. Hydrogen bonds for **3.6**.

D-H...A	d(D-H)	d(H...A)	d(D...A)	<(DHA)
N(1A)-H(1AN)...O(4A)	0.88	2.11	2.968(2)	166
N(2A)-H(2AN)...O(2B)#1	0.88	2.15	2.928(2)	147
N(4A)-H(4AN)...O(1A)	0.88	1.98	2.854(2)	171
O(6A)-H(6A)...O(61)#1	0.84	1.93	2.745(3)	162
N(6A)-H(6AN)...O(10A)	0.88	1.98	2.837	163
N(7A)-H(7AN)...O(2A)#2	0.88	2.04	2.900(2)	164
N(9A)-H(9AN)...O(7A)	0.88	2.02	2.873(2)	163
N(10A)-H(10A)...O(62)	0.88	2.54	3.233(3)	136
O(12A)-H(12A)...O(6A)	0.84	1.97	2.810(2)	178
N(1B)-H(1BN)...O(4B)	0.88	2.11	2.959(2)	162
N(2B)-H(2BN)...O(8B)#3	0.88	2.04	2.779(2)	141
N(4B)-H(4BN)...O(1B)	0.88	1.96	2.836(2)	171
N(6B)-H(6BN)...O(10B)	0.88	1.96	2.811(2)	164
O(6B)-H(6BO)...O(12B)	0.84	2.2	3.019(3)	164
O(6B)-H(6BO)...O(12C)	0.84	1.7	2.535(11)	170
N(7B)-H(7BN)...O(8A)#1	0.88	2.32	3.133(3)	153
N(9B)-H(9BN)...O(7B)	0.88	2.02	2.873(2)	163
N(10B)-H(10B)...O(62)	0.88	2.41	3.158(3)	143
O(12B)-H(12B)...O(63)	0.84	2.28	2.973(4)	141
O(12C)-H(12C)...O(63')	0.84	2.06	2.880(9)	164
O(61)-H(61A)...O(3B)	0.858(10)	1.881(13)	2.723(3)	167(4)
O(62)-H(62A)...O(11A)	0.858(10)	1.898(10)	2.755(3)	178(3)
O(62)-H(62B)...O(11B)	0.855(10)	2.075(13)	2.902(3)	163(3)
O(63)-H(63A)...O(62)	0.866(10)	2.28(4)	2.983(4)	138(5)
O(63)-H(63B)...O(9A)#1	0.851(10)	2.01(3)	2.737(3)	143(4)
O(64)-H(64A)...O(12A)	0.850(10)	2.20(2)	3.002(3)	157(5)
O(64)-H(64B)...O(3A)#2	0.849(10)	2.26(4)	3.010(3)	148(6)

REFERENCES

1. Hawksworth, D. L., *Mycol. Res.* **1991**, *95*, 641-655.

2. O'Brien, H. E.; Parrent, J. L.; Jackson, J. A.; Moncalvo, J.-M.; Vilgalys, R., *Applied and Environmental Microbiology* **2005**, *71*, 5544-5550.

3. Hawksworth, D. L., *Mycol. Res.* **2001**, *105*, 1422-1432.

4. Gloer, J. B., Applications of Fungal Ecology in the Search for New Bioactive Natrual Products. In *The Mycota IV: Enviromental and Microbial Relationships*, 2nd ed.; Kubicek, C. P.; Druzhinina, I. S., Eds. Springer-Verlag Berlin Heidelberg: 2007; Vol. X, pp 257-282.

5. AFLATOXINS : Occurrence and Health Risks. http://www.ansci.cornell.edu/plants/toxicagents/aflatoxin/aflatoxin.html (accessed 10/14/2013).

6. Bad Bug Book: Foodborne Pathogenic Microorganisms and Natural Toxins Handbook Aflatoxins. http://www.fda.gov/Food/FoodborneIllnessContaminants/CausesOfIllnessBadBugBook/ucm071020.htm (accessed 12-02-2013).

7. Aflatoxin Handbook. http://www.gipsa.usda.gov/publications/fgis/handbooks/aflatoxin/aflatoxin-ch01.pdf (accessed 12-02-2013).

8. Demain, A. L., *Ann. N.Y. Acad. Sci.* **1974**, *235*, 601-612.

9. Hopwood, D. A., *Mol. Microbiol.* **2007**, *63*, 937-940.

10. Schrettl, M.; Carberry, S.; Kavanagh, K.; Haas, H.; Jones, G. W.; O'Brien, J.; Nolan, A.; Stephens, J.; Fenelon, O.; Doyle, S., *PLoS Pathog* **2010**, *6*, e1000952.

11. Scharf, D. H.; Remme, N.; Heinekamp, T.; Hortschansky, P.; Brakhage, A. A.; Hertweck, C., *J. Am. Chem. Soc.* **2010**, *132*, 10136-10141.

12. Amnuaykanjanasin, A.; Daub, M. E., *Fungal Genetics and Biology* **2009**, *46*, 146-158.

13. Gardiner, D. M.; Jarvis, R. S.; Howlett, B. J., *Fungal Genetics and Biology* **2005**, *42*, 257-263.

14. Chanda, A.; Roze, L. V.; Kang, S.; Artymovich, K. A.; Hicks, G. R.; Raikhel, N. V.; Calvo, A. M.; Linz, J. E., *Proc. Natl. Acad. Sci.* **2009**, *106*, 19533-19538.

15. Sirikantaramas, S.; Yamazaki, M.; Saito, K., *Proc. Natl. Acad. Sci.* **2008**, *105*, 6782-6786.

16. Marahiel, M. A., *J. Pept. Sci.* **2009**, *15*, 799-807.

17. Denning, D. W., *The Lancet* **2003**, *362*, 1142-1151.

18. Weber, G.; Schörgendorfer, K.; Schneider-Scherzer, E.; Leitner, E., *Curr. Genet.* **1994**, *26*, 120-125.

19. Alberts, A. W.; Chen, J.; Kuron, G.; Hunt, V.; Huff, J.; Hoffman, C.; Rothrock, J.; Lopez, M.; Joshua, H.; Harris, E.; Patchett, A.; Monaghan, R.; Currie, S.; Stapley, E.; Schonberg, G.; Hensens, O.; Hirshfield, J.; Hoogsteen, K.; Liesch, J.; Springer, J., *Proc. Natl. Acad. Sci.* **1980**, *77*, 3957-3961.

20. Lee, K. K. Novel Cyclic Peptides And Depsipeptides From Coprophilous Fungi. University Of Iowa, Iowa City, 1997.

21. Thali, M., *Mol, Med. Today* **1995**, *1*, 287-291.

22. Du, L.; Sánchez, C.; Chen, M.; Edwards, D. J.; Shen, B., *Chem. Biol.* **2000**, *7*, 623-642.

23. Finking, R.; Marahiel, M. A., *Annu. Rev. Microbiol.* **2004**, *58*, 453-488.

24. Schwarzer, D.; Finking, R.; Marahiel, M. A., *Nat. Prod. Rep.* **2003**, *20*, 275-287.

25. Schmatz, D. M.; Abruzzo, G.; Powles, M. A.; McFadden, D. C.; Balkovec, J. M.; Black, R. M.; Nollstadt, K.; Bartizal, K., *J. Antibiot.* **1992**, *45*, 1886-1891.

26. Balkovec, J. M.; Hughes, D. L.; Masurekar, P. S.; Sable, C. A.; Schwartz, R. E.; Singh, S. B., *Nat. Prod. Rep.* **2014**.

27. Schwartz, R. E.; Sesin, D. F.; Joshua, H.; Wilson, K. E.; Kempf, A. J.; Goklen, K. A.; Kuehner, D.; Gailliot, P.; Gleason, C.; White, R.; Inamine, E.; Bills, G.; Salmon, P.; Zitano, L., *J. Antibiot.* **1992**, *45*, 1853-1866.

28. Bills, G. F.; Platas, G.; Peláez, F.; Masurekar, P., *Mycol. Res.* **1999**, *103*, 179-192.

29. Chen, L.; Yue, Q.; Zhang, X.; Xiang, M.; Wang, C.; Li, S.; Che, Y.; Ortiz-Lopez, F.; Bills, G.; Liu, X.; An, Z., *BMC Genomics* **2013**, *14*, 339.

30. Kurtz, M. B.; Douglas, C.; Marrinan, J.; Nollstadt, K.; Onishi, J.; Dreikorn, S.; Milligan, J.; Mandala, S.; Thompson, J.; Balkovec, J. M.; Bouffard, F. A.; Dropinski, J. F.; Hammond, M. L.; Zambias, R. A.; Garcia, M. L., *Antimicrob. Agents Chemother.* **1994**, *38*, 2750-2757.

31. Bartizal, K.; Abruzzo, G.; Trainor, C.; Krupa, D.; Nollstadt, K.; Schmatz, D.; Schwartz, R.; Hammond, M.; Balkovec, J.; Vanmiddlesworth, F., *Antimicrob. Agents Chemother.* **1992**, *36*, 1648-1657.

32. Fujie, A., *Pure Appl. Chem.* **2007**, *79*, 603-614.

33. Iwamoto, T.; Fujie, A.; Sakamoto, K.; Tsurumi, Y.; Shigematsu, N.; Yamashita, M.; Hashimoto, S.; Okuhara, M.; Kohsaka, M., *J. Antibiot.* **1994**, *47*, 1084-1091.

34. Kanasaki, R.; Sakamoto, K.; Hashimoto, M.; Takase, S.; Tsurumi, Y.; Fujie, A.; Hino, M.; Hashimoto, S.; Hori, Y., *J. Antibiot.* **2006**, *59*, 137-144.

35. Kanasaki, R.; Abe, F.; Furukawa, S.; Yoshikawa, K.; Fujie, A.; Hino, M.; Hashimoto, S.; Hori, Y., *J. Antibiot.* **2006**, *59*, 145-148.

36. Kanasaki, R.; Abe, F.; Kobayashi, M.; Katsuoka, M.; Hashimoto, M.; Takase, S.; Tsurumi, Y.; Fujie, A.; Hino, M.; Hashimoto, S.; Hori, Y., *J. Antibiot.* **2006**, *59*, 149-157.

37. Kanasaki, R.; Kobayashi, M.; Fujine, K.; Sato, I.; Hashimoto, M.; Takase, S.; Tsurumi, Y.; Fujie, A.; Hino, M.; Hashimoto, S.; Hori, Y., *J. Antibiot.* **2006**, *59*, 158-167.

38. Shiono, Y.; Tsuchinari, M.; Shimanuki, K.; Miyajima, T.; Murayama, T.; Koseki, T.; Laatsch, H.; Funakoshi, T.; Takanami, K.; Suzuki, K., *J. Antibiot.* **2007**, *60*, 309.

39. Shigemori, H.; Wakuri, S.; Yazawa, K.; Nakamura, T.; Sasaki, T.; Kobayashi, J. i., *Tetrahedron* **1991**, *47*, 8529-8534.

40. Lee, Y. M.; Dang, H. T.; Hong, J.; Lee, C.-O.; Bae, K. S.; Kim, D.-K.; Jung, J. H., *Bull. Korean Chem. Soc.* **2010**, *31*, 205-208.

41. Lee, Y. M.; Dang, H. T.; Li, J. L.; Zhang, P.; Hong, J.; Lee, C.-O.; Jung, J. H., *Bull. Korean Chem. Soc.* **2011**, *32*, 3817-3820.

42. Xu, D.; Ondeyka, J.; Harris, G. H.; Zink, D.; Kahn, J. N.; Wang, H.; Bills, G.; Platas, G.; Wang, W.; Szewczak, A. A.; Liberator, P.; Roemer, T.; Singh, S. B., *J. Nat. Prod.* **2011**, *74*, 1721-1730.

43. Cruz, L. J.; Insua, M. M.; Baz, J. P.; Trujillo, M.; Rodriguez-Mias, R. A.; Oliveira, E.; Giralt, E.; Albericio, F.; Cañedo, L. M., *The Journal of Organic Chemistry* **2005**, *71*, 3335-3338.

44. Haritakun, R.; Sappan, M.; Suvannakad, R.; Tasanathai, K.; Isaka, M., *J. Nat. Prod.* **2009**, *73*, 75-78.

45. Sy-Cordero, A. A.; Graf, T. N.; Adcock, A. F.; Kroll, D. J.; Shen, Q.; Swanson, S. M.; Wani, M. C.; Pearce, C. J.; Oberlies, N. H., *J. Nat. Prod.* **2011**, *74*, 2137-2142.

46. Amagata, T.; Morinaka, B. I.; Amagata, A.; Tenney, K.; Valeriote, F. A.; Lobkovsky, E.; Clardy, J.; Crews, P., *J. Nat. Prod.* **2006**, *69*, 1560-1565.

47. Liu, B.-L.; Tzeng, Y.-M., *Biotechnol. Adv.* **2012**, *30*, 1242-1254.

48. Pedras, M. S. C.; Irina Zaharia, L.; Ward, D. E., *Phytochemistry* **2002**, *59*, 579-596.

49. Tsunoo, A.; Kamijo, M.; Taketomo, N.; Sato, Y.; Ajisaka, K., *J. Antibiot.* **1997**, *50*, 1007-1013.

50. Oh, S. U.; Yun, B. S.; Lee, S. J.; Kim, J. H.; Yoo, I. D., *J. Antibiot.* **2002**, *55*, 557-564.

51. Fuente-Núñez, C. d. l.; Whitmore, L.; Wallace, B. A., Chapter 22 - Peptaibols. In *Handbook of Biologically Active Peptides (Second Edition)*, Kastin, A. J., Ed. Academic Press: Boston, 2013; pp 150-156.

52. Marsh, D., *Biochem. J* **1996**, *315*, 345-361.

53. Summers, M. Y.; Kong, F.; Feng, X.; Siegel, M. M.; Janso, J. E.; Graziani, E. I.; Carter, G. T., *J. Nat. Prod.* **2007**, *70*, 391-396.

54. Duclohier, H.; Wróblewski, H., *J. Membrane Biol.* **2001**, *184*, 1-12.

55. Oh, S.-U.; Lee, S.-J.; Kim, J.-H.; Yoo, I.-D., *Tetrahedron Lett.* **2000**, *41*, 61-64.

56. Schiell, M.; Hofmann, J.; Kurz, M.; Schmidth, F. R.; Vertesy, L.; Vogel, M.; Wink, J.; Seibert, G., *J. Antibiot.* **2001**, *54*, 220-233.

57. Krasnoff, S. B.; Reátegui, R. F.; Wagenaar, M. M.; Gloer, J. B.; Gibson, D. M., *J. Nat. Prod.* **2004**, *68*, 50-55.

58. Komatsu, K.; Shigemori, H.; Kobayashi, J. i., *J. Org. Chem.* **2001**, *66*, 6189-6192.

59. Strobel, G.; Daisy, B., *Microbiol. Mol. Biol. Rev.* **2003**, *67*, 491-502.

60. Neff, S. A.; Lee, S. U.; Asami, Y.; Ahn, J. S.; Oh, H.; Baltrusaitis, J.; Gloer, J. B.; Wicklow, D. T., *J. Nat. Prod.* **2012**, *75*, 464-472.

61. Sy, A. A. Chemical Investigation of Fungicolous and Mycoparasitic Fungi from Florida and Hawaii. University of Iowa, Iowa City, IA, 2007.

62. Jiao, P.; Mudur, S. V.; Gloer, J. B.; Wicklow, D. T., *J. Nat. Prod.* **2007**, *70*, 1308-1311.

63. Joshi, B. K. New Bioactive Natural Products from Coprophilous and Mycoparasitic Fungi. University of Iowa, Iowa City, IA, 1999.

64. Stodola, F. H.; Weisleder, D.; Vesonder, R. F., *Phytochemistry* **1973**, *12*, 1797-1798.

65. Marumo, S.; Hattori, H.; Katayama, M., *Agric. Biol. Chem* **1985**, *49*, 1521-1522.

66. McCorkindale, N. J.; Hutchinson, S. A.; McRitchie, A. C.; Sood, G. R., *Tetrahedron* **1983**, *39*, 2283-2288.

67. Singh, S. B.; Zink, D. L.; Liesch, J. M.; Dombrowski, A. W.; Darkin-Rattray, S. J.; Schmatz, D. M.; Goetz, M. A., *Org. Lett.* **2001**, *3*, 2815-2818.

68. Singh, S. B.; Zink, D. L.; Liesch, J. M.; Mosley, R. T.; Dombrowski, A. W.; Bills, G. F.; Darkin-Rattray, S. J.; Schmatz, D. M.; Goetz, M. A., *J. Org. Chem.* **2002**, *67*, 815-825.

69. Isaka, M.; Suyarnsestakorn, C.; Tanticharoen, M.; Kongsaeree, P.; Thebtaranonth, Y., *J. Org. Chem.* **2002**, *67*, 1561-1566.

70. An, Y.; Zhao, T.; Miao, J.; Liu, G.; Zheng, Y.; Xu, Y.; Van Etten, R. L., *J. Agric. Food. Chem.* **1989**, *37*, 1341-1343.

71. Stack, M. E.; Mazzola, E. P., *J. Nat. Prod.* **1989**, *52*, 426-427.

72. Stack, M. E.; Mazzola, E. P.; Page, S. W.; Pohland, A. E.; Highet, R. J.; Tempesta, M. S.; Corley, D. G., *J. Nat. Prod.* **1986**, *49*, 866-871.

73. Arnone, A.; Nasini, G.; Merlini, L.; Assante, G., *J. Chem. Soc., Perkin Trans. 1* **1986**, 525-530.

74. Bouillant, M. L.; Bernillon, J.; Favre-Bonvin, J.; Salin, N., *Z. Naturforsch., C: Biosci.* **1989**, *44c*, 719-723.

75. Höller, U.; Gloer, J. B.; Wicklow, D. T., *J. Nat. Prod.* **2002**, *65*, 876-882.

76. Bouillant, M. L.; Favre-Bonvin, J.; Salin, N.; Bernillon, J., *Phytochemistry* **1988**, *27*, 1517-1519.

77. Nakajima, H.; Isomi, K.; Hamasaki, T.; Ichinoe, M., *Tetrahedron Lett.* **1994**, *35*, 9597-9600.

78. Wheeler, M. H.; Stipanovic, R. D.; Puckhaber, L. S., *Mycol. Res.* **1999**, *103*, 967-973.

79. Hazuda, D. J.; Felock, P.; Hastings, J.; Pramanik, B.; Wolfe, A.; Bushman, F.; Farnet, C.; Goetz, M. A.; Williams, M.; Silverman, K. C.; Lingham, R. B.; Singh, S. B., *Antiviral Chem. Chemother.* **1999**, *10*, 63-70.

80. Lee, H. L.; Gloer, J. B.; Wicklow, D. T., *Bull. Korean Chem. Soc.* **2997**, *28*, 877-879.

81. Edwards, R. L.; Gill, M., *J. Chem. Soc., Perkin Trans. 1* **1973**, 1529-1537.

82. Edwards, R. L.; Elsworthy, G. C.; Kale, N., *J. Chem. Soc. C* **1967**, 405-409.

83. Jiao, P.; Swenson, D. C.; Gloer, J. B.; Campbell, J.; Shearer, C. A., *J. Nat. Prod.* **2006**, *69*, 1667-1671.

84. Singh, S. B.; Zink, D. L.; Dombrowski, A. W.; Dezeny, G.; Bills, G. F.; Felix, J. P.; Slaughter, R. S.; Goetz, M. A., *Org. Lett.* **2000**, *3*, 247-250.

85. Kimura, Y.; Nakadoi, M.; Nakajima, H.; Hamasaki, T.; Nagai, T.; Kohmoto, K.; Shimada, A., *Agric. Biol. Chem* **1991**, *55*, 1887-1888.

86. Takahashi, C.; Numata, A.; Ito, Y.; Matsumura, E.; Araki, H.; Iwaki, H.; Kushida, K., *J. Chem. Soc., Perkin Trans. 1* **1994**, 1859-1864.

87. Caddy, B.; Kidd, C. B. M.; Robertson, J.; Tebbett, I. R.; Tilstone, W. J.; Watling, R., *Experientia* **1982**, *38*, 1439-1440.

88. Zou, X.; Niu, S.; Ren, J.; Li, E.; Liu, X.; Che, Y., *J. Nat. Prod.* **2011**, *74*, 1111-1116.

89. Damm, U.; Mostert, L.; Crous, P. W.; Fourie, P. H., *Persoonia* **2008**, *20*, 87-102.

90. Reátegui, R. F.; Wicklow, D. T.; Gloer, J. B., *J. Nat. Prod.* **2006**, *69*, 113-117.

91. Sano, T.; Takagi, H.; Kaya, K., *Phytochemistry* **2004**, *65*, 2159-2162.

92. Cvak, L.; Jegorov, A.; Sedmera, P.; Havlicek, V.; Ondracek, J.; Husak, M.; Pakhomova, S.; Kratochvil, B.; Granzin, J., *Journal of the Chemical Society, Perkin Transactions 2* **1994**, 1861-1865.

93. Leimer, K. R.; Rice, R. H.; Gehrke, C. W., *J. Chromatogr. A* **1977**, *141*, 121-144.

94. Ohnuki, T.; Yano, T.; Takatsu, T., *J. Antibiot.* **2009**, *62*, 551-557.

95. Ohnuki, T.; Yano, T.; Furukawa, Y.; Takatsu, T., *J. Antibiot.* **2009**, *62*, 559-563.

96. Han, S.-Y.; Joullié, M. M.; Fokin, V. V.; Petasis, N. A., *Tetrahedron: Asymmetry* **1994**, *5*, 2535-2562.

97. Wong, H., *Aust. J. Chem.* **1984**, *37*, 327-333.

98. Angelotti, T.; Krisko, M.; O'Connor, T.; Serianni, A. S., *J. Am. Chem. Soc.* **1987**, *109*, 4464-4472.

99. Horton, D.; Wałaszek, Z., *Carbohydr. Res.* **1982**, *105*, 111-129.

100. Petersson, G.; Samuelson, O.; Anjou, K.; Sydow, E. V., *Acta Chem. Scand.* **1967**, *21*, 1251-1256.

101. Hakami, R. M.; Ruthel, G.; Stahl, A. M.; Bavari, S., *Trends Microbiol.* **2010**, *18*, 164-172.

102. Barash, J. R.; Arnon, S. S., *J. Infect. Dis.* **2013**.

103. Sobel, J., *Clin. Infect. Dis.* **2005**, *41*, 1167-1173.

104. Roos, R. Scientists find new botulinum toxin, withhold genetic details. http://www.cidrap.umn.edu/news-perspective/2013/10/scientists-find-new-botulinum-toxin-withhold-genetic-details (accessed 11/14/2013).

105. Schantz, E. J.; Johnson, E. A., *Microbiol. Rev.* **1992**, *56*, 80-99.

106. Arnon, S. S.; Schechter, R.; Inglesby, T. V.; et al., *JAMA* **2001**, *285*, 1059-1070.

107. Roxas-Duncan, V.; Enyedy, I.; Montgomery, V. A.; Eccard, V. S.; Carrington, M. A.; Lai, H.; Gul, N.; Yang, D. C. H.; Smith, L. A., *Antimicrob. Agents Chemother.* **2009**, *53*, 3478-3486.

108. Cardellina, J. H.; Roxas-Duncan, V. I.; Montgomery, V.; Eccard, V.; Campbell, Y.; Hu, X.; Khavrutskii, I.; Tawa, G. J.; Wallqvist, A.; Gloer, J. B.; Phatak, N. L.; Höller, U.; Soman, A. G.; Joshi, B. K.; Hein, S. M.; Wicklow, D. T.; Smith, L. A., *ACS Med. Chem. Lett.* **2012**, *3*, 387-391.

109. Koyama, K.; Natori, S.; Iitaka, Y., *Chem. Pharm. Bull.* **1987**, *35*, 4049-4055.

110. Soman, A. G. Chemical Investigations of *Chaetomium Globosum* and Mycoparasitic and Coprophilous Fungi. University of Iowa, Iowa City, IA, 1998.

111. Suzuki, K.; Nozawa, K.; Nakajima, S.; Udagawa, S.-i.; Kawai, K.-i., *Chem. Pharm. Bull.* **1992**, *40*, 1116-1119.

112. Grove, C. I.; Di Maso, M. J.; Jaipuri, F. A.; Kim, M. B.; Shaw, J. T., *Org. Lett.* **2012**, *14*, 4338-4341.

113. Mason, S. F.; Seal, R. H.; Roberts, D. R., *Tetrahedron* **1974**, *30*, 1671-1682.

114. Koyama, K.; Natori, S., *Chem. Pharm. Bull.* **1987**, *35*, 578-584.

115. Singh, S. B.; Zink, D. L.; Bills, G. F.; Teran, A.; Silverman, K. C.; Lingham, R. B.; Felock, P.; Hazuda, D. J., *Bioorg. Med. Chem. Lett.* **2003**, *13*, 713-717.

116. Ugaki, N.; Yamazaki, H.; Uchida, R.; Tomoda, H., *J. Antibiot.* **2012**, *65*, 21-24.

117. Koyama, K.; Natori, S., *Chem. Pharm. Bull.* **1988**, *36*, 146-152.

118. Friscic, T.; MacGillivray, L. R., *Chem. Commun.* **2005**, 5748-5750.

119. Wiese, J.; Ohlendorf, B.; Blümel, M.; Schmaljohann, R.; Imhoff, J. F., *Mar. Drugs* **2011**, *9*, 561-585.

120. Rivero-Cruz, J. F.; Macías, M.; Cerda-García-Rojas, C. M.; Mata, R., *J. Nat. Prod.* **2003**, *66*, 511-514.

121. Evidente, A.; Lanzetta, R.; Capasso, R.; Andolfi, A.; Bottalico, A.; Vurro, M.; Zonno, M. C., *Phytochemistry* **1995**, *40*, 1637-1641.

122. Fausto Rivero-Cruz, J.; García-Aguirre, G.; Cerda-García-Rojas, C. M.; Mata, R., *Tetrahedron* **2000**, *56*, 5337-5344.

123. Cimmino, A.; Andolfi, A.; Fondevilla, S.; Abouzeid, M. A.; Rubiales, D.; Evidente, A., *J. Agric. Food. Chem.* **2012**, *60*, 5273-5278.

124. Pedras, M. S. C.; Abrams, S. R.; Seguin-Swartz, G.; Quail, J. W.; Jia, Z., *J. Am. Chem. Soc.* **1989**, *111*, 1904-1905.

125. Chen, X. S.; Da, S. J.; Yang, L. H.; Xu, B. Y.; Xie, Z. X.; Li, Y., *Chin. Chem. Lett.* **2007**, *18*, 255-257.

126. Seo, C.; Oh, H.; Lee, H. B.; Kim, J. K.; Kong, I. S.; Ahn, S. C., *Bull. Korean Chem. Soc.* **2007**, *28*, 1803-1806.

127. Butts, C. P.; Jones, C. R.; Towers, E. C.; Flynn, J. L.; Appleby, L.; Barron, N. J., *Organic & Biomolecular Chemistry* **2011**, *9*, 177-184.

128. Person, R. V.; Monde, K.; Humpf, H.-u.; Berova, N.; Nakanishi, K., *Chirality* **1995**, *7*, 128-135.

129. Murphy, W. S., *J. Chem. Educ.* **1975**, *52*, 774.

130. Dowd, P. F., *Entomologia Experimentalis et Applicata* **1988**, *47*, 69-71.

131. Brady, O. L.; Elsmie, G. V., *Analyst* **1926**, *51*, 77-78.